Une méthodologie d'aide à la décision basée sur l'ACV dynamique pour la gestion du budget carbone des bâtiments

Lucas Neves Mosquini

THÈSE

Pour obtenir le grade de

DOCTEUR DE L'UNIVERSITÉ GRENOBLE ALPES

École doctorale : EEATS - Electronique, Electrotechnique, Automatique, Traitement du Signal (EEATS)
Spécialité : Génie électrique
Unité de recherche : Laboratoire de Génie Electrique

Une méthodologie d'aide à la décision basée sur l'ACV dynamique pour la gestion du budget carbone des bâtiments

A dynamic LCA-based decision-making methodology for carbon budget management of buildings

Présentée par :

Lucas NEVES MOSQUINI

Direction de thèse :

Benoit DELINCHANT PROFESSEUR DES UNIVERSITES, Grenoble INP - UGA	Directeur de thèse
Thomas JUSSELME Associate professor, Haute École d'ingénierie et d'architecture de Fribourg	Co-directeur de thèse

Rapporteurs :

Robin GIRARD
DIRECTEUR DE RECHERCHE, École des Mines Paris PSL
Monika WOLOSZYN
PROFESSEURE DES UNIVERSITES, UNIVERSITE DE CHAMBERY

Thèse soutenue publiquement le **27 septembre 2024**, devant le jury composé de :

Benoit DELINCHANT, PROFESSEUR DES UNIVERSITES, Grenoble INP - UGA	Directeur de thèse
Thomas JUSSELME, ASSOCIATE PROFESSOR, Haute École d'ingénierie et d'architecture de Fribourg	Co-directeur de thèse
Robin GIRARD, DIRECTEUR DE RECHERCHE, École des Mines Paris PSL	Rapporteur
Monika WOLOSZYN, PROFESSEURE DES UNIVERSITES, UNIVERSITE DE CHAMBERY	Rapporteure
Fréderic WURTZ, DIRECTEUR DE RECHERCHE, CNRS DELEGATION ALPES	Président
Bruno PEUPORTIER, DIRECTEUR DE RECHERCHE, École des Mines Paris PSL	Examinateur
Mathilde LOUERAT, INGENIEURE DOCTEURE, Centre scientifique et technique du bâtiment	Examinatrice

Invités :

Stéphane PLOIX
PROFESSEUR DES UNIVERSITES, Grenoble INP - UGA

Acknowledgements

To my supervisors, who have assisted me through thick, thin, and even thinner, I am incredibly grateful. For your incredible patience and for always believing in me when I most doubted myself, thank you, Benoit and Thomas. I truly believe I am not only a better engineer but also a more complete person than I was 4 years ago.

I am also thankful to Grenoble-Alps University for this PhD, which was the result of a collaboration between the G2ELab and the SmartLivingLab. Thanks as well to all my colleagues in both institutions for their companionship.

I would also like to thank my family as well, specially my parents, Adriana and Everson, and my brother, Guilherme. Thank you for your support and for your unconditional love. Last, but not least, thank you Kent for the long days and nights helping me.

As I struggled with this PhD, I lost myself. During this period of self-doubt, I isolated myself from friends and family. With this loss, it took me realizing I'm not the sum of my accomplishments to finally reconnect. Instead, I found that I am the sum of the people who love me and whom I love. To these people, I am truly sorry.

Lucas Hajiro Neves Mosquini

Abstract

Addressing the global challenge of environmental sustainability in the building sector, this thesis focuses on advancing methodologies for greenhouse gas (GHG) budget compliance in building post-occupancy stages. It emphasizes the need for dynamic assessment in the decision-making processes to enhance the process of ensuring carbon budget compliance.

The research employs a multifaceted approach, beginning with an exploration of current methodologies for building GHG budget compliance. This includes a thorough examination of carbon budgets, Life Cycle Assessment (LCA), and Dynamic Life Cycle Assessment (DLCA). The study then progresses to refine the DLCA methodology, focusing on reducing simulation times and optimizing the number of dynamic parameters. Techniques such as linear interpolation, surrogate modelling, feature selection, sensitivity and uncertainty analysis are tested for these tasks. Then, through a case-study, the importance of decarbonization of the industrial, waste and energy sectors in dynamic GWP calculations are highlighted.

Furthermore, the enhanced DLCA methodology is applied in the context of retrofit decision-making, showcasing its utility in adapting to carbon budget deviations throughout a building's life cycle. This application is exemplified through the same case-study of a single-family home in the Paris region, demonstrating the methodology's effectiveness in guiding retrofit decisions in alignment with carbon budgets and broader environmental objectives. However, the findings also reveal the scenario-dependent nature of these decisions, indicating that budget-compliant buildings can exhibit diverse characteristics based on different DLCA assumptions.

Overall, this research emphasizes the critical role of integrating dynamic parameters in retrofit decision-making processes. Simultaneously, it also challenges and assesses the applicability of these methods within the framework of carbon budget compliance, providing a detailed evaluation of their impact on sustainable building practices.

Résumé

Le secteur du bâtiment est un des principaux contributeurs de la crise environnementale mondiale et doit impérativement maitriser ses émissions de gaz à effet de serre (GES). Cette thèse vise à contribuer à l'atteinte de cet objectif en s'intéressant plus particulièrement à la phase d'occupation des bâtiments. Il est nécessaire d'agir lors de cette phase pour respecter un budget carbone défini dès la conception et maintenu sur toute la durée de vie du bâtiment. Cette contribution souligne la nécessité d'une évaluation dynamique dans les processus de prise de décision afin de tenir compte des scenarios d'évolution sur les années restantes.

Une analyse des méthodologies actuelles telle que l'Analyse du Cycle de Vie (ACV) nous conduit à étudier plus spécifiquement l'ACV Dynamique. Nous nous intéressons en particulier à la réduction des temps de simulation et l'optimisation du nombre de paramètres dynamiques. Des techniques telles que l'interpolation linéaire, les modèles de substitution, la sélection des caractéristiques importantes, l'analyse de sensibilité et d'incertitude sont mise en œuvre pour y parvenir. A travers une étude de cas, l'importance de la décarbonisation des secteurs industriels, des déchets et de l'énergie est mise en évidence dans les calculs du Potentiel de Réchauffement Planétaire dynamique.

La méthodologie d'ACV Dynamique que nous proposons est appliquée dans le contexte de la prise de décision pour la rénovation, démontrant son utilité pour s'adapter aux écarts du budget carbone tout au long du cycle de vie d'un bâtiment. L'étude de cas d'une maison individuelle dans la région parisienne montre l'efficacité de la méthodologie pour guider les décisions de rénovation en accord avec les budgets carbone. Cependant, les résultats révèlent également que ces décisions dépendent fortement des scénarios envisagés, indiquant que les bâtiments conformes au budget peuvent présenter une variété de caractéristiques en fonction des différentes hypothèses de modélisation de l'ACV Dynamique.

Plus globalement, nos travaux apportent une méthode pour rationaliser et faciliter l'utilisation généralisée de l'ACV en tenant compte des incertitudes et des sensibilités des différents paramètres dynamiques. Nous montrons que l'ACV Dynamique ainsi mise en œuvre a un impact significatif dans les processus de prise de décision pour la rénovation afin d'assurer une meilleure adaptation aux budgets carbone tout au long du cycle de vie des bâtiments.

Contents

List of Figures

List of Tables

Glossary

B

BAU Busisness-As-Usual. 96, 100, 111–114, 117, 121, 163, 164, 172

BIM Building Information Modelling. 16

BOQ Bill of Quantities. 41, 44, 96, 97

C

CB Carbon Budget. xi, 2, 5, 6, 9–11, 13, 17, 18, 21–24, 32, 35–39, 42, 46, 89, 91, 95, 105, 111, 115

CI Carbon Intensity. 36, 50–55, 62, 76, 83, 85, 99, 100, 104, 117, 118, 161, 162, 167

CMM Carbon Mitigation Measure. xii, 89–91, 95–97, 99, 101, 105, 108–111, 113–115, 119–123, 161–164, 167, 169, 172, 173

CMV Controlled Mechanical Ventilation. 98, 108

COP Coefficient Of Performance. 58, 59

D

DHW Domestic Hot Water. 45, 97, 98, 104

DLCA Dynamic Life Cycle Assessment. 6, 16–19, 21, 22, 27, 29, 30, 36–44, 56, 61, 63, 65–67, 70, 72, 76, 82, 83, 85–87, 92, 94, 101, 104, 117, 119, 120, 122, 123, 125–128, 164, 166

DM Decision-Making. 3–6, 10, 11, 21–25, 27, 29–32, 36–38, 43, 65, 70, 89–97, 101, 102, 104, 105, 111, 118, 119, 122, 123, 125–127, 129, 156, 159–161, 169

DP Dynamic Parameters. 20, 36, 39, 40, 42, 43, 47, 57, 58, 60, 62, 64, 66–70, 72–74, 76, 80, 81, 83–86, 89, 93, 94, 96, 102, 104, 112, 117–119, 122, 123, 126, 127, 129, 161, 162, 167, 169, 170

DTS Dynamic Thermal Simulation. 63, 67

E

EE Embodied Emission. 4, 11, 21, 23, 35, 36, 41, 43–45, 52, 63, 65, 74, 83, 86, 91, 92, 94, 96, 98, 100, 101, 105, 108, 111–115, 117, 119, 126, 161, 163, 167, 169, 170, 172, 173

EI Environmental Impact. 4, 12–20, 22, 26, 30, 33, 37, 39, 41, 97, 100, 117

EOL End-Of-Life. 12, 14, 15, 19–21, 24, 57, 63, 83, 91, 101, 108, 110, 112, 119, 169

EPD Environmental Product Declaration. 2, 14, 15, 41–44, 63, 86, 91, 97–101, 126, 155, 156, 159, 160

G

GA Genetic Algorithm. 34

GCB Global Carbon Budget. 1, 2, 9–11

GHG Greeenhouse Gas. 1–5, 9–11, 16, 19–22, 35, 37, 38, 41, 42, 46, 47, 50, 56, 63, 66, 122, 124, 125, 127

GWP Global Warming Potential. 2, 4, 13, 17, 18, 20, 21, 23, 26–28, 31, 33, 36, 39, 41–44, 46, 60, 63, 65–67, 69, 76, 78, 80–87, 89–91, 93, 94, 96–100, 108–114, 117–120, 122, 123, 126–128, 161, 163, 167, 169, 170, 172

I

IPCC Intergovernmental Panel for Climate Change. 1, 9, 10, 47, 50, 128

L

LCA Life Cycle Assessment. 2–6, 9–13, 15–18, 20, 22, 23, 26, 29, 36–38, 40–42, 44, 50, 53, 54, 61, 66, 76, 77, 80, 83, 85, 86, 89, 91, 94, 98, 100, 118, 124, 125, 128, 169, 170

LCI Life Cycle Inventory. xiii, 4, 42–44, 77, 86, 159

LCIA Life Cycle Impact Assessment. 18, 41, 42

M

MOO Multi-Objective Optimization. 30, 31, 34, 91, 92, 95, 96, 113, 115

O

OE Operational Emissions. 4, 11, 21, 23, 29, 31, 35, 40, 42–45, 50, 51, 55, 60, 63, 65–69, 72, 73, 75, 81, 85, 86, 90–92, 94, 96, 98, 100, 101, 105, 108, 111–115, 117, 119, 126, 161, 163, 167, 169, 170, 172, 173

P

PCP Parallel Coordinates Plot. 29, 95, 105–108, 111, 162, 172

POE Post-Occupancy Evaluation. 23, 129, 130

R

RE2020 Reglémentations Environnementale 2020. 2, 13, 18, 21, 42, 44, 46, 61, 63, 64, 85, 94, 111, 117, 119, 123, 124, 127, 128, 161

RMSE Root Mean Square Error. 66, 69, 70, 74, 86, 103

R^2 Coefficient of Determination. 66, 69, 70, 72, 74, 86, 103

S

SA Sensitivity Analysis. 26–28, 75, 85, 93, 111

SM Surrogate Model. 29, 30, 71–75, 78, 82, 86, 101, 102, 104, 123, 126

SNBC Stratégie Nationale Bas Carbone. 2, 9, 10, 55, 56

1 Introduction

The introductory chapter for this thesis serves to define the context, the problem statements, and the subsequent research objectives and questions.

1.1 Research Background

With the planet's warming reaching 0.8°C to 1.2°C since before the industrial era [1], the United Nations has been regularly organizing international conferences on the subject. The Climate Change Conference in 2015 (COP 21) is of particular importance, during which the Paris Agreement was signed by 196 countries. In it, each nation proposed its Nationally Determined Contributions (NDCs) aiming to limit the global average temperature increase to 2°C [2]. This target had been proposed earlier by the Intergovernmental Panel for Climate Change (IPCC)'s Assessment Report of 2007 [3], identifying the severe consequences to the environment and human life if this threshold was to be surpassed.

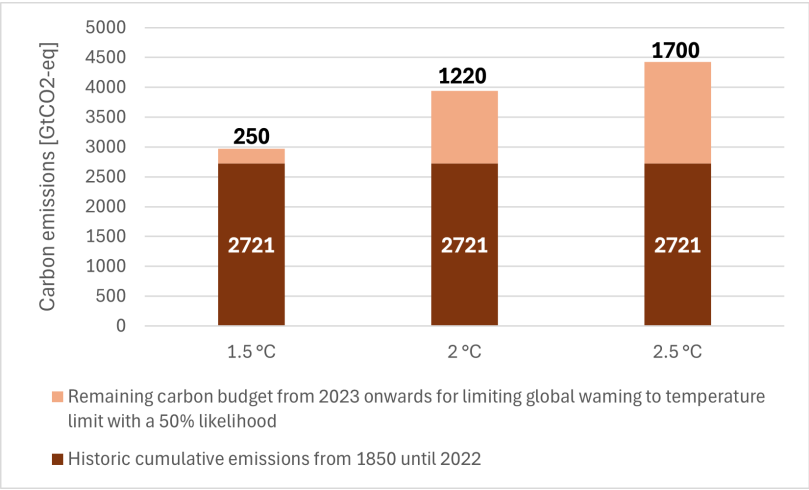

Figure 1.1: The dark orange columns represent the historic emissions since the industrial revolution and in light orange are the remaining budgets for the respective global warming targets as of 2023. From left to right, the targets are 1.5 °C, 2 °C and 2.5 °C with a likelihood of 50 %. Adapted from [4].

In 2018, the IPCC published its Special Report [5], advocating that limiting global warming to 1.5 °C remains viable and significantly more beneficial for life on Earth. The report outlines necessary Greeenhouse Gas (GHG) emission pathways over the coming decades, utilizing the Global Carbon Budget (GCB). From 2023

onwards, the remaining Carbon Budget (CB) for achieving this target is 250 $GtCO_2-eq$, which is equivalent to six years of current emissions [4]. The report also compares CBs for various global warming targets, as illustrated in Figure 1.1. Additionally, it warns that adherence to current NDCs will still result in surpassing the GCB before 2050. Given that the building sector accounts for 34% of final energy consumption and 37% of global GHG emissions [6], an extensive effort is underway to decarbonize this sector.

One of France's responses to this environmental challenge came in the form of the National Low-Carbon Strategy[1] or *Stratégie Nationale Bas Carbone* (SNBC) [7]. In this documentation, national carbon reduction targets are set periodically for specific economic sectors until the year 2050, including agriculture, transportation, industry, waste and building sectors.

Additionally, to further enhance building environmental performance, recent initiatives such as the E+C-[2] experimentation and the RE2020[3] regulation are key national initiatives. RE2020, evolving from the previous RT 2012 regulation, extends its focus beyond the energy performance of new buildings. It sets more stringent requirements for energy efficiency and introduces limits on whole life cycle carbon emissions [8] through CBs at the building level, aligning operational and embodied carbon considerations with environmental objectives. This marks a shift from merely considering energy efficiency to adopting a holistic view of Greeenhouse Gas (GHG) emissions.

Historically, the building sector prioritized energy consumption and energy-efficient design, following the oil crisis of 1973 [9]. Recently, considerable efforts have been directed towards accounting for the embodied impacts of buildings [10], particularly through Life Cycle Assessment (LCA). This environmental evaluation methodology, introduced in the 1960s in other sectors [11], was not applied to buildings until the 1990s [12]. Among various environmental impact indicators (e.g., ozone layer depletion, resource depletion, acidification, water consumption, and eutrophication [13]), the LCA assesses the Global Warming Potential (GWP) of a product in equivalent kilograms of carbon dioxide ($kgCO_2-eq$), an indicator particularly relevant in the context of climate change [12].

The LCA methodology was standardized for general consumer products by ISO 14040/14044 [13], [14]. In the construction sector, the EN 15804 [15] standardizes the Environmental Product Declaration (EPD) of building materials, while EN 15978 [16] specifies an LCA approach detailing the different stages of a building's life cycle, which are depicted in Figure 1.2.

The stages include:

1: The SNBC, published in August 2015, came right after the Paris Agreement was signed and it establishes a target for French national emissions to be net-zero by 2050. By 2021, it was found that between 2015 and 2018 the allocated budget had been surpassed by 3.7%, so the SNBC was revised and new targets were established. For more information: ecologie.gouv.fr/suivi-strategie-nationale-bas-carbone.

2: The E+C- (Positive energy building and carbon reduction) experimentation evaluated thousands of French buildings for relative performance per livable area in both energy and GHG emissions. This led to the creation of a label and the RE2020. For more information: batiment-energiecarbone.fr/.

3: In addition to its environmental efforts, RE2020 (Réglementations Environnementale 2020) also emphasizes stricter thermal performance and summer internal comfort in new buildings. For more information: ecologie.gouv.fr/reglementation-environnementale-re2020.

- **Initial Emissions (Phase A1-A5):** Occur during material extraction, manufacturing, construction, and transportation. These phases are critical due to the high energy consumption and GHG emissions related to material production and logistics.
- **Recurrent Embodied Emissions (B1-B5):** Linked to renovations and maintenance approximately every 50 years, involving the replacement of building components.
- **Operational Emissions (B6-B7):** Span the building's usage phase, influenced by energy consumption for heating, cooling, lighting, etc., dependent on the building's energy efficiency and occupant behaviour.
- **End-of-Life Emissions (C1-C4):** Associated with disassembly, demolition, and waste processing at the end of the building's life cycle.

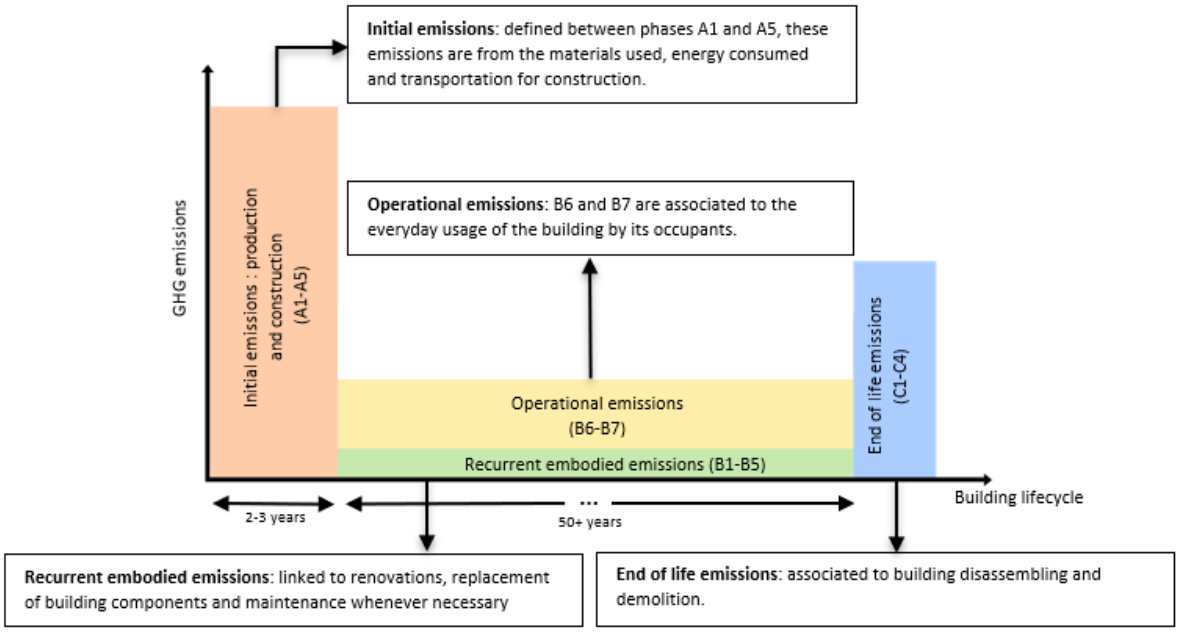

Figure 1.2: Representation of the GHG emissions profile over the life cycle of a building. Based on [17] and [16].

LCAs also function as a Decision-Making (DM) support tool [18], facilitating the comparison of various building component options to identify the most environmentally favourable choices. However, applying LCA to the building sector presents unique challenges due to each building's uniqueness, the long life cycles exceeding 50 years, the complexity arising from numerous components, and the low digitalisation level of the construction sector, leading to complexities in establishing the material quantity take off, which adds significant uncertainty to their assessments [12, 19].

Building on these foundational standards, various European countries have implemented specific regulations to further integrate LCA into their construction practices. In the European Union, reg-

ulations and directives like the Energy Performance of Buildings Directive (EPBD) and national laws emphasize the integration of LCA in construction. For instance, France's RE2020 regulation, Switzerland's SIA 390 and Denmark mandate LCAs for new buildings, enforcing specific CO2 emission thresholds.

1.2 Problem Statement

LCA, an essential DM tool for building design, is conducted during the design phase, where it plays a crucial role in planning and verifying compliance with GHG budgets. Traditionally, LCA uses a static model, assuming no significant changes in the building's structure or functionality throughout its life cycle. This approach can lead to significant discrepancies between projected and actual Environmental Impact (EI).

Recent studies have highlighted a consistent discrepancy between predicted and actual energy performances in modern, energy-efficient buildings, questioning the reliability of static LCA methods [20–23]. As the focus in building assessments shifts from mere energy consumption to comprehensive life cycle performance, it becomes evident that a broader range of assumptions and estimates inherent in LCA outcomes contribute to this unreliability [24–26]. Notably, building LCAs, which are often projected over fifty years or more, encompass these broad estimates.

The challenge extends beyond the design phase, as there is often a lack of mechanisms to verify Life Cycle Inventory (LCI) inputs such as material quantities, transport distances, and energy consumption once construction begins. Ensuring the completeness of LCA is crucial to accurately reflect the EI throughout the entire life cycle of a building. LCA completeness involves capturing all relevant stages and impacts from raw material extraction to material disposal, ensuring every stage is represented and all relevant inputs and outputs are accounted for [27].

Röck et al. [28] noted that buildings constructed before stricter regulations took effect attributed approximately 80-85% of life cycle GWP to Operational Emissions (OE), whereas buildings complying with newer standards showed a reduction in this ratio to about 60-65%. Moreover, Moncaster et al. [29] attributed 64% of Embodied Emission (EE)s to the production phase (A1-5). These works highlight the amount of emissions that lack supervision at post-occupancy stages, underscoring the importance of comprehensive LCA practices to ensure all stages are adequately monitored and verified.

The significance of these findings emphasizes the necessity for continuous assessments and interventions throughout the building's life cycle—not just during the design phase—to achieve sustainability goals. LCA must evolve from a tool used mainly for compliance and DM in the initial phase to a dynamic process that tracks emissions and enables corrective actions during the operational phases. This approach ensures that buildings consistently meet their intended CB and can adjust to any deviations from their projected environmental performance.

Addressing these challenges is critical for advancing LCA's effectiveness beyond initial compliance, enabling it to function as a continuous feedback mechanism throughout the building's lifespan. The following sections will outline research objectives and questions aimed at refining LCA methodologies to support ongoing environmental improvements and ensure that buildings achieve their CB commitments over time.

1.3 Research Objectives

Having identified this necessity of scientific production on the matter of ensuring that buildings respect their budget, this doctoral thesis' main objective is to propose a DM support methodology for managing building CB using LCA. This objective has been divided into the following sub-objectives:

- As LCA becomes a mandatory method in the building design process, it often involves assumptions and estimations about future conditions over a 50-year period. The first objective, therefore, is to propose a methodology that better navigates these uncertainties for CB compliance verification.
- Upon calculating life cycle GHG emissions, it is imperative to take post-occupancy actions towards reducing future GHG emissions in case of CB over-expenditure. Thus, the second objective of this thesis is to propose a methodology towards decision-making of short and long-term retrofit actions towards ensuring budgetary compliance.

1.4 Research Questions

With these objectives set, it is now possible to underline the specific research questions that should be answered throughout the thesis:

- How can long-term uncertainties be taken into account in building LCA?

- How impactful are long-term dynamic uncertainties in the context of building carbon budget compliance?
- How can decision-makers minimize the impacts of uncertainties and create a robust retrofit plan to ensure carbon budget compliance?

The broader inquiry regarding the implementation of a more detailed LCA approach will be addressed through the research efforts of this thesis. These questions will find answers in the third and fourth chapters, which are dedicated to the development of the proposed methodology.

1.5 Thesis Outline

This first introduction chapter has served to give context and justify the interest in developing these research works.

The following second chapter is the result of an extensive literature review on the main topics of this thesis. It starts by defining the primary motivator of this thesis: CBs and the challenge of translating these global targets to the building scale. Subsequently, a review of the state of the art of LCA will be conducted, with a focus on incorporating time-dependence into the assessment methodology. Chapter 2 then includes a review of complementary tools to LCA that assist decision-makers in the building sector in maintaining a certain level of performance at the post-occupancy stage.

In Chapter 3, a DLCA workflow is built specifically for the chosen case-study, around which this thesis is developed. This application allows us to understand the main challenges towards including long-term dynamics into building LCAs into DM processes. Finally, a battery of mathematical tools is studied and tested to find recommendations that facilitate some of the identified challenges of DLCA.

Subsequently, Chapter 4 explores if and how a DLCA method improves the DM process, following the improvements presented in Chapter 3. Applications to the same case-study under different static and dynamic LCA approaches investigate how different assumptions affect DM from the perspective of CBs.

The fifth and last chapter includes an outlook for improving the proposed methodology of this thesis within the topic of building carbon budget compliance and the conclusion of the entire body of work.

1.6 Publications

The following is a list of the publications that I've co-authored during the PhD, in chronological order.

S. Hodencq, J. Coignard, N. K. Twum-Duah, and **L. H. Neves Mosquini**, "Including greenhouse gas emissions and behavioural responses in the optimal design of PV self-sufficient energy communities", COMPEL - The international journal for computation and mathematics in electrical and electronic engineering, vol. 41, no. 6, pp. 2072–2083, Jan. 2022, doi: 10.1108/COMPEL-10-2021-0392.

L. H. Neves Mosquini, V. Tappy, and T. Jusselme, "A carbon-focus parametric study on building insulation materials and thicknesses for different heating systems: A Swiss case study", IOP Conf. Ser.: Earth Environ. Sci., vol. 1078, no. 1, p. 012102, Sep. 2022, doi: 10.1088/1755-1315/1078/1/012102.

N. K. Twum-Duah, **L. H. Neves Mosquini**, M. S. Shahid, F. Wurtz, and B. Delinchant, 'Feedback Indicators for Providing Carbon Impact of Vehicle Charging to Electric Vehicle Users', Transportation Research Procedia, vol. 70, pp. 347–355, 2023, doi: 10.1016/j.trpro.2023.11.039.

L. H. Neves Mosquini, B. Delinchant, and T. Jusselme, "Application of sensitivity analysis on building dynamic lifecycle assessment of GHG emissions: a French case study", J. Phys.: Conf. Ser., vol. 2600, no. 15, p. 152003, Nov. 2023, doi: 10.1088/1742-6596/2600/15/152003.

L. H. Neves Mosquini, B. Delinchant, and T. Jusselme. "Dynamic LCA Methodology to Support Post-Occupancy Decision-Making for Carbon Budget Compliance", Energy and Buildings 309 (April 2024): 114006. https://doi.org/10.1016/j.enbuild.2024.114006.

N. K. Twum-Duah, **L. H. Neves Mosquini**, M. S. Shahid, S. Osonuga, F. Wurtz, and B. Delinchant, "The Indirect Carbon Cost of E-Mobility for Select Countries Based on Grid Energy Mix Using Real-World Data," Sustainability, vol. 16, no. 14, p. 5883, Jul. 2024, doi: 10.3390/su16145883.

The State of the Art of Methods Towards Post-Occupancy GHG Budget Compliance of Buildings

2

This chapter comprises the literature review for this research work. It is organized into three main topics as illustrated in Figure 2.1, starting with an in-depth analysis of Carbon Budget (CB), initially introduced in the research background. After establishing its significance, the chapter describes Life Cycle Assessment (LCA) as the crucial methodology for advancing the building sector's budgetary compliance. However, this alone is insufficient. The chapter then discusses the need for corrective measures when deviations from the CBs are detected to ensure alignment with the Greeenhouse Gas (GHG) trajectory. Finally, the chapter concludes by identifying and discussing the research gap in the current literature.

2.1 Carbon budgets in buildings

Advocates for Global Carbon Budget (GCB) laud it as an unambiguous technique to communicate the nuances of Earth Sciences to policymakers [30]. Recent reports from the IPCC have incorporated GCB, as mentioned in the Chapter 1.1. Defined by the IPCC [1], to maintain global warming within certain limits, the accumulation of human-induced GHG emissions since the XVII century must not surpass specified thresholds. GCBs offer a myriad of benefits, including simplifying comprehension challenges for policymakers.

Bridging this concept to practical applications, for decision-makers in the building sector, having target benchmarks for GHG emissions throughout the various stages of a building's life cycle is crucial for effective sustainable design. Consequently, this creates a need for target values to evaluate the environmental performance of individual buildings [31]. However, allocating GCBs to smaller geographical scales or different sectors is a high complexity task [32].

In the context of national sector scales, the Stratégie Nationale Bas Carbone (SNBC) has set bold targets for the building sector, striving for a reduction in the current levels of emissions of 49%

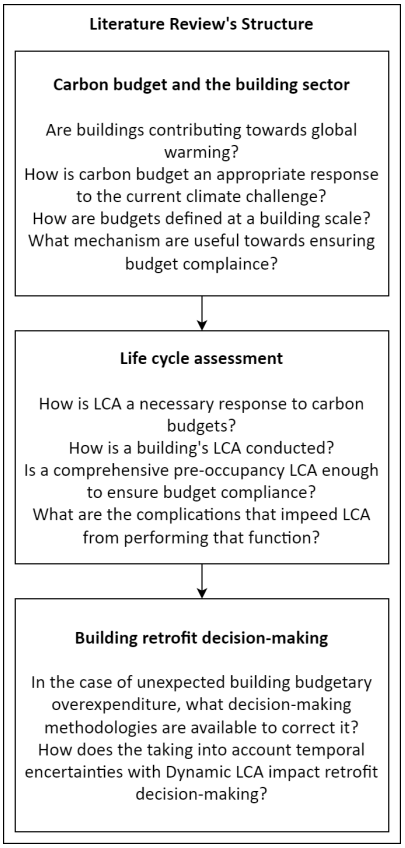

Figure 2.1: Diagram of Chapter 2's structure.

by 2030, and aiming for a net carbon-neutrality sector by 2050 [33]. However, these targets primarily focus on the operational phase of residential buildings.

A building's life cycle, in contrast, encompasses emissions that cut across various sectors: the manufacturing of products is tied to the industrial sector; the transportation of components falls within the transport sector; and the recycling of components is associated with the waste sector. Despite this, French standards have not yet assigned a life cycle perspective budget to the building sector.

To admit a Carbon Budget (CB) at the building scale then, two methodologies can be discerned: top-down and bottom-up approaches.

2.1.1 Top-Down Approach

A top-down or "externally motivated approach" can serve as a possible strategy for transforming GCB to the building or even component scale [34]. This method stems from the calculation of science-based targets that align with the IPCC's 1.5 °C targets. For instance, Priore et al. [35] utilized the 6th IPCC Assessment Report's GCB [1] to establish carbon targets at the building' operational and embodied emissions for new and renovated constructions in Switzerland. Horup et al. [36] formulated and computed a method that investigates and compares different dynamic budget allocation strategies: by population and by economic affluence of a country. Rezaei et al. [37] goes even further and determines budgets at the building component level, with the idea to make them a DM tool. However, this process of down-scaling global targets into clear and manageable targets is difficult and is yet to be harmonized [31, 36].

One major difficulty is the fact that buildings aggregate emissions from different sectors, such as industry, energy and waste. Country-level CBs, such as in France, are typically defined for each of these sectors and do not include imported emissions, limiting themselves to accounting national GHG emissions[1]. In contrast, budgets at the building level are defined with a LCA approach, where emissions across all sectors and nations are accounted for [38]. Indeed, building emissions as per the French SNBC only account for fossil fuel and biomass emissions at the operational phase.

1: In France, CITEPA (Technical Reference Center for Air Pollution and Climate Change) is responsible for reporting emissions and it follows the Secten format for sectorial emissions, much like the SNBC. For more information: citepa.org/fr/secten/

2.1.2 Bottom-Up Approach

Bottom-up strategies are prevalent in the building sector and depend on a comprehensive database of existing building performances. Targets derived from this method reflect the performance

levels possible when the database was established, enabling a comparative analysis of an individual building against the broader building stock.

Zimmermann et al. [39] analyzed 60 buildings to establish benchmarks for LCA modules and building materials, determining average and 95th percentile GHG emissions per square meter to set an emissions budget. Similarly, Lavagna et al. [40] examined 24 statistically-selected European residential building archetypes to compute average GHG emissions per dwelling, per capita, and per surface area.

However, this approach faces several challenges. First, it is inherently dynamic as the building stock continuously evolves [31]. Second, there is a significant issue of alignment, as the benchmarks generated may not consistently correlate with GCB standards [36]. Additionally, whole-building LCA databases are rare and have a low population of buildings.

2.1.3 Scope of Carbon Budgets in This Study

Defining CB is a complex task and consequently, it is not within the scope of this thesis, despite being a major input of the methodology to be developed. Indeed, the entire Decision-Making (DM) process is set to revolve around CB compliance. However, in the French context, under which this thesis is being developed, the RE2020 has recently established GHG budgets for new constructions. These budgets were defined based on the E+C- experimentation, which included a national effort to benchmark French constructions that included over 1200 buildings[2].

The RE2020 defines GHG budgets for OE and EE separately based on multiple criteria, including total surface area, climate, building type, attic surface and parking area. The complexities involved in the sizing methodology mean they are tailored to the building and thus, cannot be generalized.

In summary, complying with CBs within the building sector is crucial for fostering sustainable growth and addressing climate change. The framework provided with GCBs facilitates the reduction of GHG, but is not enough for decision-makers. Consequently, the ensuing sections of this chapter will delve into methodologies that enable practitioners to achieve compliance with CBs, ultimately pinpointing the methodological gaps that warrant additional investigation.

2: E+C- or "Bâtiments à Énergie Positive et Réduction Carbone" or "Positive Energy and Low Carbon Construction" is an experiment that aimed at developing a calculation method and requirement levels for real buildings' environmental performance. It was then, used as the basis for the development of the new environmental regulation. For more information: observatoire.batiment-energiecarbone.fr/statistiques

2.2 Life Cycle Assessment

As sustainable development becomes a main requirement towards limiting climate change and other environmental disasters, evaluating the Environmental Impact (EI) of products and services is key. Every product has a "life": from its design, development and raw material extraction to its production, use and End-Of-Life (EOL) [41]. All aforementioned steps have an environmental cost, such as the depletion of natural resources or the emission of substances.

First introduced in the '60s as a means to reduce waste of soda bottles, LCA has evolved into a methodological framework that allows the assessment of environmental costs from each phase in a product's "life" [11]. Then, at the turn of the century, the methodology was standardized by the ISO 14040-43 norms and officially defined as a "compilation and evaluation of the inputs, outputs and the potential environmental impacts of a product system throughout its life cycle" [13].

2.2.1 An Overview of General LCA

The most general and thus incumbent norms are the ISO 14040 [13] and ISO 14044 [42], which encompasses the principles and the framework of LCA. This framework is summarized in Figure 2.2 and is composed of 4 distinctive steps:

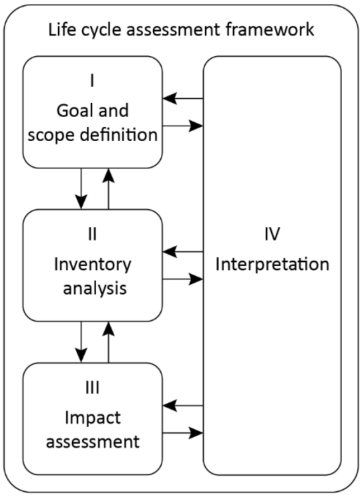

Figure 2.2: LCA framework, as defined by the [13].

I. Goal and scope definition This initial step involves defining the purpose of the study, the system, and the intended audience. It sets the boundary and scope of the LCA, including the functional unit, system boundaries, and data requirements.

II. Inventory analysis This step involves the collection and quantification of inputs and outputs for a product system. It includes data collection related to raw materials, energy inputs, and environmental releases associated with the product from its production to disposal.

III. Impact assessment Here, the EIs of resource use and emissions identified in the inventory analysis are evaluated. This phase involves the selection of impact categories, category indicators, and characterization models, leading to the assessment of the magnitude and significance of the potential EIs.

IV. Interpretation In this final step, the findings from inventory analysis and impact assessment are evaluated in relation to the defined goal and scope. It involves identifying significant issues, evaluating completeness, sensitivity, and consistency

checks, and drawing conclusions and making recommendations based on the study findings.

EIs assessed in LCA are diverse, ranging from resource depletion to ecological consequences. Among these, Global Warming Potential (GWP) emerges as a critical factor, especially in the context of climate change. GWP quantifies the relative radiative forcing of different greenhouse gases over a specific time horizon, typically 100 years [3], as compared to carbon dioxide (CO_2), the reference gas with a GWP of 1. Methane (CH_4), on the other hand, has a characterization factor of 29.8 [43].

This metric enables the comparison of emissions from various sources and the assessment of their long-term effects on global temperatures. Therefore, CBs also are defined in terms of an equivalent mass of CO_2 released into the atmosphere.

2.2.2 Building LCA

Furthermore, due to specific complexities in buildings as compared to other products and services that are often targets of LCA, the CEN / TC 350[3] developed a Framework for European buildings that included sustainable practices such as LCA standards, both at the building and the product levels.

Product stage			Construction stage		Use stage							End of life stage				Benefits beyond the life cycle
A1	A2	A3	A4	A5	B1	B2	B3	B4	B5	B6	B7	C1	C2	C3	C4	D
Raw materials supply	Raw materials transport	Manufacturing	Transport to site	On-site processes	Use	Maintenance	Repairs	Replacement	Refurbishment	Operational energy use	Operational water use	Deconstruction-demolition	Waste transport	Waste processing	Disposal	Reuse, recycling, recovery, etc. (reported separately)

Figure 2.3: Building's life cycle stages and modules, as per the EN 15978 [16].

Within the EN 15643-1 [44] standard that defined the framework for assessment of building environmental performance, two norms are referred to at the building level (EN 15978) and at the product level (EN 15804).

Within the building context, the functional unit has to be defined with the type of building, type of use, technical or functional requirement, and a service life [45]. For French buildings then, the RE2020 differentiates the square metre of floor area of commercial

3: The European Committee for Standardization/Technical Committee 350 (CEN/TC350) is responsible for the development of standardized methods for the assessment of sustainable construction (EN 15643-1) [44], including environmental (EN 15643-2), social (EN 15643-3) and economic (EN 15643-4) performances. For more information: cencenelec.eu/areas-of-work/cen-sectors/construction/

and residential buildings, while setting their life cycle at 50 years [8].

2.2.2.1 Stages and Modules Life Cycle Assessment

In the temporal dimension, this life cycle is segmented into 5 stages, as shown in Figure 2.3: production, construction, use, EOL and benefits. Within each stage, further segmentation is found, totalling 17 distinct modules:

Product stage (A1-3) This stage covers the production of materials up to the manufacturer's gate, also known as cradle-to-gate analysis. These modules, mandatory for all Environmental Product Declaration (EPD), involve data on raw materials, transportation to the manufacturing plant, and energy for production [15]. More detail on EPDs will be given in the following sub-chapter.

Construction stage (A4-5) The impact of the transportation module (A4) varies based on the distance between the construction site and the manufacturer's plant, contributing up to 8% of embodied primary energy [46]. Subsequently, the construction module (A5) includes activities such as the energy consumed by machinery and equipment, concrete pumping and pouring and in-site transportation. Both of these values are included in the French EPDs.

Use stage (B1-7) This comprehensive module covers various aspects including use (B1), maintenance (B2), repair (B3), replacement (B4), refurbishment (B5), operational energy use (B6), and water use (B7). These modules do not apply to every component.

End-Of-Life stage (C1-4) This stage includes demolition (C1), transportation to waste processing (C2), waste processing (C3), and disposal (C4). It relies on current scenarios and technology, which may differ significantly from future practices.

Beyond the life cycle (D) This module accounts for benefits beyond the system boundaries, such as energy recovery from waste incineration. However, assessing these benefits introduces complexities, especially considering the long lifespan of buildings and potential changes in energy mix and waste management practices over time [47].

These modules highlight the complexities in assessing the EIs of buildings, considering factors like material production, transportation, construction, use, and End-Of-Life (EOL). However, thanks to EPDs, this task has been drastically simplified.

2.2.2.2 EPDs and Databases

The EN 15804 [15] norm provides a standardized framework for EPDs specifically tailored to construction products. It establishes the rules for the assessment of the environmental performance of building materials and elements, ensuring consistency and comparability across different products. EN 15804 covers the entire life cycle of construction products, from raw material extraction to EOL, and includes criteria for declaring their EIs. This standard is crucial for the construction industry, enabling informed decision-making based on reliable environmental information.

In practice, the application of EN 15804 has led to the development of several EPD databases, each serving as a repository for the environmental data of building materials and products. Prominent examples of these databases include the INIES [48], in France; the Ökobaudat [49], in Germany; and the KBOB [50], in Switzerland. These databases play a vital role in providing accessible and standardized environmental information, fostering sustainable design and construction practices in line with the principles of EN 15804.

2.2.2.3 Limitations of LCA

LCA is characterized by its holistic approach, which is both its major strength and limitation [51]. The main limitations identified by Hollberg [52] of LCA are:

1. Potentials instead of absolute values: LCA results indicate potential environmental impact rather than predicting precise impacts [52]. The method relies on models valid within specific contexts [53].
2. Time independence: LCA models lack temporal dimensions and are typically linear steady-state models [51]. Dynamic LCA, which considers changing conditions, adds complexity and is not a standard part of LCA [54].
3. Limitations of impact categories: Not all relevant environmental aspects are covered by the impact categories [53].
4. Assumptions: LCA involves technical assumptions and value choices, affecting results [51]. Transparency in these assumptions is essential for objectivity.
5. Uncertainties: LCA has various uncertainties, including parameter, model, and normative uncertainties [53, 55].

Some of the limitations listed above, however, are somewhat overlapping, as the lack of time-dependent models could be considered an uncertainty. Indeed, LCA models describe the future behaviour of the system, but this can only be an educated guess, at best. In this

thesis then, we will classify time-dependent parameters as a source of uncertainty, although many other sources can simultaneously exist, such as modelling errors, which are not treated here.

The recognition of inherent limitations of traditional LCA sets the stage for exploring advanced methodologies capable of addressing these constraints. However, this thesis does not tackle every aforementioned limitation, as it focuses on the uncertainty problem, mainly in the time-domain.

Therefore, DLCA, which aims to capture the temporal aspects and variability of environmental impacts [56] will be investigated Chapter 2.2.3.

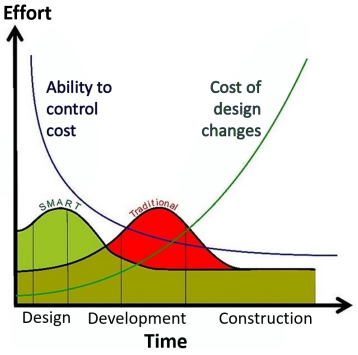

Figure 2.4: MacLeamy curve of effort to make design changes over time. The area painted in red represents the traditional design approach, where most effort is put into the latter, whereas in the IDP, painted in green, the most effort is put into the early design stages, when the cost of changes is lower and the ability to control cost is higher. [57].

2.2.2.4 Buildings' GHG Emissions Through Time

Time introduces significant uncertainty in LCA. This subsection explores emissions timelines, emphasizing the design stage's critical role in efficient building design via the Integrated Design Process (IDP). This process incorporates performance targets early in the design phase, leveraging lower costs for design changes and enhanced cost control, as illustrated by the MacLeamy curve in Figure 2.4.

Early integration of LCA empowers decision-makers to optimize sustainable design. A brief design period can determine a significant portion of a building's environmental impact over its 50-year lifespan. Techniques like parametric workflows [52], data-driven methodologies [58] and BIM-integration [59] have been developed to enhance LCA's early-stage usability.

However, early design stages are fraught with uncertainties due to limited detail [60]. Consequently, the LCA process must be iterative, assisting decision-makers from the initial design through to the documentation submission for approval. Even so, the final EI assessments conducted before construction or delivery, which are crucial for carbon budget compliance, may not fully align with predicted performances. Indeed, Vuarnoz et al. [25] highlight deviations in energy demand based on occupant behaviour, emphasizing that accurate data only becomes available during post-occupancy, thereby illustrating the discrepancy between expected and actual building performance.

These insights highlight the dynamic nature of the building sector's carbon footprint and the importance of incorporating them to LCA. Post-occupancy evaluations, capturing actual energy usage and occupant behaviours, are crucial for refining LCAs. Finally, a DLCA approach, enriched by post-occupancy data, allows for continuous optimization of a building's EI, addressing deviations in GHG

emissions trajectory and allowing timely correction towards CB compliance. The following Sub-Chapter 2.2.3 then, will explore existing DLCA frameworks.

2.2.3 Building Dynamic LCA

Dynamic Life Cycle Assessments have emerged as a response to the limitations of traditional static LCA approaches in capturing the temporal variability of EIs in the building sector [61, 62]. While static LCAs provide a snapshot of a building's EIs throughout its life cycle, they often fail to account for their time-dependent nature, which can vary due to changes in material properties, energy use, and other factors [63]. DLCA addresses this issue by incorporating time-dependent input variables and dynamic EI factors, providing a more comprehensive understanding of a building's environmental performance over its life cycle [64].

By considering the temporal variability of EIs, DLCA allows for a more informed decision-making process when designing, constructing and operating buildings, ultimately leading to more sustainable and low-carbon solutions [62].

2.2.3.1 Considering Time in the LCA Framework

As demonstrated in the framework shown in Figure 2.2, LCA is comprised of different methodological steps. Thus, the temporal dimension can be independently included into each of them [65]:

Dynamic scope Dynamism included in the goal and scope definition phase of LCA can impact product lifetime and functional unit [66]. For instance, Hoxha et al. [67] investigates the impact varying a building's service life on GWP per year.

Dynamic process inventory This refers to the process of capturing and incorporating time-dependent variations in material and energy flows, as well as emissions and other environmental exchanges, that occur during the life cycle of a product or system. This approach contrasts with traditional LCA, which often uses static or average data, failing to account for temporal changes [65].

Dynamic systems inventory Dynamic systems inventory refers to the inclusion of time-dependent changes in the background systems that support the product's life cycle but are not directly part of it. This includes changes in the electricity grid mix, transportation systems, waste management practices, and other external systems that indirectly influence the environmental impacts of the product's life cycle [68]. By incorporating these dynamics, the LCA can capture the

broader temporal shifts in the systems that the product interacts with. Vuarnoz and Jusselme [69], for instance, compared the use of hourly conversion factor for electricity in a building LCA to the traditional yearly average.

Dynamic characterization This aspect involves applying time-dependent factors during the Life Cycle Impact Assessment (LCIA). Dynamic characterization accounts for the varying significance of EIs at different times, as it considers the temporal distribution of emissions, and the varying sensitivity of ecosystems and human health to impacts at different times [70]. In [71], Negishi et al. assess three dynamic indicators: instantaneous radiative forcing, cumulative radiative forcing and global mean temperature change instead of GWP100 (equivalent mass of CO_2 over a 100-year time horizon).

Dynamic weighting This refers to a methodological approach where the relative importance or weight given to different environmental impacts is allowed to vary over time [72]. This step systematically comes last, after LCIA, and incorporates social, political and ethical values [73].

In this thesis, however, a deliberate decision was made to limit the methodology to dynamic inventories (for both process and system). The reason to leave dynamic scope and characterization aside was due to the objective of this thesis to improve CB compliance strategies. Indeed, CBs are defined in GWP100 for a pre-determined life cycle of 50 years[4]. Since the focus is on aligning with these compliance strategies, only the dynamic inventories were considered relevant. As for Dynamic Weighting, it could be argued the RE2020's dynamic approach involves a weighting mechanism, which will be described in the following chapter on the existing methodologies.

4: In France, the building life cycle has been determined at 50 years by the RE2020 regulation [74].

2.2.3.2 Dynamic LCA Methodologies

DLCA is still in its developmental stages, with the earliest scholarly articles appearing around 2010 [68]. Consequently, various methodological proposals are currently being explored in academic research. This brief section will focus on describing three methodologies that have been applied specifically to buildings. These are outlined in the only building-focused DLCA literature review known to date by Su et al. [64], along with the methodological proposal from the RE2020 regulation.

(a) Dynamic Matrix model

Dynamic matrix modelling, spearheaded by Collinge et al. [63], has significantly advanced DLCA research. Collinge et al.'s model integrates four matrices: C_t, B_t, A_t, and f_t, which represent temporal characterization factors, environmental interventions, upstream process changes, and varying materials and energy requirements, respectively. The model's formula, $h_t = \sum_{t_0}^{t_e} C_t \times B_t \times A_t^{-1} \times f_t$, encapsulates the dynamic interactions among these components.

This methodology facilitates dynamic assessments by quantifying the effects of temporal and environmental variables on life cycle phases, encompassing everything from raw material extraction to EOL processes. Collinge applied this dynamic approach to diverse studies, including human health impact quantification [75] and comparisons of green and net zero energy buildings [76]. Moreover, other researchers like Hu [77] adapted this framework, introducing alternative matrices, such as the "M" matrix for user-specific value assessments, and analyzing different environmental priority archetypes. Simplifications of this model by Fouquet et al. [78] and Pittau et al. [79] focused on dynamic global warming impacts using GHG emission vectors and environmental system dynamics.

(b) Data Transformation–Based Model

This dynamic model, established with Su et al. [80] and further explored in subsequent studies, emphasizes the transformation of calculation data in EI assessment. The core concept of the model is the data transformation pathway, which is essential for calculating the final dynamic impact results.

The methodology involves a series of steps. Initially, data on building materials and energy consumption throughout the life cycle are gathered annually. This dynamic consumption data is then transformed into dynamic inventory results, incorporating time-dependent variations in the energy mix. The next stage involves the adoption of dynamic characterization factors, which consider the timing of pollutant release, leading to the creation of dynamic impact category indicators. The final step employs dynamic weighting factors to quantify the impact severities at different times, resulting in the output of annual impact assessments.

(c) Static Model + Dynamic Variables

Negishi et al. [81] proposed an innovative approach for EI assessment, combining a static LCA model with dynamic variables, aptly named the “static model + dynamic variables”. This methodology was then applied to a case-study in [71] and it involves integrating dynamic factors into a traditionally static LCA framework to better capture the temporal aspects of EI.

The dynamic model comprises five key steps. Initially, it involves the collection of building data, focusing on identifying and discussing dynamic aspects. The second step entails the development of a static model that represents the life cycle system. Subsequently, dynamic variables relevant to the model are thoroughly analyzed and modelled, considering various scenarios to simulate different conditions. The fourth and fifth steps involve conducting a dynamic inventory analysis and a dynamic characterization process, respectively, to determine temporal EI.

This hybrid approach maintains the static LCA system as a foundational structure, with the addition of various dynamic variables. These dynamic elements are seamlessly integrated into the static framework, enabling a more comprehensive and temporally sensitive dynamic assessment.

(d) RE2020

The RE2020 methodology is defined in the most recent French building environmental regulation. In this method, a "weighting factor" is applied to building emissions year-by-year. These are the DPs that are linked to social and policy developments. Su et al. [62] defined the weighting factor as the DP linked to governmental environmental policy and planning reports [62] or to a population’s willingness to pay to avoid climate change [82].

France’s weighting factor then, is built as a linear reduction of GHG emissions with time. Effectively, the further in the future an action is taken, the lower its EI. This weighting factor represents the decarbonization process that will occur in all building-adjacent sectors in the next few decades. In practice, the weighting factor linearly decreases from 1 to 0.58 from year "zero" until the building’s EOL. This weighting factor is not a variable, however, meaning this method, unlike the others, is not inherently parametric.

Equation 2.1 summarizes the calculations, where GWP_{total} represents the overall life cycle GWP, GWP_y is the GWP at a given year y and F is the weighting factor, which is itself calculated as per Equation 2.2.

$$GWP_{total} = \sum_{y=0}^{50} GWP_y \times F_y \tag{2.1}$$

$$F_y = 1 - (\frac{1 - 0.58}{50} \times y) \tag{2.2}$$

Note that both OE and EE are treated equally in this methodology and thus multiplied by the same factor. Also note that upfront emissions linked to production and construction phases (A1-5, as per [15]) are not affected by F.

Consequently, this method of calculating GWP favours some types of components over others by reducing the importance of EOL emissions, notably, it incentivizes the use of bio-based materials.

(e) Comparing Methodologies

The aforementioned DLCA methods have distinct strengths and limitations. The dynamic matrix model is valued for its general applicability and clear structure, but it lacks depth in representing the dynamic specifics of buildings and in detailed temporal analysis. The data transformation–based model effectively links temporal data with traditional assessment methods, allowing easy integration of dynamic variables into existing frameworks. However, it falls short when deeply analyzing the temporal aspects of these variables.

Finally, the RE2020 offers the simplest approach deal with dynamics, however, this comes with many limitations, such as the strict applicability to French buildings and the fact that it's not parametric. Since this thesis also uses the CBs by the RE2020, it also will explore its DLCA method.

For a more holistic approach, it was found that the static model + dynamic variables method had the best compromise between the detail of time-dependent variables and the associated complexities. Therefore, this method will also be included in the methodological development.

2.2.4 Advantages and Disadvantages of Dynamic LCA

DLCA offers a nuanced approach to environmental impact analysis, particularly in forecasting GHG emissions over a product's life cycle. This section explores the advantages and disadvantages of DLCA in the context of its application and role in the DM processes.

2.2.4.1 Advantages of DLCA

- Enhanced Forecast and Comprehensive Overview: DLCA enables more holistic forecasting and a more complete overview of future GHG emissions. By taking into account the temporal variation and evolution of processes, DLCA allows for an educated guess of the life cycle GHG, leading to a more nuanced understanding of EIs over time [55].
- Parametric Flexibility: The parametric nature of DLCA provides flexibility in modelling. It accommodates various scenarios and changing conditions, making it a versatile tool for assessing EIs under different circumstances [71].

2.2.4.2 Disadvantages of DLCA

- Computational Intensity: The parametric nature of DLCA necessitates multiple computing simulations to account for various scenarios and temporal changes. This can be resource-intensive and time-consuming, limiting its practicality in certain contexts [83].
- Frequent Calculation of Energy Needs: DLCA requires the frequent calculation of annual energy needs for dynamic operational emissions. This process is often iterative and complex, posing challenges in terms of data accuracy and processing time [83].
- Complexity in Modeling Dynamic Parameters: The modelling of dynamic parameters in DLCA is complex, often hindered by a lack of comprehensive data and a unified database [63].
- DLCA as One of Many Adaptations: DLCA represents just one of the adaptations of the traditional LCA methodology. While it offers depth in temporal analysis, it may not fully address all aspects of EI, necessitating complementary approaches [84].

Clearly, DLCA comes with significant complexity and resource requirements. Therefore, its integration with other tools and methodologies presents notable challenges. However, the amalgamation of long-term uncertainties to a CB compliance method seems particularly relevant and necessary advancement.

Indeed, up until now, the use of LCA towards CB compliance has been restricted to the design stages of building, despite LCA method already being commonly integrated into renovations [85]. Thus, a post-occupancy DM method, informed by DLCA, plays a potentially pivotal role in aligning building performance with budgetary goals.

For this reason, Sub-Chapter 2.3 will explore DM methods in building design that could also inform decision-makers of retrofitting plans towards budgetary compliance.

2.3 Building Post-Occupancy Decision-Making

The preceding sections established CBs as important instruments towards the future of the built environment and LCA as a crucial methodology to assess the budgetary compliance of buildings. Now, this section will explore methodologies in the current literature that support decision-makers towards ensuring building energy and environmental performance at post-occupancy stages. To start then, some terms first need to be defined, starting with post-occupancy.

2.3.1 Post-Occupancy

2.3.1.1 Definition of Post-Occupancy

In line with the LCA framework, a building's life cycle is categorized into 17 modules across 5 stages (see Figure 2.3). The product and construction stages (A1-5) contribute to the upfront Embodied Emission (EE). Post-occupancy starts after delivery, encompassing the building's utilization until its life cycle concludes [5]. Hereafter then, post-occupancy emissions will correspond to the use (B1-7) and end-of-life (C1-4) stages, including Operational Emissions (OE) (B6 and B7) and EE (B1-5 and C1-4).

2.3.1.2 The Relevance of Post-Occupancy Evaluation

Post-Occupancy Evaluation is pivotal in managing the uncertainty inherent in the assessment of a building's GWP over a complete life cycle. Such evaluation allows for the actual measurement and correction of performance gaps that emerge with time, thereby addressing the limitations of predictive assessments.

Defined by Li et al. as "the general approach of obtaining feedback about a building's performance in use" [5], POEs involve comprehensive audits and evaluations throughout the building's lifespan [86]. These evaluations generate both subjective feedback, through interviews and surveys with occupants, and objective data, from measurements of indoor air quality, energy usage, water consumption, etc. [5].

Importantly, the true measure of a building's sustainability is reflected in its operational performance, not just its intended design [5]. To this end, certification and rating systems like the Energy

Results Guarantee[5] in France serve to ensure ongoing energy performance through continuous monitoring and recommendations for energy savings.

Another key example is the International Performance Measurement and Verification Protocol (IPMVP)[6], which offers an approach for validating and calculating the effectiveness of energy saving measures in buildings.

These certifications and protocols underscore the role of building experts in analyzing performance data to identify and rectify deviations. This process not only supports the immediate goal of optimizing building performance but also contributes to the broader objective of sustainable development. In this context, the inclusion of DM processes becomes crucial as these evaluations inform strategies to address performance issues.

2.3.2 Decision-Making in Building Renovations

During post-occupancy, as defined in Chapter 2.3.1.1, the building has already been constructed and is being occupied. Therefore, the design choices available at this stage are now restricted to refurbishment, maintenance, replacement and EOL measures. Indeed, when considering the life cycle modules in Figure 2.3, all A-phase emissions have now passed and the focus to ensure CB compliance is on B- and C-phase emissions: usage and EOL stages. To manage the post-occupancy CB then, design decisions can still be made to curb emission trajectories in renovations.

Within Europe, 80% of the occupied buildings in 2050 have already been built [87]. Therefore, renovating the current building stock will be an essential stepping stone towards respecting the CBs of the sector. Indeed, annual renovation rates in Europe are expected to jump from 1% to 2% in the next years [88]. This less ambitious goal was set after a target of 3% by 2020 had not been achieved [89].

Given the relevance of renovations, methodological developments towards supporting the DM process at this crucial life cycle stage are important. Despite the DM process during pre- and post-occupancy stages being fundamentally similar, the main differential between them being the number of constraints [90].

Bazerman and Moore [91] have defined a general workflow for DM in building renovations, which includes the following: problem definition, identification of objectives and criteria, criteria weighting, generation of alternatives, rating each alternative on each criterion and lastly computing the optimal solution. In the context of building renovations then, Nielsen et al. [90] assembled

5: In French, the Garantie de Résultats Energétique (GRE) mechanism is a part of the Garantie de Performance Energétique (GPE) plan. This 2-part plan consists of ensuring the intrinsic quality of the work realized during construction or renovation, then ensuring a maximum level of energy consumption. For more information: expertises.ademe.fr/batiment/

6: The International Performance Measurement and Verification Protocol (IPMVP). For more information: evo-world.org/en/products-services-mainmenu-en/protocols/ipmvp

the works of Ferreira et al. [92] and Alanne [93] in a literature review to summarize the DM process for building renovations into six areas displayed in Figure 2.5. Within each of the six areas then, the methodological steps, together with the primary actors responsible have been included.

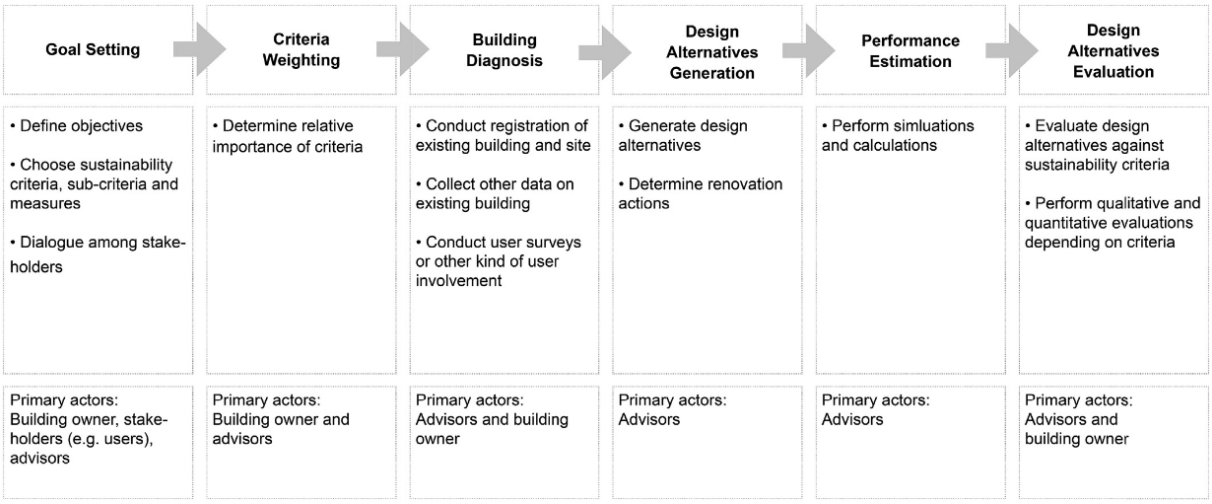

Figure 2.5: The six areas towards DM in building renovations [90].

2.3.3 Techniques for Solution Exploration

Decision-Making methodologies encompass various methods aiding building decision-makers to achieve better-performing buildings. These methods consider factors such as cost, energy consumption, indoor air quality, and intervention times [94]. Østergård et al. [95] identify the following DM support techniques for building design: statistical methods, optimizations, and CAD-BPS[7] interoperability, which integrates CAD[8] with building performance simulations to streamline the design process.

For existing buildings, statistical methods, optimizations, and CAD-BPS interoperability are particularly useful. The last method, however, falls outside this research's scope and is reviewed in detail by Tan et al. [96], focusing on BIM integration into the DM process.

7: BPS, or Building Performance Simulation, is a process that uses computer-based models to simulate the performance of a building under various conditions.

8: CAD, or Computer-Aided Design, software allows the building geometry to be visualized by the decision-maker.

2.3.3.1 Statistical Methods in Building Design

Statistical methods, as Østergård et al. [95] outline, utilize extensive energy simulations alongside statistical techniques for design support. This approach encompasses uncertainty analysis, sensitivity analysis, multivariate analysis, and visualization techniques, forming a comprehensive framework for analyzing building design data.

Building on this foundation, Hollberg [52] introduces a parametric LCA method. By parametrizing inputs like building geometry and materials, this approach facilitates real-time EI calculations, allowing for swift adjustments to enhance environmental performance.

Jusselme [58] further refines this by applying a data-driven methodology to early-stage low-carbon building design. His method overcomes traditional barriers to LCA application through tools such as parametric assessment, enabling the exploration of myriad design alternatives to assess their carbon impact.

(a) Uncertainty Analysis

Uncertainty analysis is used to assess the impact of potential uncertainty in the input parameters, model structure, and data on the outputs of a model or system. In building energy simulations, it's already been established that reality can differ from prediction for multiple different reasons: thermal properties of materials, air-tightness, weather data, occupant behaviour, etc [97].

In the context of building design though, uncertainty analysis brings better insight into the robustness of decisions, as well as a range of possible results [95]. Several studies that apply uncertainty analysis have focused on HVAC sizing. Kim et al. [98], for instance, propose a stochastic approach to evaluate and compare two HVAC system alternatives under uncertainty. In their conclusion, the authors highlight the importance of the occupant's preferences in choosing the correct system. Sun et al. [99] propose a framework based on uncertainty analysis and sensitivity analysis that includes five groups of uncertainty sources: meteorological weather, microclimate, building, system, and occupant. They then find that occupants have the largest impact on heating system sizing, whereas, for cooling systems, building materials' characteristics are the major contributors.

Within building LCAs, uncertainties have also been instrumental for the improvement of the methodology. Pannier et al. [100], for instance, identifies the major sources of uncertainties for different EI indicators with SA methods. Meanwhile, Hoxha et al. [101] focused on studying the impact of uncertainties linked to construction materials (notably their expected service lives, quantities and characterization factors) on non-renewable energy, waste and GWP.

Galimshina et al. [102] also recognizes that selecting a renovation strategy involves many uncertainties due to the long service life of buildings and the variability in design and external parameters

(like climate and energy costs). To address these uncertainties, the paper defines probability distributions for 74 uncertain parameters related to renovation scenarios.

In broader building design, outside HVAC sizing, uncertainties are more often integrated into optimizations, through robustness analysis. Therefore, this topic will be investigated further ahead.

Within the scope of DLCA, which acknowledges temporal changes as a form of uncertainty, there emerges an intriguing application of this mathematical tool, which will be explored in Chapter 3.

(b) Sensitivity Analysis

As seen above, studies investigating both sensitivity and uncertainty analysis often overlap, much like in [103], [102] and [104]. Indeed, SA is a technique used to determine how variations of an input variable affect a particular output variable. Therefore, it is a common application of SA to define the input variance as an uncertainty interval, together with a probability function.

However, SAs still are directly used in building design. For instance, Jusselme [58] calculated the Sobol indices of 14 design parameters, such as window-to-wall ratio, insulation quantity, heating system, floor and wall covering and PV surface. In a case study application, the author ranked these parameters in order of most to least influential, concluding that the choice of horizontal elements had the greatest impact on GWP.

Rezaei et al. [105] use SA to rank the impact of the design parameter on the embodied GWP and on daylight performance. The authors find that wall type has the highest impact on embodied carbon emissions, while window head height has the highest impact on daylight factor. Gauch et al. [106] also applies SA to design parameters to find their impacts on heating and cooling loads, embodied GWP and construction costs. Additionally, they also investigate how different climates, from Singapore to London, impact this SA results.

Then, when applied to DM, SA indicates to the decision-maker, which design choice requires more focus by ranking the parameters that are most sensitive in the output, thereby reducing the complexity of the multi-parameter problem [105]. In addition, SA can also "help to identify trade-offs and synergies between different design objectives and to find optimal or near-optimal solutions" [106].

Therefore, to assess the impact of various parameters GWP, SA is incredibly powerful. For this reason, a couple of techniques have been identified and described hereafter.

Morris Method

The Morris Method [107], a global sensitivity analysis technique, efficiently screens for the most influential parameters in a model. This method, also known as the Elementary Effects Test, involves a systematic alteration of input parameters to observe corresponding output changes. By evaluating the mean and standard deviation of these changes, the method distinguishes between parameters with significant, negligible, or no impact on the output. Furthermore, it identifies factors causing non-linear effects or interactions with other parameters. This method is particularly useful in the preliminary stages of model analysis, as it provides a broad overview of parameter influence without the need for extensive computational resources.

Sobol Method

The Sobol Method [108], another prominent global sensitivity analysis approach, provides a more detailed and quantitative assessment of parameter influences. It decomposes the variance of the model output into fractions attributable to each input parameter, including their higher-order interactions. This variance-based method allows for a comprehensive understanding of how individual parameters and their combinations affect the model's results. By quantifying the total, first-order, and higher-order effects, the Sobol Method delivers an in-depth analysis of parameter interactions, crucial for complex, non-linear models. This approach is especially valuable when precise quantification of parameter impacts is required for model optimization or decision-making processes.

(c) Multivariate Analysis

Multivariate analysis is used to analyze data that involves multiple variables to understand relationships among them. It helps examine how variables interact with each other. Applications include methods like principal component analysis, factor analysis, cluster analysis, multivariate regression, and discriminant analysis.

Olofson et al. [109] applied Principal Component Analysis and Partial Least Squares to Latent Structures to a dataset of 112 multifamily buildings in Sweden, and obtained various results and insights about the impact of different building design parameters on energy performance measures. Meanwhile, Bilous et al. [110] created a multivariate regression model for predicting the internal air temperature of a building, depending on various internal and external factors.

Most commonly in building design though, multivariate analysis methods are used to simplify and quicken energy simulations. Hygh et al. [111], for instance, used multivariate linear regression to build a Surrogate Model (SM) with around 2% average prediction error with 1000 training inputs. Therefore, for methodologies that require thousands of iterations of a complex model's simulation, such as building energy performance and, subsequently, in LCA, SM becomes an important tool. For instance, while optimizing retrofitting solutions, Asadi et al. [112] used Artificial Neural Networks to drastically reduce simulation time.

As mentioned as one of its key disadvantages, DLCA is associated with significant computational costs. However, multivariate analysis hold the potential to mitigate the computational burden of 50-year OE calculations with SM.

(d) Visualization Techniques

Ritter et al. [113] advocate for the integration of human-computer interaction in informed DM. This integration allows decision-makers to adjust to constraints that might not be accounted for in simulations. An exemplary tool for this interaction is the Parallel Coordinates Plot (PCP), a prevalent exploration technique in building design.

Indeed, Jusselme et al. [114] compare different visualization techniques, notably PCP and decision trees. They then conclude on the former's flexibility and effectiveness for data exploration and filtering and the latter's ease of use while being more limited in data representation and interaction.

Additionally, the extra information provided by DLCA necessitates careful management to avoid overwhelming the decision-maker [52]. Thus, developing visualization and exploration tools becomes critical. Indeed, DLCA enhances the decision-making process by incorporating a time dimension, which static LCA did not offer.

(e) Statistical Methods Within this Thesis

The utilization of statistical methods in the realm of building design and renovation stands as a testament to their indispensability in enhancing DM processes. These methods, through their multifaceted applications, provide complementary information for decision-makers. They enable the exploration of diverse design solutions while navigating the complexities and uncertainties inherent in building performance considerations.

Furthermore, by integrating advanced statistical tools with DM methodologies, this thesis aims to not only streamline the integration of DLCA into the DM landscape with SMs, but also to directly bolster the DM process itself.

However, a more efficient way to navigate the solution space is with optimizations, which will be explored in the following Sub-Chapter 2.3.3.2.

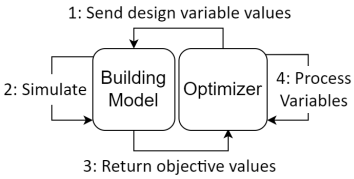

Figure 2.6: Optimization process [115]

2.3.3.2 Optimizations in Building Design

Where the inputs of the statistical methods are determined by a sampling method, independently from the outputs, optimizations use the output of each iteration to inform the next iteration's input and thus approach a predetermined objective: to maximize or minimize a given performance indicator [116]. This process is repeated until a stopping criterion is met [116]. Figure 2.6 depicts the iterative nature of the optimization process and so, in the following sub-chapters, these presented bricks will be explored.

(a) Objective Functions

Objective functions determine the target of the optimization, such as minimizing life cycle cost and EIs [117]. Indeed, optimizations can have a single or multiple objective functions. When dealing with Multi-Objective Optimization (MOO), the different design criteria then, usually have conflicting behaviours, such as minimum energy consumption and maximum indoor comfort hours [116].

A common method to deal with MOO is known as scalarization, where a weighting factor is given to the different objectives and a sum of all targets [118]. However, another way of dealing with multiple objectives is through a Pareto front, where a set of optimal trade-off solutions are identified, as shown in Figure 2.7.

In the context of building renovations, Asadi et al. [119] apply MOO with two criteria: maximize energy savings and minimize retrofit

costs. Asadi et al. [112] then expand the framework by including total hours of discomfort as a criterion.

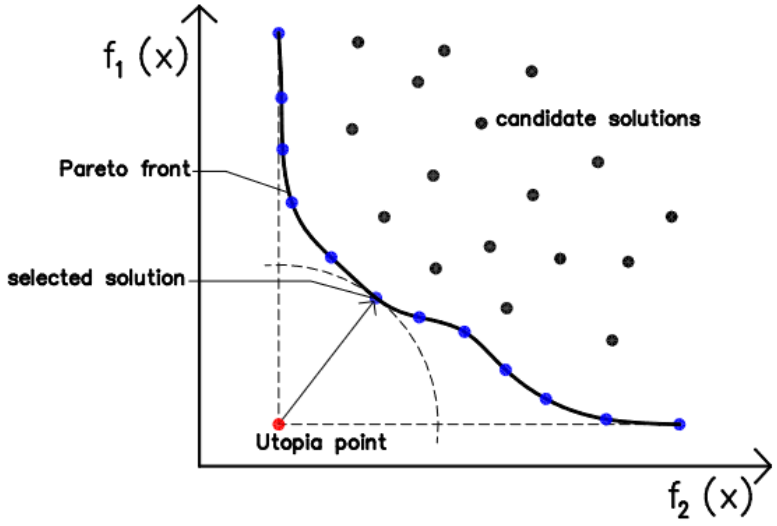

Figure 2.7: Example of a Pareto plot [116]

Shao et al. [115] apply an MOO to an office building to identify retrofitting strategies that aim to minimize operational GWP, initial investment cost, and operational energy. They discovered a Pareto relationship between operational indicators and investment costs. In contrast, a positive and linear relationship was observed between GWP and energy. This implies that in the absence of antagonistic objectives, a unique optimal solution exists. Rosso et al. [120] also considered carbon emissions in their criteria selection process, delineating a Pareto front between GWP and investment costs in a European multi-family residential building.

Shadram et al. [121] explore the relationship between embodied and operational energy through a MOO and find that a conflicting relationship exists between the two: larger embodied investments usually render lower operational burden. This trade-off relationship is true in some design decisions, but for certain parameters, a different relationship appears. Indeed, we showed in our publication [122] that, for certain bio-based insulation materials, greater insulation thickness does not necessarily yield greater embodied GWP, while still reducing OEs. In fact, when considering the stored carbon in these materials, the optimizer will recommend the maximum insulation thickness possible, since it reduces energy needs while serving as carbon sequestration [123].

Thorel [94] proposes an even more holistic methodology towards retrofit DM, by including criteria often left aside for their complexity, such as the time and intrusiveness of an intervention, acoustic quality and fire safety.

Additionally, Abbass Raad et al. [124] introduce a hybrid discrete-continuous multi-criterion optimization approach for building

design. The first key idea is the use of a weak coupling approach between the optimization algorithm and the simulation model, which is defined as a web service, allowing the model to be accessed without being directly provided. The second idea involves a bi-objective CAPEX/OPEX optimization of a building, analyzing the impact of considering the discrete nature of components.

Building upon the insights from previous studies on optimization in building design, this thesis recognizes this tool as a key DM tool. Drawing from the comprehensive review of optimization techniques and their application in various contexts, this work should refine the intersection between retrofitting and carbon budget management. Specifically, it intends to integrate a nuanced understanding of trade-offs, namely those between embodied and operational emission, into the DM process of ensuring CB compliance.

(b) Optimization Algorithms

Optimization algorithms are pivotal in determining how a function will converge through successive iterations. These algorithms can be broadly classified into enumerative, stochastic and deterministic approaches [125].

Enumerative

Enumerative methods are the most primitive, as it involves evaluating the objective function for every point in a discretized solution space [125]. This is of course very limited in the case of an entire building's design, so it is only applied to specific building components' sizing, such as insulation thickness and materials [122].

Deterministic

Deterministic algorithms "are based on the rigorous mathematical expression of objectives, or their gradients" [125]. This means they always provide the same output for a given set of inputs, ensuring reproducibility and predictability.

Several deterministic algorithms are instrumental in various optimization problems:

LP and MILP: Linear Programming (LP) deals with the optimization of a linear objective function, subject to linear equality and inequality constraints. Mixed-Integer Linear Programming (MILP) extends LP by allowing some or all of the

decision variables to take on integer values, adding complexity and expanding its applicability to discrete problems. Hodenq et al. [126] uses Gurobi, a MILP optimization tool, to optimize PV and storage systems' GWP and self-sufficiency rates in energy communities. Ashouri et al. [127] employed a MILP approach for optimizing the sizing of heating systems, thermal energy storage, and ice storage systems.

Gradient Descent: For problems with differentiable objective functions, it iteratively moves towards the minimum of the function by taking steps proportional to the negative gradient of the function at the current point. Indeed, to optimize insulation thickness, Bolatturk [128] uses the life cycle cost function's mathematical expression to calculate its derivative's equality to zero. Due to its limitations, its use in building design is rare, however, it's widely applied in machine learning for minimizing loss functions.

Dynamic Programming (DP): This method breaks down a problem into simpler sub-problems and solves each of these sub-problems just once, storing their solutions. The approach is effective for problems exhibiting the property of overlapping sub-problems, as seen in the optimization of resource allocation and inventory management. Favre and Peuportier [129] use DP to optimize electricity costs and EI with load-shifting strategies of the heating system thanks to the case-study's thermal mass.

Quasi-Newton: This is a powerful method for solving constrained nonlinear optimization problems. It also operates by solving a series of quadratic programming sub-problems, each aiming to approximate the nonlinear problem more closely. Hodenq et al. [130] uses an open-source optimization tool with sequential quadratic programming to find the optimal sizing of PV and battery systems while minimizing GWP and maximizing locally produced energy coverage rate.

Stochastic

Conversely, stochastic algorithms incorporate randomness, leading to different outcomes for the same initial conditions on different executions.

Genetic Algorithm (GA): GA is notably prevalent in performance-driven design, with Nguyen et al. [116] observing its application in 40 out of over 200 studies. GA begins with a population of potential solutions, evolving iteratively to select and recombine the "fittest" solutions for subsequent iterations. This process helps circumvent local minima with a sufficiently large population. Asadi et al. [119], Wright et al. [118], and

Abbasi et al. [131] have utilized GA for optimizing renovation design choices, energy cost and thermal comfort, and life cycle embodied and operational energy, respectively.

Particle Swarm Optimization (PSO): This class of algorithms operate with a swarm of candidate solutions moving according to mathematical rules based on their position and velocity, influenced by their best-known positions and those of the swarm. This mechanism aims to guide the swarm towards optimal solutions. Delgarm et al. [132] applied PSO to minimize energy use in heating, cooling, and lighting through design choices.

Simulated Annealing: Drawing inspiration from the process of annealing in metallurgy, this is a probabilistic technique for approximating the global optimum of a given function. Nielsen [133] uses simulated annealing to optimize the discrete design variables of the building design problem.

Wetter and Wright [134] compared nine algorithms using EnergyPlus building models. In this study, they note the inadequacy of methods requiring function smoothness due to large discontinuities in the models' cost functions. They found that a hybrid PSO and Hooke-Jeeves algorithm yielded the best results, whereas GA required the fewest simulations. Therefore, stochastic algorithms have been predominantly favoured in building simulations for their independence from initial predictions, objective function regularity, and reduced risk of local minima [135].

(c) Optimization Within this Thesis

In the exploration of optimization algorithms, particular attention has been paid to their ability to navigate complex, multidimensional, and non-linear problems, characteristic of this field. Among these, the robustness of GA in handling discrete variables and their capability to avoid local optima through mechanisms of selection, crossover, and mutation are noteworthy. Therefore, after thorough consideration, GA was chosen as the primary method for this thesis.

This decision stems from the method's flexibility and broad search capabilities, positioning it as a potent tool for uncovering innovative solutions that enhance the sustainability and resilience of the built environment. The scope of this thesis does not extend to comparing it with other algorithms; rather, it concentrates on demonstrating the effectiveness of MOO within the specific context of sustainable building retrofits.

(d) Optimization Constraints

Optimization constraints are conditions or limitations that define the boundaries within which an optimization problem must be solved. In the context of buildings, common performance constraints are: physical and cost limits; performance standards; material availability and regulatory compliance.

In this thesis then, CB will clearly be defined as a constraint for the output EE and OE.

2.3.3.3 Robust Optimization

As alluded to before, uncertainty is often attached to optimizations to aid in robustness analysis. By now in this Chapter 2, the reason why deviations from predicted performance are expected should be clear. Nevertheless, these uncertainties are rarely taken into account in design or renovation by decision-makers [136].

For Homaei and Hamdy [137] then, "robustness is defined as the ability of a building to perform effectively and remain within the acceptable margins under the majority of possible changes in internal and/or external environments". They then propose a methodology to produce robust designs under climate and occupant uncertainties on energy consumption and internal discomfort with an innovative key performance indicator.

Robustness analysis can be carried out through probabilistic- and scenario-based approaches. However, for the former, probability density functions are necessary, information that is unavailable in the context of deep uncertainty, meaning the latter approach is preferable [138].

Galimshina et al. [102] uses a robust optimization approach to minimize the sensitivity of renovation strategies to uncertainties. This involves multi-objective optimization using the Genetic Algorithms to find a balance between life cycle costs and GHG emissions. In addition, they perform a probabilistic assessment of the optimal solutions to evaluate their performance under different scenarios, including heating system replacements and renovation scenarios. This probabilistic approach ensures resilience to uncertainties.

Walker et al. [139] investigate the effects of global warming and electricity grid decarbonization in the retrofit decision-making process. To do so, they evaluate the performance of different retrofit strategies for residential buildings in six European contexts under future scenarios through a method that calculates the embodied and operational GHG emissions of retrofit measures under multiple scenarios and then transforms them into a robustness value.

They end up concluding that heating system choice is the most decisive factor for retrofit robustness, followed by the envelope insulation. The paper recommends using heat pump systems in most contexts, except for those with very low grid CI, where EE become dominant.

Effectively then, given that DLCA has been characterized by the assessment of uncertainties over time, integrating DPs into the DM methodology for architectural design constitutes a robust analytical approach. This thesis specifically seeks to incorporate long-term uncertainties into GWP estimations to enhance the likelihood of achieving CB compliance over by the end of the building's life cycle through retrofitting actions.

2.4 Research Gaps

The exploration into current methodologies for ensuring CB compliance in the construction sector reveals discernible research gaps, particularly during the post-occupancy phase.

Although LCA stands as a robust method for evaluating a product's environmental impact and is crucial for ensuring CB adherence, its application alone falls short in guaranteeing compliance over a building's entire life cycle, especially during post-occupancy. This shortfall underscores a knowledge gap that merits attention.

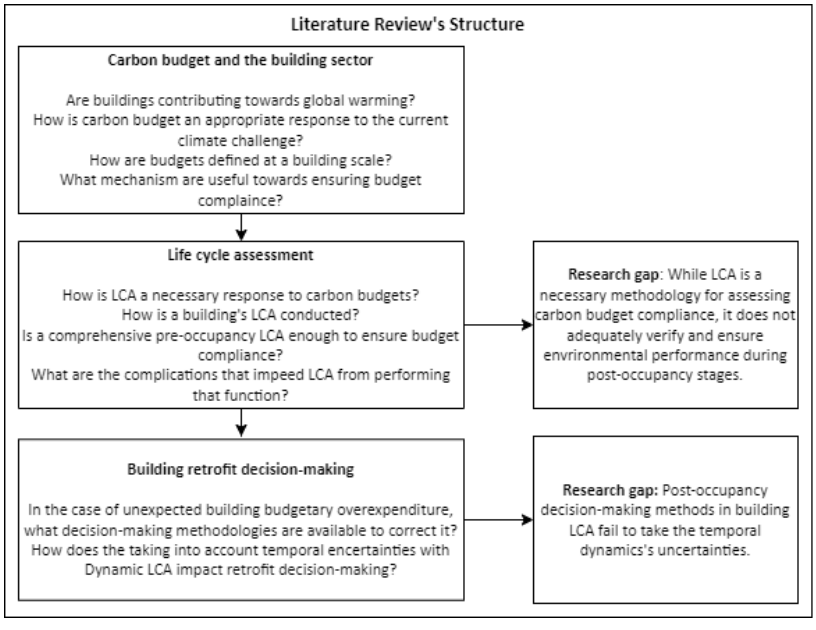

Figure 2.8: Illustration of the research gap identified throughout Chapter 2.

This chapter has outlined two primary research gaps, shown in Figure 2.8. First, while LCA serves as a fundamental approach for sustainable design, it alone does not suffice to confirm CB compliance due to anticipated discrepancies between projections and actual outcomes. With the pressing climate crisis, ensuring

buildings adhere to their CBs, despite uncertainties, is paramount. Moreover, when buildings fail to meet their CBs, there is currently no methodology to support the DM process to mitigate and correct GHG effectively.

To this end, incorporating Dynamic Life Cycle Assessment (DLCA) emerges as a vital enhancement to a CB compliance methodology. It addresses uncertainties associated with the long-term life cycle of buildings and fosters a more nuanced understanding of GHG emissions over time.

Nonetheless, the integration of DLCA into a CB compliance framework presents its challenges, marked by its inherent complexity. Thus, identifying and mitigating factors that could hinder its widespread adoption becomes crucial.

Moreover, the identification of deviations from budgetary constraints necessitates corrective measures. Current post-occupancy DM methods, especially those focusing on renovations, often overlook these temporal uncertainties. Incorporating these uncertainties can enhance the robustness of the DM process, thus ensuring a building's compliance with its CB, despite unforeseeable futures.

Numerous methods, such as sensitivity and uncertainty analysis, optimizations, and meta-models, have been identified as potent tools in the DM process for performance-driven design. However, the integration of these tools into DLCA and their influence on DM during retrofitting remain unclear.

2.5 Conclusion

This chapter has examined building GHG threshold compliance, DLCA, and post-occupancy DM processes in sustainable building design and operation.

The analysis highlighted the significance of CBs in promoting sustainable practices within the building sector and the challenges involved in their effective allocation and interpretation. It was established that LCA is a critical tool for assessing the EIs of buildings, though its static nature and limitations necessitate the incorporation of DLCA to address temporal uncertainties in environmental impact assessment.

In the post-occupancy phase, the importance of continuous monitoring and adaptive DM was underscored as vital for ensuring ongoing compliance with GHG budgets. Despite the availability of various techniques, such as statistical methods and optimization strategies, the review identified significant gaps, particularly the

lack of methodologies that fully integrate temporal dynamics into the decision-making process.

The key conclusion drawn is that while existing methodologies provide a strong foundation for sustainable building practices, they fall short in addressing the complexities of post-occupancy performance and the dynamic nature of environmental impacts. Specifically, LCA alone is inadequate for ensuring CB compliance, and current post-occupancy DM approaches are insufficiently equipped to handle temporal variability.

Moving forward, the development of more integrated and dynamic methodologies that incorporate DLCA and robust decision-making frameworks is crucial. Such advancements will better address the temporal uncertainties and enhance the effectiveness of strategies aimed at achieving GHG budget compliance.

The subsequent chapters, Chapter 3 and Chapter 4, will delve deeper into these identified gaps and propose solutions to bridge them. Furthermore, the outlook section of Chapter 5 will outline areas for future research not fully covered in this study.

Exploring Dynamic Life Cycle Assessment Simplification Strategies

3

Chapter 3 explores the introduction of Dynamic Life Cycle Assessment (DLCA) as a more nuanced approach to Environmental Impact (EI) assessment and, more specifically, for Carbon Budget (CB) verification. However, in the preceding chapter, potential difficulties have been highlighted, such as computational intensity and the complexity of Dynamic Parameters (DP) modelling.

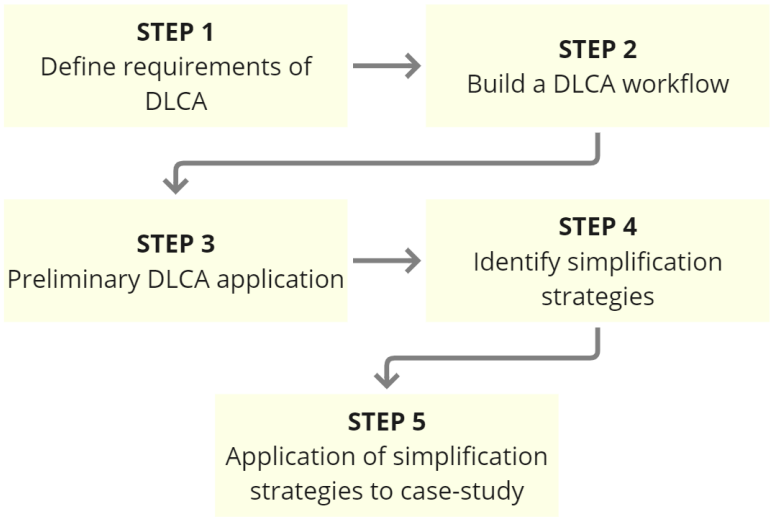

Figure 3.1: Methodology for the identification of DLCA simplification strategies.

To structure this exploration, this chapter is organized into five steps, as described in the methodological framework shown in Figure 3.1.

First, it is paramount to establish and gather the foundational requirements of DLCA together with a workflow proposal for dynamic calculations. Thereafter, a feasibility test rooted in a case study will be conducted to gauge the intricacies involved in implementing it, detailing the difficulties of DLCA.

Given the complexities identified in the literature review, the next step is to identify strategies that would simplify and thus facilitate the inclusion of DPs in GWP calculations. Finally, by applying these strategies to the case study, a simplified DLCA will be proposed towards CB verification.

3.1 Building the DLCA workflow

3.1.1 Workflow Inputs

This section will define the different pre-requisites of a DLCA workflow and will highlight the intricacies that come with bringing dynamics to environmental calculations over static LCAs.

3.1.1.1 Dynamic Parameters

The modelling of DPs emerge as a notably intricate aspect of DLCA, predominantly due to data scarcity and the absence of a unified database [62, 63]. To address this, a comprehensive literature review is essential, encompassing both scholarly articles and documents from governmental agencies. This is a step not required of current building LCA practitioners.

In accordance with this observation, the present Sub-Chapter 3.1.1.1 will offer an overview of the DPs incorporated into this DLCA workflow based on other works. Initially, these parameters are categorized based on their levels: external, building, and occupant. This taxonomical work draws inspiration from the schema proposed by Negishi et al. [71], as delineated in Figure 3.2.

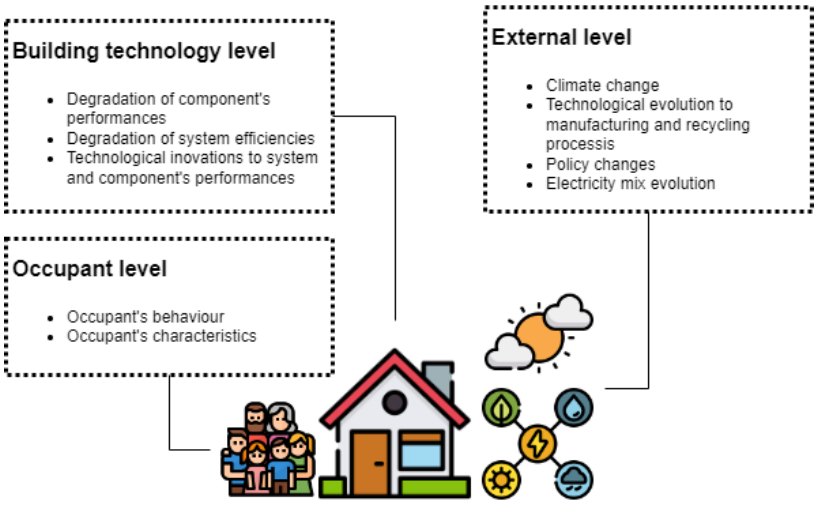

Figure 3.2: Categorization of Dynamic Parameters (DP) by perimeter, adapted from [71]

3.1.1.2 Energy Model and Weather Data

Energy modelling and simulation is a crucial component of LCAs, more specifically, in Operational Emissions (OE) calculation. In DLCA, energy modelling enhances precision by modelling building-level and occupant-level changes, as exemplified in the preceding Sub-Chapter 3.1.1.1. However, to the best the author's knowledge, no study on DLCA has created a workflow that allows

energy simulations to be executed at a yearly time step. For instance, [56] realises 2 energy simulations over the building life span, while [140] realises them at 10-year time-steps.

Another pre-requisite closely associated with the energy model is the weather data. This requirement is no different from a static approach. However, the intricacy of DLCA lies in the necessity for future weather forecasts, driven by the imperative to model climate change and its inevitable impact on the built environment.

3.1.1.3 Building Components

The final requirement for the DLCA methodology involves the Bill of Quantities (BOQ) of building components used in construction, which are linked to their respective Environmental Product Declaration (EPD)s, similar to a static LCA approach. However, the DLCA diverges from the static method in calculating recurrent Embodied Emission (EE)s, despite the majority of EEs being emitted during construction.

A further requirement for the BOQ is detailed information on emission modules as defined by the component's EPDs. Since A1-A3 emissions occur at a different time than C1-C4 emissions, they are accounted for differently in the overall GWP, unlike in static LCA methodologies.

Having identified the inputs of DLCA, the following sections will be dedicated to building the workflow, starting by defining its perimeter.

3.1.2 Workflow Perimeter

This research emphasizes compliance with the GHG budget, defined in terms of equivalent emissions of carbon dioxide ($CO_2 - eq$). Consequently, the only EI incorporated in the methodological workflow is the GWP, also measured in CO_2 equivalent emissions.

Furthermore, certain modules within the EN 15804 framework were excluded from the calculations. Specifically, only the modules marked in red in Figure 3.3 were not included in the scope of this workflow: B1 - Use, B3 - Repair and B7 - Operational Water Use. This selection was primarily influenced by the completeness of French Environmental Product Declaration (EPD)s available on the INIES database [48].

Additionally, the DLCA developed in this chapter does not encompass a dynamic Life Cycle Impact Assessment (LCIA), meaning the characterization factors of various GHGs are not considered.

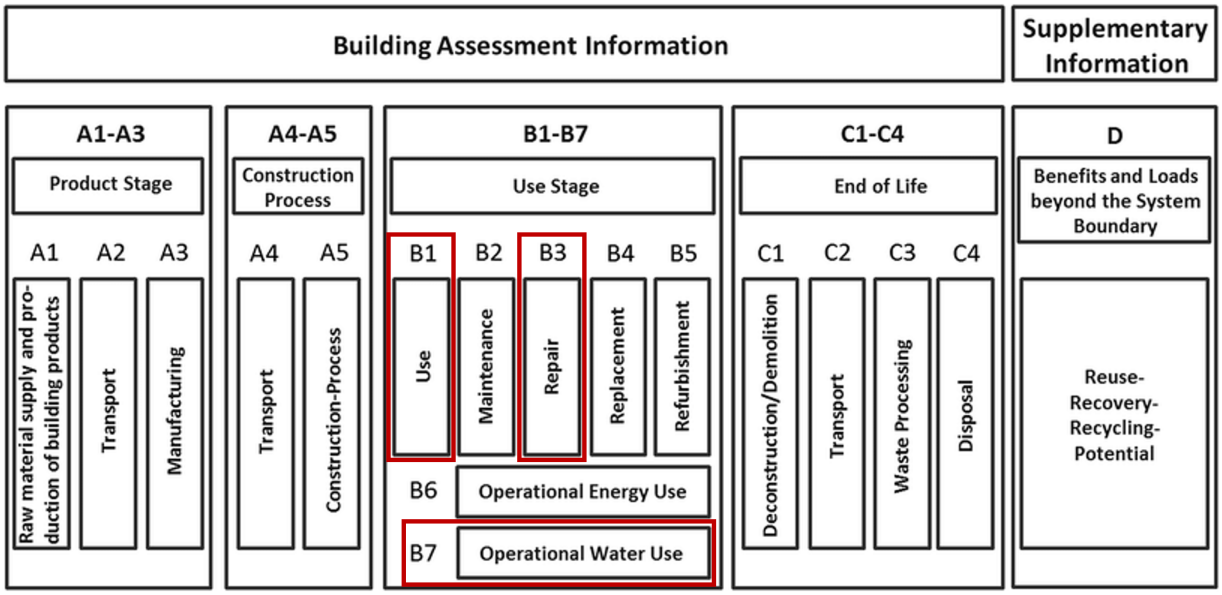

Figure 3.3: LCA modules defined by the EN 15804 [15] not included in this workflow marked in red.

To include this step, with GWP calculations based on radiative forcing, for instance, would require converting CBs accordingly.

Dynamic LCIA also demands information on each type of GHG (e.g., CO_2, CH_4, NO_2, refrigerants). However, such details are not mandated in EPDs as per EN15978 and the French EPD database follows suit. In building LCA then, where Life Cycle Inventory (LCI) and Life Cycle Impact Assessment (LCIA) merge into one phase, other DLCA studies in literature do not utilize EPDs. To render both phases dynamic, as proposed by [81], they must be conducted separately.

3.1.3 Workflow Description

Having defined its inputs and perimeter, Figure 3.4 demonstrates the proposed workflow for dynamic GWP calculation. This approach combines all the aforementioned pre-requisites, establishing the DLCA workflow of this thesis. The process starts with the DP, positioned on the left side of the diagram. It is crucial to note that the DPs are integrated into the calculations at different stages.

The "Calculations" section begins by modifying the energy model and weather data. Here, 50 yearly simulations[1] are executed, covering the complete life cycle of the building. After this 50-year energy simulation, the building's hourly energy consumption is utilized in the post-processing stage of the OE assessment. In this phase, system efficiency is evaluated, and energy is converted into carbon emissions.

1: In the French regulation RE2020, buildings have a reference life cycle of 50 years, hence, the same number of yearly simulations are realized.

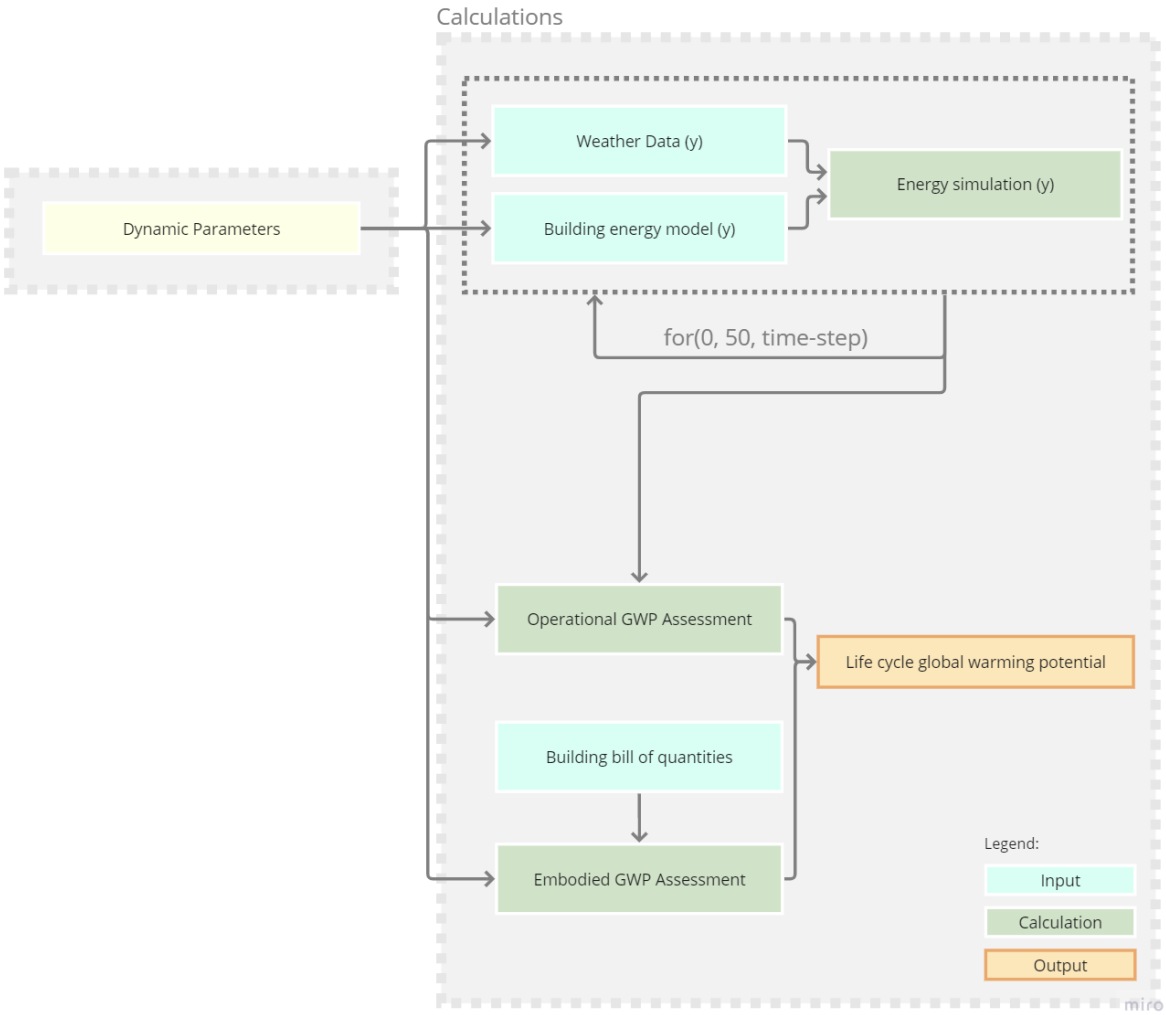

Figure 3.4: DLCA parametric workflow, depicting how various DPs models influence the dynamic GWP calculation at distinct stages.

Simultaneously, the Embodied Emission (EE)s calculations involve the Life Cycle Inventory (LCI) of the building, which includes associating component quantities with EPDs and incorporating DPs. The final step is the aggregation of the 50-year vectors for EE and OE, culminating in the overall dynamic GWP result.

3.2 Preparing Case-Study Application and Testing Feasibility

With the framework established, the objective of this sub-chapter is to evaluate the feasibility of the DLCA workflow and to identify the main hurdles associated. Through a feasibility study then, we will better understand the problems that create impedance in the way of making DLCA a core part of the DM process in building design.

This application will also serve as a baseline for the simplification strategies that will be investigated hereafter. Indeed, this first case-study application will be used as a reference in terms of both simulation time and GWP accuracy.

3.2.1 Case-study Presentation

Figure 3.5: 3D rendering of a similar house as described in this subchapter. Picture from [141].

The case study illustrated in Figure 3.5 is a single-family French home in the Parisian region, as they represent 55% of dwellings in the country [142]. Thanks to previous research works at the same institution, the necessary information about the building, including an energy model and a Bill of Quantities (BOQ), was readily available.

In this particular building, constructed in 2017, this BOQ of the components was associated with EPDs found in the INIES database [143]. The resulting LCI can be found in Appendix B. The LCA tool used for this building is Vizcab[2], as it allows the user to export the building's components list and LCA results to be acquired through an Excel file. This drastically facilitated the automation of the workflow.

2: Vizcab is a French building LCA SaaS (Software as a Service) tool capable of executing static and dynamic assessments according to the RE2020 regulation. This software uses the French INIES database for EPDs. For more information: vizcab.io/.

Table 3.1 then, summarizes the main characteristics of the building, including RE2020 DLCA results in terms of GWP. An EE of 569 $kgCO_2 - eq/m^2$ and an OE of 261 $kgCO_2 - eq/m^2$ were obtained, meaning this relatively recent building has an overall GWP of 701 $kgCO_2 - eq/m^2$, 69% of which embodied.

For energy simulations, a detailed profile of the wall compositions modelled is illustrated in Figure A.1, Figure A.2 and Figure A.3 in Appendix A. In summary, this building has around 10 cm of PU insulation in vertical opaque surfaces and in its flooring. A thicker

layer of 14 cm of PU is installed on the roof. As for glazed surfaces, double-glazed and PVC-framed windows are found.

Table 3.1: The main characteristics of the case-study.

Characteristics	Value
Year of construction	2017
Horizontal structure	Cast concrete
Façade structure	Cinder block
Insulation material	Polyurethane (PU)
Insulation Conductivity	0.03 W/(m.K)
Opaque surface conductance	0.23 W/(m².K)
Thermal Bridging	0.1 W/(m.K)
Glazing type	Double-glazing
Glazing frame	PVC + Aluminium
Glazed surface conductance	1.2 W/(m².K)
Ventilation system	Simple-flow
Infiltration (n50)	0.6 ac/h
Heating system	Electrical radiators
Domestic Hot Water Production	Thermodynamic Tank
Indoor surface area	160 m²
Building life cycle	50 years
Embodied Emission	569 $kgCO_2 - eq/m^2$
Operational Emissions	261 $kgCO_2 - eq/m^2$

This is a relatively low thermal performance, especially considering the inefficient heating system that is found in the building: Joules-effect electrical radiators. For Domestic Hot Water (DHW) production, however, a much more efficient heat-pump, or thermodynamic tank, is used.

Table 3.2: Embodied emission per lot, as defined by the French RE2020 regulation.

RE2020 Lot	Static Emission $[kgCO_2/m^2]$	Share of All Lots [%]
Lot 1: Roads and Miscellaneous Networks	13.49	2.01%
Lot 2: Foundations and Infrastructure	23.22	3.47%
Lot 3: Superstructure - Masonry	176.42	26.33%
Lot 4: Roofing - Waterproofing - Framing - Zinc Work	18.26	2.73%
Lot 5: Partitioning - Lining - Suspended Ceilings - Interior Carpentry	31.03	4.63%
Lot 6: Facades and Exterior Carpentry	96.56	14.41%
Lot 7: Coverings - Screed - Paints - Decorative Products	92.27	13.77%
Lot 8: HVAC	21.08	3.15%
Lot 9: Sanitary Installations	108.10	16.13%
Lot 10: Energy Networks - High Current	87.83	13.11%
Lot 11: Energy Networks - Low Current	1.74	0.26%
Total	700.82	

To categorize the EE of the case study, the RE2020 divides it

into "lots". These lots include various elements from construction materials that have been included in Table 3.2.

3.2.2 Defining Case Study's RE2020 Carbon Budget Threshold

Ensuring adherence to a carbon threshold is a primary focus of this research. However, the task of establishing a science-based carbon budget for buildings and the broader building industry is a highly complex endeavour, one that extends beyond the scope of this thesis.

Consequently, this research adopts the carbon threshold as defined at the building scale by the French RE2020. This regulation provides a methodology for calculating CBs, considering factors such as geographical location, terrain, indoor surface areas, parking facilities, etc. [74]. For this case-study, the budgets have been calculated in accordance with these parameters and are presented in Table 3.3. However, it is important to note that the RE2020 is only applicable to new construction and its application to this residence built in 2017 is theoretical.

Table 3.3: RE2020 carbon budgets for the case-study.

Carbon Budget	**Value** $(kgCO_2 - eq/m^2)$
Current Embodied Budget	610
2025 Embodied Budget	550
2028 Embodied Budget	453
2031 Embodied Budget	396
Operational Budget	150

The RE2020 regulation defines four embodied CBs, as it intends to reduce the French building sector's GHG emissions over the next decades. The current budget applies to buildings constructed before 2024. Then, three additional budgets are set for buildings constructed during the following periods: 2025-2027, 2028-2030, and from 2031 onwards. In contrast, a single operational budget is defined, which will remain in effect until the introduction of the next regulation.

A discrepancy between the embodied CBs and the GWP values in Table 3.1 has been manifested, indicating that while the current embodied budget is compliant, the operational budget does not align with the expected values. This discrepancy will be thoroughly explored and questioned in Chapter 4.

3.2.3 Dynamic Parameter Modeling for Case Study

Having established the case-study, various DPs will be modelled hereafter. This Sub-Chapter is divided into the perimeters identified in Figure 3.2.

3.2.3.1 External-level

External-level DPs are those that fall outside the direct influence and control of the building and its occupants. These parameters encompass a range of external variables, including shifts in regulatory and policy frameworks, the evolving dynamics of climate change, and changes in the composition of the electrical grid. The following discussion will offer a detailed examination of five key parameters.

(a) Global Warming

The inexorable advance of global warming over the forthcoming decades is a settled scientific fact; what remains uncertain, however, is the magnitude of its impact on global temperatures and the efficacy of existing and prospective policies to mitigate Greeenhouse Gas (GHG) emissions. The Intergovernmental Panel for Climate Change (IPCC)'s Fifth Assessment Report employed Representative Concentration Pathways (RCPs) to outline distinct scenarios that capture the prospective impact of anthropogenic activities on global warming by the end of the century [144], as depicted in Figure 3.6.

These RCP scenarios are correlated with projected temperature elevations [1]:

- RCP 2.5: Envisions a 67% probability of constraining global warming to 2°C.
- RCP 4.5: Constitutes an intermediate scenario with a 50% probability of capping global warming at 3°C.
- RCP 8.5: Represents a pessimistic outlook, positing a 50% likelihood of global temperatures exceeding the 4°C threshold.

In order to contextualize global climate changes for a specific area, namely the Parisian territory in this case, future weather data was procured using Meteonorm software[3]. This data is derived from the CMIP5 (Coupled Model Intercomparison Project)[4]. The CMIP5 incorporates a diverse array of models, including atmosphere-ocean and Earth system models, to simulate various climate system variables for each RCP scenario. These simulations are conducted

3: Meteonorm is a comprehensive global weather database that offers both historical and current climate data. It enables the extraction of time-series weather files for any location and simulates future weather based on the IPCC's RCP scenarios. For more details: meteonorm.meteotest.ch/.

4: CMIP5 data can be accessed at climateknowledgeportal.worldbank.org/cmip5.

for different time horizons and locations globally, with a resolution of approximately 100 km by 100 km [145].

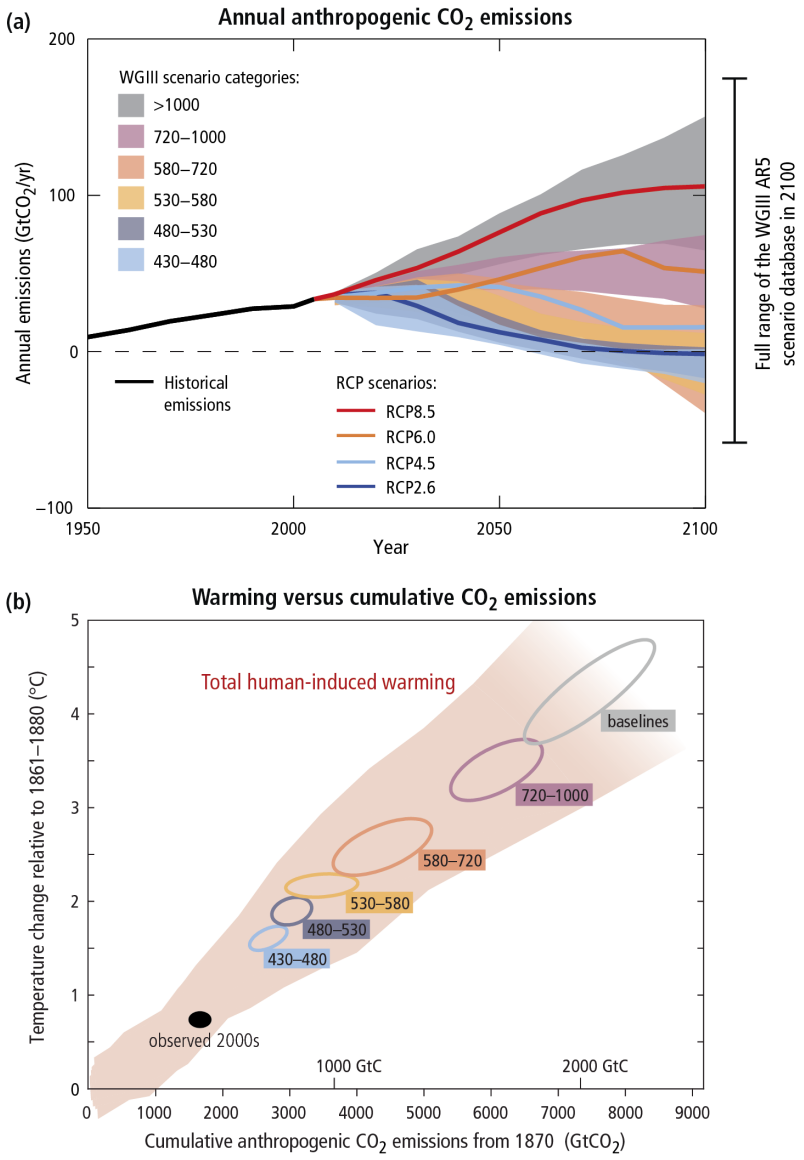

Figure 3.6: (a) The different Representative Concentration Pathways (RCPs) scenarios in terms of annual $GtCO_2$ emissions. The values of the RCP scenarios relate to the expected radiative forcing in 2100 in W/m^2. (b) The second graph illustrates the correlation between the increasing surface temperature and the concentration of CO_2 in the atmosphere. These plots were obtained from the 5th IPCC Assessment Report [144]

Meteonorm effectively generates weather files at ten-year intervals from 2020 to 2100, covering each of the RCP scenarios mentioned. Other studies on climate change implications for long-term building energy simulations have employed a technique known as 'morphing.' This method involves altering a reference weather file, with changes observed on a monthly scale as noted in [146] and on a daily scale in [140].

To gain a deeper understanding of the projected weather changes over the coming decades under these scenarios, Table 3.4 was created using the obtained data. This table provides a comparative analysis of temperature and humidity across different RCP scenarios, with a typical meteorological year (TMY) serving as the baseline for current climatic conditions. The data indicates a signif-

icant increase in temperature, with average dry-bulb temperatures expected to rise by 0.44°C to 2.5°C.

Table 3.4: Comparison of weather parameters for different RCP scenarios. The table shows the averages of the meteorological years and compares the difference with the reference weather data: a TMY (typical meteorological year).

	TMY	2070-RCP2.6		2070-RCP4.5		2070-RCP8.5	
	Avg	Avg	Diff	Avg	Diff	Avg	Diff
Dry-Bulb Temp (°C)	13.89	14.33	+0.44	15.14	+1.25	16.39	+2.50
Wet-Bulb Temp (°C)	7.33	8.19	+0.86	8.98	+1.65	10.14	+2.81
Relative Humidity (%)	67.98	68.26	+0.28	68.26	+0.28	68.11	+0.13

Additionally, to investigate how climate change might impact energy needs, the heating degree-days (HDD) and cooling degree-days (CDD) were calculated for 2070 under the same 3 RCP scenarios in Figure 3.7. HDD will decrease in every scenario by 2070, while CDD increases slightly. This suggests that climate change is expected to reduce energy needs in the Parisian region, even for those equipped with air-conditioning units.

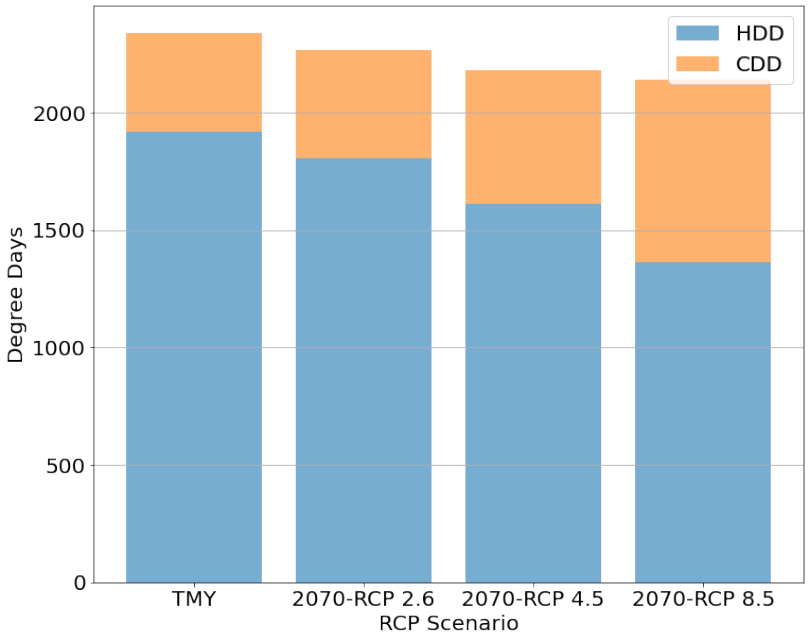

Figure 3.7: A comparison between today's TMY and 2070's data under different climate change scenarios of cooling degree-days (CDD) and heating degree-days (HDD), with a base temperature of 18°C.

$$T(y,m) = T(y_{TMY},m) + \frac{T(y_{TMY},m+10) - T(y_{ref},m)}{10} \times (y - y_{TMY}) \tag{3.1}$$

The strategy implemented here is similar to what has been implemented in [140], where the average monthly temperatures seen in Figure 3.8 are used to gradually modify the TMY weather data. In this plot, it is evident that global warming affects temperature the most during the summer seasons. Since weather data is available every ten years, this monthly interpolation is done between the available years. This process is merely executed for dry-bulb and

wet-bulb temperatures, as is shown in (3.1), where $T(y, m)$ represents the hourly temperature vector for the year y and month m, with y_{TMY} serving as the baseline temperature vector.

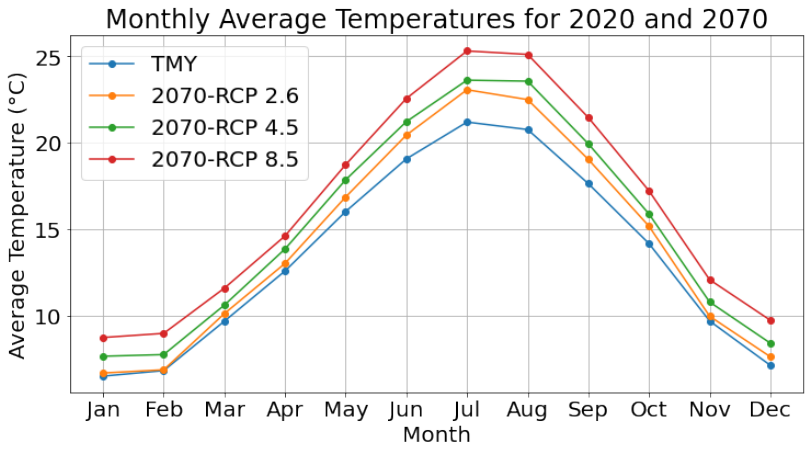

Figure 3.8: Monthly average temperature variation for TMY and 2070, under the different scenarios

(b) Electricity Electricity Mix

Hourly Variations

The Carbon Intensity (CI) of electricity fluctuates as a function of the instantaneous energy mix supplying the grid, adjusting dynamically in response to variations in demand. Within the ambit of the Continental Europe Synchronous Area[5], which includes France, the power grid integrates multiple energy sources. Typically, static LCA workflows rely on annual average values that can lead to over- and under-estimations of up to 10% for operational GHG calculations [147]. The CI for such a complex grid reflects on short-term variations. To model these variations, historical data on electricity CI and fuel-based power generation, provided by the French transmission system operator, RTE (Réseau de Transport d'Electricité)[6] were employed.

It is important to note that the CI values calculated by RTE solely take into account direct emissions. Consequently, sources like solar (PV), nuclear, and wind are treated as zero-emission power sources. However, this interpretation is inconsistent with an LCA approach. Therefore, the CI for each energy source was recalculated to include life cycle emissions, as detailed in Table 3.5. This adjusted data is grounded on research by Scarlat et al. [148] and an IPCC report's Annex [149]. The "Eco2mix" column in Table 3.5 represents the CI values provided by RTE [150], which accounts emissions through a different methodology, most noticeably, assuming zero OE for renewable and nuclear energies.

Upon completing this data manipulation, a striking revelation emerged concerning the electricity's CI in France from 2012 until

5: Comprised of 24 countries, most European countries and some parts of Africa and Asia are interconnected by the largest synchronous electrical grid, known as the Continental Europe Synchronous Area.

6: This data, available from 2012 to 2020 and aggregated in 30-minute intervals, as of writing this manuscript in Excel format on RTE's website: rte-france.com/eco2mix/.

2020. When life cycle emissions were factored in, the average CI was more than double compared to calculations solely based on direct emissions. This discrepancy is vividly illustrated in Figure 3.9. The figure further underscores the high volatility of carbon intensity, ranging from sub-40gCO_2/kWh to exceeding 140gCO_2/kWh. The dynamic nature of electricity's CI exerts a noticeable influence on a building's Operational Emissions. Consequently, the study will account for this variable characteristic in its forthcoming analyses.

Electricity source	Carbon Intensity ($gCO_2 - eq/kWh$)	
	Eco2mix [150]	[148, 149]
Coal	986	990
Oil	777	790
Natural Gas	429	480
Biomass	494	65
Solar PV	0	41
Nuclear	0	24
Hydroelectric	0	19
Offshore wind	0	16.5
Wind	0	11
Germany and Belgium	-	410
Italy	-	371
England	-	282
Spain	-	262
Switzerland	-	78

Table 3.5: Life cycle emission intensity of electricity sources, including from exchanges with bordering nations of France [148, 149]

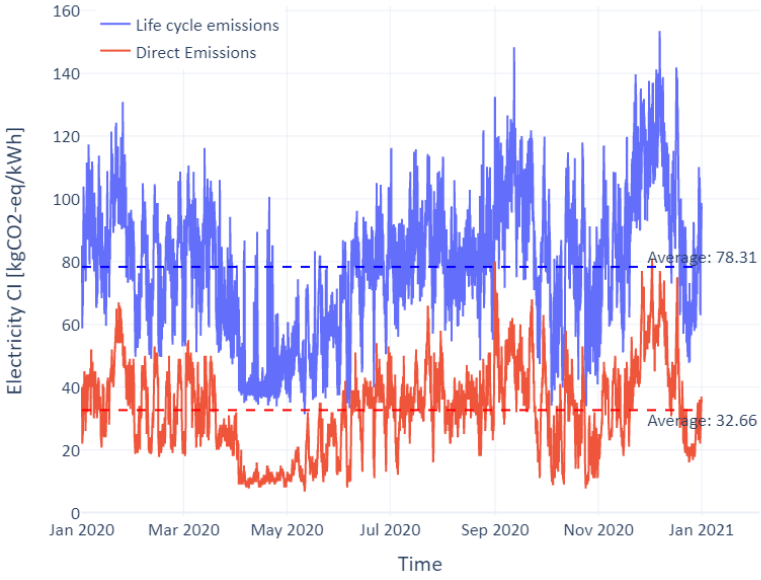

Figure 3.9: Electricity carbon intensity in France over the year 2020. This plot compares the different methodologies, the life cycle approach and the direct emissions approach.

Moreover, a closer examination during April and May 2020 revealed peaks in the blue line that do not exist in the red curve. This indicates complexities beyond a direct emission multiplication. Such discrepancies arise because certain technologies, such

as nuclear, wind, and solar power, have no direct emissions contribution. Therefore, during mid-season—when the combined cooling and heating degree-days are at their lowest—the electricity demand is met predominantly by these low-direct-emission sources. Nevertheless, these sources are associated with substantial EEs. Consequently, applying the life cycle method introduces significantly greater variability to the CI.

Production Mix Evolution

Nevertheless, the CI is not a static year-over-year either; it is anticipated to undergo significant transformation in the coming decades, principally due to escalated investments in renewable energy sources that typically boast lower CI, as substantiated in Table 3.5. To forecast the future electricity grid landscape, various organizations have developed forecasting scenarios. For instance, the International Energy Agency (IEA) has outlined a global 2050 roadmap that substantially leans on wind and solar energy, planning to entirely phase out coal and natural gas [151].

However, for this study, another alignment is found with the roadmap also provided by RTE. This roadmap delineates six distinct scenarios, each with its own set of assumptions and implications for France's energy landscape [152]. Three of these scenarios posit that France's existing nuclear power plants will not be replaced upon reaching the end of their operational lifetimes, while the remaining three scenarios project the contrary—namely, that these nuclear facilities will be displaced by new installations in the ensuing decades. These divergent futures are quantitatively expressed in terms of the sectorial energy production percentages for the year 2050, as detailed in Table 3.6. Further elucidation is provided through calculated metrics, as articulated in Equations 3.2 and 3.3.

The naming conventions in Table 3.6 are explicitly delineated by RTE in 2021 [152], with the energy mix scenario carrying its unique implications listed below.

M0 No nuclear power is anticipated by 2050. Existing nuclear plants that could potentially function in the next three decades are projected to commence decommissioning by 2030.

M1 Only extant nuclear facilities will remain operational through 2050, with the majority of energy needs met by distributed solar PV systems.

M23 This scenario aligns closely with M1, but with a heightened emphasis on investment in both onshore and offshore wind power.

N1 Construction of new nuclear plants would be limited, with a new installation every five years commencing in 2035. Renewable energy sources would still account for the majority of the energy supply.

N2 Analogous to N1, but a new plant would be established every three years starting from 2035. Two-thirds of the energy production would still originate from renewable sources.

N03 This scenario envisions the most extensive investment in nuclear power, which would contribute to half of the energy production, while the remaining half would be sourced from renewables.

To predict the CI in 2050 for each of these scenarios, the proportionality assumption is employed: each energy source would contribute proportionally to its production to the CI. For assessing the changes in CI from the present day to 2050, a linear trajectory of improvement is assumed. This progression is graphically represented in Figure 3.10 via a CI multiplier. After 2050, this reduction factor is presupposed to remain constant until the conclusion of the building's life cycle, given the 2050 endpoint of the roadmap.

Equation 3.2 details how the production shares specified in the roadmap will be leveraged to approximate the CI for each 2050 scenario. Equation 3.3 calculates the anticipated improvement in CI for each scenario in comparison to today's grid, which, as seen in Figure 3.9, has an average of 78 $gCO_2 - eq/kWh$.

$$CI_{estimated} = \sum_{sources} CI_{source} \times Share\_of\_Prod_{source} \tag{3.2}$$

$$CI_{improvement} = \frac{CI_{estimated}(2050)}{CI_{estimated}(2020)} \tag{3.3}$$

The scenarios proposed by RTE have varying implications for the evolution of the CI of electricity in France. By taking into account the energy mix projected for 2050 under each scenario, we can better understand how the electricity CI will shift over time, which is of paramount importance for LCAs in the building sector.

To estimate the CI in 2050, an approach that factors in the proportionate contributions of each energy source to the total energy production is utilized. Equation 3.2 formalizes this by summing up the products of the CI for each source and its share of total production.

Additionally, to evaluate the rate of improvement in the CI, Equation 3.3 is employed. This equation represents the ratio of the estimated CI in 2050 to the current value, which is approximately 78 $gCO_2 - eq/kWh$, as evidenced in Figure 3.9.

Table 3.6: Roadmap of electricity production mix in terms of percentage energy production over a year. Based on [152]. The CI is the same as shown in Table 3.5 in addition to tidal turbine, obtained from [153] and offshore wind, obtained from [154].

Source	Carbon Intensity ($gCO_2 - eq/kWh$)	Current Mix (2020)	M0	M1	M23	N1	N2	N03
PV	41	2.5%	36%	35%	23%	20%	16%	13%
Hydro	19	13.6%	9%	9%	9%	9%	10%	10%
Offshore Wind	16.5	1.98%	31%	23%	31%	24%	19%	12%
Wind	11	8.06%	21%	17 %	21%	17%	15%	13%
Nuclear	12	68.08%	0%	13%	13%	27%	38%	50%
Tidal Turbine	33.8	0%	1%	1%	1%	1%	0%	0%
Biomass	65	1.97%	2%	2%	2%	2%	2%	2%
Oil	790	0.19%	0%	0%	0%	0%	0%	0%
Coal	990	0.28%	0%	0%	0%	0%	0%	0%
Gas	480	7%	0%	0%	0%	0%	0%	0%
Estimated CI ($gCO_2 - eq/kWh$)		78.3	25.5	24.9	21.8	20.6	19.1	17.9
Improvement to CI in 2050 in relation to 2020 (%)			33%	32%	28%	26%	24%	23%
Yearly reduction in average CI (%/year)			**2.32**%	2.35%	2.49%	2.54%	2.61%	**2.66**%

The proposed method assumes a linear trend in CI improvements from the present day to 2050, depicted as a reduction factor in Figure 3.10. After the year 2050, this factor is assumed to remain constant, serving as a reasonable estimate for any lifecycle assessments extending beyond that year. This framework provides a structured approach to factor in future electricity CI changes, thereby enhancing the robustness of this study.

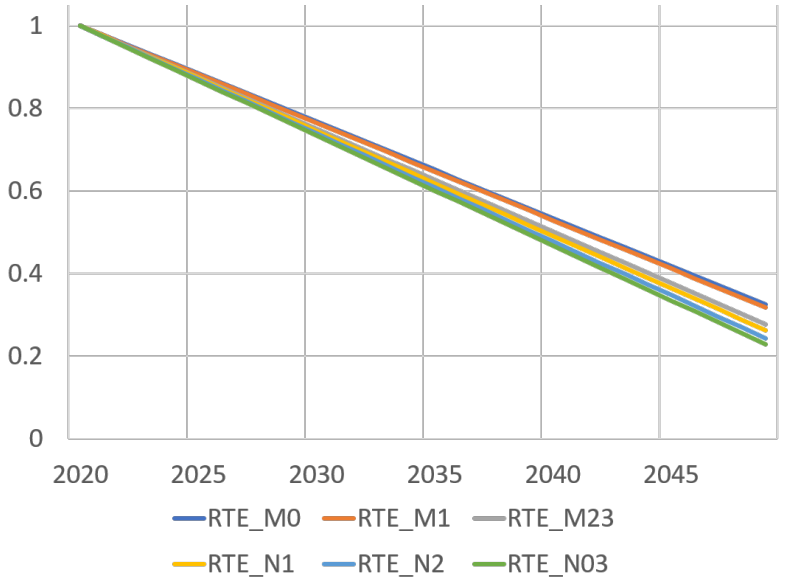

Figure 3.10: Improvement factor of electricity CI between 2020 and 2050.

To incorporate the improvement factor into building LCA, it is applied as a multiplier to the hourly CI vectors, exemplified by the red line in Figure 3.9. Given that this vector only represents the year 2020, an average over the past 5 years of data should provide a more accurate representation of the current grid.

The procedure for this calculation is outlined in Equation 3.4. Here, CI refers to the hourly CI vector spanning one year, and CI_{ref} is the average reference vector over the past 5 years and y_{ref} is the reference year, which in this case, is defined as 2020. This approach ensures that the OE calculations are not solely based on a snapshot of a single year but take into account a more extended period, therefore providing a more reliable estimate.

$$CI(y) = CI_{ref} \times (1 - \frac{1 - CI_{improvement}}{2050 - y_{ref}}) \times (y - y_{ref}) \tag{3.4}$$

(c) Industrial Sector Evolution

The transformational shift towards sustainability is not confined solely to the energy sector. Multiple sectors, including industry—which encompasses raw material extraction and the manufacturing of building components—are undergoing significant metamorphoses. In France, such prospective advancements have been formally articulated through the National Low-Carbon Strategy, denoted as SNBC. This framework delineates sector-specific national emission budgets for the coming decades.

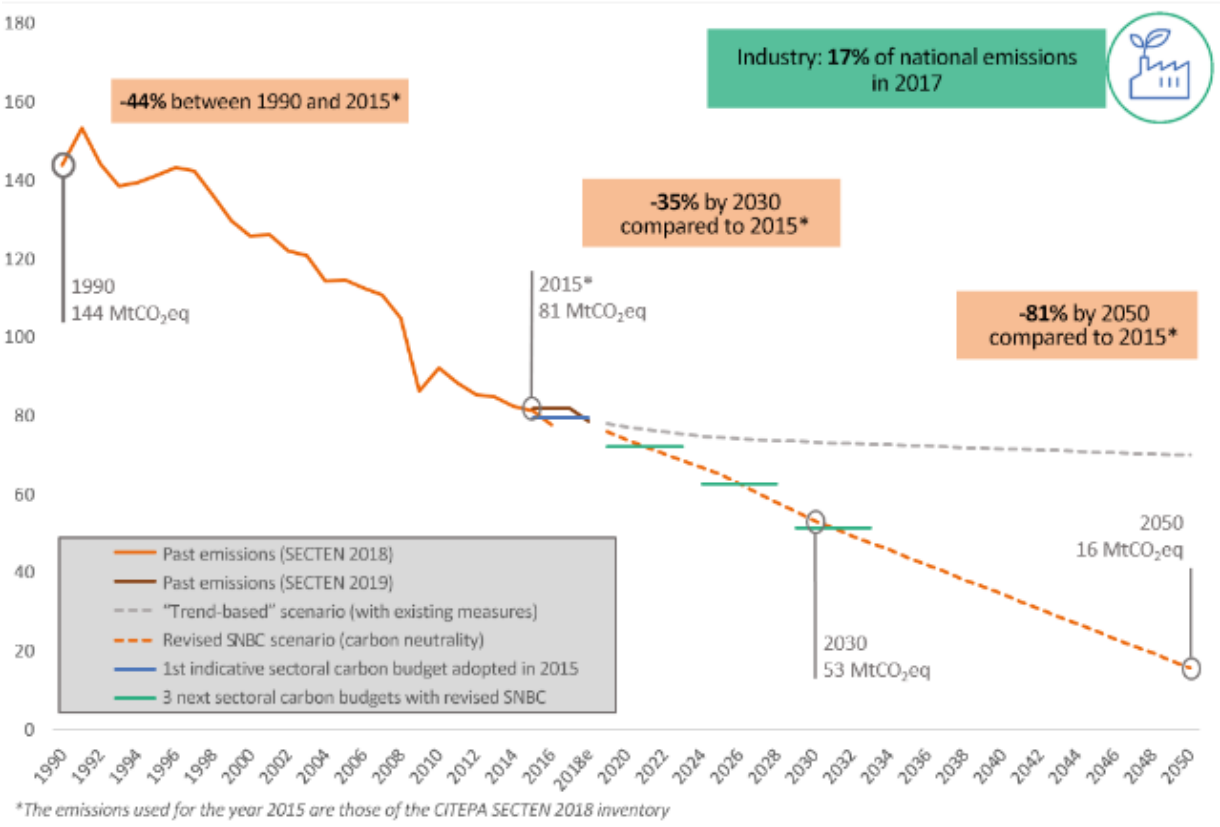

Figure 3.11: Historic and predicted emissions of the industry sector between 1990 and 2050 in $MtCO_2 - eq$. Figure obtained from [155]

Clearly, the industrial sector, responsible for 17% of France's total GHG emissions [155], aims to reduce its emissions by a substantial 81% from 2015 levels, decreasing from 81 to 16 $MtCO_2 - eq$ in line with SNBC objectives. The arduous path toward this target is graphically depicted in Figure 3.11 in the dotted orange line. In contrast, the grey dotted line represents forecasts based on current trends, showing a much less noticeable improvement of 13.6% by 2050, when yearly emissions would still be around 70 $MtCO_2 - eq$.

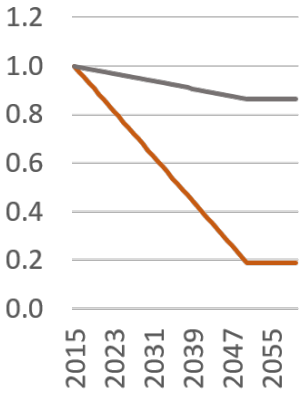

Figure 3.12: The reduction factor in production processes of building components in order to follow the SNBC target for the industrial sector.

Amongst the pivotal mechanisms to attain the dramatic reduction proposed by the SNBC and improve on current trends are the enhancement of energy efficiency, the incorporation of circular economy frameworks, and the deployment of innovative solutions such as carbon sequestration.

In this study, the DLCA workflow incorporates the assumption that the reduction in GHG emissions within the industrial sector will have a downstream impact on the environmental footprint of all building components across their production cycles. Consequently, replacement components incorporated over the lifespan of a building will exhibit a different emission profile than those used in the initial construction. It should be noted that this 81% reduction is benchmarked to emission levels recorded in 2015. This equates to a linear annual reduction rate of 2.31% over a 35-year timeline, culminating in the year 2050. Beyond 2050, the model presupposes that no additional reductions will occur, effectively stabilizing the reduction factor at zero. This temporal evolution is depicted in Figure 3.12, where the reduction factor serves as a multiplicative coefficient for the material and product-related emissions (A1-3) of building components as a function of the emission year.

(d) Waste Sector Evolution

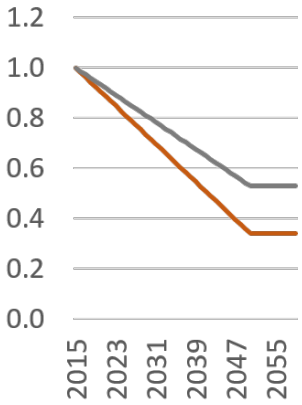

Figure 3.13: The reduction factor in production processes of building components to follow the SNBC target for the industrial sector.

The waste sector emissions are analogous to the aforementioned industry sector, as they are projected to decrease by 66% by 2050 in relation to 2015 levels, from 17 to 6 $MtCO_2 - eq$ [7], as shown in Figure 3.14 in the dotted orange curve. Then, similar to the industry sector, a reduction factor is also assumed to follow a linear reduction trajectory, resulting in -1.89%/year until 2050, as shown in Figure 3.13.

However, Figure 3.14 also identifies the current trends in the dotted grey line. If existing measures are maintained, a reduction of 47.1% in waste-sector emissions is still expected. This highlights a more positive trend than the industry sector, but it falls short of the SNBC targets. This gap can be observed in Figure 3.13, where the current trends are compared to the SNBC scenario assuming a linear

reduction between 2015 and 2050. This waste reduction factor is then used as a multiplier for EOL emissions of all components (C1-4).

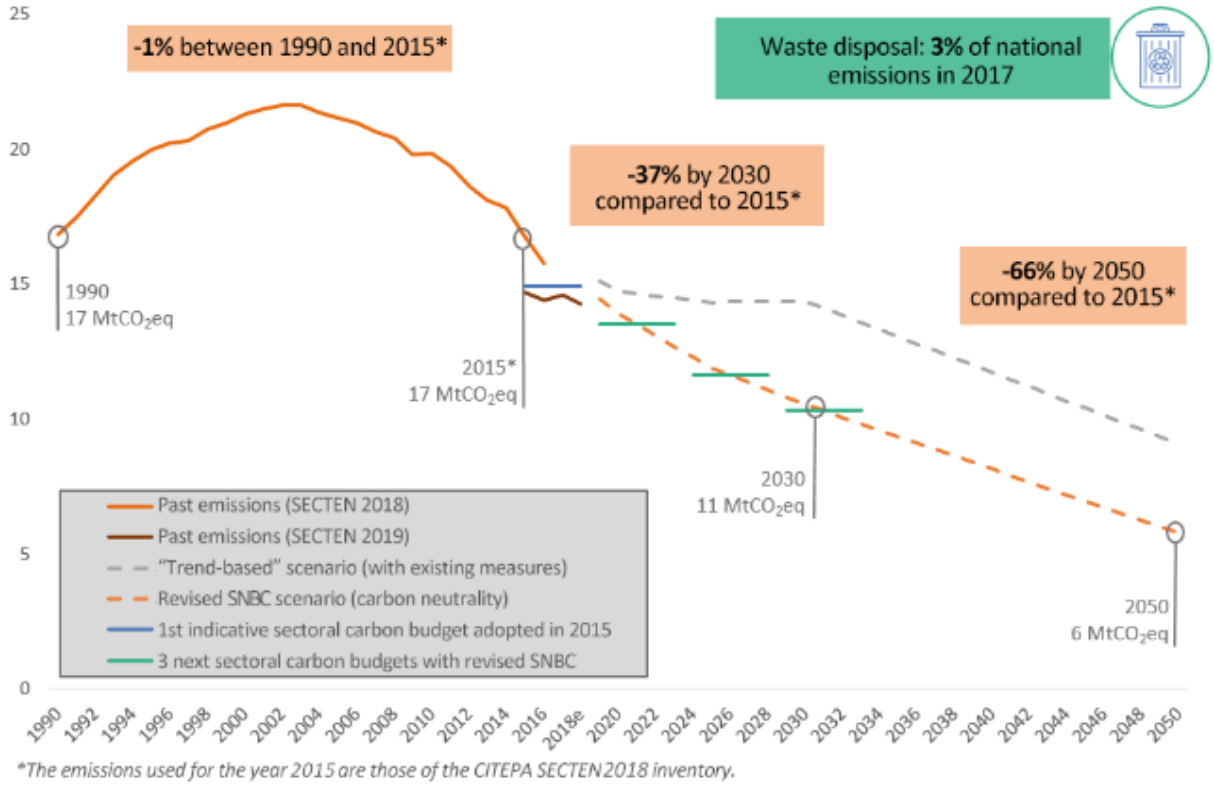

Figure 3.14: Historic and predicted emissions of the waste sector between 1990 and 2050 in $MtCO_2 - eq$. Figure obtained from [155]

(e) Limitation of External-Level DPs

Now, having identified external-level parameters throughout Sub-Chapter 3.2.3.1, it is worth taking a step back to recognize the limitations of these parameters, where each have been modelled independently from one other. However, in reality, these parameters are all intertwined and could be modelled with greater levels of detail. Meanwhile, it is relevant to recognize the inherent complexity of forecasting the evolution of entire economic sectors over half a century and the inherent need to simplify it.

With that said, the following section zooms into building-level parameters, which are associated with the equipment, materials and performance of the building itself.

3.2.3.2 Building Level

At the building-level, a further differentiation can be made amongst the DPs: ageing and technological advancements. The technolog-

ical advancement can be seen in multiple components, such as insulation material and glazed surfaces. Indeed, new and innovative equipment and materials have contributed to the energy efficiency improvements of recent decades. However, in this study, only the evolution of the heating system was included.

(a) Heat-pump Technological Improvement

The evolution of Heat-pump COP has been modeled in accordance with [156], assuming a compound improvement rate of 0.15%/year to the efficiency of these heating systems until 2052. Meanwhile, [71] uses an improvement rate much higher of 1% a year. Therefore, in this parametric approach, the DP will vary from 0.15% to 1%. Since the building requires a new heat-pump every 15 to 20 years and thus, this performance improvement only comes into play when it is replaced. Equation 3.5 demonstrates the compound efficiency improvement to COP, where $COP_{nominal}(y)$ is the nominal COP of the system when new at year y, $COP_{current}$ is the COP that current heat-pump technology allows, imp is the rate of improvement discussed earlier in this paragraph and $y_{construction}$ is the year the building is built, making the exponent is the age of the building.

$$COP_{nominal}(y) = COP_{current} \times imp^{(y - y_{construction})} \tag{3.5}$$

(b) Heat-pump Performance Degradation

Meanwhile, these same heat-pump are also expected to lose performance with time. Negishi et al. [71] and Eleftheriadis et al. [157] have modelled this parameter at much higher values than the rate of improvement found above, with both studies modelling this degradation process as a 1% to 3% yearly reduction to COP. The yearly COP due to degradation is calculated in similar fashion as the improvement, as shown in Equation Equation 3.6.

$$COP(y) = COP_{nominal} \times (1 - deg)^{(y - y_{nominal})} \tag{3.6}$$

Where $COP(y)$ is the efficiency of the heat-pump calculated yearly for year y, $COP_{nominal}$ is the nominal efficiency of the heat-pump when new, calculated in Equation 3.5, deg is the yearly degradation rate and $y_{nominal}$ is the year when the heat-pump was last replaced. This means the exponent of deg is simply the age of the heat-pump being used.

Finally, the yearly COP profile of a heat-pump assuming it has a service life of 17 years and a current COP of 3, with both parameters

affecting its performance is illustrated in Figure 3.15. This plot includes 2 scenarios to illustrate its impact:

- Worst case (in orange), combining the highest degradation of 3% degradation and lowest improvement rate of 0.15% improvement.
- Best case (in blue), combining 1% degradation and 1% improvement.

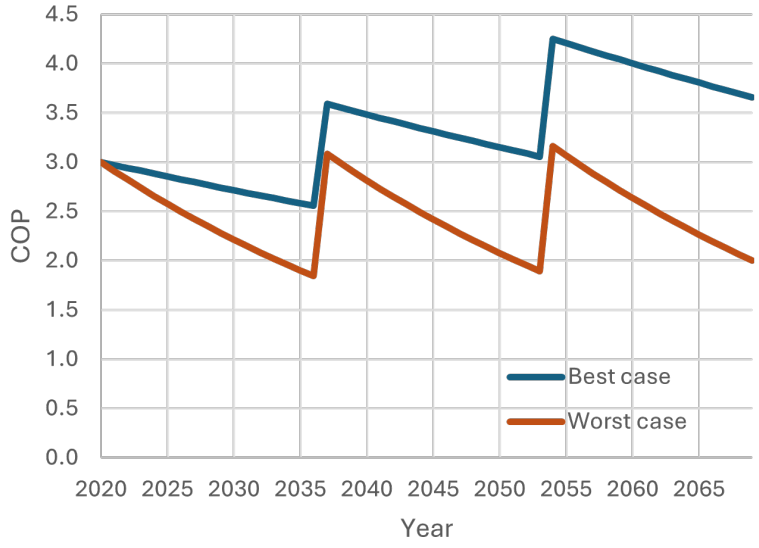

Figure 3.15: Heat-pump's COP profile for two scenarios over a building's life cycle of 50 years, considering a product service life of 17 years and an initial coefficient of 3.

(c) Insulation's Thermal Conductivity Degradation

The heating system is not the only building component to be affected by the ageing process. The insulation material is also expected to evolve. However, it is important to note that the commercial U-value given to the product by its manufacturers already includes some of the degradation that naturally occurs at the beginning of a material's life cycle, which includes testing for the material-specific norms. For instance, the EN 13163 defines the measurement guidelines of the thermal insulation for Expanded Polystyrene (EPS) [158] and the EN 13162 does the same for mineral wool products [159]. Therefore, in this study, only the degradation after the insulation material settles will be taken into account, in practical terms, only the degradation that occurs after 5 years was taken into account from the literature found on the subject. The result of this work is shown in Table 3.7.

As presented in Table 3.1, the insulation material used in the case-study building is Polyurethane and thus, the insulation degradation parameter varies from 0.43%/year to 1.1%/year.

Table 3.7: Insulation degradation in terms of linear yearly increase to thermal conductivity after the first 5 years of operation. The table is the result of a literature review that included multiple materials, mostly petroleum-based closed-cell foam.

Insulation Material	Yearly Degradation (%/y)	Source
EPS #1	0.37	[160]
EPS #2	0.23	[160]
EPS #3	0.71	[160]
EPS #4	0.27	[160]
EPS	1.65	[161]
PU 40K	1.10	[160]
PU 50K	0.43	[160]
XPS	0.04	[157]
Average	0.65	

(d) Air Tightness Degradation

As air infiltration is a large contributor to thermal losses in building energy simulation[7], it was important to include it in this study. Research on the durability of building air-tightness has been assembled quite comprehensively in the International Energy Agency (IEA) Energy in Buildings and Communities (EBC)'s AIVC Technical Note 71 [163]. This publication included real case-study testing, where most buildings were found to degrade in terms of air-tightness over time. However, there is a high variability amongst the buildings found. In addition, it was found that neither the initial air-tightness nor the construction material correlates with this degradation in terms of relative increase to infiltration. Due to the variability and lack of established correlations, infiltration degradation is defined to be between 0% and 1% per year, based on [164] and [61].

7: For French single-family homes, air renovation and infiltration represent around 20% and 25% of thermal losses [162].

(e) PV Performance Degradation

Finally, the last building-level DP to be included in this work is the performance degradation of the PV panels' power production relative to the same insulation, as it relates to ageing. The median value for this long-term degradation rate of over 2000 panels is around 0.5%/year while the mean was found to be around 0.8%/year [165]. Moreover, for monocrystalline Silicium technology, the 95% confidence interval for annual degradation ranges around 0.3% to 0.7% and for our analysis, we will use these values for the DP modelling.

3.2.3.3 User-Level

As explained in the Chapter 2.2.3, occupancy is the largest source of uncertainty in a building's energy simulation results. This trend should continue in GWP, especially in terms of OE. Four types of

user-level parameters were identified, although many others could be included:

- Occupant behaviour: when, what and how much energy is consumed and internal gains are produced by the users in activities such as cooking, reading, watching TV, indoor exercising, etc.
- Occupant density: how many people occupy a given space or building nominally and hourly.
- Heating temperature setpoint: The temperature setpoint for the heating systems.
- Cooling temperature setpoint: The temperature setpoint for the cooling system.

Defining these parameters dynamically at an hourly time-step is far from innovative, with national regulations such as the RE2020, standardizing daily occupancy profiles. However, to start considering these user-level uncertainties in a dynamic LCA approach, one might start thinking about how a building's occupants evolve through the decades. As individuals age and start families, their behaviors and household density naturally evolve. One might also consider how a population will become more sustainably conscious and thus be aware of energy and resource sufficiency. This behaviour change might also stem from policy incentives.

In some of the other DLCA applications in the literature, the definition of this parameter was strictly qualitative. Notably, Negishi et al. [71] used a Japanese single-family home to tell the story of how a couple eventually had children and thus, expanded their house to build extra rooms. These bedrooms would then be emptied as the kids moved out for their studies. On the other hand, Su et al. [166] used Chinese demographic forecasts to build user-level scenarios of occupancy and energy consumption. For the French context, data on usage behaviour for energy modelling, such as appliances, lighting and other devices is available. This data has been largely investigated by Vorger et al. [167], leading to the development of a stochastic method for sub-hourly occupant behaviour modelling. Although this study does not include forecasting.

The difficulty of making this parameter dynamic, due to insufficient data and extensive research on uncertainties in building energy simulations, led to a further simplification of this category of parameters. Instead of allowing them to evolve, they are simulated statically in this thesis, essentially being treated as uncertainties.

The modelling stage in this chapter aims to be comprehensive, enabling the exploration of simplification techniques. It is particularly conducive to examining the edge cases in parameter intervals. Consequently, the modelling of user-level parameters is defined as

a static uncertainty, as demonstrated in the presence hours density model in Figure A.4.

After establishing the residential case study, including its characteristics and context in the French Parisian region, the DP is modelled as closely as possible to the specific case. To summarize the findings, Table 3.8 was constructed.

Table 3.8: Table summarizing all the included Dynamic Parameters (DP) in this chapter.

Dynamic parameter name	Dimension	Time-Step	Form	Value Interval	Data Source
Global warming	Outdoor temperature	yearly	RCP models (2.6, 4.5, 8.5)	+0.016°C, +0.037°C and +0.063°C	[1]
Electricity mix's CI evolution	CI	Yearly	Linear	-2.6% to -2.3%	[152]
Electricity Production CI	CI	Hourly	-	-	[150]
Industrial sector's evolution.	A1-3 GWP	Yearly	Linear	-2.31% to -1.85%	[155]
Waste sector's evolution.	C1-4 GWP	Yearly	Linear	-1.89% to -1.34%	[155]
Heat-pump technology improvement	COP	Yearly	Exponential	0.15% to 1%	[61, 156, 168]
PU insulation ageing	Thermal conductivity	Yearly	Exponential	0.43% to 1.1%	[169]
Air tightness ageing	Infiltration airflow	Yearly	Linear	0% to 1%	[71]
Heat-pump ageing	COP	Yearly	Exponential	-3% to -1%	[71, 157]
Photovoltaic system ageing	Efficiency	Yearly	Linear	-0.2 to -1%	[165]
Occupant density	Persons	Static	-	2 to 8	-
Presence hours	Hours	Static	-	13h to 20h	[170]
Heating temperature setpoint	Temperature	Static	-	18°C to 22°C	[106, 171]
Cooling temperature setpoint	Temperature	Static	-	23°C to 27°C	[106]

3.2.4 Energy Model and Reference Weather Data

Having defined the case-study and the appropriate DPs, we must assemble all other requirements listed in Chapter 3.1. The energy model, as mentioned, must be in a flexible and adaptable format that would allow its automated manipulation. EnergyPlus[8] was found to be the most suitable option given these constraints along with python libraries that facilitate this process: EPPY[9], which is used to modify EnergyPlus energy models in the .idf format and launch parallel simulations, and OpyPlus[10], which is used to modify the weather files in .epw format.

8: EnergyPlus is an open-source building simulation engine developed by the U.S. Department of Energy's (DOE) Building Technologies Office (BTO). For more information: energyplus.net/.

9: For EPPY's documentation: eppy.readthedocs.io/.

10: For OpyPlus' documentation: opyplus.readthedocs.io.

However, EnergyPlus alone is not well-suited for the geometric modelling of buildings. Thus, DesignBuilder[11], a building design and assessment tool, utilises EnergyPlus as its Dynamic Thermal Simulation (DTS) engine and features a graphical user interface for the 3D modeling of building geometry. DesignBuilder subsequently creates an .idf file, the energy model standard used by EnergyPlus.

11: DesignBuilder's product page: designbuilder.co.uk/.

The EE calculations in this thesis were strictly based on the RE2020 methodology. This, of course, includes the use of French EPDs. Meanwhile, the OE calculations have been done based on an EnergyPlus model. This choice to deviate from the energy simulation methods described by the norm was based on the extra flexibility that an open-source calculation engine afforded.

As specific as the building model is the weather data for the DTS. EnergyPlus simulations require the weather data in "EPW" format and to generate representative weather information about the building's location, the PVGIS[12] tool was used. It enables the export of EPW files with typical meteorological year (TMY) data for a given geographical location, which is then used as a reference for the remainder of the building life cycle.

12: PVGIS, or Photovoltaic Geographical Information System, is a tool developed and maintained by the European Commission Joint Research Center for solar resource assessment. For more information: re.jrc.ec.europa.eu/pvg_tools.

3.2.5 Preliminary Case-study Application

Having presented the case-study information and all requirements established in Chapter 3.2.1, we can now apply it to the DLCA workflow.

But first, it is important to understand the inputs used in this simulation, which have been listed in Table 3.9, as the inputs shown in Table 3.8 give an interval instead of an absolute value.

Hereafter, for simplification purposes, we assume that the building starts operating on the 1st of January 2020 and the EEs are also indexed to the year 2020. Indeed, Figure 3.16 displays the yearly carbon emissions from 2020 until 2070, with two vertical axes. To the left, represented in green, is the yearly overall GWP in $kgCO_2 - eq$ and to the right, in red, is the cumulative sum of these same emissions.

From this profile, a major peak in emission is observed at year zero, due to the building's construction and another GHG emission peak is seen at year 50, due to the building's EOL. Between them, a "plateau" of emissions can be seen linked to the building's operation with some noticeable peaks that are explained by the replacement of the following components, which are also highlighted in Figure 3.16:

1. (Orange) Both the heating and ventilation systems have a service life of 17 years, prompting replacements after 17 and then 34 years of operation.
2. (Purple) A lot of components in the bathroom and kitchen of the residence have a 20-year service life, resulting in two replacements.
3. (Yellow) Plenty of components linked to the electrical installation have a service life of 25 years, requiring replacement during the building's lifetime.
4. (Blue) The double-glazing windows have a service life of 30 years, thus undergoing replacement only once.

Table 3.9: List of inputs used for the feasibility study.

Dynamic Parameter	**Dimension**	**Value**
Global warming	Outdoor temperature	+0.037 °C/year
Electricity mix evolution	Carbon Intensity	-2.45 %/year
Industry evolution	A1-3 GWP	-2.08 %/year
Waste evolution	C1-4 GWP	-1.62 %/year
Heat-pump improvement	COP	+0.58 %/year
Insulation degradation	Thermal conductivity	+0.94 %/year
Air tightness degradation	Infiltration airflow	-0.5 %/year
Heat-pump degradation	COP	-2 %/year
PV degradation	Efficiency	-0.6 %/year
Occupant density	Persons	5 occupants
Daily presence	Hours	16h30 / 24h
Heating setpoint	Temperature	20°C

In addition, the dotted horizontal lines in Figure 3.16 have been drawn to represent the carbon budgets defined for the case-study, according to the RE2020. As shown in Table 3.3, this regulation defines different budgets depending on when the building is built. This is why the 2025 budget was also included in the dotted orange line.

Most importantly for this preliminary application to a case-study are the following identified issues:

Dynamic Parameters modelling: This issue has been identified in the literature review and the experience for this French case-study was no different. Determining which parameters to consider and the appropriate values for these parameters is a complex task, so that results are more reliable than the static workflow.

Simulation time: This is an inherent issue of DLCA as it deals with more data and more calculations. This issue is even more relevant when considering that the accuracy of dynamic GWP comes from its parametric nature, which is particularly useful in decision-making. The simulation took 3min7s[13] with all 50 simulations being executed in parallel simultaneously. Additionally, this is the time required for a single simulation. Optimisation and sensitivity analysis algorithms require thousands of iterations to be run and this would cause simulation times to quickly jump to days.

13: This simulation was run in a 40-core, 80-threads Intel Xeon E5-2498 server running at 2.2 GHz and 256GB of memory RAM. Current laptop-grade CPUs with 8 to 12 cores would require some EnergyPlus simulations to be run in series

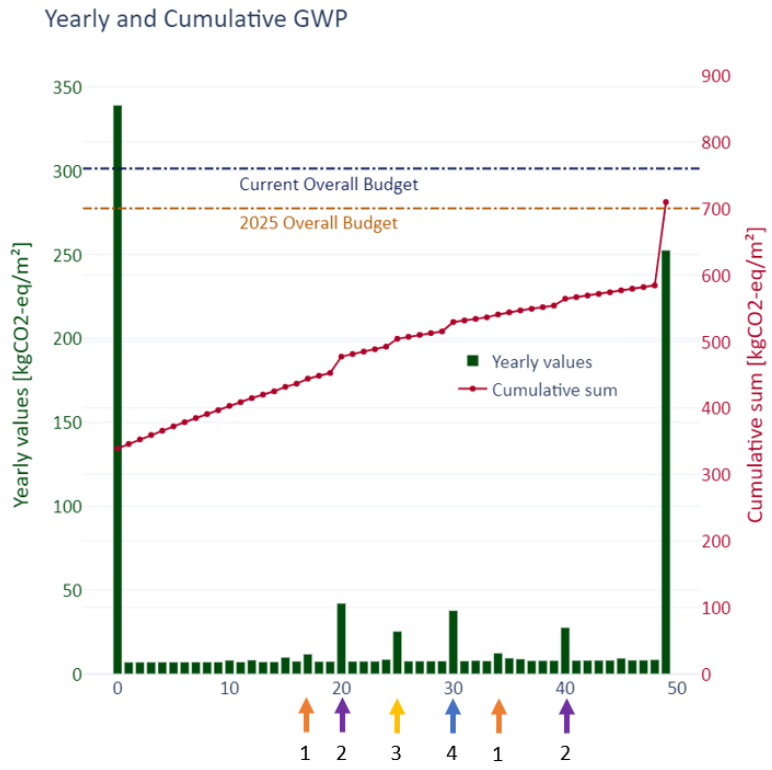

Figure 3.16: Overall dynamic GWP results of the DLCA applied to the case-study in $kgCO_2-eq$ from 2020 until 2070, in terms of yearly and cumulative emissions.

An important addition to the simulation time discussion is that 186s of the 187s it took to obtain these results, were dedicated to the OE calculation. Only 1s was related to EE calculation, as it simply involves adding and multiplying values in a table at a yearly time-step. This discrepancy in calculation times is inversely proportional to the relative impacts of OEs and EEs, where 75% of the overall GWP was embodied.

Depending on the application, these simulation times are acceptable. However, this thesis delves into the topic of DM in building design, particularly at post-occupancy stages. In this context shorter simulation times are highly desirable, allowing exploration of design options and a better understanding of the alternatives.

3.3 Proposing a DLCA simplification methodology

For the two problems identified then, this sub-chapter is subdivided into proposing a solution to each of them: reducing simulation times and simplifying the DP modelling process.

3.3.1 Reducing Simulation Times

As found in Chapter 2, other DLCA applications have steered away from making life-cycle energy simulations. Indeed, most research has been limited to 2 to 5 interpolated simulations for OE [56, 140]. The workflow developed in this thesis though, executed 50-year hourly energy simulations, offering the flexibility to test different regression techniques, linear or otherwise, while evaluating the simulation times.

In a first approach, as done in other works, a linear interpolation will be applied where the number of simulations for life cycle operational GHG is reduced to a given time-step. The second approach involves meta-models. Using model regression algorithms, other research has been successful in the context of building energy simulations, most notably for optimisations.

In this comparison of techniques, three indicators will be used to identify the optimal strategy: simulation time, Root Mean Square Error (RMSE)[14] and Coefficient of Determination (R^2)[15]. The latter two indicators are commonly used in the context of evaluating the performance of computational models [172]. To calculate the RMSE and R^2 a representative sample of the inputs and outputs are needed. Thus, a Monte Carlo sample of the input parameters with a uniform probability distribution between the intervals was created.

14: Root Mean Square Error (RMSE) is a measure of the differences between predicted and observed values, calculated as the square root of the average of squared differences. Lower values indicate better fit.

15: R-squared (R^2) is the proportion of variance in the dependent variable that is predictable from the independent variable(s). Higher values indicate a better fit.

3.3.2 Reducing the Number of Dynamic Parameters

As established in Chapter 2, another issue commonly identified in the literature towards including DPs to the LCA process is their modelling, due to the absence of a unified database Thus, reducing the number of parameters should also reduce the barrier of entry to building DLCA.

Based on this logic, we decided to find the parameters with the largest impact on the results of the dynamic GWP results in two main studies. The first study investigates the impact of turning each parameter of the LCA from static to dynamic, thus identifying which of them should be prioritized if a decision-maker does

decide to model them dynamically. The second study investigates the uncertainty with each of the identified DPs found throughout this chapter, determining which ones contribute the most variance in the GWP.

3.4 Case Study Application I: Reducing Calculation Times

With the simplification strategies established towards reducing simulation times, we shall now apply them to the same case-study presented in Chapter 3.2.1.

3.4.1 Interpolation

3.4.1.1 Interpolation Framework

This approach aims to reduce the simulation time of the DLCA method discussed previously. The energy simulation is the most time-consuming part of the workflow. To address this, we modified the method to perform simulations every few years and use linear interpolation to estimate values for the intervening years. Only the OE suffers from decreased accuracy, as DTS times are the most time-consuming, making interpolation unnecessary for the embodied calculations.

In this study, the time step is variable and its impact on accuracy and simulation times is analyzed. The latter depends on the number of parallel energy simulations that can be executed. During the feasibility study, all 50 simulations were executed simultaneously on a server. However, on less powerful machines, the differences in time steps would be more pronounced. Thus, simulation times referenced here are based on a portable computer[16] instead of a calculation server.

16: This portable PC with only 4 cores and 8 threads can run up to 8 EnergyPlus simulations at once. However, to avoid errors, a maximum of 6 simulations were executed simultaneously.

The following interpolation periods were studied:

Full workflow Energy simulations were executed every year of the building's life cycle. The portable computer divided the simulations into 9 batches of up to 6 running in parallel, serving as the reference baseline.

Every 5 years Executing 10 simulations, spaced every 5 years, with linear interpolation between these points. This reduced the number of batches to 2.

Every 10 years Increasing the sampling period to 10 years, reducing the number of simulations to 5, necessitating only one batch.

Every 24 years Ensuring 3 simulations in a single batch at years 1, 24, and 49.

Every 49 years Simulating only the first and last years of OEs, with interpolation between these points.

The OE calculations between these simulations are performed using the linear interpolation described in Equation 3.7 and illustrated in Figure 3.17:

$$OE_t = OE_{t_0} + \frac{OE_{t_1} - OE_{t_0}}{t_1 - t_0} \cdot (t - t_0) \tag{3.7}$$

where:

- OE_t is the interpolated operational emissions at time t
- OE_{t_0} and OE_{t_1} are the operational emissions at the nearest simulated times t_0 and t_1
- t is the time at which the interpolation is being calculated

Subsequently, the life cycle OE is assessed as per Equation 3.8, where OE_{LC} is the total life cycle OE and T is the total number of years in the building's life cycle.

$$OE_{\text{LC}} = \sum_{t=0}^{50} OE_t \tag{3.8}$$

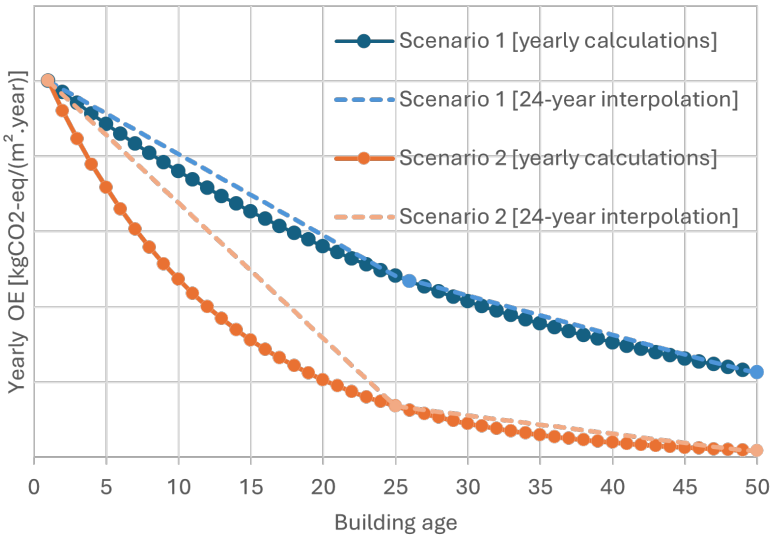

Figure 3.17: Illustration of two interpolation scenarios showing 24-year steps and their impact on OE.

This approach was applied to 100 different scenarios, each with a unique set of DPs. The interpolated results were compared to actual values simulated for each year to assess the accuracy and efficiency of this method. By choosing time steps of 1, 25, and 49 years, we balanced reducing computational load with maintaining the accuracy of the interpolated OE.

To exemplify the framework, considering the 24-year interpolation, the following steps were undertaken:

1. Simulate the operational emissions for the 1^{st}, 25^{th}, and 49^{th} years.
2. Apply the interpolation from Equation 3.7 to estimate emissions for the intermediate years.
3. Calculate the life cycle OE with Equation 3.8.
4. Compare the interpolated values against yearly simulation results to evaluate interpolation accuracy.
5. Repeat steps 1 through 4 for all scenarios.
6. Calculate the relative RMSE and R^2 to quantify interpolation accuracy.

3.4.1.2 Interpolation Results

The results demonstrated that linear interpolation using these key points provides a good approximation of operational emissions while significantly reducing the number of required simulations. The results are shown in Table 3.10.

Interpolation period	Relative RMSE	R^2	Simulation time
1 year	0%	1	5min 47s
5 years	0.6692%	0.9973	1min 10s
10 years	0.8143%	0.9960	38s
24 years	4.075%	0.8988	23s
49 years	21.27%	-1.760	19s

Table 3.10: Comparison of interpolation results.

For an interpolation period of 1 year, the baseline, RMSE and R^2 are 0% and 1, respectively.

Reducing the sampling period from yearly to every 5 or 10 years negligibly impacts accuracy, with RMSE smaller than 1% and R^2 greater than 0.99.

Reducing the number of simulations to only 3, with 24-year time-steps, significantly decreases performance, with an R^2 value below the recommended 0.9 for energy simulations [173].

Executing only 2 simulations (49-year time-step) continues this trend, presenting a relative RMSE in the double digits and a negative R^2. A negative R^2 indicates that the interpolation is a worse representation of yearly OE than a simple average of the two available true values, due to non-linear DP models.

Simulation times, dependent on the computer's capabilities[17], showed significant improvements when reducing the time-step from yearly to every 5 years, as the number of batches of parallel EnergyPlus simulations reduced from 9 to 2. Increasing the time

17: When comparing the portable computer to the server used in the feasibility study, for the same dynamic GWP calculation, the smaller PC took 2min30s longer than the server.

step to 10 or 24 years led to diminishing returns as the number of batches reduced to one.

Figure 3.18 compares simulation times with R^2 and RMSE, helping determine the ideal simulation time step for this case study. Each point in the orange and blue curves defines a simulation time-step from 1 to 49 years, as per Table 3.10. The curves show that the point of diminishing returns is reached quickly, at one simulation every 10 years, allowing a single batch of 5 simulations and preserving good fidelity to the original calculations.

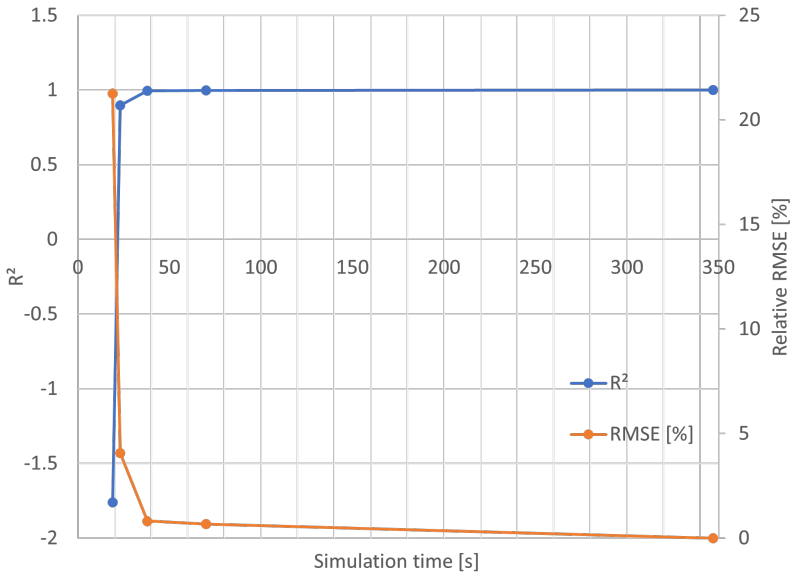

Figure 3.18: Comparing simulation times, R^2 and relative RMSE of full and interpolated operational emissions. Longer simulation times correspond to more simulations due to decreasing time steps.

The results in this sub-chapter vary based on the case study, the DP models, and the computer used for simulations. Linear interpolation has proven accurate with at least 4 simulations, but simulation times are still somewhat long, at 38 seconds, especially in the context of parametric simulations and optimizations.

3.4.2 Surrogate Modelling

3.4.2.1 Surrogate Modelling in Building Simulations

To further improve simulation times, this section investigates surrogate modelling techniques. As building data has massively grown over the past few decades, the models that are used to describe them have also evolved. This leads to an increased computational complexity and, consequently, simulation times [174]. This is especially problematic in the context of parametric workflows, which are essential to DM processes and DLCA. Surrogate- or meta-models offer a solution to these long computational times of high-fidelity models by replacing them with statistical models trained on a set of in- and output data of the original building physics [175].

In the context of building simulations, Surrogate Model (SM) is far from an innovative concept, being used for many applications. For early-design stage [59, 174, 176–178], for variance-based sensitivity analysis applications [59, 179–181], for uncertainty analysis in energy performance [178, 182], for optimisations [176, 181, 183–185] and many other applications, which has been summarized in a literature review on the matter by Westermann and Envins [175].

3.4.2.2 Modelling Techniques

In addition to seeing many applications in the building simulation sphere, a wide range of SM techniques have been explored. This sub-chapter then, will list the most commonly found in the literature.

Most common of all SMs techniques are linear regressions [175]. They are used to model the relationship between a dependent variable and one or more independent variables by fitting a linear equation. As SMs, they are computationally efficient and easy to interpret, making them good choices for problems with a linear or nearly linear relationship between variables. However, they perform poorly when the underlying system is nonlinear or complex, and they lack the flexibility to capture intricate patterns in the data [173], similar to what was observed in the in Sub-Chapter 3.4.1.

Artificial neural networks (ANNs) are also frequently used in building simulations. They are computational models for machine learning, consisting of interconnected layers of artificial neurons. They excel at complex pattern recognition and nonlinear function approximation [184]. ANNs are often effective as SM for high-dimensional and complex systems where traditional methods may struggle. However, they can be computationally expensive to train, require large datasets for accuracy, and may become "black boxes," making it difficult to interpret or to explain their predictions [186].

Additionally, Support Vector Machines (SVMs) are supervised learning algorithms used for classification and regression tasks. As SM, they are effective for high-dimensional spaces and can handle nonlinear relationships through kernel trick. However, they may require careful tuning of hyperparameters and can be computationally intensive for large datasets [173].

Meanwhile, Multivariate Adaptive Regression Splines (MARS) is a form of non-linear regression that uses piecewise linear basis functions to model complex relationships. As SM, MARS is good for capturing non-linearities and interactions between variables, while still being relatively interpretable. However, the model can become complex and overfit if not properly regularized [173].

Finally, Gaussian Processes (GPs) are probabilistic models used for regression and classification. They are particularly strong as SM for capturing uncertainty and complex, smooth relationships in the data. They are computationally expensive (like SVMs and MARS), especially for large datasets, but offer the advantage of providing confidence intervals for predictions [173].

3.4.2.3 Dealing with Integer and Categorical Variables

Numerous techniques are available, yet when dealing with buildings, an additional challenge arises when working with SMs due to the presence of categorical and integer variables. Garrido-Merchán and Hernández-Lobato [187] proposed a solution that includes rounding the prediction to the nearest integer with a Kriging algorithm, which is a GP-based process. This method is applied in the SMT[18] python library. Although integer problems are not addressed in this chapter, they will become relevant in Chapter 4.

18: The Surrogate Modelling Toolbox is a complete open-source library with plenty of modelling algorithms.For more information smt.readthedocs.io/

3.4.2.4 Sampling and Training Surrogate Models

Out of all the options listed above, the Kriging technique was selected as the best alternative for the application in this thesis, demonstrating consistent superior performance in terms of R^2 across training sample sizes ranging from 64 to 1024 [186] and its capability to handle mixed-integer problems. While GP does have its disadvantages, such as long training times for large datasets, this is a one-time process and the prediction times remain fast, making the trade-off worthwhile for achieving high-fidelity results.

In the scope of this study, a parametric DLCA workflow, the SM is trained with the input being the different DPs, while the output is the OEs of a given year. In other words, from the perspective of the SM, this is a single-year OE calculation. However, before training the model, there must be conversion of the DPs into modifiable building characteristics. For instance, instead of training the model with the insulation degradation, it will be trained on the range of thermal conductivity within which it is expected to operate, even after 50 years. This same process is repeated for all 10 parameters, and the results of this work are shown in Table 3.11.

As a result, the SM has 10 inputs for the single output, as illustrated in Figure 3.19. Thus, for the DLCA simulation, 50 iterations of the SM must be executed.

Prior to operating this model, a sample of 1100 input vectors was created with the Latin Hyper-Cube method (LHS), 100 of which were reserved for the model validation. The true outputs of the

Table 3.11: The inputs for the surrogate model training.

Dynamic Parameters	Training Parameter	Parameter Type	Training Interval	Unit
Insulation Degradation	Material Conductivity	$\mathbb{R}$	0.02 to 0.07	$W/(m^2.K)$
Occupant Density	Number of occupants	$\mathbb{Z}$	2 to 8	person
Presence Hours	Average number of hours daily with occupancy	$\mathbb{R}$	13 to 20	hours
Heating Setpoint	Heating Temperature Setpoint	$\mathbb{R}$	18 to 22	°C
Cooling Setpoint	Cooling Temperature Setpoint	$\mathbb{R}$	23 to 27	°C
Air tightness Degradation	Infiltration	$\mathbb{R}$	0.6 to 0.9	ac/h
Global Warming	Modified Weather File	Categorical	RCP 2.6, 4.5 and 8.5	-
PV degradation	PV efficiency	$\mathbb{R}$	100 to 70	%
Heat-pump Degradation and Improvements	Heat-pump Coefficient of Performance (COP)	$\mathbb{R}$	2.6 to 5	COP
Electricity Mix Evolution	Average Carbon Intensity	$\mathbb{R}$	17.9 to 78.3	gCO_2/kWh

1000 samples were calculated over 1h44min[19], resulting in a 1000-point single-dimension array with the resulting OEs. Additionally, for the Surrogate Model training, an extra 8 minutes need to be accounted for.

19: This simulation was also executed on a server equipped with a 40-core CPU, allowing many simulations to be run in parallel.

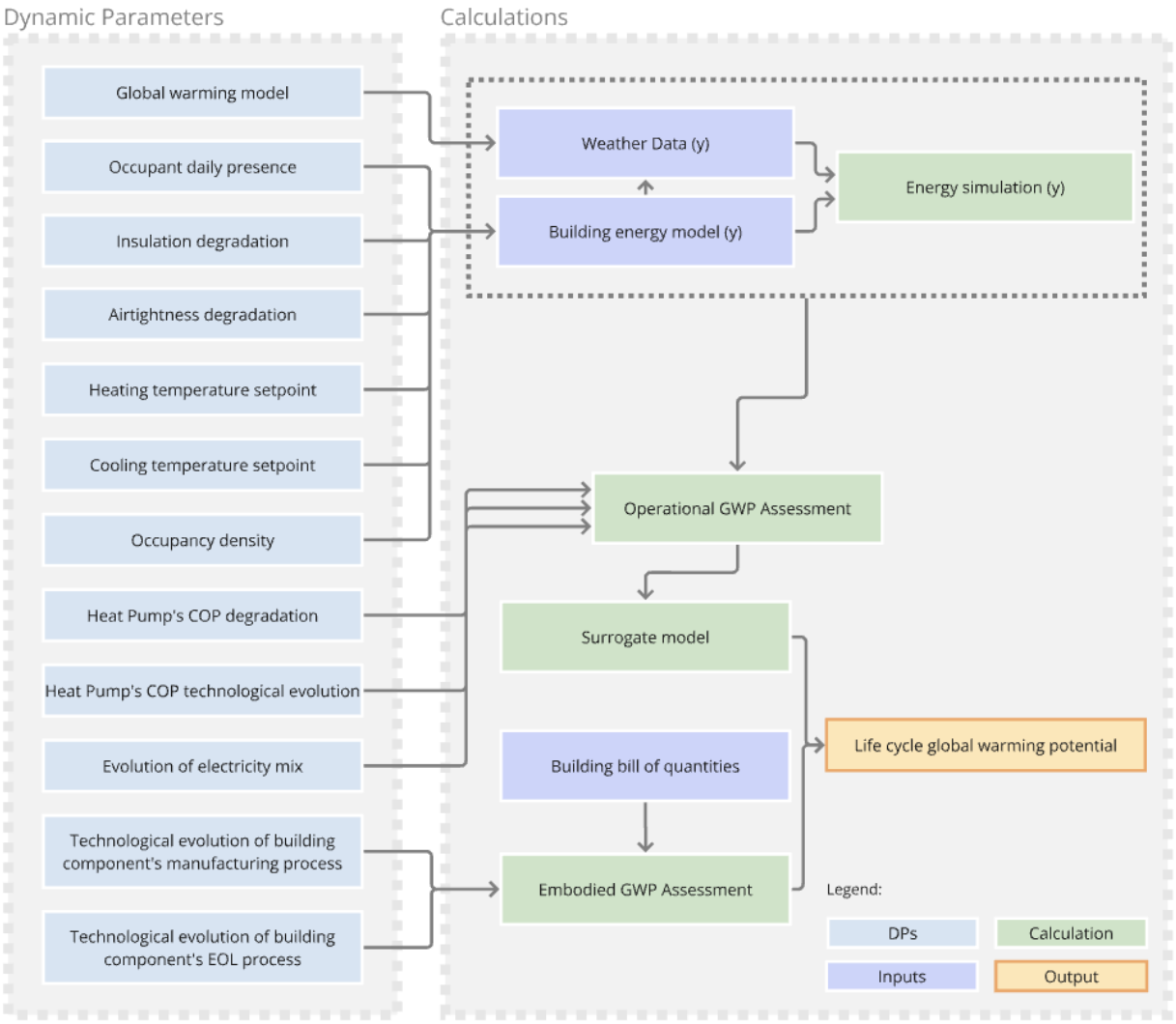

Figure 3.19: Meta-modelling method employed to reduce simulation times.

3.4.2.5 Results

With the input and output arrays prepared, we trained multiple SM models to examine how the number of samples affects the meta-model's accuracy in replicating the original system's behaviour. We varied the sample size from 100 to 1000. For each model, we used the same validation sample to evaluate the Relative RMSE and the R^2. The outcomes of this study are detailed in Table 3.12 and visualized in Figure 3.20.

These findings reveal that with just 200 samples, the model achieved an R^2 value greater than 0.98. This high degree of linearity is particularly pronounced within the bounds of the DPs modelled earlier. As a result, the newer, faster statistical model significantly reduces simulation times from 38 seconds to between 0.5 and 0.7 seconds, depending on the machine's capabilities. This is a 98.15% to 98.68% improvement. Despite this improvement, Embodied Emission (EE) calculations remain time-consuming compared to

Operational Emissions (OE) calculations, which now take only 117 milliseconds to run 50 times with 1000 samples.

Number of samples	Relative RMSE	R^2	Prediction time
100	20.14%	0.9517	60 µs
200	13.03%	0.9797	110 µs
300	11.03%	0.9855	150 µs
400	9.264%	0.9897	240 µs
500	7.945%	0.9925	579 µs
600	7.352%	0.9935	1.05 ms
700	7.130%	0.9940	1.13 ms
800	6.701%	0.9947	9.50 ms
900	6.129%	0.9955	12.5 ms
1000	6.103%	0.9955	15.0 ms

Table 3.12: The results in terms of R^2 and RMSE of varying the number of samples used in the training of a surrogate model.

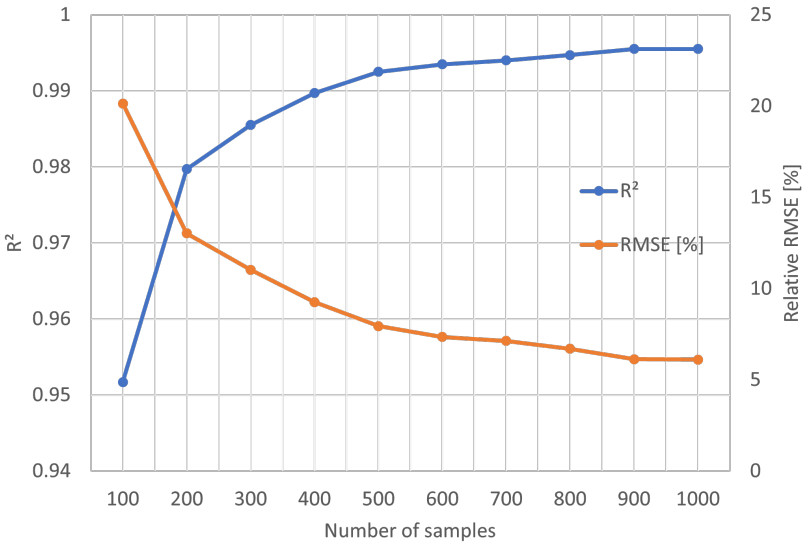

Figure 3.20: Comparing R^2 and relative RMSE of the surrogate models trained with 100 to 1000 samples. The more points available for training, the more accurate the surrogate model will be, but there is a point of diminishing returns debatably beyond 500 samples.

This experiment also highlights that the most accurate models require longer simulation times, which increase linearly due to the Kriging method used in training. It is important to consider the time needed for collecting training data, training, and validating the model. If a practitioner or researcher does not require thousands of iterations, it may be more efficient to interpolate OE values throughout the building's life cycle.

However, for extensive iterative use of this Surrogate Model in variance-based Sensitivity Analysis (SA), the rapid simulation times provided by this model are highly advantageous.

3.5 Case Study Application II: Reducing the Number of Parameters

In Chapter 3.3, the complexities associated with modelling DPs were identified as significant challenges within DLCA. This subsection aims to determine the parameter that has the greatest impact on GWP. Accordingly, the investigation is divided into two separate analyses, outlined in Table 3.13: the first analysis is detailed in Chapter 3.5.1, and the subsequent uncertainty analysis is conducted in Chapter 3.5.2.

Table 3.13: This table compares the two approaches to classifying the most affluent parameters.

Criteria	GWP Sensitivity to Static and Dynamic LCA approaches	Uncertainty in Dynamic GWP results
Objective	Identify parameters to prioritize in a dynamic approach	Identify largest source of uncertainty in DLCA
Comparison Methods	Best feature selection, difference of means and Sobol analysis	
Sampling Method	Full factorial design of static and dynamic parameters	Random sampling of inputs defined by uniform probability functions
Parameters Variation	Binary: static or dynamic	Operating intervals of DPs

To further clarify the differences between these analyses, we focus on the electricity mix evolution parameter. Previous discussions anticipated a reduction in the CI of electricity, with an annual decrease of 2.3% to 2.6% in France until 2050, contrasting with static LCA methods that assume no change.

In the "GWP's Sensitivity to Static and Dynamic LCA approaches" analysis, we examine the impact of modelling CI as either constant or reducing at an average rate of 2.45% per year. Conversely, the "Uncertainty in Dynamic GWP Results" analysis explores the impact of varying the reduction rate of CI between 2.3% and 2.6% per annum on GWP results. This nuanced comparison sheds light on how static and dynamic modelling choices, as well as parameter uncertainties, uniquely influence GWP outcomes.

3.5.1 GWP Sensitivity to Static and Dynamic LCA approaches

To facilitate a comparative analysis between static and dynamic LCA methodologies, two distinct sets of parameters have been developed. These will be detailed in the following section. Subsequently, the GWP results derived from each set will be rigorously

calculated and juxtaposed. The primary objective of this comparison is to identify the parameters that exhibit the most significant impact when transitioning from a static to a dynamic LCA approach.

Upon the completion of this sub-section, a hierarchical ranking of parameters, in terms of their significance for the case study, will be established. It is important to note, however, that while this ranking is specific to the case study and may not be universally applicable, the underlying methodology developed for this comparison possesses broader applicability and can be generalized to other studies.

3.5.1.1 Dynamic and Static Scenarios

To build a representative set of dynamic LCA scenarios, the intervals identified in Table 3.8 were used to build an average dynamic scenario, which will be referred to as a "representative dynamic scenario". However, not all parameters of the table were included here, since user-level inputs were modelled statically. Indeed, since they do not evolve through time, an average value already is used for the static scenario. This limitation could be amended simply by turning these parameters dynamic, which, due to lack of pertinent data, remained stationary in this thesis.

Table 3.14 then, displays the set of parameters: (1) a representative dynamic scenario, which was built with the exact mean between the bounds defined in Chapter 3.2.3, with the only exception being the global warming scenario, where the RCP 4.5 was chosen and (2) the static inputs, which were much simpler to define, as the LCI remains unchanged from year zero to 50 and for the weather data, the TMY dataset is used.

Table 3.14: Defining representative dynamic and static LCA calculation hypothesis.

Parameter	**Dynamic LCA** [%/year]	**Static LCA** [%/year]
Global warming	RCP 4.5	TMY
Electricity mix's evolution	-1.87%	0%
Industrial sector's evolution	-2.08	0%
Waste sector's evolution	-1.62	0%
Heat pump technology improvement	0.58%	0%
Insulation degradation	0.94%	0%
Air tightness degradation	0.5%	0%
Heat-pump ageing	2%	0%
PV system ageing	0.6%	0%

3.5.1.2 Full Factorial Sampling

To comprehensively assess the impact of varying parameters, an exhaustive sampling approach was adopted. This involved running a full factorial design, thereby calculating all possible combinations of dynamic and static parameters. This method ensures a thorough exploration of the solution space, albeit within the constraints of the nine selected parameters.

The 512 (2^9) iterations required were then executed with the full workflow[20], without interpolations or the SM explored in Chapter 3.4.

20: These 512 simulations ran with all 50 one-year EnergyPlus simulations in parallel over 7h38min, averaging around 50.7s per iteration

3.5.1.3 Methods to Rank Parameter's Influence

The ranking of parameters based on their influence on the GWP was conducted using several statistical techniques. The goal was to establish a hierarchical understanding of each parameter's relative impact on the dynamic GWP results.

(a) Pick and Freeze

The Pick and Freeze analysis consists of generating pairs of outputs by holding the value of a variable of interest (frozen variable) and sampling the other variables (picked variables) [188]. For example, by choosing the industrial evolution parameter as the frozen variable, the remaining 8 parameters are the picked variables. Consequently, the first group of 256 results comprises all outcomes assuming a 0% yearly emission reduction, while the second group includes outcomes with a -2.08% yearly reduction rate, as detailed in Table 3.14. Thereafter, averages for each group are calculated, and the difference between them is analyzed in Table 3.15.

The differences highlight the influence of each parameter on GWP. A higher value indicates a more significant impact, as depicted in Figure 3.21. It becomes evident that the waste, electricity, and industrial sector's decarbonization are the most influential, by a substantial margin, compared to system-level parameters or global warming itself. The evolution of the waste sector alone accounts for a difference of 129 $kgCO_{2-eq}/m^2$, representing about 20% of the total embodied budget outlined in Table 3.3. Further, more comprehensive conclusions will be drawn after the subsequent studies.

Table 3.15: Analysis of Parameter Influence on LCA Results.

Parameter	Dynamic ($kgCO_2 - eq/m^2$)		Static ($kgCO_2 - eq/m^2$)		Difference ($kgCO_2 - eq/m^2$)
	Mean	Std Dev	Mean	Std Dev	
Industrial sector's evolution	839.97	79.66	777.95	79.66	-62.03
Insulation degradation	807.26	85.65	810.66	85.32	+3.40
Infiltration Deg	809.83	86.45	808.09	84.54	-1.74
Global warming	812.39	85.37	805.54	85.51	-6.85
Heat-pump ageing	805.45	84.77	812.47	86.10	+7.02
Electricity mix's evolution	763.31	72.08	854.61	72.40	+91.31
Heat pump technology improvement	812.90	86.22	805.02	84.60	-7.88
Waste sector's evolution	873.63	55.80	744.30	55.80	-129.33
PV system ageing	811.03	85.68	806.89	85.29	-4.14

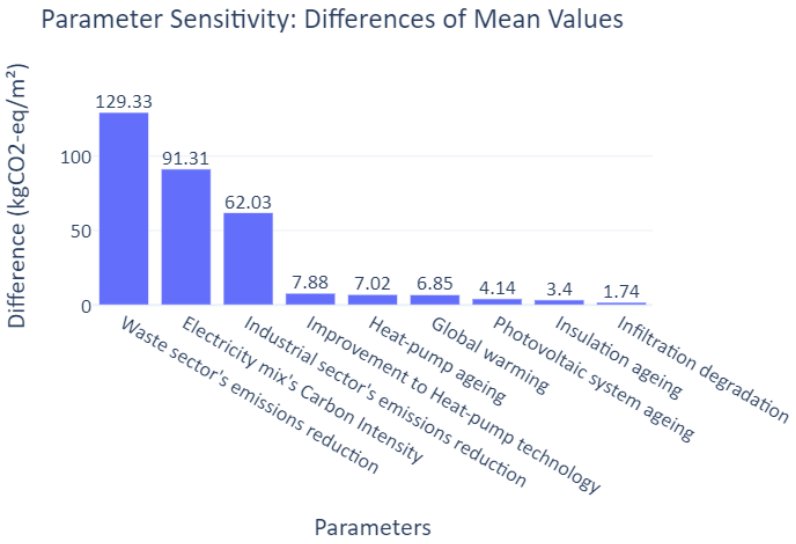

Figure 3.21: Results from the pick and freeze method. The plot shows the ranking of the difference between dynamic and static mean values.

(b) Feature Selection

Feature selection, a widely used technique in machine learning, aims to select a subset of input variables by eliminating irrelevant or non-predictive features [189]. It has been applied in building simulations for predicting energy consumption [190–193], managing smart buildings [194], and identifying key parameters in simulations [195].

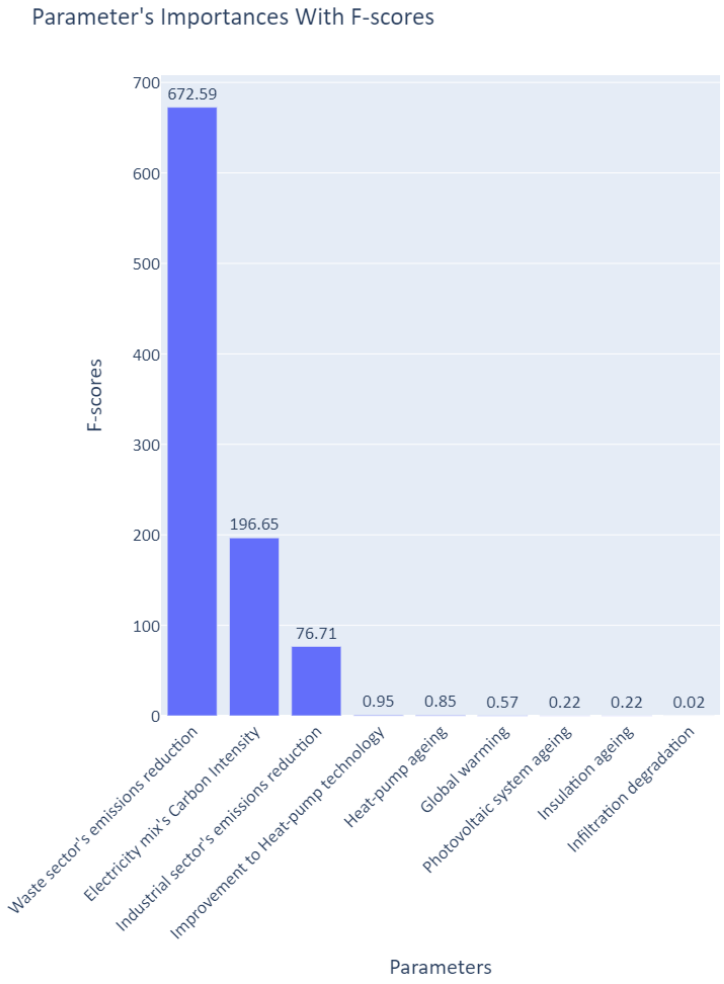

Figure 3.22: Results from feature regression using f-scores.

Feature selection techniques are broadly classified based on the output type of the function: categorical outputs utilize classification algorithms, while continuous outputs apply regression algorithms. In this study, addressing GWP as a continuous value, the "f_regression" technique from the Python library SciKitLearn[21] was employed. This method utilizes the F-statistic from ANOVA (Analysis of Variance) to assess the linear relationship between each feature and the target variable in regression analysis. The ranking of F-scores applied to DPs are shown in Figure 3.22.

21: SciKit Learn is an open-source machine learning library in Python. More information at scikit-learn.org

3.5.1.4 Comparing Results

After evaluating two distinct studies, the same factors consistently impact GWP when transitioning from static to dynamic modelling in the case-study's LCA: waste sector's emissions reduction, electricity mix decarbonization, and industrial sector's emissions reduction. These findings align with expectations, as this DPs indicate substantial decarbonization efforts, even though they are not the most optimistic scenarios.

Conversely, system-level DPs show minimal impact in the shift from static to dynamic modelling. This is expected since they primarily affect OEs and do not evolve as significantly as, for example, the electricity mix. Interestingly, global warming is among the least influential parameters, which is surprising given its common consideration in building performance studies [139, 146, 196–199], often more so than parameters like waste sector's decarbonization.

However, this analysis overlooks user-level parameters, widely recognized in the literature as a significant source of uncertainty in building energy performance [200]. To incorporate these impacts, the discussion will progress to the next sub-chapter.

When juxtaposing these findings with existing studies, such as those by Walker et al. [201], there's a consensus on the critical role of electricity and construction materials decarbonization in the future of the building sector. Similarly, comparable observations are noted regarding global warming.

3.5.2 Uncertainty in Dynamic GWP results

In Chapter 2, the use of Uncertainty and Sensitivity analysis have been identified and highlighted in the context of building simulations.

3.5.2.1 Defining Objective

In this study specifically, the objective is to identify the most influential DPs on the dynamic GWP results so that the modelling process of these parameters can be focused on the ones that generate the most variance.

In the previous sub-chapter, we identified the parameters that gain the most from dynamic modelling, as opposed to being treated statically. These parameters are represented with a range of plausible values in Table 3.8. This analysis aims to determine which of these parameters, within their plausible ranges, have the greatest impact on the variance of the resulting dynamic GWP.

3.5.2.2 Sampling Input Parameters

The Sobol method, recognized for its comprehensive quantitative results, was chosen for this study. However, before the Sobol indices can be computed, it is essential to generate a representative sample of the solution space. Typically, for accurate results, about 1000 iterations per parameter are needed [173]. Given this requirement, at least 13,000 samples were deemed necessary for our case study. To

meet and slightly exceed this threshold, the quasi-random Saltelli sampling method [202] was employed, generating a total of 14,336 samples. This number is derived from the formula $2^N \times (2 * D + 2)$, where 2^N represents the base sample size (with N=13 for our study) and D is the number of parameters being analyzed.

Because of the drastically higher number of samples than in the preceding Sub-Chapter 3.5.1, the SM trained in Chapter 3.4.2 was re-used. These simulations took around 3h14min, with an average of 0.81s per resulting dynamic GWP.

3.5.2.3 Sobol Results

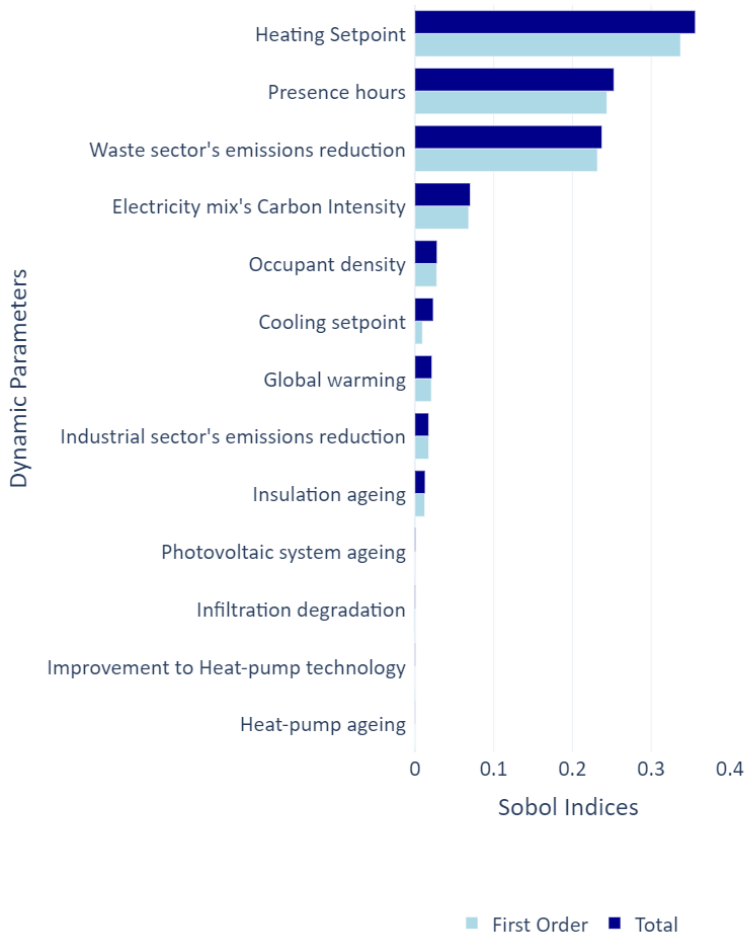

Figure 3.23: Sobol sensitivity analysis results of the dynamic parameters.

Figure 3.23 illustrates the resulting Sobol indices obtained for the DLCA, where we can observe that the occupant-level parameters are the most impactful with heating setpoint temperature and presence hours. This seems reasonable as the main source of uncertainty between energy simulations and reality is occupant behaviour [21, 203].

Third to this parameter is the waste sector's decarbonization, which seems to align with other DLCA studies, such as [83, 166] since, especially in bio-based materials, most EOL emissions occur at the end of the building's life cycle. This gives this sector ample time to evolve, highlighting a great deal of pressure on recycling technologies and on circularity as the current building stock ages. Fourth is CI evolution, despite the French electricity grid already being quite low-carbon. This is supported by Walker's study on LCA assumptions' impact on decision-making [204].

Assuming the building is equipped with a cooling system, the other 2 occupant-level parameters also appear in the top half of the parameters. This significant impact of cooling is tied to the considerations of global warming and the poor thermal performance of the building. This is evidenced by the fact that this parameter has, relatively, the highest interdependence of any other parameter, as the sum of the Sobol indices for "Cooling setpoint" is much greater than the first order index ($ST_{CoolingSetpoint} \gg S1_{CoolingSetpoint}$).

To round up the top half though, is global warming, which is somewhat unexpected, given that other studies, such as [204] have found it to be quite irrelevant towards building GWP.

The 8^{th}-ranked parameter is the decarbonization of the industrial sector, which has a high impact, despite only affecting component replacements. Indeed, in the feasibility study, 66% of the EE were upfront emissions in the A1-5 modules of the building life cycle. Still, the remaining 44% emitted in renovation and replacements are then heavily impacted by the decarbonization prospects of the sector. The remaining Sobol results are all building-level parameters, including all the degradation and individual equipment's technological improvements.

Another point to emphasize from these Sobol results is the very low interactivity between the DP, as evidenced by the very close values of the total and first-order Sobol indices. This observation suggests minimal interaction effects among the parameters, except the cooling setpoint, as highlighted above.

For the context of this analysis, a difference of less than 5% between the total and first-order indices has been considered negligible, indicating insignificant interactivity. This low level of interactivity is explained by how the DPs have been modelled. For example, the decarbonization of the energy sector has been considered in isolation from the evolution of waste and industry sectors, despite the potential for improvements in one sector to influence the others in reality.

3.5.3 Comparing Results

Comparing the results of Sub-Chapter 3.5.1's ranking to Sub-Chapter 3.5.2's, the lack of occupant-level parameters is immediately obvious, as heating setpoint and presence hours together represent around 60% of the total variance observed in the dynamic GWP results.

However, even when ignoring the lack of occupant-level parameters in preceding studies, the rankings still are different, most notably, with the industrial sector's decarbonization being less relevant than global warming. This difference is explained by the very different nature of inputs from each study. While Chapter 3.5.1 compared the sensitivity of the resulting GWP to each parameter being modelled dynamically or statically, Chapter 3.5.2 studied the influence of the different parameters on the variance of dynamic GWP results. Then, the operating range for industry decarbonization, identified in Table 3.8, is tighter than for global warming.

3.5.4 The Impact of Reducing the Number of Parameters

Now, having identified the most influential parameters in the dynamic GWP calculation, we can compare what the results look like if instead of simulating all 13 parameters, only top parameters identified in Figure 3.23 were included. To do that, the maximum and minimum results were calculated with varying quantities of DP. The results are illustrated in Figure 3.24, where dynamic GWP is given by an interval of values. Notably, we highlight that, by cutting down to 7 of the original 13 parameters, a 46% reduction in DPs, the range of values is cut by 26 $kgCO_2 - eq/m^2$, or an 13% loss of information[22].

22: Loss of information here is being defined as the reduction of the dynamic GWP range (light red in Figure 3.24) relative to the interval calculated with all parameters.

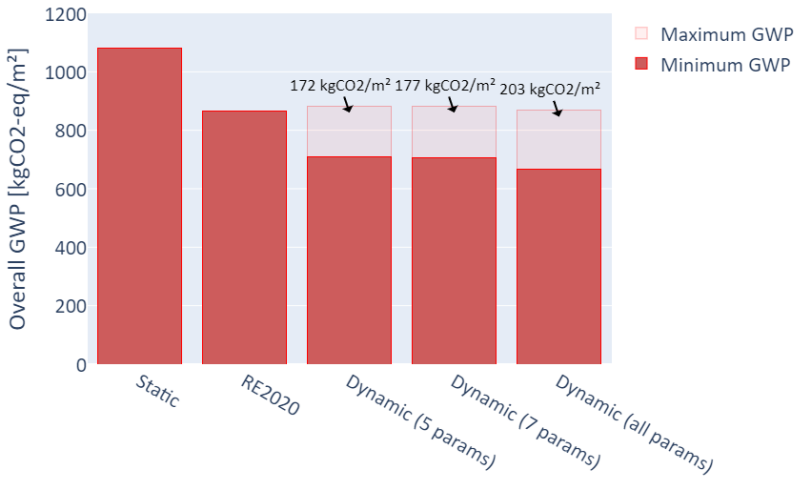

Figure 3.24: Comparing static and dynamic results and the impact of reducing the number of DPs from 13 to 7 and 5 on dynamic GWP.

Reducing the number of DPs to 5 still showed comparable results, with a loss of information of 15% (31 $kgCO_2 - eq/m^2$) despite a 62% cut in Dynamic Parameters.

It is also important to note that the static GWP does not fall within the range of the maximum and minimum values derived from DLCA calculations. This outcome aligns with expectations, as even the conservative forecasts for DPs indicate some level of improvement in aspects like the decarbonization of building-related sectors. This observation is consistent with existing literature, which shows dynamic LCA generally results in lower GWP outcomes, reflecting ongoing policy trends. This occurs even though certain parameters, such as degradation decrease energy performance thereby increasing OE. However, as the SA results indicate, building-level parameters do not significantly impact the overall findings.

One can also see that RE2020 is conservative, yielding a result comparable to the Maximum GWP, but with greater efficiency in terms of calculation length and complexity. However, this efficiency comes at the cost of reduced transparency and detail in the regulatory calculation, since the weighting factor hides the nuance of the different DPs.

3.6 Limitations of the Methodology

This methodology has many limitations and they will be identified in this section. To start, an attributional approach is used in the DLCA application, as opposed to a consequential one. This means that this study does not affect global environmental burdens. However, an interesting development would be to study the effect that a widened application specifically of external level DP would have on the parameters themselves. For instance, with reducing CI of electricity versus the electrification observed in recent years. A consequential approach should take into account the limited capacity of renewable energy. Furthermore, electricity mix scenarios do not impact industry and waste sector decarbonization in this research, as aforementioned.

In addition, the Dynamic Parameters modeling is a major topic when it comes to the limitations of this DLCA application seen in this thesis. A great deal of work is needed to homogenize and facilitate the integration of dynamism into LCA, however, this study does little to advance that subject. Indeed, only DPs for the context of the case-study were modeled, making them difficult to generalize. Specifically, the integration of prospective LCA, which includes the evaluation of the environmental performance of current and emerging technologies [205], remains inadequately

addressed. This aspect is crucial for accurately predicting long-term environmental impacts and ensuring that future innovations align with sustainability goals. Future research should focus on developing universal dynamic parameters that can be applied across various industries and regions to enhance the adaptability and predictive accuracy of LCA methodologies.

When it comes to the simplification techniques demonstrated in this chapter, it is important to highlight that the results obtained do not serve as direct recommendations to future DLCA studies. Instead, this research provides a methodology to identify the ideal simplification approach to each case-study and context. The application to a plethora of distinct buildings would be required for generalised recommendations.

3.7 Conclusions

After identifying Dynamic Life Cycle Assessment (DLCA) as a necessary accuracy-improving methodology to ensure building carbon threshold compliance, this chapter has explored strategies to simplify it in two key ways: by reducing simulation times and by reducing the number of Dynamic Parameters (DP)s.

To identify these improvements, a preliminary case-study was necessary. A workflow based on the literature found in Chapter 2 was built and a research of DPs for the case-study building was executed. This led to 13 total parameters, each of them having an operating interval of uncertainty. The probability density function was assumed constant.

The proposed DLCA workflow was built with an LCI based on the French EPD database (INIES) for the EE calculation. The OE was based on the EnergyPlus calculation engine at an hourly time step for the 50 years of operation of the building. In this DLCA workflow then, 99% of the simulation time was dedicated to OE, despite operational impact representing 25% of total GWP.

To speed up simulation times, two techniques were studied: a linear interpolation between different time steps and the use of Surrogate Model (SM) for the Operational Emissions (OE) calculations. SM emerged as a scientifically sound and efficient option. It substantially reduces simulation times by 98% while RMSE is kept below 7% and R^2 above 0.99. Additionally, the model's uncertainty primarily manifests in the operational emissions calculations, which represent approximately 25% of the overall GWP.

Concerning the modelling of Dynamic Parameters (DP), a battery of analysis aimed at identifying the most impactful parameters was executed. Thanks to this analysis, the number of parameters

could be simplified while keeping a similar level of uncertainty calculation with the dynamic GWP. Indeed, after ranking the parameters in order of impact on dynamic GWP, cutting the number of parameters by 63% resulted in a loss of information of 13%. Thus, the methodology successfully identified some parameters on which more detailed modelling should be focused for this case-study. Indeed, additional parameters such as the building lifecycle and that of the different building components could also be integrated and have shown to be great contributors towards GWP, as demonstrated in [67, 102].

Now, with flexible and manageable simulation times, DLCA can be brought to the decision-making process more easily, which shall be explored in the following chapter.

Integrating Dynamic LCA into Retrofit Decision-Making Methods

4

Chapter 3 highlighted some of the uncertainties associated with the multi-decade lifespan of buildings and their impacts on Life Cycle Assessment (LCA). It also discussed the simplification of these dynamic variables in relation to Global Warming Potential (GWP) assessment.

This fourth chapter builds upon the established knowledge and framework, proposing a method to guide the Decision-Making (DM) process towards compliance to French regulation carbon threshold. It involves developing action plans that take into account the main Dynamic Parameters (DP) identified in Chapter 3, thereby enhancing the robustness of decisions.

4.1 Building the Framework for Decision-Making Support

As buildings age, it becomes crucial to consider their maintenance as a part of their lifespans. Given the high prevalence of energy-inefficient buildings requiring substantial renovations, and with European renovation rates projected to rise to between 2 and 3% [89], post-occupancy DM methods become essential developments.

In this section, a post-occupancy DM methodology will be developed, starting with the process of identifying potential Carbon Mitigation Measure (CMM)s for CB compliance.

4.1.1 Identifying Carbon Mitigation Measures in Post-Occupancy Stages

4.1.1.1 Carbon-Mitigation Measures and Its Perimeter

CMMs encompass actions that enhance a building's environmental performance, including system and envelope improvements, changes in occupant behaviour, etc. CMMs during post-occupancy then, impact only the B and C modules.

For example, encouraging lower scheduler setpoints temperatures in heating systems is a CMM. However, this thesis excludes occupant-related measures from the DM process, focusing solely on refurbishments - actions that enhance an existing building's performance through renovations and the addition of renewable energy production [206]. The reason to leave occupant-level measures aside is due to the intricacies of optimizing such actions, which only impact Operational Emissions (OE)s. Since this study fails to consider other performance indicators, such as indoor comfort, the outcome of a DM process that only evaluates GWP would be unsurprising.

4.1.1.2 Distinguishing Renovation and Replacement

In addition, the terminology in the field of building adaptation projects in the literature (ie. retrofit, renovation, replacement) is not very consistent [206]. Then, to maintain accordance with the EN 15978 norm, we propose to define and distinguish the terms renovation and replacement as per Table 4.1, while retrofit will be used an umbrella term including both.

Table 4.1: Comparison of renovation and replacement in building adaptation projects.

Aspect	Renovation	Replacement
Definition	Addition of building components that change the building's energy and environmental performance.	Substitution of building components that have a reference service lives inferior to that of the buildings.
Purpose	To enhance energy and environmental performance of the building.	To maintain the functional integrity while improving the environmental performance of the building.
Examples	Installing renewable energy systems on an unequipped building	Replacing existing HVAC systems.

To identify the possible replacement actions a three-step filtering process of the building components was executed:

1. Identify the building components that have a service life that is less than the building's life cycle.
2. Identify the components that have an impact on both the building's operational and embodied emissions.
3. Rank the remaining components in terms of overall Global Warming Potential.

The first step filters out all components that are not replaced during the building's reference service life. The second is introduced to simplify the DM process, as comparing components that only

impact Embodied Emission (EE), which do not require a Multi-Objective Optimization (MOO). Indeed, the difficulty of the DM process comes from the intricate relationships that exist between EEs and OEs. The third step helps to prioritise the components that contribute the most to the building's CB and, since this is a permutation problem, reducing the number of variables is a crucial step towards reasonable simulation times.

As for identifying renovation measures, the process is less generic and more building-dependent. In the literature, the most typical renovation choices relate to improvements to the thermal envelope's performance together (ie. thermal insulation of opaque and glazed surfaces) and with the production of local renewable energy, namely with photovoltaic (PV) panels.

Keeping with the trend of this thesis of including time as a variable, another CMM included in this work is supporting decision-makers in choosing *when* these actions should be implemented.

4.1.1.3 Scheduling Carbon-Mitigation Measures

As discussed in Chapter 3, incorporating time into building GWP evaluations significantly impacts LCA results, warranting its inclusion in CB assessments. This chapter now argues for integrating this temporal aspect into the DM process, especially concerning renovations and replacements.

This integration utilizes the reference service lives of building components from their EPDs, as defined by EN 15804 [207]. These service lives are set by manufacturers and, in typical LCA approaches, components are replaced by identical ones at the end of their lifespans.

However, in reality, they can be replaced by any functionally equivalent component, not only at the end of their lifespan but at any point until then. Therefore, the timing of replacements is incorporated into the CMM as defined in Equation 4.1, where $y_{current}$ denotes the current year and $y_{ComponentEOL}$ the year the component reaches its End-Of-Life.

$$y_{replacement} \in [y_{current}, y_{ComponentEOL}[\quad , y \in \mathbb{Z} \tag{4.1}$$

Conversely, for renovations, the upper bound is nonexistent since they involve adding new components, thereby modifying building performance. Thus, $y_{renovation}$ is defined in Equation 4.2, where $y_{BuildingEOL}$ is the building's EOL.

$$y_{renovation} \in [y_{current}, y_{BuildingEOL}[\quad , y \in \mathbb{Z} \tag{4.2}$$

4.1.2 Full Workflow Proposal

The Decision-Making support methodology in this thesis is based on the diagram shown in Figure 4.1.

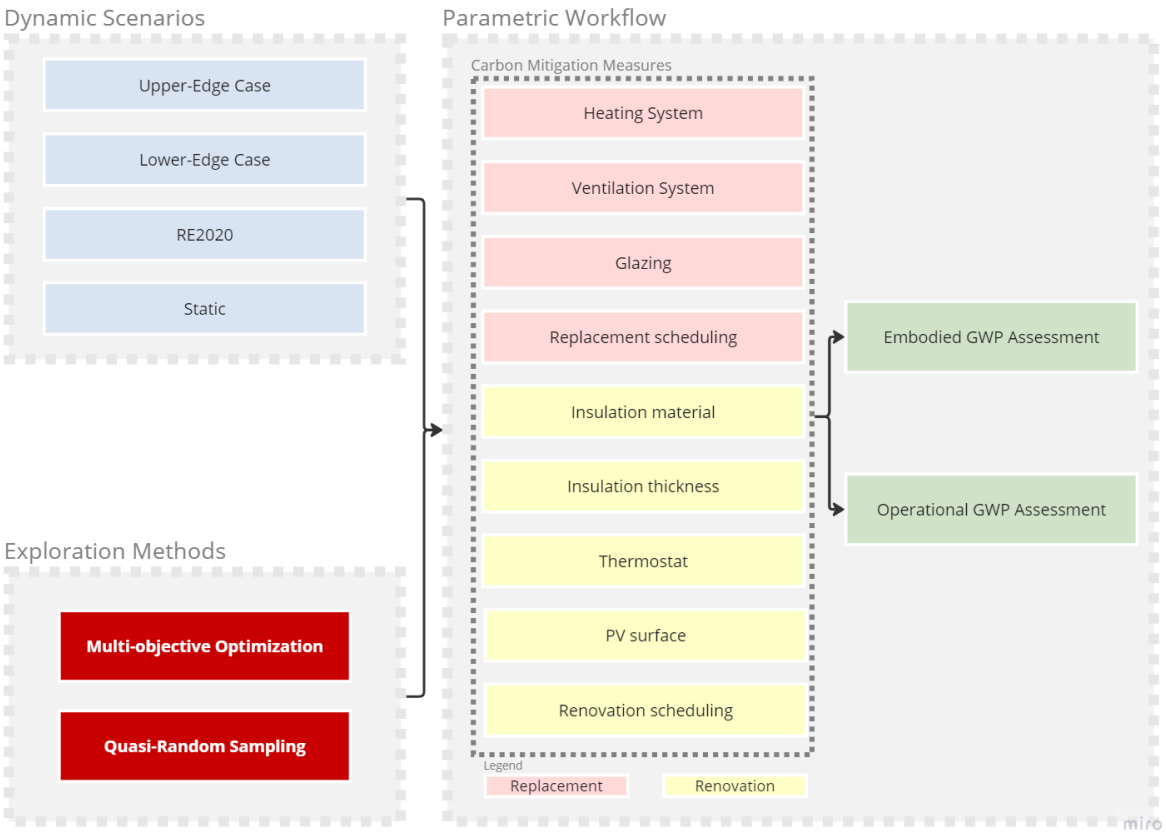

Figure 4.1: Full workflow for the Decision-Making process.

The DM parametric workflow evaluates EE and OE separately since the budgets for these values are defined separately. The solution space will be explored through two methods: a Multi-Objective Optimization (MOO) and a statistical evaluation, following the recommendations from the literature uncovered in Chapter 2.3.3.

Of course, the DLCA approach is also integrated into the methodology, so the next sub-section will be dedicated to detailing the dynamic scenarios listed in Figure 4.1.

4.1.3 The Dynamic Parameter Integration in the Decision-Making Process

DLCA involves accounting for uncertainties related to temporal factors. When it comes to uncertainties in DM, robustness analysis is crucial. It aims "to identify strategies that perform well and are minimally affected by uncertain future conditions" [204].

Robustness analysis is generally divided into two categories: probability-based and scenario-based. Probabilistic methods need detailed information about uncertainties, such as probability density functions, enabling evaluation in terms of probabilities and confidence intervals [208]. However, in cases like this, where the probabilities of DP are unknown, scenario-based methods are more appropriate [208], as it was established in Chapter 2.

4.1.3.1 The Scenarios for Decision-Making

This part of the thesis then, will be dedicated to constructing said scenarios. However, before implementing the DM workflow with all DPs, came the recognition that only a few of them represent the most variance in terms of the results obtained. Indeed, thanks to the Sensitivity Analysis (SA) demonstrated in Figure 3.23, only the most influential parameters will be included in this study, those being: electricity mix evolution, waste sector evolution, heating setpoint temperature, daily presence hours, industrial sector evolution, occupant density and global warming.

The choice to include 7 parameters, instead of fewer was partially due to the willingness to include climate change in this study, as global warming is often included in long-term building simulations such as this one. Despite this being relatively low in the rankings (in 7^{th}).

(a) Edge-Case Dynamic Scenarios

Table 4.2: The dynamic and static scenarios to be used in the decision-making methodology application.

Dynamic Parameters	Lower-Edge	Upper-Edge	Static
Yearly Electricity mix's evolution	-2.3%	-2.6%	0%
Yearly Waste sector evolution	-1.34%	-1.89%	0%
Heating temperature setpoint	22°C	18°C	19°C
Presence Hours	20h	13h	16h30
Yearly Industrial sector evolution	-1.85%	-2.31%	0%
Number of occupants	8 persons	2 persons	5 persons
Global warming	RCP8.5	RCP2.6	TMY

Upon choosing the DPs then, with two single-objective optimizations, the overall GWP was maximized and minimized to find the combination of DPs that yield the lowest and highest results within the intervals defined in Table 3.8. The parameter's values were then used to construct edge case scenarios shown in Table 4.2. The

upper-edge case produces the highest GWP and the lower-edge produces the lowest.

(b) Dynamic RE2020 Scenario

In addition to these two dynamic scenarios, another DLCA approach included in this work is based on RE2020, which follows the French regulatory framework. This method, described in Chapter 2.2.3.2, is unique to France, as it is the only country to incorporate Dynamic Life Cycle Assessment in its building performance regulations. However, the RE2020 DLCA framework differs significantly from the one implemented in this thesis, as it proposes only one scenario for its single DP.

(c) Static Scenario

Finally, to be able to compare aforementioned DLCA approaches to a baseline, a static LCA has been included. Since the RE2020 also includes such a methodology, this thesis largely follows this regulation.

Consequently, this LCA approach bears no changes to the building or its environment throughout its life cycle. This assumption also has been quantified in Table 4.2. However, for user-level parameters, which already are static, a simple mean value has been taken between the bounds.

4.1.4 Exploring the Solution Space

In the building DM process, identifying the most suitable solution is intricate and time-intensive, as this combinatorial challenge grows exponentially with each added parameter. For instance, a comprehensive parametric study aiming to minimize energy consumption across 5 parameters, each with 4 options, necessitates 4^5 (or 1024) simulations. Consequently, exhaustive simulations are impractical for complex DM processes typical in building design. Indeed, such extensive parametric workflows can lead to an overwhelming amount of information [58].

To manage this complexity, two approaches have been previously outlined in Chapter 2.3.3. The first approach involves a statistical sampling of input parameters to gain a representative understanding of the solution space. The second approach focuses on optimizing variables to minimize OE and EE, thus efficiently navigating the solution space.

In this section, the utility of these approaches will be detailed and in the case-study application, a comparison between the approaches will be made. A secondary objective of this chapter then, is to identify appropriate techniques for DM process in the way of CB compliance.

4.1.4.1 Statistical evaluation

As observed in Chapter 2, statistical evaluations serve various purposes. In addition to visualization techniques such as Parallel Coordinates Plot (PCP), they are instrumental for conducting sensitivity, uncertainty, and multivariate analyses. Employing the same random sample creates an extensive knowledge database that can be leveraged by various DM assistance methods [58].

Two methods incorporated into this work include the PCP for interactive exploration of design solutions and the calculation of Sobol indices for CMMs. This dual functionality enhances the DM process by providing a comprehensive tool for exploring solution spaces and gaining insights into the impact of different design choices.

However, despite being constructed with a statistically representative set of input parameters, a large sample size remains necessary. An alternative method for navigating the solution space more efficiently is the use of optimization algorithms, which also present their own set of challenges and drawbacks.

4.1.4.2 Optimization

While optimizations may not provide a comprehensive exploration of the entire solution space, they are a widespread tool in building design, particularly when employing Multi-Objective Optimization (MOO), which assemble a subspace of optimal solutions that can be explored.

(a) Multi-Objective Optimization Algorithm

In building design and renovation, a variety of optimization algorithms are available. However, as discussed in Chapter 2.3.3, genetic algorithm (GA) is most often used in studies of this field, as it is particularly suitable for handling non-linear and non-differentiable objective functions while circumventing local minima issues [117].

(b) Objective Functions

The MOO in this study focuses on two objectives: Embodied Emission and Operational Emissions. The decision to optimize these objectives separately is based on how they are typically defined and measured in different contexts.

The calculation of EE involves straightforward arithmetic based on the BOQ presented in Appendix B. While OE will be reliant on the same energy simulations detailed in Chapter 3.

4.2 Preparing the Case-Study for the Methodology

Now that the methodology has been delineated, it is essential to delve into the specifics of the case study that will serve as the initial testing ground for this approach.

4.2.1 Introduction to the Case Study

The case study for this DM support methodology is consistent with the one detailed in Table 3.1 of Chapter 3. In this section, we will examine the building's envelope and systems more closely to pinpoint potential CMMs. Subsequently, a Busisness-As-Usual (BAU) scenario will be formulated.

4.2.1.1 Determining the Building's Age

Similar to Chapter 3, the case-study's life cycle is set at 50 years, which corresponds to the French regulation for new buildings but is used also for this recent building.

To identify the CMMs, the building's age needs to be determined first. As previously mentioned in Chapter 4.1.1.3, the timing of applying the methodology is a crucial factor in shaping the retrofit plan's schedule. The current workflow allows for renovations and replacements to begin from the methodology's implementation date. The building's GWP is evaluated annually, so it's presumed that the CMMs influence the OE at the start of each year. For simplicity, the EEs are also tallied in the same year.

Referring to Table 3.1, the building was erected in 2017. Given that the DPs in Chapter 3 were identified using data and insights from between 2020 and 2022, it's assumed for this case study that the building has been operational for 4 years, when the owners opt to implement this thesis's methodology. Consequently, the earliest

feasible time for retrofit actions to have an impact of yearly GWP is from the building's 5^{th} year.

With this critical temporal variable in the DM process at post-occupancy stages established, we can now define the CMMs pertinent to this particular case study.

4.2.1.2 Carbon Mitigation Measures for the Case Study

Reflecting on Chapter 4.1.1, the identification of suitable CMM is divided into renovations and replacements. These will be delineated separately for this case-study.

(a) Replacements

An analysis of the building's BOQ revealed 4 components that meet the criteria in Chapter 4.1.1.2: a service life shorter than the building's life cycle, impact on both operational and embodied emissions, and highest overall GWP. These components, detailed in Table 4.3, require replacement and have both embodied and operational impacts.

Table 4.3: The components listed in this table were chosen to be included in the replacement measures. These components are taken from the INIES database [143] and represent a slice of the components listed in Table B.1

Component	Functional Unit	Quantity	Service Life (years)	Interval (years)	LC phases (kgCO2-eq/unit)		
					A	B	C
Joules Effect Electrical Radiator	1 unit providing up to 1 kW of heating	9	17	[5, 17]	512	1800	6.61
Thermodynamic Water Heater	1 heat-pump producing DHW with a 200L tank	1	17	[5, 17]	2320	4880	347
Humidity-Controlled Simple-Flow Ventilation	1 ventilation unit ensuring up to 59 m^3/h of fresh air	3	17	[5, 17]	46	97	4.17
Double-Glazed Windows with Aluminium/PVC Framing	1 m^2 of opening with U = 1.2 W/(m^2.K)	10	30	[5, 30]	304	0	9.7

It's important to note that the heating and Domestic Hot Water (DHW) systems are linked to energy and water consumption in their use phases (modules B6 - Operational water use - and B7 - Operational energy use). These emissions, stated in the components' EPDs, are based on standardized usage values and are used here to identify the major contributors to the building's EIs. However, these

emission values are not used in this thesis' OE calculations. Indeed, B6 emissions are calculated through an EnergyPlus simulation, while B7 is outside the scope of this LCA.

With the identification of components for potential replacement, alternatives were explored. The next three tables present alternative options, starting with heating and DHW systems, which are closely linked. The chosen systems will be evaluated together, as illustrated in Table 4.4. This includes considering a shared air-water heat-pump for both heating and DHW, in contrast to other options that require separate systems.

All components and associated values listed in this section have been taken from the INIES database of EPDs. The unitary values and specific component names can be found in Appendix C.

Table 4.4: Heating and DHW production systems considered to improve the buildings' environmental performance. Specific information about the EPDs used can be found in Table C.1.

Heating System	DHW System	Unit	Efficiency / COP	Embodied GWP (kgCO2-eq)
Joules Effect Radiator (BAU)	Thermodynamic Water Heater	1 unit producing up to 1 kW of heat	1.00 / 3.5	826
Wood-pellet Boiler	Thermodynamic Water Heater	1 unit producing up to 1 kW of heat	0.93 / 3.5	1645
Air-Water Heat-Pump	Same Heat-Pump	1 unit producing up to 1 kW of heat	3.72	1940
Air-Air Heat Pump	Thermodynamic Water Heater	1 unit producing up to 1 kW of heat	3.15/3.5	1923

For Controlled Mechanical Ventilation (CMV), the choice was between maintaining the existing single-flow system or upgrading to a more material-intensive double-flow system with heat recovery is shown in Table 4.5. The latter system, while having a higher embodied GWP, offers significant thermal energy recovery. The EE costs are linked to the extensive air distribution system required to extract and supply air in a double-flow arrangement. However, the associated intervention that is required to install those ducts has not been taken into account.

Table 4.5: Ventilation systems studied to improve the buildings' environmental performance. Specific information about the EPDs used can be found in Table C.1.

Ventilation System	Functional Unit	Heat recovery	Embodied GWP (kgCO2-eq)
Single-flow CMV (BAU)	1 unit	No	792
Double-flow CMV + PVC ducts	1 unit	85%	4450

Lastly, the case study considers replacements for glazed surfaces.

Initially equipped with double-glazed PVC windows, various alternative options with different thermal performances and materials were identified, as listed in Table 4.6.

Table 4.6: Glazing alternatives studied to improve the buildings' environmental performance. In this table, in addition to the glazing type, frame material and embodied GWP, are the U-value and the Solar Heat Gain Coefficient (SHGC) of each design alternative. Specific information about the EPDs used can be found in Table C.2.

Glazing type	Funcitonal Unit	Frame Material	U-value (W/(m².K)	SHGC	Embodied GWP (kgCO2-eq/m²)
Double-glazed (BAU)	1m² of glazed surface	Alu + PVC	1.2	0.8	128
Triple-glazed	1m² of glazed surface	Alu + PVC	1.0	0.5	170
Double-glazed	1m² of glazed surface	Wood	1.4	0.7	51
Triple-glazed	1m² of glazed surface	Wood	1.2	0.5	66
Double-glazed	1m² of glazed surface	Wood + Alu	1.1	0.7	195
Triple-glazed	1m² of glazed surface	Wood + Alu	0.8	0.5	368

This detailed examination of potential replacements paves the way for pinpointing the optimal CMM for enhanced environmental performance and adherence to carbon budgets. However, to complete the picture, it is essential to consider renovations as well.

(b) Renovations

For renovations, two key measures frequently examined in the literature are identified: enhancing the building's thermal insulation and incorporating renewable energy generation, particularly photovoltaic (PV) panels. The former aims to reduce heating energy requirements, while the latter decreases the average electricity Carbon Intensity (CI). In addition, we also study the installation of a scheduler for the heating system.

Following the approach used for replacements, the renovation alternatives will also be presented in tabular format. The first table, Table 4.7, includes all a combination of materials and thicknesses for external insulation. For each combination, the table lists the thickness and embodied GWP per square meter of installation. This approach ensures a comprehensive overview of the insulation options, allowing for an informed decision on the most effective and sustainable choice. The environmental cost of the intervention and wall coverings for the new external insulation is not taken into account.

The exploration of PV systems and schedulers as part of the renovation measures adds another layer to the building's potential for energy efficiency and carbon mitigation.

Table 4.7: Insulation materials and thicknesses alternatives studied to improve the buildings' environmental performance. Specific information about the EPDs used can be found in Table C.3.

Material Embodied GWP [$kgCO_2-eq/m^2$]	**PU**	**Cotton Wool**	**Glass Wool**	**Wood Fibre**	**Compressed Straw Panel**	**Wood Straw**
λ (W/m.K)	0.026	0.038	0.035	0.036	0.039	0.052
Thinnest	BAU (10cm)	6 cm | -0.30	14 cm | 3.2	4 cm | -0.13	10 cm | 0.22	10 cm | -11
Thin	5.4 cm | 14	8 cm | -0.39	16 cm | 3.8	8 cm | -0.48	20 cm | 0.44	20 cm | -17
Thick	10 cm | 17	10 cm | -0.45	20 cm | 5.2	10 cm | -0.84	30 cm | 0.66	30 cm | -24
Thickest	14 cm | 20	16 cm | -0.78	22 cm | 6.4	20 cm | -2.6	40 cm | 0.88	40 cm | -30

For the PV system, an EPD detailing the EI of a square meter of roof-mounted PV panels was identified. This includes not just the panels themselves but also associated components like converters, cables, connectors, and mounting systems. The inclusion of these components provides a comprehensive view of the PV system's environmental footprint.

As for the OE of the renewable energy production, the energy that is produced and consumed locally has no net impact on GWP. However, for excess energy exported to the grid, a symmetrical value was assumed, where exported energy assumes the grid's negative CI at that given time. This is a simple, but often criticized method [126].

In contrast, Walker et al. recommended the pro-rata method [201], where the EEs of the PV panels are allocated to the building's LCA in proportion to the self-consumption rate [209].

However, in this thesis' dynamic OEs calculations, energy demand as well as PV production and electricity CI vary not only hourly, but also at an yearly time-steps. This renders the calculation of dynamic self-consumption rate another methodological hurdle to be investigated. Since this additional complexity lies outside the scope of the thesis, the more simplistic approach was chosen.

Additionally, the production location of PV panels significantly affects their EE. For instance, the Voltec panels considered here involve a complex supply chain: silicon is sourced from Norway, upgraded in Germany, then returned to Norway for monocrystal

formation, and finally processed into cells in Taiwan. Each step's energy mix and transport impacts the panels' EE.

Alongside the PV system, the potential benefits of installing a scheduler are also considered. This tool can facilitate more effective management by occupants during unoccupied hours of the heating system, allowing for a reduction in the heating setpoint by 4°C. Without a scheduler, it is assumed that the temperature setpoint remains constant, potentially leading to unnecessary energy usage and increased emissions.

Given their interrelated benefits and impacts, the PV system and scheduler options are combined in Table 4.8.

Table 4.8: Information on the PV panel and scheduler installation as renovation measures. Specific information about the EPDs used can be found in Table C.4.

Added Component	Functional Unit	Service Life	Embodied GWP $[kgCO_2 - eq]$
PV system	1 m² of PV installation and associated converter and mounting system	30 years	137
Scheduler	1 wall-mounted scheduler to control a zone's set-point temperature	10 years	134

The scheduling of the identified CMMs is a critical aspect of the DM process, especially for renovations. As outlined in Equation 4.3, the timeline for implementing these measures in the case-study extends from the 5^{th} year of the building's life cycle up to the 49^{th} year, just before its EOL.

$$y_{renovation} = [5, 50[\quad , y \in \mathbb{Z} \tag{4.3}$$

This Equation 4.3 sets the framework within which renovations can be undertaken. A crucial assumption here is that any renovations implemented will influence the timing of subsequent replacements. For example, if a PV system is installed in the building's 5^{th} year, the life cycle of this addition will be factored into future replacement schedules. In this instance, the PV system would be due for replacement after 30 years, in the building's 35^{th} year.

This past Sub-Chapter 4.2.1.2, detailed then, the EE calculations for the DM. However, OE calculations are the most time-consuming step in DLCA and thus, in the following section, a technique to solve this issue will be explored.

4.2.1.3 Surrogate Model for Decision-Making

In the Chapter 3 application of DLCA, the advantages of using a Surrogate Model (SM) in building energy simulations were

demonstrated and thus, this tool's use is extended to this chapter on DM support as well. These statistical models are used differently in the field, as noted in Chapter 2, however here, its purpose is to accelerate simulation times so that the statistical and optimization results are obtained in a matter of minutes rather than days.

(a) Modelling Inputs

To enhance the complexity of modelling various design alternatives, this thesis incorporates DPs identified in preceding chapters. A new model is proposed, expanding the number of input parameters beyond those initially listed in Table 3.11. Concurrently, the refinement process in Chapter 3 has led to the exclusion of certain parameters, ensuring that only the most pertinent DPs are integrated into the DM process. The selected input variables and their training intervals are detailed in Table 4.9, distinguishing DPs from inputs specific to the DM process in the "Input Classification" column.

Newly incorporated inputs include insulation design options. The SM ideally considers two factors: insulation thickness and thermal properties. To maintain thermal resistance comparability, markedly different thicknesses were assigned to each material, as outlined in Table 4.7. Modelling diverse material conductivities require training across a broad thickness range, from 5 cm to 50 cm. Therefore, the model would include 40 cm of EPS insulation, an unrealistic amount. To avoid this impractical scenario, the model is trained using varied thicknesses of a single insulation material: EPS. Subsequent additions of other materials are converted to an equivalent PU thickness for the same thermal conductivity.

For example, adding 16 cm of cotton fibre insulation to an existing 10 cm PU layer (10cm, thermal conductivity 0.03 W/(m.K)) involves separate thermal resistance calculations for each layer, later combined to determine the new resistance. This process, detailed in Equation 4.4 through Equation 4.7, simplifies training by reducing the parameter count and necessary sample size for achieving the same coefficient of determination.

As a consequence of this methodological choice, it does not consider the difference in the new material's heat capacity. However, considering this extra insulation is installed in the exterior of the walls, this inertia would not play a big role in the building's indoor temperature.

$$R_{PU} = l_{BAU}/\lambda_{PU} = 3.33 m^2.K/W \tag{4.4}$$

$$R_{CottonFibre} = l_{added}/\lambda_{CottonFibre} = 4.21m^2.K/W \quad (4.5)$$

$$R_{renovated} = R_{PU} + R_{CottonFibre} = 7.54m^2.K/W \quad (4.6)$$

$$l_{EPS_equivalent} = R_{renovated} * \lambda_{PU} = 0.22m \quad (4.7)$$

Meanwhile, glazing alternatives have 2 input parameters associated with them: the glazing surface's U-value and Solar Heat Gain Coefficient (SHGC), since these two variables impact the thermal performance of the building differently, through conduction and radiation, respectively.

As for ventilation and scheduler modelling, both are boolean decisions, as defined in the preceding sub-section. Finally, for PV system modelling, the installation's surface is varied from zero to 32 m². This upper value has been defined by analysing the case-study and identifying the maximum roof surface facing the southernmost orientation. This simplification assumption is the optimization of the panel's orientations and positions to maximize self-sufficiency rates is not the objective of this work.

(b) Model Sampling and Training

Having defined the inputs, we can now initiate the sampling process. The "Parameter Type" column in Table 4.9 indicates whether a parameter's intervals are continuous ($\mathbb{R}$) or integers ($\mathbb{Z}$). This distinction is crucial during sampling, particularly for variables like ventilation, which are boolean; in such cases, floating points between 0 and 1 are not applicable.

From this point forward then, the choices in tools for this work will be important due to the mixed-integer nature of the problem. For this reason, Surrogate Modelling Toolbox was chosen for this important methodological step. SAlib[1] Python library bases on the work by Saves et al. [210], where the authors propose a new kernel-based Gussian Process approach to handling mixed-integer problems, denoted Exponential Homoscedastic Hypersphere.

1: For more information: salib.readthedocs.io/

Associated to a Latin Hypercube Sampling (LHS) also capable of handling mixed-integer sampling, the resulting model achieved an Coefficient of Determination (R^2) and relative Root Mean Square Error (RMSE) of 0.992 and 8.06%, respectively, with 1000 training samples.

Table 4.9: List of the training inputs and intervals for the second SM of this thesis, which excludes some half of the DPs, but includes the different design alternatives. The purpose of each parameter is differentiated in the column "Input Classification", where DP represents parameters used in the DLCA calculation and DM represents the different design choices simulated.

Input Classification	Paramater Name	Model Variable	Parameter Type	Training Interval	Unit
DP	Electricity Mix Evolution	Average Carbon Intensity	$\mathbb{R}$	[17.9, 78.3]	gCO_2/kWh
DP	Heating Setpoint	Heating Temperature Setpoint	$\mathbb{R}$	[18, 22]	°C
DP	Presence Hours	Average number of hours daily with occupancy	$\mathbb{R}$	[13, 20]	hours
DP	Occupant Density	Number of occupants	$\mathbb{R}$	[2, 8]	person
DP	Global Warming	Modified Weather File	$\mathbb{Z}$	RCP 2.6, 4.5 and 8.5	-
DM	Heat+DHW Replacement	Efficiency/COP & CI	$\mathbb{Z}$	[0, 3]	-
DM	Ventilation Sys. Replacement	Heat Recovery	Boolean	(0, 1)	W/(m².K)
DM	Glazing Replacement	U-Value	$\mathbb{R}$	[0.5, 0.8]	-
DM	Glazing Replacement	SHGC	$\mathbb{R}$	[0, 5]	-
DM	Insulation Renovation	Thickness	$\mathbb{R}$	[10, 50]	cm
DM	PV Renovation	PV panel surface	$\mathbb{Z}$	[0, 32]	m²
DM	scheduler Renovation	Unoccupied Heating Setpoint	Boolean	(0, 1)	-

This sample is not to be confused with the sample used directly in the DM process. Here, the LHS is used strictly to create the sample for the SM training.

4.3 Results of Case-study Application Under Different Scenarios

In this section, the results of applying the methodology to the upper-edge case scenario will be presented and thoroughly discussed. The other scenarios have also been simulated and their results have been included in Appendix D.

4.3.1 Upper-Edge Scenario

4.3.1.1 Statistical Evaluation Results

For a representative overview of the solution space, statistical methods are an appropriate exploration tool. The Monte-Carlo Saltelli method was chosen for this application, similar to Chapter 3, with 13,000 samples to create a representative array of the solution space. Given the presence of 12 CMMs, there are more than 1,000 samples per DM parameter. With the sampling method established, the first graphical representation to be explored in this results section is a PCP.

Parallel coordinates, effective in representing multi-dimensional data [211], allow for the visualization of complex datasets across various fields [212]. This method displays data as polylines intersecting parallel axes, enabling the assessment of multiple parameters simultaneously [114]. Interactive features like brushing facilitate data filtering, crucial in building design.

In Figure 4.2 then, the 12 CMMs are drawn along the horizontal space in addition to OE, EE and overall emissions. Each vertical line has all values that a given parameter can assume, both for continuous values, such as the resulting emissions, and for discrete values, such as the choice of insulation material.

To test the interactivity aspect of PCP, the CBs have been applied to OE and EE in Figure 4.3, represented by the pink intervals. Accordingly, thousands of lines that were visible before, have been greyed out, leaving only a couple of combinations of parameters left.

Further analysis indicates that some measures are no longer feasible options, starting with the heating system. In the first vertical line, no solution is available neither with wood pellet boiler nor with electrical radiators. Additionally, it seems that this replacement of this component needs to be made before year 11, or in 6 years. There is, of course, the possibility that a solution is possible by replacing the heating at year 13 or after, since this PCP was not built by exhaustively simulating all possible combinations.

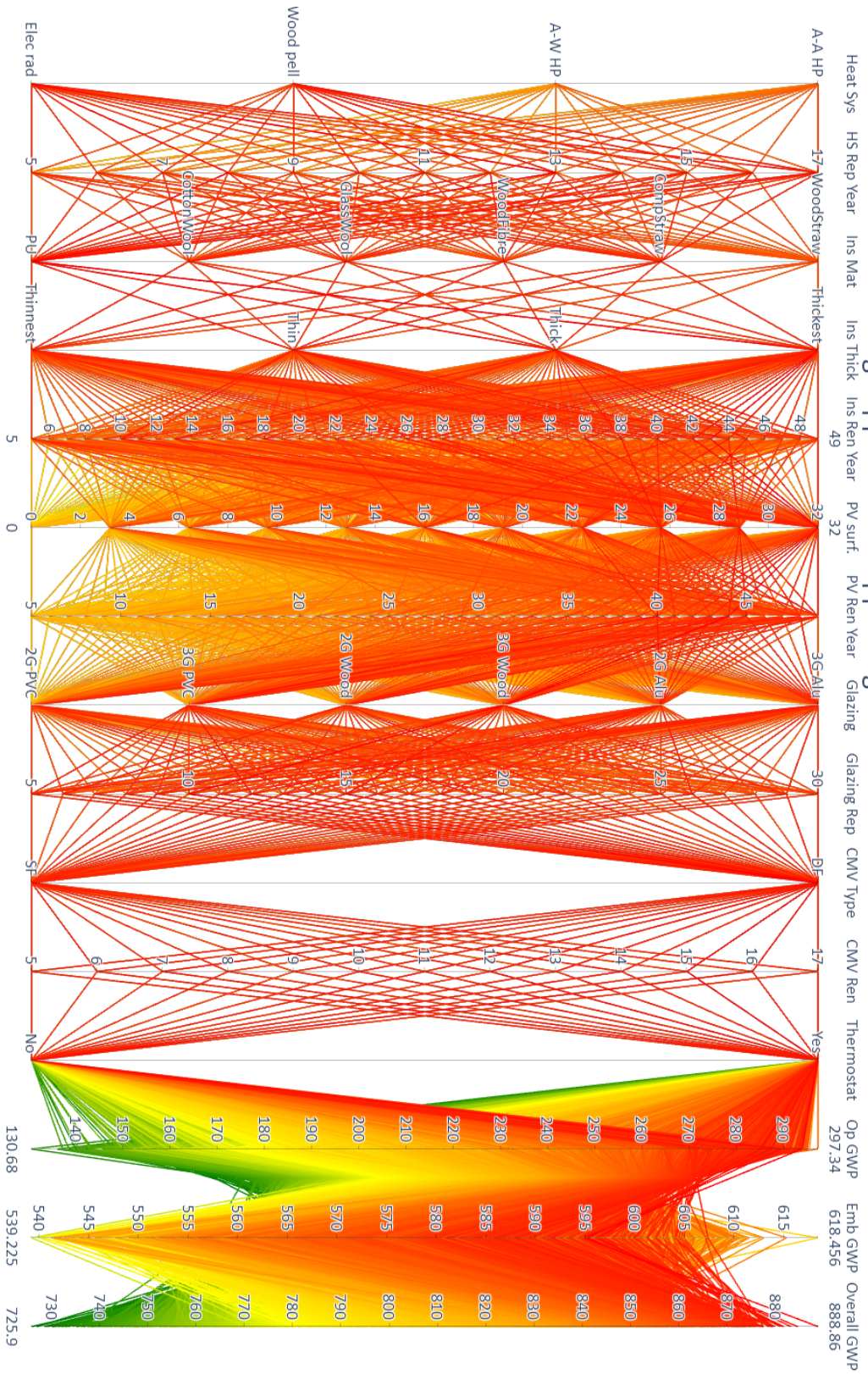

Figure 4.2: This PCP includes over 13k simulations under the Upper-Edge scenario, allowing the decision-makers to find solutions that follow their own constraints.

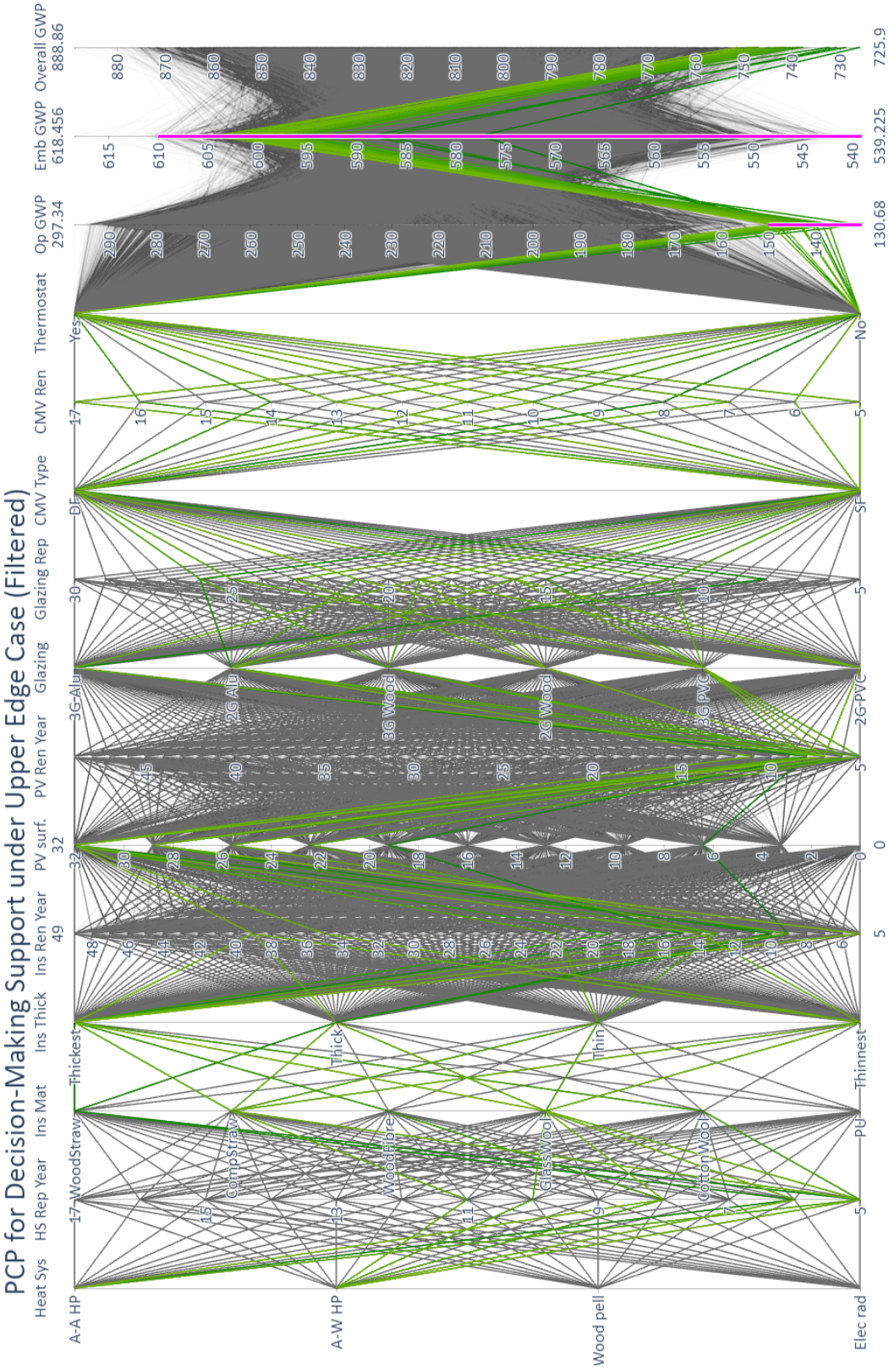

Figure 4.3: This PCP includes over 13k simulations under the Upper-Edge scenario with the carbon budgets appearing as filters.

Indeed, a random sample of the parameters was used. But given the significant number of simulations realized, this graphical representation gives the ability for the decision-maker to explore the parameters and find combinations that answer to other limitations, that an optimization might not consider. An example of a constraint that is not taken into account in this thesis is cost or architectural limits, such as wall thickness. For instance, the optimization always recommended the installation of 40 cm of wood straw which could, for instance, present architectural challenges. In a PCP though, the decision-maker can filter out solutions that rely on such practice, according to their needs and constraints.

To make more conclusions on this dataset, Figure 4.4 was built. In it, the reader will find the frequency each design choice appears among all 42 carbon-compliant solutions, of the 13k simulations initially executed. This analysis provides a more holistic understanding of which measures most often contribute towards budgetary compliance.

When analyzing these results, the same conclusion on the heating system can be made as before: heat-pump should be installed before year 11. Although now, the decision-maker doesn't know which combination of parameters corresponds to a budget-compliant result, unlike with the PCP. Indeed, there is no indication as to which heat-pump is to be installed if the decision to wait 6 more years before is preferred.

In the CMV, some preference is observed towards the simple flow solution to be replaced at year 10, whereas the triple-glazed windows are preferred. Amongst the renovation CMMs, a preference for larger PV surface is also seen from years 5 to 11, while having a scheduler is slightly preferred over not having one at all.

The most surprising of the results in Figure 4.4 however, is the glass wool insulation material that is much more likely to satisfy the budgets than others, despite having neither the highest thermal resistivity nor the lowest embodied GWP. The reason behind this is the good balance between these two performances, which results in good, if unexceptional, OE and EE. To that point, PU has even better thermal performance, but clearly, its embodied cost does not compensate the energy savings, unlike for glass wool.

In this context, it is also important to note that the EOL process plays a critical role in these assessments. For materials like wood fibre and other bio-based materials, incineration or landfill might be considered standard practices. However, for these materials, their performance could be significantly influenced by the EOL scenario. Incineration of bio-based materials can lead to high emissions, which impacts their overall impact unfavorably. If recycling or long-term storage is considered instead, the environmental impact

could be reduced, suggesting a potential improvement area for future decision-making strategies.

Then, it is evident that Figure 4.4 allowed new insights to be drawn, but this graphical form is not explanatory. In fact, it is clear that this graphic only supplements and facilitates conclusions to be made on the results given in Figure 4.2.

Figure 4.4: Solution frequency of budget compliant solutions under Upper-Edge scenario.

The sampling method chosen for this quasi-random evaluation was inspired. Indeed, by using a Saltelli sampling, we are now able to calculate the Sobol indices with the same sample. This Sobol application then, will indicate which CMMs have the most influence in the resulting overall GWP. But before presenting the results, it is important to highlight that the CMMs related to scheduling are defined by Equation 4.1 and Equation 4.2[2].

2: For both renovations then, PV and insulation installations, the boundaries for their scheduling is defined between years [5, 50[.

Consequently, as shown in Figure 4.5, the PV addition year was found to be the most influential parameter in the variance found in the resulting overall GWP. The reason for this is the large influence is the wide range of values considered. In an optimization, the algorithm should avoid renovations too close to the building's EOL, but in a quasi-random evaluation with uniform probability through the entire range, some of the simulations will be run with PV installations happening at year 49. Thus, the Sobol index of this CMM has been inflated.

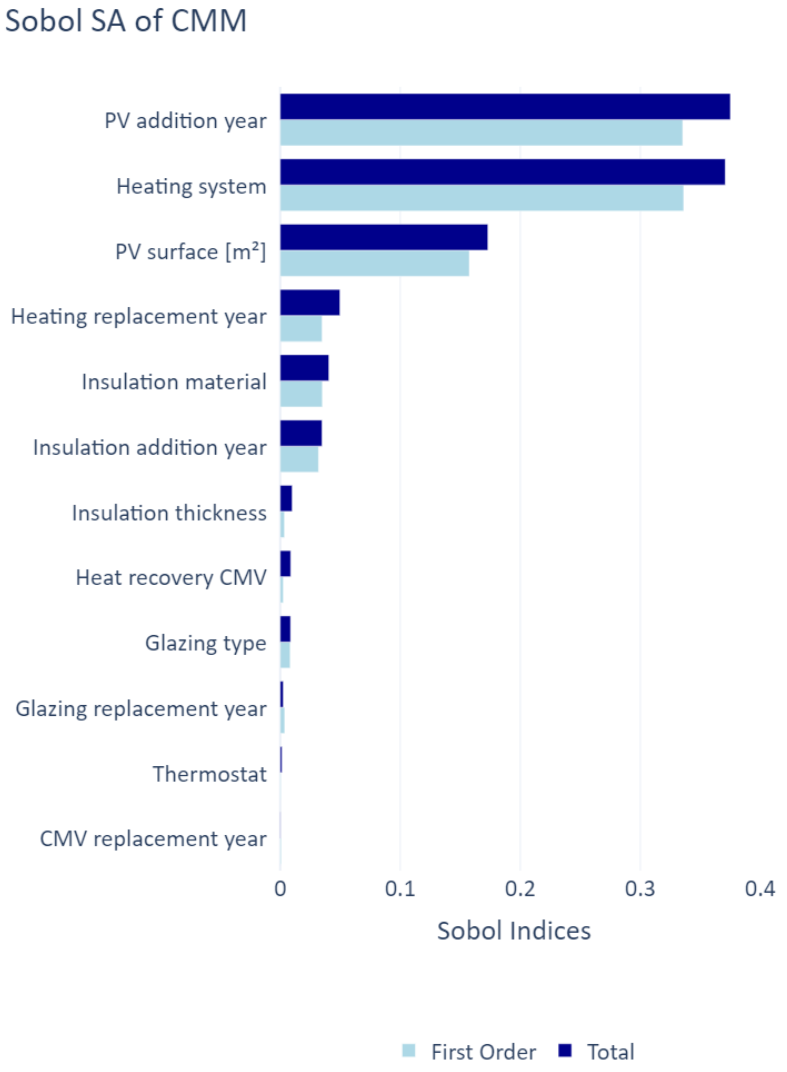

Figure 4.5: Sobol indices of CMMs under Upper-Edge Scenario.

Second to that is the heating system replacement is considered almost as influential as the PV addition year, with the surface of the PV installation being a far third place in terms of influence in overall GWP variance. Heating replacement scheduling, insulation material choice and insulation addition year round up the top half of influential parameters. The impact of all remaining CMMs is somewhat negligible, but as shown in Table 4.10, glazing- and scheduler-related choices can still represent the difference between carbon budget compliance and over-expenditure.

These results shown in the form of the Sobol indices highlight to the decision-makers, which CMMs should be prioritized and require more attention.

Statistical methods then, are useful for interactive DM and prioritizing CMMs with PCP and Sobol SA, respectively. However, the sampling required is an inefficient way to explore the solution space, unlike optimizations. For this reason, the next sub-chapter will present results from an optimization application.

4.3.1.2 Optimization Results

To start, the optimization's results will be shown in a Pareto plot. Each point then, represents what will be referred to as a "Solution Set": a combination of CMMs that result in the pair of values plotted on the Cartesian plane. Here, the trade-off between objectives can be identified through the Pareto front: the set of solutions that best minimize the optimization functions.

Since the objective of this optimization workflow is to ensure CB compliance, the RE2020 budgets have been added to the plot as dotted horizontal and vertical lines. To better compare the results with the budgets, the GWP values have been normalized to the m² of habitable indoor area. In addition, a colour scale was added based on the sum of both values, also known as the overall GWP.

For the first scenario then, the Pareto plot is shown in Figure 4.6. Here, both vertical and horizontal axis have been defined between 0 and 800 $kgCO_2 - eq/m^2$, to give a holistic perspective of where the solutions are with respect to the budgets. Based on the fact that the solutions are agglomerated in the bottom right corner demonstrates that OEs and EEs operate at 2 very different scales. To reflect this, a closer plot is shown to the right of Figure 4.6.

Another immediate observation from this plot is that, in this lower-edge case scenario, compared to the budgets, a number of viable solutions exist. Indeed, every solution simulated has a lower EE than the current budget of 610 $kgCO_2 - eq/m^2$ and in fact, the BAU case follows even the 2025 embodied budget. Indeed, the future embodied budgets have been added to demonstrate the decarbonization pathway set by the RE2020 over the next decade. The operational budget of 150 $kgCO_2 - eq/m^2$ is another story though, with the BAU case exceeding the budget by 40%.

Despite this, the CMMs prove to be enough to curb the operational emissions trajectory, while keeping the embodied budget within bounds.

On the Pareto front, highlighted with the red contour, 3 clusters of solutions have been identified with dark red rings and named

from A to C. These clusters can be largely differentiated by the following characteristics:

A. This first cluster involves keeping the heating system as is, the electrical radiators. These are the solutions with the lowest EE, since this is the lowest embodied GWP heating system considered, but these are the least efficient options, as the high OEs suggest. The variation within this cluster exists from measures such as adding heat recovery to the ventilation and PV panels.

B. Cluster B consists of replacing the BAU heating system with the most efficient option investigated: the air-water heat pump, despite it being the most emissive in terms of EE. The variation within this cluster originates from the scheduling of this replacement. The earlier the radiators are replaced, the lower the life cycle OEs will be. Conversely, delaying this intervention reduces the EOL of the current system and the embodied GWP of the new component. This reduction stems from the DPs included in this analysis. Both clusters B and C include PV installations, with variations primarily due to the PV surface area.

C. Cluster C also involves replacing the heating system with the air-water heat pump. However, all solutions in this cluster advocate for transitioning to the heat pump as early as possible, specifically by year 5. The variation within this cluster is also is linked to the size of the PV system. The greater the PV surface, the higher the EEs and the lower the OEs. Both clusters B and C include PV installations, with most variation due to the PV surface area.

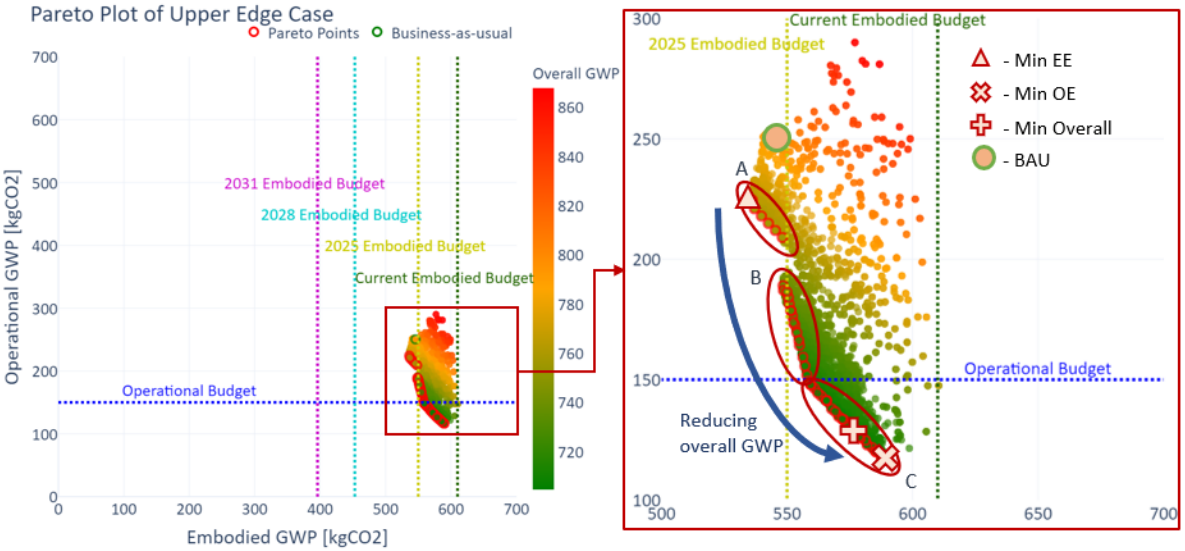

Figure 4.6: Pareto plot of the optimization solution found in the Upper-Edge case-study. The points with a red contour represent the Pareto front and the one with a green contour is the BAU case. To the right are the same points at a different scale.

From Figure 4.6, it is also clear that there's more flexibility in terms of OE than EE, as the interval of possible values in the Pareto front for the former is 120 $kgCO_2 - eq/m^2$ and only 53 $kgCO_2 - eq/m^2$ for the latter.

This is explained by the fact that only five years have passed since construction, meaning only 22% of the operational budget has been used. Therefore, plenty of solutions exist that help align the operational carbon trajectory with the blue horizontal line, despite the OE of the BAU being more than 80 $kgCO_2 - eq/m^2$ over budget.

Another factor relates to the selected case study, which, while not particularly energy-efficient, has a low life-cycle embodied GWP. If a net-zero energy building were considered instead, the main challenge would likely shift to meeting the embodied budget. In essence, the starting point threshold compliance will highly depend on the building characteristics.

Meanwhile, for EE, by the same year, 55 % of the embodied budget (green vertical line) has already been depleted, since construction represents the largest share of embodied GWP. This suggests the importance of ensuring first and foremost the EE's compliance to the embodied budget, as fewer CMMs will be available to correct an eventual deviation in its trajectory.

Of the 50 solutions found in the Pareto Front, 3 can have been highlighted in Table 4.10. The solutions that minimize: (1) overall GWP; (2) OE and (3) EE. As a reminder, replacement year measures are indexed to the building's age. Therefore, if a value reads 5, this represents that at year 5 (the current age of the case-study, as-soon-as possible), the intervention should be made.

When comparing the optimal EE solution with the BAU, it is clear that the 2 solutions are not far from each other, with the MOO recommending only the installation of thickest wood-straw insulation as-soon-as possible. The minimal overall solution however, is closer to the minimal OE solution, indicating how CMM are, in general, worth the investments, aside from PV surface, which is the only difference between these two solutions.

To compare how the recommended CMMs affect emissions over time, a plot of cumulative emissions was built to show carbon emissions trajectories. In this fan plot, emissions between years 0 and 4 are the same for all solutions, as those emissions are assumed to have already occurred. It is only after year 5 that the CMMs can start taking effect. In Figure 4.7, the four scenarios described in Table 4.10 are included. The first thing to notice in this figure is that the minimal overall solution is very similar to the minimal operational solution, as the green and yellow curves almost overlap.

Table 4.10: This table includes 3 sets of solutions found in the Pareto front under Upper-Edge Case scenario and identifies all CMMs to achieve the resulting GWP displayed.

CMM	Best Overall Solution	Minimal OE Solution	Minimal EE Solution	BAU
	1	2	3	
Heat recovery CMV	Simple flow Ventilation	Simple flow Ventilation	Simple flow Ventilation	Simple flow Ventilation
CMV replacement year	17	17	17	17
Glazing type	Triple Glaz Wood	Triple Glaz PVC	Double Glaz Wood	Double Glaz PVC
Glazing replacement year	16	14	30	30
Insulation material	Wood Straw	Wood Straw	Wood Straw	EPS
Insulation thickness	Thickest	Thickest	Thickest	Thinnest
Insulation addition year	5	5	7	5
Heating system	Air-water HP	Air-water HP	Electric rad	Electric rad
Heating replacement year	5	5	17	17
PV surface [m^2]	19.2	32.0	0.0	0.0
PV addition year	5	5	-	-
Scheduler	Scheduler	Scheduler	No scheduler	No scheduler
Operational GWP	128.62	116	224.54	250.44
Embodied GWP	576.10	589.81	536.18	545.76
Overall GWP	704.71	706.21	760.72	796.20

The only difference between them is the replacement year of the windows and the ventilation system.

However, as useful as the illustration of the carbon trajectories is, only 4 solutions were visible at a time. Including more solutions makes the figure very hard to read. Therefore, to better understand the solutions proposed by the Pareto front as a whole, the next graphical interpretation will be extremely useful.

To identify the patterns within the Pareto front, another analysis was made: a frequency analysis for each measure. Figure 4.8 then, shows how often each parameter is selected for the 12 CMMs studied.

For some CMMs, the benefits of realizing a given action are so beneficial, that all Pareto solutions include said action. In the case of ventilation, for instance, the optimizer never found the extra investments in EE for a double-flow system never compensated the heating energy savings that it causes. However, upon further analysis of the energy balance, these energy savings in heating performance does not compensate even the energy used to run

the additional fans of the double-flow installation. This result is a testament of how important the appropriate sizing of this type of ventilation system is, which was clearly not well executed enough in this case-study application.

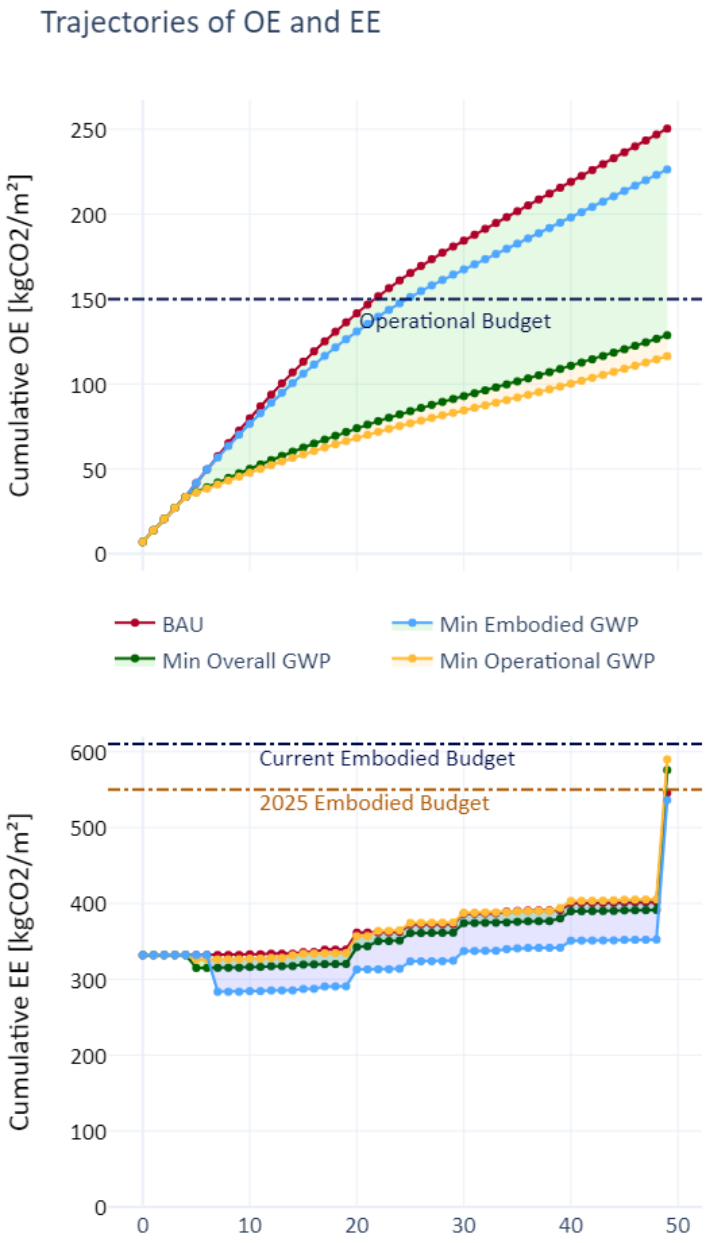

Figure 4.7: This fan plot shows the cumulative OE, on top, and EE, underneath. The different lines represent the different trajectories future emissions could take, depending on which set of CMM, as identified by the different colours.

In the meantime, for insulation, 100% of the solutions included the addition of carbon-absorbing wood-straw as soon as possible, at year 5. This is simply explained by the fact that this measure reduces both OE and EE by improving thermal resistance and storing carbon in the envelope, respectively. This raises the question of whether to include this material in a MOO, but it is worth emphasizing how beneficial and useful these materials are for CB compliance. In fact,

the use of bio-based materials is the only way to correct towards compliance.

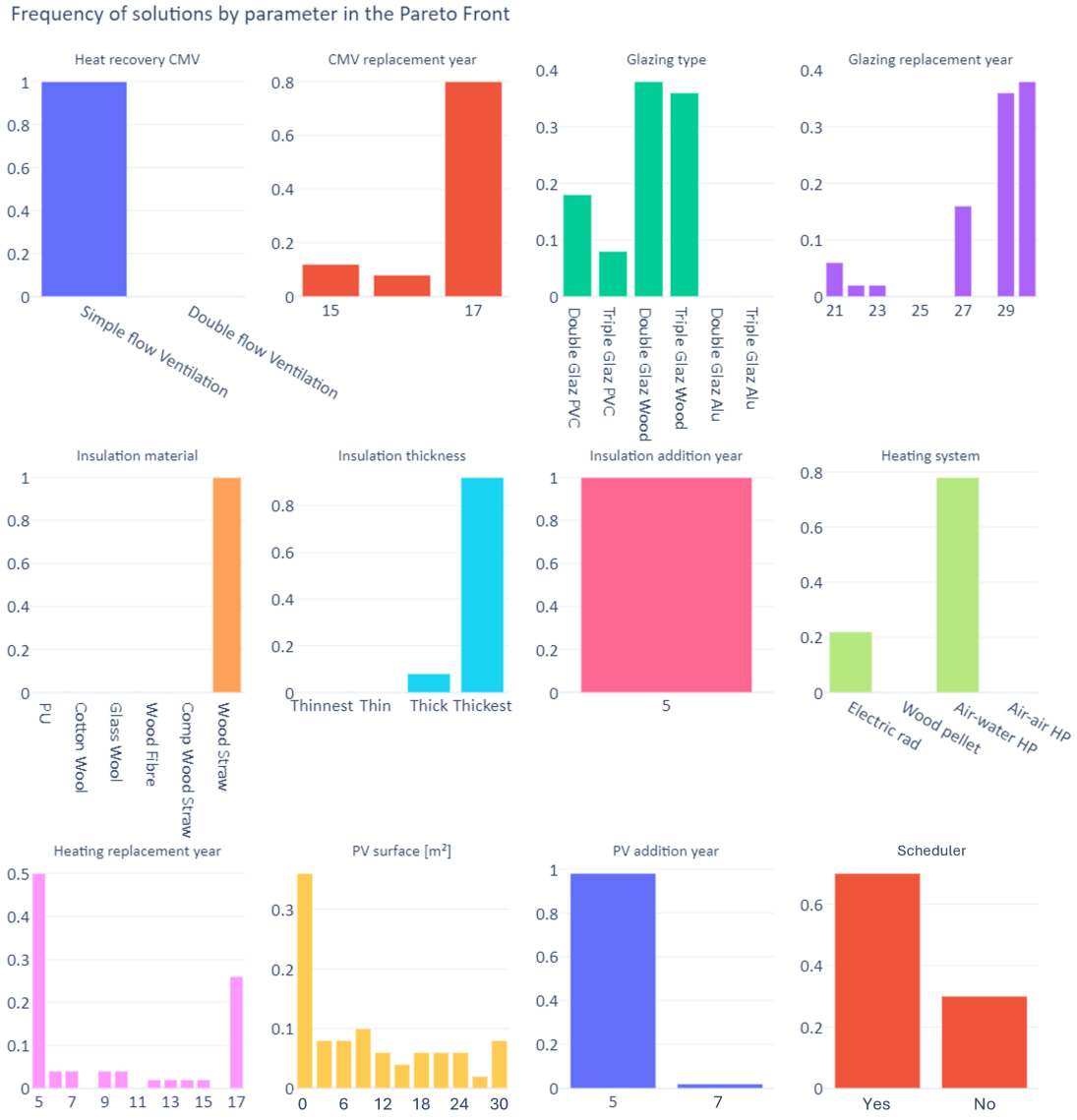

Figure 4.8: Frequency of solutions for each variable in the Pareto front under Upper-Edge scenario.

For other parameters, it is more difficult to see patterns, where a more even distribution exists, such as for glazing type. For instance, in close to 80% of solutions, wood framing was preferred, again highlighting the use of bio-based materials, however, in some other 20%, PVC frames are more beneficial, as they have better thermal performance. Concerning the scheduling aspect of this component, no replacement is ever recommended before year 20 and 40% of them take place at the current window's EOL, at year 30.

Heating systems seem to come down to only two choices: electrical radiators and air-water heat-pump. Although it might be

surprising to see a system as inefficient as electrical radiators in this Pareto front, it is important to highlight that these are extremely inexpensive solutions in terms of EEs, since no distribution system is required, except for the electrical installation. Additionally, electricity in France is relatively low-carbon and its CI is comparable to wood pellets. The scheduling of the replacement seems to be arbitrary, but in fact, it largely depends on the heating system of choice and the priority given to each objective by the decision-maker.

When considering local renewable energy production, around 35% of solutions find it unnecessary, however, when it is installed, this action should be realized as soon as possible, by year 6. In fact, the addition of PV panels can still reduce OE, as shown in cluster C of Figure 4.6.

4.4 Comparing and Discussing Scenario-Based Results

To start this section then, a rundown on the results will be made, so that results can be compared more directly between the different scenarios, whose results have been listed in Appendix D.

4.4.1 Comparing the Impact on GWP Values

It is unquestionable, from Chapter 4.3, that in terms of raw GWP results, the different dynamic scenarios produced extremely different values. To drive this point home then, Table 4.11 compares the results of BAU under the 4 scenarios. Additionally, we can observe how the different scenarios affect OE and EE differently.

First, it is worth highlighting quantitatively that the lowest overall GWP in Table 4.11 is upwards of 39% lower than the highest value. This interval that ranges from 629 to 1030 $kgCO_2 - eq/m^2$ demonstrates the importance of further evolving and improving the DLCA methodology for more accurate EI assessment, which will, subsequently, strengthen the process of ensuring carbon budget compliance.

Visibly, the RE2020 scenario is the closest to the static values, with an overall GWP around 20% lower. Additionally, since the weighting factor impacts the operational and embodied GWP equally, their relative reductions are close at 21% and 19%, respectively. However, it is important to note that RE2020 is closer to the upper edge of the range than any other scenario.

In contrast, under the Lower-Edge case, the different DPs affect OE and EE very disproportionately. The former is reduced by 58%

Table 4.11: Comparison of GWP metrics across different scenarios in the 'Business-as-usual' solution, including percentage reductions relative to the Static scenario. The reduction columns are the reference to the static values in the last row.

Scenario	**OE**		**EE**		**Overall**	
	Value ($kgCO_2 - eq/m^2$)	Reduction (%)	Value ($kgCO_2 - eq/m^2$)	Reduction (%)	Value ($kgCO_2 - eq/m^2$)	Reduction (%)
Upper-Edge	250.44	-23.9	545.76	-22.1	796.20	-22.7
Lower-Edge	138.54	-57.9	490.27	-30.1	628.81	-38.9
RE2020	260.58	-20.9	568.99	-18.8	829.57	-19.5
Static	329.31	-	700.82	-	1030.13	-

relative to the equivalent static value, while the latter is reduced by 30%. Of course, this is highly dependent on how the different DPs are modelled and on their contexts. In this scenario's case then, the improvements to the electricity CI seem to be very effective.

The Upper-Edge case's overall GWP is close to the RE2020 results, being 23% lower than the static value, as shown in Figure 4.9.

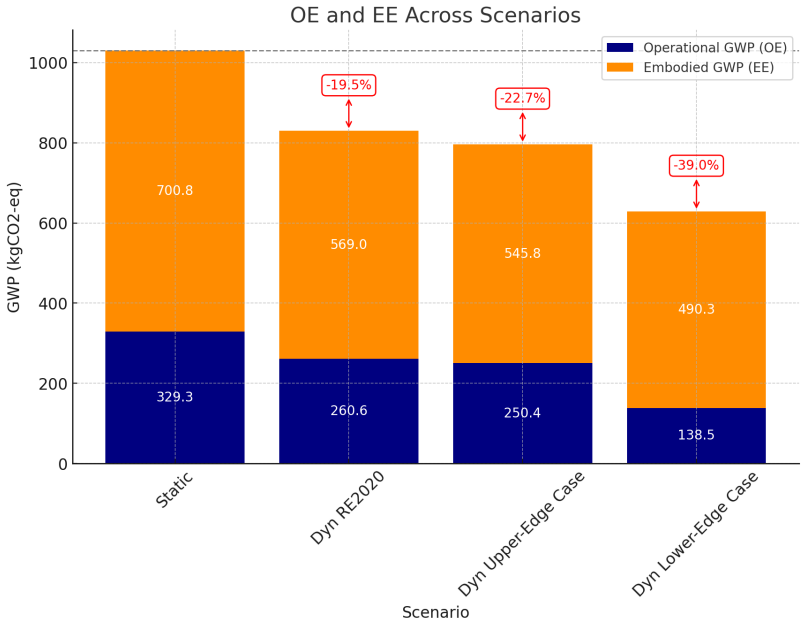

Figure 4.9: Resulting GWP of BAU under different scenarios. The percentage values in red are the reduction in overall GWP from the static scenario.

It is worth highlighting again that these results are particular to this case-study. The results are not only affected by the modelling of the DPs, but also by its technical characteristics, such as the electrical radiator heating system, which will be more sensitive to the electricity mix evolution. Meanwhile, bio-based materials will benefit most from improvements in the waste sector.

With this caveat established, it is still pertinent to question the impact that the different approaches have on building carbon budget compliance and DM. Indeed, the LCA method chosen and the DP

models established can make the difference between no interventions being needed to major renovations being imperative.

4.4.2 Comparing the Impact on Decision-Making

It is still unclear, however, if and how these different scenarios impact the DM. Thus, this sub-section is dedicated to comparing the solutions provided under the 4 scenarios and discourse on the differences and similarities.

The first comparison to be made is between static and RE2020 results and here, the differences are hard to notice, as the optimization yielded very similar Pareto solutions. One big particularity of the static approach, when compared to all other dynamic ones, relates to the scheduling-related CMMs. Again, since no change is accounted for in the EEs, as long as the measure improves energy efficiency, the optimizer will simply suggest performing said measure as early as possible, since there is no benefit to waiting to realize said intervention. However, in all other dynamic approaches, there are increasing benefits to waiting for the current component's EOL before it is replaced, either in the form of the weighting factor or in the DPs linked to industry and waste sector evolution.

At the same time though, OEs also evolve through time in DLCA, making the energy savings less valuable with each year that passes, since the electricity sector will never be more carbon intensive than it is today. This makes the DM process all the more interesting and unpredictable.

Aside from this difference however, the other CMMs saw little change, which is somewhat disappointing, as one of the objectives of the RE2020's weighting factor was to incentivize the use of bio-based materials. These were recommended in the RE2020's Pareto front, but so it was in the static's. The similarities in optimization solutions can be explained by the fact that OE and EE are equally impacted by the weighting factor.

The solutions for the Upper-Edge scenario were also very similar to the ones above, especially the RE2020's, also because the ratio between operational and embodied GWP was similar to the aforementioned ones.

Finally, the Lower-Edge case had the most distinguished results, correlating to the balance between OE and EE being most affected under this scenario. Under these assumptions, the optimizer deems the EE for PV installation not worth the reduction in grid electricity needs, unlike all other scenarios. For example, under the Lower-Edge case scenario, a building with no local renewable energy

production and an electric radiator heating system results in a 15% lower overall GWP compared to a building equipped with 32 m² of PV panels and an air-water heat pump under the Upper-Edge case scenario.

When putting the carbon budget into perspective, the difference in raw values make a big difference. It is a much simpler task to curb the emission trajectories of the RE2020 approach than the static, of course. This poses the question if DLCAs in the context of carbon budgets are simply a way to make buildings more easily compatible with them.

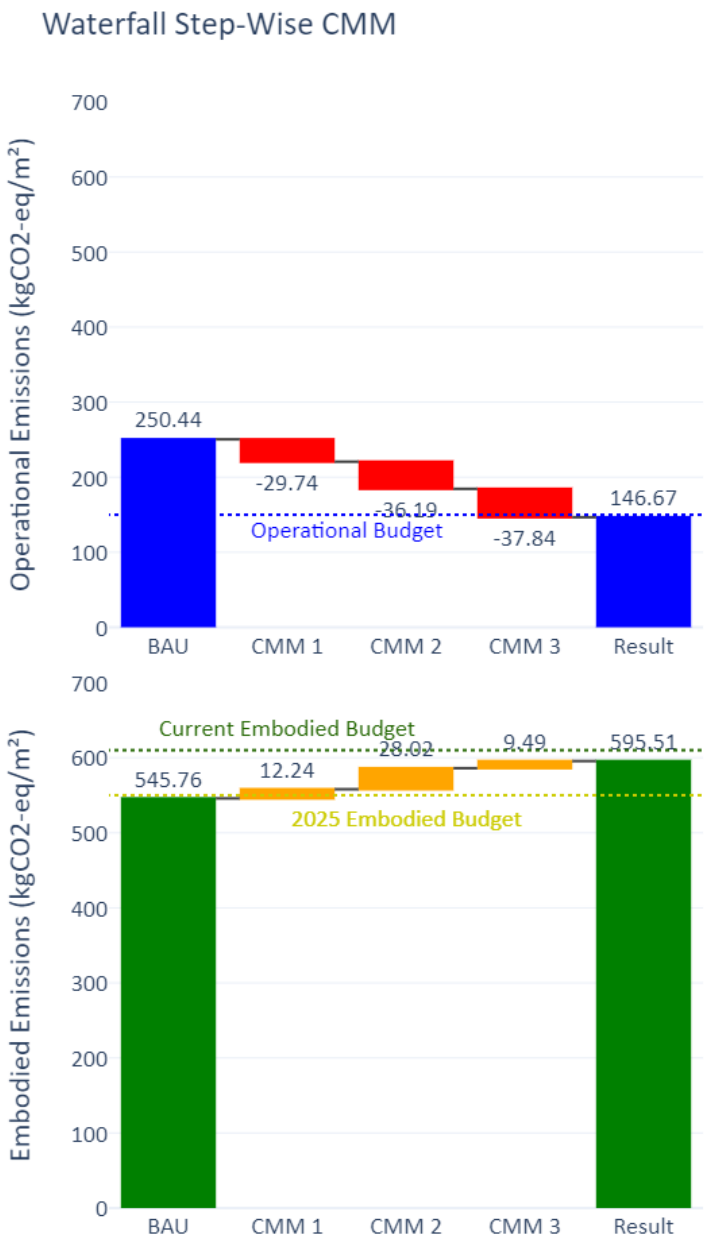

Figure 4.10: Waterfall plot of step-by-step CMMs applied to the case-study under the Upper-Edge case: (1) replacement of heating system, (2) addition of PV panels and (3) anticipating the replacement of the heating system by 12 years.

CMM	**Lower-Edge Case**	**Upper-Edge Case**
Heat recovery CMV	Simple flow Ventilation	Simple flow Ventilation
CMV replacement year	17	17
Glazing type	Double Glaz PVC	Double Glaz PVC
Glazing replacement year	30	30
Insulation material	PU	PU
Insulation thickness	Thinnest	Thinnest
Insulation addition year	-	-
Heating system	**Electric rad**	**Air-water HP**
Heating replacement year	**17**	**5**
PV surface [m²]	**0.0**	**32.0**
PV addition year	**-**	**5**
Scheduler	Yes	Yes
Operational GWP	138.54	146.67
Embodied GWP	490.27	595.51
Overall GWP	628.81	742.18

Table 4.12: This table includes 2 sets of solutions: in lower-edge and upper-edge scenarios. These solutions represent the minimal number of CMMs for ensuring carbon budget compliance.

To highlight how different a budget-compliant building looks like under different dynamic scenarios, Table 4.12 was built. It shows two solutions, one in lower-edge and the other under upper-edge case. To find these solutions, a step-wise approach was applied following the order of CMM shown in Figure 4.5. By applying one CMM at a time and verifying carbon budget compliance, the number of interventions is minimized, since the most impactful measures are being prioritized.

For the Upper-Edge case, a couple of measures had to be introduced, as shown in the waterfall plot in Figure 4.10, where steps 1 through 3 represent the following:

1. Replacement of heating system (electrical radiators) for an air-water heat-pump.
2. Addition of 32 m^2 of PV panels at year 5.
3. Anticipating replacement of heating system by 12 year: from year 17 to year 5.

These 3 measures represent the minimum amount of intervention under this dynamic scenario that ensured carbon-budget compliance, whereas under the lower-edge scenario, the BAU solution already complies with budgetary constraint, making this, the lowest-effort solution possible.

Under the lower-edge case scenario, a building with no local renewable energy production and an electric radiator heating system results in a 15% lower overall GWP compared to a building equipped with 32 m² of PV panels and an air-water heat pump under the upper-edge case scenario.

To evaluate the viability of following the French regulation's carbon thresholds under the different scenarios, Table 4.13 compares the number of budget-compliant solutions in the quasi-random evaluation out of the 13,312 samples. The number of solutions from Lower-Edge case to Upper-Edge case reduces from 8124 to only 42 solutions, showcasing how distinct these two scenarios are. The reduced number of solutions suggests that carbon compliance requires a more specific set of CMMs.

Table 4.13: Comparison of GWP metrics across different scenarios in the 'Business-as-usual' solution, including percentage reductions relative to the Static scenario. The reduction columns are the referenced static values in the last row.

Scenario	Number of Carbon-Compliant Solutions	Percentage of Carbon-Compliant Solutions (%)
Upper-Edge	42	0.32
Lower-Edge	8124	61.03
RE2020	110	0.83
Static	0	0

4.5 Conclusions

This Chapter has explored the integration of Dynamic Life Cycle Assessment into retrofit Decision-Making processes, a crucial step towards carbon budget-compliant buildings. The research has been anchored in the understanding that buildings, due to their long lifespans, are subject to a myriad of uncertainties that can significantly impact their environmental performance. The development and application of a comprehensive DM methodology that incorporates Dynamic Parameters offer a robust and future-proof approach to building retrofits, ensuring long-term environmental sustainability.

The methodology proposes a distinction between renovations and replacement, the former being the addition of building components while the latter is the substitution of existing ones. This differentiation is crucial towards creating a workflow that considers the current context of the building at post-occupancy stages and institutes the prerequisite for the iterative and continuous GHG budget compliance.

Moreover, this study extends beyond just identifying replacement and renovation measures. It delves into the timing of these interventions, using dynamic parameters to determine the most appropriate

schedules for implementation. This aspect of the research is particularly innovative, as it integrates temporal considerations into the decision-making process, a crucial element given the evolving nature of building performance and environmental impact over time.

Upon determining a case-study, its specific renovation and replacement measures were identified, based on which components have the most potential impact in life cycle Global Warming Potential. To assist Decision-Making in building design, statistical and optimization methods were found to be ideal. However, these are computationally expensive and so the Dynamic Life Cycle Assessment simplification techniques explored in Chapter 3 were brought over into this chapter. Indeed, reducing the number of Dynamic Parameters and the training of Surrogate Model were crucial steps towards building an easy to use methodology.

Through a scenario-based integration of long-term dynamic uncertainties, two scenarios were built: an upper-edge case and a lower-edge case. With the case-study application, drastically different life cycle GWPs were obtained, ranging from 796 $kCO_2 - eq/m^2$ to 629 $kCO_2 - eq/m^2$. This variation, driven by changes in the Dynamic Parameters modelling assumptions, including electricity mix evolution, industrial and waste sector decarbonization, etc., could represent the difference between remaining comfortably within budget and irreparably surpassing it. Compared to the static GWP, these results indicate an up to 39% reduction.

These differences in the resulting GWP will influence DM regarding CMM. In other words, two buildings that comply with carbon standards may exhibit significantly different characteristics depending on the dynamic scenario. For example, under a lower-bound scenario, a building without local renewable energy production and using an electric radiator heating system can still achieve a 15% lower overall GWP compared to a building equipped with 32 m² of photovoltaic panels and an air-water heat pump under the upper-bound scenario.

Importantly, this research also takes into account the French regulatory framework, particularly the RE2020, to ensure that the proposed methodology is not only academically sound but also somewhat coherent with current regulations. The proposed dynamic LCA approach was compared to the French regulation and the resulting GWP appears to be somewhat close to the upper-edge case scenario, only a 33 $kgCO_2 - eq/m^2$ difference in overall GWP.

When it comes to the optimization results, very little difference was observed between the CMMs that appeared in each scenario's Pareto fronts. The major difference was in where these solutions

were located in the Cartesian plane, particularly relative to the RE2020 life cycle GHG emissions. Indeed, a recommendation that appears throughout is the use of bio-based insulation for carbon storage and the replacement of the existing electrical radiators for air-water heat-pumps as early as possible.

This chapter represents a step forward in the integration of dynamic LCA into building retrofit decision-making. It provides a comprehensive framework that can guide decision-makers in retrofitting buildings in a manner that follows pre-established carbon budgets. As the building industry continues to grapple with the challenges of climate change and its uncertainties, the findings and methodologies presented in this research offer valuable insights and tools for advancing towards a more sustainable future.

Conclusions and Outlook 5

5.1 Conclusions

In this thesis, strides in advancing methodologies for GHG emission evaluation in the building sector were made, with a focus on low-carbon building retrofit decision-making.

The state of the art of methods towards building GHG threshold compliance

The journey began in Chapter 2, where an exploration of the state of the art is carried out. It starts by emphasizing the importance of carbon thresholds, towards limiting global warming to 1.5°C or 2°C targets. As buildings represent a significant portion of current yearly global emissions, a major effort is necessary in the task of rendering the sector net zero GHG emissions by 2050.

Within this context of climate emergency, Life Cycle Assessment (LCA) appears as a key methodology for all products and services, including buildings. Throughout the review presented in this chapter, however, it becomes clear that buildings are particularly difficult to calculate life cycle environmental impacts for, due to their inherently long lifespans. Indeed, within the context of carbon emission targets, long-term uncertainties can cause deviations from predicted GHG emissions.

Dynamic Life Cycle Assessment (DLCA) is then identified as key research area for GHG threshold-compliant buildings. Indeed, this methodological framework takes into account long-term dynamics of the building and its associated systems, such as the electricity grid's decarbonization or climate change. This methodology offers a more detailed and comprehensive result, but it comes with its challenges. Nonetheless, in Chapter 2, the inclusion of these uncertainties is judged necessary.

But as comprehensive as DLCA is, it is not enough to simply assess budgetary deviations. For this reason, Chapter 2 also investigates post-occupancy Decision-Making (DM) methods as possible tools

to correct carbon threshold over-expenditure. These methods include sensitivity analysis, uncertainty analysis, optimizations, and visualization techniques often associated with building design DM.

Exploring Dynamic Life Cycle Assessment Simplification Strategies

Building on these conclusions, Chapter 3 presents an examination of the DLCA as an essential methodology for enhancing accuracy in ensuring building carbon threshold compliance. It details strategies aimed at simplifying DLCA through two primary means: reducing simulation times and the number of Dynamic Parameters (DP)s. The DLCA workflow incorporates the French Environmental Product Declaration (EPD) database INIES for Embodied Emission (EE) calculation and EnergyPlus for Operational Emissions (OE) calculations over a 50-year operational period, revealing that 99% of simulation time was dedicated to OE, which represents only 25% of the total Global Warming Potential (GWP).

To address the challenge of lengthy simulation times, the chapter explores two solutions: linear interpolation between different time steps and a Surrogate Model (SM) for OE calculations. Linear interpolation with a modest setup capable of 6 parallel simulations reduced simulation times by 90% with a minor accuracy compromise while SM drastically cut down simulation time to less than a second for both operational and embodied GWP calculations. This efficiency was achieved with only 500 simulations, which took 52 minutes to simulate.

To address the challenge of lengthy simulation times, the chapter explores two solutions: linear interpolation between different time steps and a Surrogate Model (SM) for OE calculations. Linear interpolation with modest computing power capable of 6 parallel simulations reduced simulation times by 90% with a minor accuracy compromise. Meanwhile the SM drastically cut down simulation times by 98% to less than a second.

Furthermore, the chapter discusses the refinement of DP modelling through an analysis aimed at identifying the most impactful parameters for dynamic GWP. By focusing on the parameters with the greatest impact, 47% of the DPs were responsible for 87% of the variance in dynamic life cycle GWP. Thus, a strategic selection of DPs can significantly simplify the modelling process by focusing only on the most impactful DPs, which, in the case-study were: occupant behaviour and decarbonization of industry, waste and electricity sectors.

With these advancements, DLCA's integration into the DM process is significantly facilitated, setting the stage for further exploration in the subsequent chapter. This progress underscores the potential for more accessible and efficient DLCA applications. However, it is important to note that each new project requires reapplying the methodological framework, as it is case-specific. In contrast, the interpolation of GWP is less challenging, as it can be quickly applied to each new building.

Integrating Dynamic LCA into Retrofit Decision-Making Methods

Chapter 4 advanced the discourse by integrating DLCA into retrofit DM processes, aiming to align building's emission trajectories with threshold requirements. It highlights the critical role of understanding the long-term uncertainties buildings face, which significantly influence their environmental performance. By developing a comprehensive DM methodology that includes DP, the research provides a data-driven approach to ensure buildings follow long-term environmental objectives. This methodology differentiates between renovations (adding components) and replacements (substituting components), essential for creating a workflow that adapts to the building's post-occupancy stage and facilitates ongoing GHG threshold compliance verification.

The study extends its analysis to the timing and scheduling of retrofit measures, employing dynamic parameters to optimize intervention schedules. This consideration is innovative, as it incorporates temporal dynamics into retrofit decisions, acknowledging the evolving nature of a building's performance and its context. In addition, this approach aligns with the limited investment capacity of building owners, who often cannot implement all retrofit measures simultaneously.

Through a case study, specific renovation and replacement measures were identified based on their potential to impact the life cycle GWP, acknowledging the computational intensity of statistical and optimization methods implemented. This was facilitated by the DLCA simplification techniques, emphasizing the importance of streamlining methodologies.

As scenario-based analysis reveal significant differences in life cycle GWP outcomes, demonstrating the impact of dynamic parameter assumptions on retrofit decisions. For example, changing DP modelling assumptions resulted in life cycle GWP variations from 796 $kgCO_2/m^2$ to 629 $kgCO_2/m^2$. Furthermore, the research acknowledges the French RE2020 regulatory framework, ensuring the proposed methodology's relevance to current standards.

The choice to base the methodology on the RE2020 carbon threshold was made to ensure compatibility with current regulatory standards, though no weighting factor was applied in this study. It is also recognized that carbon budgets (e.g., IPCC) exist, which are calculated using different assumptions. Despite its design for building construction, the RE2020 threshold was applied to an existing building (recently built), with the focus placed on dynamic modeling and uncertainties.

As a general conclusion, this thesis presents arguments for the integration of dynamic LCA into building design and retrofit decision-making. The methodologies proposed include a method to streamline and facilitate the widespread use of DLCA and a framework to guide decision-makers towards ensuring threshold compliance, despite long-term uncertainties in calculating building life cycle GWP.

As the world grapples with the imperatives of climate change, the insights and tools presented in this research are small contributions to the pursuit of a sustainable future in the building industry.

5.2 Outlook: Towards a Post-Occupancy Decision-Making Methodology for Carbon Threshold Compliance

Despite proposing a general methodology, this work has drawn many conclusions based on a single case-study application. However, as highlighted before, they are not "extrapolatable" to other buildings in other contexts. Therefore, a straightforward, but demanding follow-up to this thesis would be to apply the same Dynamic Life Cycle Assessment (DLCA) methodology to a dataset that is representative of the building stock to draw a general conclusion about the future of the building sector.

Additionally, the case-study used in Chapter 3 and in Chapter 4 was somewhat specific, since the building wasn't, in fact, subject to the RE2020 carbon threshold. This choice came down simply to the accessibility to this particular building's data. This thesis then, assumes that the owner of this house built in 2017 willingly decided to follow this new carbon threshold. However, another interesting scenario is comprised of buildings that are initially designed to follow their imposed thresholds and require CMMs to be enacted due to post-occupancy deviations. Nevertheless, as years pass by, they end up surpassing their budgets from premature and excessive renovations, from over-consumption of energy or several other uncertainties or DPs that were studied in this work.

Therefore, it would be interesting to apply this methodology to an occupied case-study and, together with Post-Occupancy Evaluation (POE), iteratively evaluate, at a reasonable time-step, carbon threshold compliance. Such a workflow has been drafted in Figure 5.1 are:

1. **Assessment of Threshold Expenditure**: This step, not covered in this thesis, involves gathering extensive real-world data from a case-study building. The objective is to create an as-built material bill of quantities and a calibrated energy model. This area of research, though beyond the scope of this thesis, is explored by researchers in large dimensional BIM (Building Information Modelling) [213–215] and digital twins [216, 217].
2. **Assessment of Threshold Compliance**: As detailed in Chapter 3, this step involves using DP modeling to verify compliance with long-term budgetary constraints. The key addition here would be integrating real-world data and calibrated models for more accurate forecasts. Moreover, re-calibrating DPs as uncertainties decrease over time is a developing area that requires a standardized database for consistent updates. For the French residential building in this thesis, 3 years of energy consumption data is available, therefore this step is was not viable.
3. **Post-Occupancy Decision-Making Support**: Defined in Chapter 4, this step involves applying the DM support method once budgetary deviations are identified. The main difference in this advanced outlook would be the utilization of more accurate data and models.

In future works then, to study this complete workflow through a case-study is essential. However, due to time constraints during the making of this thesis, it was not executed for the developments of Chapter 4.

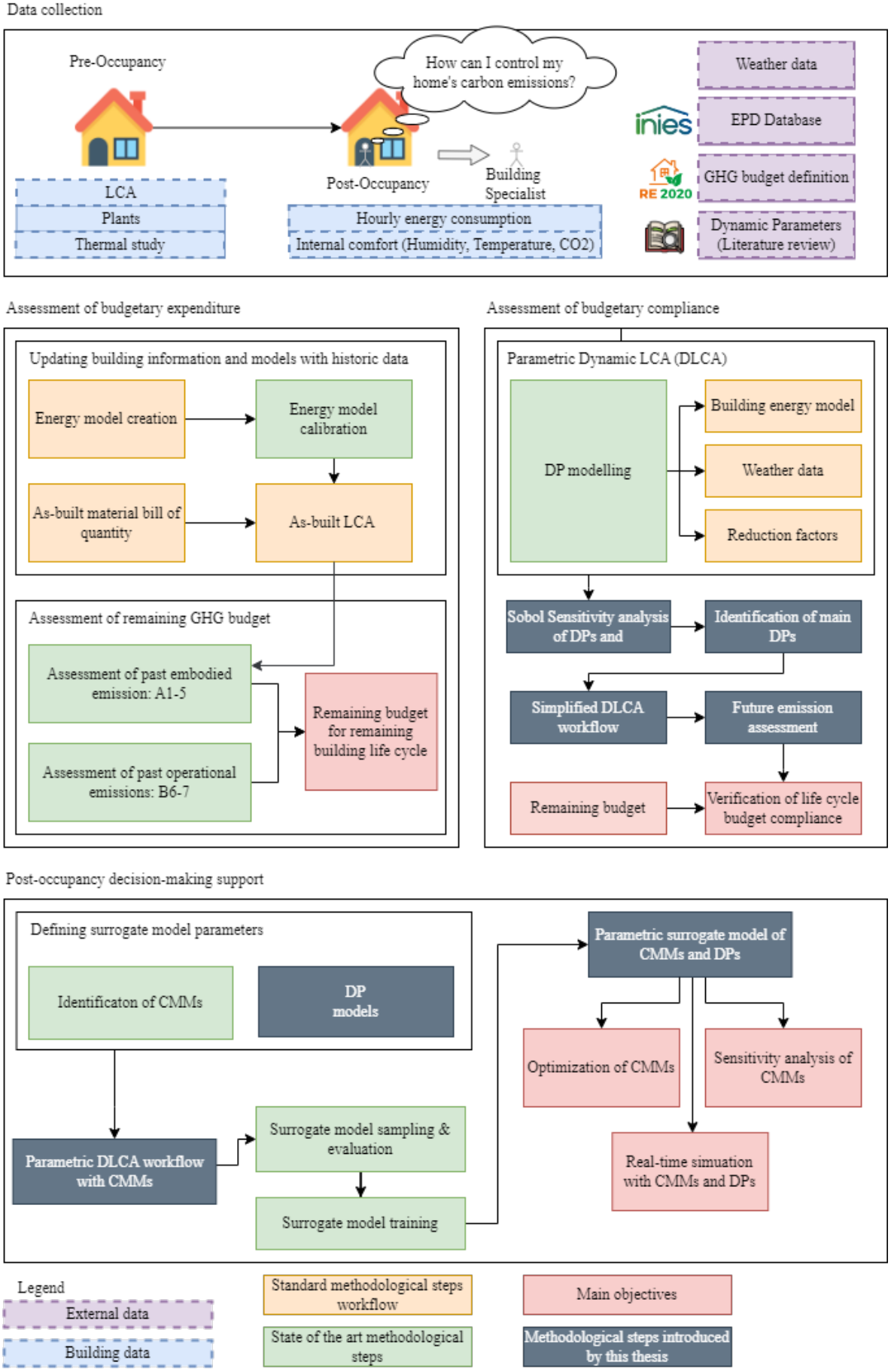

Figure 5.1: Proposal of methodology for the inclusion of POE into the methodological developments of this thesis.

Bibliography

Here are the references in citation order.

[1] Katherine Calvin et al. *Climate Change 2023: Synthesis Report - Summary for Policymakers*. IPCC Assessment Report. Edition: First. Intergovernmental Panel on Climate Change (IPCC), July 25, 2023. DOI: 10.59327/IPCC/AR6-9789291691647. (Visited on 08/16/2023) (cited on pages 1, 9, 10, 47, 62).

[2] United Nations. *Paris Agreement*. 2015. URL: https://unfccc.int/sites/default/files/english_paris_agreement.pdf (cited on page 1).

[3] Lenny Bernstein et al. *Climate Change 2007: Synthesis Report*. Nov. 2007. (Visited on 04/26/2021) (cited on pages 1, 13).

[4] Robin D. Lamboll et al. 'Assessing the size and uncertainty of remaining carbon budgets'. In: *Nature Climate Change* 13.12 (Dec. 2023), pp. 1360–1367. DOI: 10.1038/s41558-023-01848-5. (Visited on 06/22/2024) (cited on pages 1, 2).

[5] Peixian Li, Thomas M. Froese, and Gail Brager. 'Post-occupancy evaluation: State-of-the-art analysis and state-of-the-practice review'. In: *Building and Environment* 133 (Apr. 2018), pp. 187–202. DOI: 10.1016/j.buildenv.2018.02.024. (Visited on 05/27/2023) (cited on pages 1, 23).

[6] United Nations Environment Programme. *2020 Global Status Report for Buildings and Construction: Towards a Zero-emission, Efficient and Resilient Buildings and Construction Sector*. 2020 (cited on page 2).

[7] Ministère de la Transition Ecologique et Solidaire. *National Low-Carbon Strategy: The ecological and inclusive transition towards carbon neutrality*. Mar. 2020 (cited on pages 2, 56).

[8] Ministère de la Transition Ecologique et Solidaire. *Réglementation environnementale RE2020*. Ministères Écologie Énergie Territoires. Feb. 17, 2023. URL: https://www.ecologie.gouv.fr/reglementation-environnementale-re2020 (visited on 04/24/2023) (cited on pages 2, 14).

[9] Nur Najihah Abu Bakar et al. 'Energy efficiency index as an indicator for measuring building energy performance: A review'. In: *Renewable and Sustainable Energy Reviews* 44 (Apr. 2015), pp. 1–11. DOI: 10.1016/j.rser.2014.12.018. (Visited on 05/27/2021) (cited on page 2).

[10] Chirjiv Kaur Anand and Ben Amor. 'Recent developments, future challenges and new research directions in LCA of buildings: A critical review'. In: *Renewable and Sustainable Energy Reviews* 67 (Jan. 2017), pp. 408–416. DOI: 10.1016/j.rser.2016.09.058. (Visited on 01/27/2021) (cited on page 2).

[11] Robert G. Hunt, William E. Franklin, and R. G. Hunt. 'LCA — How it came about: — Personal reflections on the origin and the development of LCA in the USA'. In: *The International Journal of Life Cycle Assessment* 1.1 (Mar. 1996), pp. 4–7. DOI: 10.1007/BF02978624. (Visited on 05/26/2021) (cited on pages 2, 12).

[12] Mohamad Khasreen, Phillip F. Banfill, and Gillian Menzies. 'Life-Cycle Assessment and the Environmental Impact of Buildings: A Review'. In: *Sustainability* 1.3 (Sept. 18, 2009), pp. 674–701. DOI: 10.3390/su1030674. (Visited on 05/26/2021) (cited on pages 2, 3).

[13] International Organization for Standardization. *ISO 14044:2006 Management environnemental - Analyse du cycle de vie - Exigences et lignes directrices*. 2006 (cited on pages 2, 12).

[14] International Organization for Standardization. *ISO 14040:2006 Management environnemental – Analyse du cycle de vie – Principes et cadre*. June 19, 2006 (cited on page 2).

[15] European Comitee for Standardization. *NF EN 15804:2012+A2:2019 Contribution des ouvrages de construction au développement durable — Déclarations environnementales sur les produits — Règles régissant les catégories de produits de construction*. Oct. 2019 (cited on pages 2, 14, 15, 21, 42).

[16] European Comitee for Standardization. *EN 15804:2012+A1:2013 Contribution des ouvrages de construction au développement durable - Déclarations environnementales sur les produits - Règles régissant les catégories de produits de construction*. Nov. 13, 2011 (cited on pages 2, 3, 13).

[17] T. Ibn-Mohammed et al. 'Operational vs. embodied emissions in buildings—A review of current trends'. In: *Energy and Buildings* 66 (Nov. 2013), pp. 232–245. DOI: 10.1016/j.enbuild.2013.07.026. (Visited on 04/14/2021) (cited on page 3).

[18] European Commission. Joint Research Centre. Institute for Environment and Sustainability. *International Reference Life Cycle Data System (ILCD) Handbook :general guide for life cycle assessment : detailed guidance.* LU: Publications Office, 2010. (Visited on 05/27/2021) (cited on page 3).

[19] Fida Hussain Siddiqui, Muhammad Jamaluddin Thaheem, and Amir Abdekhodaee. 'A Review of the Digital Skills Needed in the Construction Industry: Towards a Taxonomy of Skills'. In: *Buildings* 13.11 (Oct. 27, 2023), p. 2711. DOI: 10.3390/buildings13112711. (Visited on 06/26/2024) (cited on page 3).

[20] Patrick X.W. Zou et al. 'Review of 10 years research on building energy performance gap: Life-cycle and stakeholder perspectives'. In: *Energy and Buildings* 178 (Nov. 2018), pp. 165–181. DOI: 10.1016/j.enbuild.2018.08.040. (Visited on 04/13/2021) (cited on page 4).

[21] Stefano Cozza, Jonathan Chambers, and Martin K. Patel. 'Measuring the thermal energy performance gap of labelled residential buildings in Switzerland'. In: *Energy Policy* 137 (Feb. 1, 2020), p. 111085. DOI: 10.1016/j.enpol.2019.111085. (Visited on 05/31/2021) (cited on pages 4, 82).

[22] Dan Wang et al. 'Evaluation of the dynamic energy performance gap of green buildings: Case studies in China'. In: *Building Simulation* 13.6 (Dec. 2020), pp. 1191–1204. DOI: 10.1007/s12273-020-0653-y. (Visited on 05/31/2021) (cited on page 4).

[23] N. Kampelis et al. 'Evaluation of the performance gap in industrial, residential & tertiary near-Zero energy buildings'. In: *Energy and Buildings* 148 (Aug. 1, 2017), pp. 58–73. DOI: 10.1016/j.enbuild.2017.03.057. (Visited on 05/31/2021) (cited on page 4).

[24] K Kanafani et al. 'Early Design Stage Building LCA using The LCAbyg Tool: New Strategies For Bridging The Data Gap'. In: *IOP Conference Series: Earth and Environmental Science* 323 (Sept. 6, 2019), p. 012117. DOI: 10.1088/1755-1315/323/1/012117. (Visited on 05/31/2021) (cited on page 4).

[25] Didier Vuarnoz et al. 'Assessing the gap between a normative and a reality-based model of building LCA'. In: *Journal of Building Engineering* 31 (Sept. 1, 2020), p. 101454. DOI: 10.1016/j.jobe.2020.101454. (Visited on 05/31/2021) (cited on pages 4, 16).

[26] Sjouke Beemsterboer, Henrikke Baumann, and Holger Wallbaum. 'Bridging the gap between assessment and action: recommendations for the effective use of LCA in the building process'. In: *IOP Conference Series: Earth and Environmental Science* 588 (Nov. 21, 2020), p. 022007. DOI: 10.1088/1755-1315/588/2/022007. (Visited on 05/31/2021) (cited on page 4).

[27] Yahong Dong and Peng Liu. 'Evaluation of the completeness of LCA studies for residential buildings'. In: *Clean Technologies and Environmental Policy* 24.1 (Jan. 1, 2022), pp. 229–250. DOI: 10.1007/s10098-021-02115-x. (Visited on 06/26/2024) (cited on page 4).

[28] Martin Röck. 'Embodied GHG emissions of buildings – The hidden challenge for effective climate change mitigation'. In: *Applied Energy* (2020), p. 12 (cited on page 4).

[29] Alice M. Moncaster et al. 'Widening understanding of low embodied impact buildings: Results and recommendations from 80 multi-national quantitative and qualitative case studies'. In: *Journal of Cleaner Production* 235 (Oct. 2019), pp. 378–393. DOI: 10.1016/j.jclepro.2019.06.233. (Visited on 04/13/2021) (cited on page 4).

[30] Bård Lahn. 'A history of the global carbon budget'. In: *WIREs Climate Change* 11.3 (May 2020). DOI: 10.1002/wcc.636. (Visited on 03/28/2023) (cited on page 9).

[31] Alexander Hollberg, Thomas Lützkendorf, and Guillaume Habert. 'Top-down or bottom-up? – How environmental benchmarks can support the design process'. In: *Building and Environment* 153 (Apr. 2019), pp. 148–157. DOI: 10.1016/j.buildenv.2019.02.026. (Visited on 03/28/2023) (cited on pages 9–11).

[32] Laura Rodríguez-Fernández, Ana Belén Fernández Carvajal, and María Bujidos-Casado. 'Allocation of Greenhouse Gas Emissions Using the Fairness Principle: A Multi-Country Analysis'. In: *Sustainability* 12.14 (July 20, 2020), p. 5839. DOI: 10.3390/su12145839. (Visited on 03/28/2023) (cited on page 9).

[33] Ministère de la Transition Ecologique et Solidaire. *Stratégie nationale bas-carbone : La transition écologique et solidaire vers la neutralité carbone (Synthèse)*. Mar. 2020 (cited on page 10).

[34] Anna Braune and Bastian Wittstock. 'Measuring environmental sustainability: The use of LCA based building performance indicators'. In: () (cited on page 10).

[35] Yasmine Dominique Priore, Guillaume Habert, and Thomas Jusselme. 'Exploring the gap between carbon-budget-compatible buildings and existing solutions – A Swiss case study'. In: *Energy and Buildings* 278 (Jan. 2023), p. 112598. DOI: 10.1016/j.enbuild.2022.112598. (Visited on 03/28/2023) (cited on page 10).

[36] Lise Hvid Horup, Harpa Birgisdóttir, and Morten Walbech Ryberg. 'Defining dynamic science-based climate change budgets for countries and absolute sustainable building targets'. In: *Building and Environment* 230 (Feb. 2023), p. 109936. DOI: 10.1016/j.buildenv.2022.109936. (Visited on 07/06/2023) (cited on pages 10, 11).

[37] N Rezaei Oghazi, T Jusselme, and M Andersen. 'Carbon budgets at the component scale and their impacts on design choices: the façade as a case study'. In: *Journal of Physics: Conference Series* 2600.15 (Nov. 1, 2023), p. 152016. DOI: 10.1088/1742-6596/2600/15/152016. (Visited on 12/11/2023) (cited on page 10).

[38] M Pellan et al. 'A holistic perspective on the French building and construction GHG footprint'. In: *IOP Conference Series: Earth and Environmental Science* 1078.1 (Sept. 1, 2022), p. 012049. DOI: 10.1088/1755-1315/1078/1/012049. (Visited on 07/06/2023) (cited on page 10).

[39] R. K. Zimmermann et al. *Whole Life Carbon Assessment of 60 buildings: Possibilities to develop benchmark values for LCA of buildings*. BUILD Report 2021:12. Polyteknisk Boghandel og Forlag, Apr. 2021 (cited on page 11).

[40] Monica Lavagna et al. 'Benchmarks for environmental impact of housing in Europe: Definition of archetypes and LCA of the residential building stock'. In: *Building and Environment* 145 (Nov. 2018), pp. 260–275. DOI: 10.1016/j.buildenv.2018.09.008. (Visited on 08/04/2023) (cited on page 11).

[41] G. Rebitzer et al. 'Life cycle assessment'. In: *Environment International* 30.5 (July 2004), pp. 701–720. DOI: 10.1016/j.envint.2003.11.005. (Visited on 05/24/2023) (cited on page 12).

[42] International Organization for Standardization. *ISO 14044:2006 Environmental Management—Life Cycle Assessment—Requirements and Guidelines*. 2006 (cited on page 12).

[43] V Masson-Delmotte et al. *Global Warming of 1.5°C: IPCC Special Report - Summary for Policymakers*. Cambridge University Press, June 9, 2022. (Visited on 08/16/2023) (cited on page 13).

[44] European Comitee for Standardization. *EN 15643:2021 Sustainability of construction works - Framework for assessment of buildings and civil engineering works*. 2021. URL: https://www.nen.nl/nen-en-15643-2021-en-285097 (visited on 11/27/2023) (cited on page 13).

[45] European Committee for Standardization (CEN). *Sustainability of Construction Works—Assessment of Environmental Performance of Buildings—Calculation Method; EN 15978*. 2011 (cited on page 13).

[46] Brüttisellen-Zurich. *SIA 2032:2020 L'énergie grise - Établissement du bilan écologique pour la construction de bâtiments*. 2020. URL: http://shop.sia.ch/collection%20des%20normes/architecte/sia%202032/f/2020/F/Product (visited on 02/12/2022) (cited on page 14).

[47] Lisa Wastiels, Laetitia Delem, and Johan Dessel. 'To module D or not to module D? The relevance and difficulties of considering the recycling potential in building LCA'. In: Nov. 5, 2013 (cited on page 14).

[48] INIES. *About the INIES database – INIES*. URL: https://www.inies.fr/about-the-inies-database/ (visited on 06/24/2021) (cited on pages 15, 41).

[49] Urban Development {and} Building Federal Ministry for Housing. *ÖKOBAUDAT*. URL: https://www.oekobaudat.de/no_cache/en/database/search.html (visited on 07/26/2021) (cited on page 15).

[50] Conférence de coordination des services de la construction et des immeubles des maîtres d'ouvrage publics KBOB. *La KBOB se présente*. URL: https://www.kbob.admin.ch/kbob/fr/home/die-kbob/kbob.html (visited on 01/20/2022) (cited on page 15).

[51] Hans De Bruijn et al., eds. *Handbook on Life Cycle Assessment: Operational Guide to the ISO Standards*. Vol. 7. Eco-Efficiency in Industry and Science. Dordrecht: Springer Netherlands, 2002. DOI: 10.1007/0-306-48055-7. (Visited on 11/24/2023) (cited on page 15).

[52] Alexander Hollberg. 'A parametric method for building design optimization based on Life Cycle Assessment'. PhD thesis. Universität Weimar: Fakultät Architektur und Urbanistik, Nov. 23, 2016. 260 pp. (cited on pages 15, 16, 26, 29).

[53] Walter Klöpffer and B. Grahl. 'Life Cycle Assessment (LCA): A Guide to Best Practice'. In: *Life Cycle Assessment (LCA): A Guide to Best Practice* (Apr. 14, 2014), pp. 1–396. DOI: 10.1002/9783527655625 (cited on page 15).

[54] Martin Pehnt. 'Dynamic life cycle assessment (LCA) of renewable energy technologies'. In: *Renewable Energy* 31.1 (Jan. 1, 2006), pp. 55–71. DOI: 10.1016/j.renene.2005.03.002. (Visited on 11/24/2023) (cited on page 15).

[55] Reinout Heijungs and Mark A J Huijbregts. 'A Review of Approaches to Treat Uncertainty in LCA'. In: () (cited on pages 15, 22).

[56] Els Van de moortel et al. 'Dynamic Versus Static Life Cycle Assessment of Energy Renovation for Residential Buildings'. In: *Sustainability* 14.11 (June 2, 2022), p. 6838. DOI: 10.3390/su14116838. (Visited on 09/22/2022) (cited on pages 16, 41, 66).

[57] Architectural/Engineering Productivity Committee of the Construction Users Roundtable (CURT). *Collaboration, Integrated Information, and the Project Lifecycle in Building Design, Construction and Operation*. Aug. 2004. URL: https://kcuc.org/wp-content/uploads/2013/11/Collaboration-Integrated-Information-and-the-Project-Lifecycle.pdf (visited on 05/27/2021) (cited on page 16).

[58] Thomas Bernard Paul Jusselme. 'Data-driven method for low-carbon building design at early stages'. PhD thesis. Ecole Polytechnique de Fédérale de Lausanne: Faculté de l'environnement naturel, architectural et construit, Mar. 30, 2020. 218 pp. (cited on pages 16, 26, 27, 94, 95).

[59] Torben Østergård, Rasmus L. Jensen, and Steffen E. Maagaard. 'Early Building Design: Informed decision-making by exploring multidimensional design space using sensitivity analysis'. In: *Energy and Buildings* 142 (May 2017), pp. 8–22. DOI: 10.1016/j.enbuild.2017.02.059. (Visited on 10/02/2023) (cited on pages 16, 71).

[60] Tove Malmqvist et al. 'Life cycle assessment in buildings: The ENSLIC simplified method and guidelines'. In: *Energy* 36.4 (Apr. 2011), pp. 1900–1907. DOI: 10.1016/j.energy.2010.03.026. (Visited on 12/06/2023) (cited on page 16).

[61] Koji Negishi. 'Development of a methodology of Dynamic LCA applied to the buildings'. PhD thesis. INSA de Toulouse: Other, June 21, 2019. 260 pp. (cited on pages 17, 60, 62).

[62] Shu Su, Xiaodong Li, and Yimin Zhu. 'Dynamic assessment elements and their prospective solutions in dynamic life cycle assessment of buildings'. In: *Building and Environment* 158 (July 2019), pp. 248–259. DOI: 10.1016/j.buildenv.2019.05.008. (Visited on 03/23/2022) (cited on pages 17, 20, 40).

[63] William O. Collinge et al. 'Dynamic life cycle assessment: framework and application to an institutional building'. In: *The International Journal of Life Cycle Assessment* 18.3 (Mar. 2013), pp. 538–552. DOI: 10.1007/s11367-012-0528-2. (Visited on 10/11/2022) (cited on pages 17, 19, 22, 40).

[64] Shu Su et al. 'Assessment models and dynamic variables for dynamic life cycle assessment of buildings: a review'. In: *Environmental Science and Pollution Research* 28.21 (June 2021), pp. 26199–26214. DOI: 10.1007/s11356-021-13614-1. (Visited on 03/23/2022) (cited on pages 17, 18).

[65] Joshua Sohn et al. 'Defining Temporally Dynamic Life Cycle Assessment: A Review'. In: *Integrated Environmental Assessment and Management* 16.3 (May 2020), pp. 314–323. DOI: 10.1002/ieam.4235. (Visited on 07/13/2022) (cited on page 17).

[66] Didier Beloin-Saint-Pierre et al. 'Addressing temporal considerations in life cycle assessment'. In: *Science of The Total Environment* 743 (Nov. 2020), p. 140700. DOI: 10.1016/j.scitotenv.2020.140700. (Visited on 11/29/2023) (cited on page 17).

[67] E Hoxha et al. 'Expanding Boundaries: Systems Thinking for the Built Environment'. In: (), p. 6 (cited on pages 17, 87).

[68] Simone Cornago et al. 'Systematic Literature Review on Dynamic Life Cycle Inventory: Towards Industry 4.0 Applications'. In: *Sustainability* 14.11 (May 25, 2022), p. 6464. DOI: 10.3390/su14116464. (Visited on 02/01/2023) (cited on pages 17, 18).

[69] Didier Vuarnoz and Thomas Jusselme. 'Temporal variations in the primary energy use and greenhouse gas emissions of electricity provided by the Swiss grid'. In: *Energy* 161 (Oct. 2018), pp. 573–582. DOI: 10.1016/j.energy.2018.07.087. (Visited on 01/27/2021) (cited on page 18).

[70] Stefanie Hellweg and Llorenç Milà I Canals. 'Emerging approaches, challenges and opportunities in life cycle assessment'. In: *Science* 344.6188 (June 6, 2014), pp. 1109–1113. DOI: 10.1126/science.1248361. (Visited on 11/29/2023) (cited on page 18).

[71] Koji Negishi et al. 'Evaluating climate change pathways through a building's lifecycle based on Dynamic Life Cycle Assessment'. In: *Building and Environment* 164 (Oct. 2019), p. 106377. DOI: 10.1016/j.buildenv.2019.106377. (Visited on 07/13/2022) (cited on pages 18, 20, 22, 40, 58, 61, 62).

[72] Shu Su, Chen Zhu, and Xiaodong Li. 'A dynamic weighting system considering temporal variations using the DTT approach in LCA of buildings'. In: *Journal of Cleaner Production* 220 (May 2019), pp. 398–407. DOI: 10.1016/j.jclepro.2019.02.140. (Visited on 10/17/2023) (cited on page 18).

[73] Göran Finnveden et al. 'Recent developments in Life Cycle Assessment'. In: *Journal of Environmental Management* 91.1 (Oct. 2009), pp. 1–21. DOI: 10.1016/j.jenvman.2009.06.018. (Visited on 11/29/2023) (cited on page 18).

[74] *RE2020 : retours contrastés des acteurs de la construction*. Batiweb. URL: https://www.batiweb.com/actualites/legislation/www.batiweb.com (visited on 06/07/2023) (cited on pages 18, 46).

[75] William Collinge et al. 'Indoor environmental quality in a dynamic life cycle assessment framework for whole buildings: Focus on human health chemical impacts'. In: *Building and Environment* 62 (Apr. 2013), pp. 182–190. DOI: 10.1016/j.buildenv.2013.01.015. (Visited on 06/13/2023) (cited on page 19).

[76] William O. Collinge et al. 'Dynamic Life Cycle Assessments of a Conventional Green Building and a Net Zero Energy Building: Exploration of Static, Dynamic, Attributional, and Consequential Electricity Grid Models'. In: *Environmental Science & Technology* 52.19 (Oct. 2, 2018), pp. 11429–11438. DOI: 10.1021/acs.est.7b06535. (Visited on 04/13/2021) (cited on page 19).

[77] Ming Hu. 'Dynamic life cycle assessment integrating value choice and temporal factors—A case study of an elementary school'. In: *Energy and Buildings* 158 (Jan. 2018), pp. 1087–1096. DOI: 10.1016/j.enbuild.2017.10.043. (Visited on 07/13/2022) (cited on page 19).

[78] Marine Fouquet et al. 'Methodological challenges and developments in LCA of low energy buildings: Application to biogenic carbon and global warming assessment'. In: *Building and Environment* 90 (Aug. 2015), pp. 51–59. DOI: 10.1016/j.buildenv.2015.03.022. (Visited on 07/13/2022) (cited on page 19).

[79] Francesco Pittau et al. 'Fast-growing bio-based materials as an opportunity for storing carbon in exterior walls'. In: *Building and Environment* 129 (Feb. 2018), pp. 117–129. DOI: 10.1016/j.buildenv.2017.12.006. (Visited on 07/13/2022) (cited on page 19).

[80] Shu Su et al. 'Dynamic LCA framework for environmental impact assessment of buildings'. In: *Energy and Buildings* 149 (Aug. 2017), pp. 310–320. DOI: 10.1016/j.enbuild.2017.05.042. (Visited on 03/12/2021) (cited on page 19).

[81] Koji Negishi et al. 'An operational methodology for applying dynamic Life Cycle Assessment to buildings'. In: *Building and Environment* 144 (Oct. 2018), pp. 611–621. DOI: 10.1016/j.buildenv.2018.09.005. (Visited on 03/24/2022) (cited on pages 20, 42).

[82] Yurong Zhang. 'Taking the Time Characteristic into Account of Life Cycle Assessment: Method and Application for Buildings'. In: *Sustainability* 9.6 (May 31, 2017), p. 922. DOI: 10.3390/su9060922. (Visited on 10/17/2023) (cited on page 20).

[83] Lucas Hajiro Neves Mosquini, Benoit Delinchant, and Thomas Jusselme. 'Application of sensitivity analysis on building dynamic lifecycle assessment of GHG emissions: a French case study'. In: CISBAT 2023. Lausane, Switzerland, Sept. 2023 (cited on pages 22, 83).

[84] Abdulrahman Fnais et al. 'The application of life cycle assessment in buildings: challenges, and directions for future research'. In: *The International Journal of Life Cycle Assessment* 27.5 (May 2022), pp. 627–654. DOI: 10.1007/s11367-022-02058-5. (Visited on 02/01/2023) (cited on page 22).

[85] Alberto Vilches, Antonio Garcia-Martinez, and Benito Sanchez-Montañes. 'Life cycle assessment (LCA) of building refurbishment: A literature review'. In: *Energy and Buildings* 135 (Jan. 2017), pp. 286–301. DOI: 10.1016/j.enbuild.2016.11.042. (Visited on 01/27/2021) (cited on page 22).

[86] Wolfgang Preiser Vischer Jacqueline, ed. *Assessing Building Performance*. London: Routledge, Nov. 23, 2004. 256 pp. DOI: 10.4324/9780080455228 (cited on page 23).

[87] Doug King. *Engineering a low carbon built environment: the discipline of building engineering physics*. OCLC: 642292689. London: Royal Academy of Engineering, 2010 (cited on page 24).

[88] Thijs Vandenbussche. 'Is the EU's building renovation wave 'fit for 55'?' In: () (cited on page 24).

[89] European Comission. *Horizon 2020 - Work Programme 2018-2020: Secure, clean and efficient energy*. Sept. 17, 2020 (cited on pages 24, 89).

[90] Anne N. Nielsen et al. 'Early stage decision support for sustainable building renovation – A review'. In: *Building and Environment* 103 (July 2016), pp. 165–181. DOI: 10.1016/j.buildenv.2016.04.009. (Visited on 10/03/2023) (cited on pages 24, 25).

[91] Max H. Bazerman and Don A. Moore. *Judgment in managerial decision making*. 8. ed. Hoboken, N.J: Wiley, 2013. 277 pp. (cited on page 24).

[92] Joaquim Ferreira, Manuel Duarte Pinheiro, and Jorge De Brito. 'Refurbishment decision support tools review—Energy and life cycle as key aspects to sustainable refurbishment projects'. In: *Energy Policy* 62 (Nov. 2013), pp. 1453–1460. DOI: 10.1016/j.enpol.2013.06.082. (Visited on 12/10/2023) (cited on page 25).

[93] Kari Alanne. 'Selection of renovation actions using multi-criteria "knapsack" model'. In: *Automation in Construction* (2004). DOI: 10.1016/J.AUTCON.2003.12.004 (cited on page 25).

[94] Mathieu Thorel. 'Aide à la décision multicritère pour la prescription de scénarios d'amélioration énergétique via une approche globale'. PhD thesis. Université de Grenoble, Oct. 16, 2014 (cited on pages 25, 31).

[95] Torben Østergård, Rasmus L. Jensen, and Steffen E. Maagaard. 'Building simulations supporting decision making in early design – A review'. In: *Renewable and Sustainable Energy Reviews* 61 (Aug. 2016), pp. 187–201. DOI: 10.1016/j.rser.2016.03.045. (Visited on 10/02/2023) (cited on pages 25, 26).

[96] Tan Tan et al. 'Combining multi-criteria decision making (MCDM) methods with building information modelling (BIM): A review'. In: *Automation in Construction* 121 (Jan. 2021), p. 103451. DOI: 10.1016/j.autcon.2020.103451. (Visited on 10/02/2023) (cited on page 25).

[97] Wei Tian et al. 'A review of uncertainty analysis in building energy assessment'. In: *Renewable and Sustainable Energy Reviews* 93 (Oct. 2018), pp. 285–301. DOI: 10.1016/j.rser.2018.05.029. (Visited on 01/31/2023) (cited on page 26).

[98] Young-Jin Kim, Ki-Uhn Ahn, and Cheol-Soo Park. 'Decision making of HVAC system using Bayesian Markov chain Monte Carlo method'. In: *Energy and Buildings* 72 (Apr. 2014), pp. 112–121. DOI: 10.1016/j.enbuild.2013.12.039. (Visited on 12/11/2023) (cited on page 26).

[99] Yuming Sun et al. 'Exploring HVAC system sizing under uncertainty'. In: *Energy and Buildings* 81 (Oct. 2014), pp. 243–252. DOI: 10.1016/j.enbuild.2014.06.026. (Visited on 12/11/2023) (cited on page 26).

[100] Marie-Lise Pannier. 'Étude de la quantification des incertitudes en analyse de cycle de vie des bâtiments'. PhD thesis. Université Paris sciences et lettres: Eco-conception, Oct. 24, 2017. 485 pp. (cited on page 26).

[101] Endrit Hoxha et al. 'Influence of construction material uncertainties on residential building LCA reliability'. In: *Journal of Cleaner Production* 144 (Feb. 2017), pp. 33–47. DOI: 10.1016/j.jclepro.2016.12.068. (Visited on 02/17/2021) (cited on page 26).

[102] Alina Galimshina et al. 'Statistical method to identify robust building renovation choices for environmental and economic performance'. In: *Building and Environment* 183 (Oct. 2020), p. 107143. DOI: 10.1016/j.buildenv.2020.107143. (Visited on 09/22/2024) (cited on pages 26, 27, 35, 87).

[103] Gloria Calleja Rodríguez et al. 'Uncertainties and sensitivity analysis in building energy simulation using macroparameters'. In: *Energy and Buildings* 67 (Dec. 2013), pp. 79–87. DOI: 10.1016/j.enbuild.2013.08.009. (Visited on 09/15/2022) (cited on page 27).

[104] Vincenzo Corrado and Houcem Eddine Mechri. 'Uncertainty and Sensitivity Analysis for Building Energy Rating'. In: *Journal of Building Physics* 33.2 (Oct. 2009), pp. 125–156. DOI: 10.1177/1744259109104884. (Visited on 09/15/2022) (cited on page 27).

[105] Nazanin Rezaei Oghazi, Thomas Jusselme, and Marilyne Andersen. 'Evaluation of daylighting strategies based on their embodied carbon emissions: a first methodological framework and case study'. In: 2021 Building Simulation Conference. Sept. 1, 2021. DOI: 10.26868/25222708.2021.30691. (Visited on 06/08/2023) (cited on page 27).

[106] H.L. Gauch et al. 'What really matters in multi-storey building design? A simultaneous sensitivity study of embodied carbon, construction cost, and operational energy'. In: *Applied Energy* 333 (Mar. 2023), p. 120585. DOI: 10.1016/j.apenergy.2022.120585. (Visited on 01/31/2023) (cited on pages 27, 62).

[107] Max D. Morris. 'Factorial Sampling Plans for Preliminary Computational Experiments'. In: *Technometrics* 33.2 (May 1991), pp. 161–174. DOI: 10.1080/00401706.1991.10484804. (Visited on 11/14/2022) (cited on page 28).

[108] I.M Sobol. 'Global sensitivity indices for nonlinear mathematical models and their Monte Carlo estimates'. In: *Mathematics and Computers in Simulation* 55.1 (Feb. 2001), pp. 271–280. DOI: 10.1016/S0378-4754(00)00270-6. (Visited on 11/14/2022) (cited on page 28).

[109] Thomas Olofsson, Staffan Andersson, and Jan-Ulric Sjögren. 'Building energy parameter investigations based on multivariate analysis'. In: *Energy and Buildings* 41.1 (Jan. 2009), pp. 71–80. DOI: 10.1016/j.enbuild.2008.07.012. (Visited on 12/12/2023) (cited on page 29).

[110] Inna Bilous, Valerii Deshko, and Iryna Sukhodub. 'Parametric analysis of external and internal factors influence on building energy performance using non-linear multivariate regression models'. In: *Journal of Building Engineering* 20 (Nov. 2018), pp. 327–336. DOI: 10.1016/j.jobe.2018.07.021. (Visited on 12/12/2023) (cited on page 29).

[111] Janelle S. Hygh et al. 'Multivariate regression as an energy assessment tool in early building design'. In: *Building and Environment* 57 (Nov. 2012), pp. 165–175. DOI: 10.1016/j.buildenv.2012.04.021. (Visited on 12/12/2023) (cited on page 29).

[112] Ehsan Asadi et al. 'Multi-objective optimization for building retrofit: A model using genetic algorithm and artificial neural network and an application'. In: *Energy and Buildings* 81 (Oct. 2014), pp. 444–456. DOI: 10.1016/j.enbuild.2014.06.009. (Visited on 02/24/2023) (cited on pages 29, 31).

[113] Fabian Ritter, Philipp Geyer, and André Borrmann. 'Simulation-based Decision-making in Early Design Stages'. In: CIB W78 Conference. Vol. 32. Eindhoven, The Netherlands, 2015 (cited on page 29).

[114] Thomas Jusselme et al. 'Visualization techniques for heterogeneous and multidimensional simulated building performance data sets'. In: (2017), p. 14 (cited on pages 29, 105).

[115] Yunming Shao, Philipp Geyer, and Werner Lang. 'Integrating requirement analysis and multi-objective optimization for office building energy retrofit strategies'. In: *Energy and Buildings* 82 (Oct. 2014), pp. 356–368. DOI: 10.1016/j.enbuild.2014.07.030. (Visited on 02/24/2023) (cited on pages 30, 31).

[116] Anh-Tuan Nguyen, Sigrid Reiter, and Philippe Rigo. 'A review on simulation-based optimization methods applied to building performance analysis'. In: *Applied Energy* 113 (Jan. 2014), pp. 1043–1058. DOI: 10.1016/j.apenergy.2013.08.061. (Visited on 12/12/2023) (cited on pages 30, 31, 33).

[117] Vasileios Machairas, Aris Tsangrassoulis, and Kleo Axarli. 'Algorithms for optimization of building design: A review'. In: *Renewable and Sustainable Energy Reviews* 31 (Mar. 2014), pp. 101–112. DOI: 10.1016/j.rser.2013.11.036. (Visited on 10/04/2023) (cited on pages 30, 95).

[118] Jonathan A. Wright, Heather A. Loosemore, and Raziyeh Farmani. 'Optimization of building thermal design and control by multi-criterion genetic algorithm'. In: *Energy and Buildings*. A View of Energy and Bilding Performance Simulation at the start of the third millennium 34.9 (Oct. 1, 2002), pp. 959–972. DOI: 10.1016/S0378-7788(02)00071-3. (Visited on 06/14/2023) (cited on pages 30, 33).

[119] Ehsan Asadi et al. 'Multi-objective optimization for building retrofit strategies: A model and an application'. In: *Energy and Buildings* 44 (Jan. 2012), pp. 81–87. DOI: 10.1016/j.enbuild.2011.10.016. (Visited on 02/24/2023) (cited on pages 30, 33).

[120] Federica Rosso et al. 'Multi-objective optimization of building retrofit in the Mediterranean climate by means of genetic algorithm application'. In: *Energy and Buildings* 216 (June 2020), p. 109945. DOI: 10.1016/j.enbuild.2020.109945. (Visited on 02/24/2023) (cited on page 31).

[121] Farshid Shadram et al. 'Exploring the trade-off in life cycle energy of building retrofit through optimization'. In: *Applied Energy* 269 (July 2020), p. 115083. DOI: 10.1016/j.apenergy.2020.115083. (Visited on 02/24/2023) (cited on page 31).

[122] L H Neves Mosquini, V Tappy, and T Jusselme. 'A carbon-focus parametric study on building insulation materials and thicknesses for different heating systems: A Swiss case study'. In: *IOP Conference Series: Earth and Environmental Science* 1078.1 (Sept. 1, 2022), p. 012102. DOI: 10.1088/1755-1315/1078/1/012102. (Visited on 10/11/2022) (cited on pages 31, 32).

[123] Lucas Hajiro Neves Mosquini, Benoit Delinchant, and Thomas Jusselme. 'Dynamic Lca Methodology to Support Post-Occupancy Decision-Making for Carbon Budget Compliance'. In: *Energy and Buildings* (Pre-Peer Review 2023). DOI: 10.2139/ssrn.4538384. (Visited on 11/29/2023) (cited on page 31).

[124] Abbass Raad et al. 'HYBRID DISCRET-CONTINUOUS MULTI-CRITERION OPTIMIZATION FOR BUILDING DESIGN'. In: () (cited on page 31).

[125] Fanny Pernodet Chantrelle et al. 'Development of a multicriteria tool for optimizing the renovation of buildings'. In: *Applied Energy* 88.4 (Apr. 1, 2011), pp. 1386–1394. DOI: 10.1016/j.apenergy.2010.10.002. (Visited on 03/03/2023) (cited on page 32).

[126] Sacha Hodencq et al. 'Including greenhouse gas emissions and behavioural responses in the optimal design of PV self-sufficient energy communities'. In: *COMPEL - The international journal for computation and mathematics in electrical and electronic engineering* 41.6 (Jan. 1, 2022). Publisher: Emerald Publishing Limited, pp. 2072–2083. DOI: 10.1108/COMPEL-10-2021-0392. (Visited on 02/24/2023) (cited on pages 33, 100).

[127] Araz Ashouri et al. 'Optimal design and operation of building services using mixed-integer linear programming techniques'. In: *Energy* 59 (Sept. 2013), pp. 365–376. DOI: 10.1016/j.energy.2013.06.053. (Visited on 12/12/2023) (cited on page 33).

[128] Ali Bolattürk. 'Determination of optimum insulation thickness for building walls with respect to various fuels and climate zones in Turkey'. In: *Applied Thermal Engineering* 26.11 (Aug. 2006), pp. 1301–1309. DOI: 10.1016/j.applthermaleng.2005.10.019. (Visited on 02/07/2022) (cited on page 33).

[129] Bérenger Favre. 'Etude de stratégies de gestion énergétique des bâtiments par l'application de la programmation dynamique'. PhD thesis. Ecole Nationale Supérieure des Mines de Paris, 2013 (cited on page 33).

[130] Sacha Hodencq, Benoit Delinchant, and Frédéric Wurtz. 'Vers l'ouverture des modèles d'optimisation de systèmes énergétiques pour l'Analyse de Cycle de Vie : cas d'étude d'un foyer en autoconsommation photovoltaïque avec l'outil open source NoLOAD'. In: *Symposium de Génie Electrique*. Vol. SGE 2020. Nantes, Nov. 18, 2020 (cited on page 33).

[131] Saman Abbasi and Esmatullah Noorzai. 'The BIM-Based multi-optimization approach in order to determine the trade-off between embodied and operation energy focused on renewable energy use'. In: *Journal of Cleaner Production* 281 (Jan. 2021), p. 125359. DOI: 10.1016/j.jclepro.2020.125359. (Visited on 03/03/2021) (cited on page 34).

[132] N. Delgarm et al. 'Multi-objective optimization of the building energy performance: A simulation-based approach by means of particle swarm optimization (PSO)'. In: *Applied Energy* 170 (May 2016), pp. 293–303. DOI: 10.1016/j.apenergy.2016.02.141. (Visited on 12/12/2023) (cited on page 34).

[133] Toke Rammer Nielsen. *Optimization of buildings with respect to energy and indoor environment*. No. R-036. Byg Rapport, Technical University of Denmark, 2003 (cited on page 34).

[134] Michael Wetter and Jonathan Wright. 'A comparison of deterministic and probabilistic optimization algorithms for nonsmooth simulation-based optimization'. In: *Building and Environment* 39.8 (Aug. 2004), pp. 989–999. DOI: 10.1016/j.buildenv.2004.01.022. (Visited on 02/11/2024) (cited on page 34).

[135] Seyed Amirhosain Sharif and Amin Hammad. 'Simulation-Based Multi-Objective Optimization of institutional building renovation considering energy consumption, Life-Cycle Cost and Life-Cycle Assessment'. In: *Journal of Building Engineering* 21 (Jan. 2019), pp. 429–445. DOI: 10.1016/j.jobe.2018.11.006. (Visited on 04/22/2021) (cited on page 34).

[136] George Mavrotas, José Rui Figueira, and Eleftherios Siskos. 'Robustness analysis methodology for multi-objective combinatorial optimization problems and application to project selection'. In: *Omega* 52 (Apr. 2015), pp. 142–155. DOI: 10.1016/j.omega.2014.11.005. (Visited on 12/13/2023) (cited on page 35).

[137] Shabnam Homaei and Mohamed Hamdy. 'A robustness-based decision making approach for multi-target high performance buildings under uncertain scenarios'. In: *Applied Energy* 267 (June 2020), p. 114868. DOI: 10.1016/j.apenergy.2020.114868. (Visited on 12/13/2023) (cited on page 35).

[138] Rajesh Kotireddy, Pieter-Jan Hoes, and Jan L.M. Hensen. 'A methodology for performance robustness assessment of low-energy buildings using scenario analysis'. In: *Applied Energy* 212 (Feb. 2018), pp. 428–442. DOI: 10.1016/j.apenergy.2017.12.066. (Visited on 12/13/2023) (cited on page 35).

[139] Linus Walker, Illias Hischier, and Arno Schlueter. 'Does context matter? Robust building retrofit decision-making for decarbonization across Europe'. In: *Building and Environment* 226 (Dec. 2022), p. 109666. DOI: 10.1016/j.buildenv.2022.109666. (Visited on 09/20/2023) (cited on pages 35, 81).

[140] Mija Frossard. 'Optimisation robuste multicritère pour l'écoconception de bâtiments zéro-énergie'. PhD thesis. Université Paris sciences et lettres, 2020 (cited on pages 41, 48, 49, 66).

[141] ByConception. *ByConception - Permis de construire et déclaration préalable | Facebook*. URL: https://www.facebook.com/byconception (visited on 04/28/2024) (cited on page 44).

[142] INSEE. *37,2 millions de logements en France au 1er janvier 2021*. URL: https://www.insee.fr/fr/statistiques/5761272#tableau-figure3 (visited on 04/27/2023) (cited on page 44).

[143] INIES. *INIES | Les données environnementales et sanitaires de référence pour le bâtiment*. URL: https://www.base-inies.fr/iniesV4/dist/consultation.html (visited on 05/23/2022) (cited on pages 44, 97, 155, 159).

[144] *Climate Change 2014: Synthesis Report*. IPCC Assessment Report. Geneva, Switzerland: Intergovernmental Panel on Climate Change, 2015 (cited on pages 47, 48).

[145] Karl E. Taylor, Ronald J. Stouffer, and Gerald A. Meehl. 'An Overview of CMIP5 and the Experiment Design'. In: *Bulletin of the American Meteorological Society* 93.4 (Apr. 1, 2012), pp. 485–498. DOI: 10.1175/BAMS-D-11-00094.1. (Visited on 09/20/2023) (cited on page 48).

[146] Charlotte Roux et al. 'Integrating climate change and energy mix scenarios in LCA of buildings and districts'. In: *Applied Energy* 184 (Dec. 2016), pp. 619–629. DOI: 10.1016/j.apenergy.2016.10.043. (Visited on 05/05/2021) (cited on pages 48, 81).

[147] Charlotte Roux, Patrick Schalbart, and Bruno Peuportier. 'Accounting for temporal variation of electricity production and consumption in the LCA of an energy-efficient house'. In: *Journal of Cleaner Production* 113 (Feb. 2016), pp. 532–540. DOI: 10.1016/j.jclepro.2015.11.052. (Visited on 01/27/2021) (cited on page 50).

[148] Nicolae Scarlat, Matteo Prussi, and Monica Padella. 'Quantification of the carbon intensity of electricity produced and used in Europe'. In: *Applied Energy* 305 (Jan. 2022), p. 117901. DOI: 10.1016/j.apenergy.2021.117901. (Visited on 08/17/2023) (cited on pages 50, 51).

[149] Steffen Schlömer et al. *Climate Change 2014: Mitigation of Climate Change. Contribution of Working Group III to the Fifth Assessment Report of the Intergovernmental Panel on Climate Change*. Cambridge, UK and New York City, USA: Cambridge University Press (cited on pages 50, 51).

[150] RTE. *Les émissions de CO2 par kWh produit en France*. URL: https://www.rte-france.com/eco2mix/les-emissions-de-co2-par-kwh-produit-en-france (visited on 07/05/2021) (cited on pages 50, 51, 62).

[151] Stéphanie Bouckaert et al. *Net Zero by 2050 - A Roadmap for the Global Energy Sector*. Paris, France: International Energy Agency, Oct. 2021 (cited on page 52).

[152] Réseau de transport d'électricité RTE. *Futurs énergétiques 2050 : Bilan de la Phase I - Synthèse et enseignements issus de la consultation publique*. June 2021. URL: https://assets.rte-france.com/prod/public/2021-06/BP50_Bilan%20de%20la%20consultation%20publique.pdf (cited on pages 52, 54, 62).

[153] Maria Apolonia and Teresa Simas. 'Life Cycle Assessment of an Oscillating Wave Surge Energy Converter'. In: (2021), p. 17 (cited on page 54).

[154] Åsa Grytli Tveten. 'Life Cycle Assessment of Offshore Wind Electricity Generation in Scandinavia'. In: () (cited on page 54).

[155] Ministère de la Transition Ecologique et Solidaire. *Stratégie Nationale Bas Carbone : La transition écologique et solidaire vers la neutralité carbone*. Mar. 2020. URL: https://www.ecologie.gouv.fr/sites/default/files/SNBC-2%20synthe%CC%80se%20VF.pdf (visited on 10/07/2022) (cited on pages 55–57, 62).

[156] Stephane Frijia, Subhrajit Guhathakurta, and Eric Williams. 'Functional Unit, Technological Dynamics, and Scaling Properties for the Life Cycle Energy of Residences'. In: *Environmental Science & Technology* 46.3 (Feb. 7, 2012), pp. 1782–1788. DOI: 10.1021/es202202q. (Visited on 06/18/2021) (cited on pages 58, 62).

[157] Georgios Eleftheriadis and Mohamed Hamdy. 'The Impact of Insulation and HVAC Degradation on Overall Building Energy Performance: A Case Study'. In: *Buildings* 8.2 (Feb. 2, 2018), p. 23. DOI: 10.3390/buildings8020023. (Visited on 09/15/2022) (cited on pages 58, 60, 62).

[158] European Comitee for Standardization. *EN 13162:2008 Thermal insulation products for buildings - Factory made mineral wool (MW) products*. 2008 (cited on page 59).

[159] European Comitee for Standardization. *EN 13163:2008 Thermal insulation products for buildings - Factory made expanded polystyrene*. 2008 (cited on page 59).

[160] Hyun-Jung Choi, Jae-Sik Kang, and Jung-Ho Huh. 'A Study on Variation of Thermal Characteristics of Insulation Materials for Buildings According to Actual Long-Term Annual Aging Variation'. In: *International Journal of Thermophysics* 39.1 (Jan. 2018). DOI: 10.1007/s10765-017-2318-3. (Visited on 07/27/2021) (cited on page 60).

[161] F. Stazi et al. 'Assessment of the actual hygrothermal performance of glass mineral wool insulation applied 25 years ago in masonry cavity walls'. In: *Energy and Buildings* 68 (Jan. 2014), pp. 292–304. DOI: 10.1016/j.enbuild.2013.09.032. (Visited on 03/23/2021) (cited on page 60).

[162] Faïez Maaloul. *Déperditions thermiques : comment réduire sa facture énergétique ?* Clim PAC. Oct. 1, 2020. URL: https://www.clim-pac.fr/comment-limiter-les-deperditions-thermiques/ (visited on 03/24/2024) (cited on page 60).

[163] Valerie Leprince, Nolwenn Hurel, and Bassam Moujalled. 'Durability of building airtightness'. In: *AIVC Technical Note 71*. International Energy Agency Implementing Agreement for a Programme of Research and Development on Energy in Buildings and Communities. INIVE, Sept. 2022 (cited on page 60).

[164] Jennifer McWilliams and Melanie Jung. *Development of a Mathematical Air-Leakage Model from MeasuredData*. LBNL–59041, 883786. May 1, 2006, LBNL–59041, 883786. DOI: 10.2172/883786. (Visited on 09/20/2023) (cited on page 60).

[165] D. C. Jordan and S. R. Kurtz. 'Photovoltaic Degradation Rates—an Analytical Review'. In: *Progress in Photovoltaics: Research and Applications* 21.1 (2013). _eprint: https://onlinelibrary.wiley.com/doi/pd pp. 12–29. DOI: 10.1002/pip.1182. (Visited on 04/17/2023) (cited on pages 60, 62).

[166] Shu Su et al. 'Dynamic global warming impact assessment integrating temporal variables: Application to a residential building in China'. In: *Environmental Impact Assessment Review* 88 (May 2021), p. 106568. DOI: 10.1016/j.eiar.2021.106568. (Visited on 07/13/2022) (cited on pages 61, 83).

[167] Eric Vorger, Patrick Schalbart, and Bruno Peuportier. 'Integration of a Comprehensive Stochastic Model of Occupancy in Building Simulation to Study how Inhabitants Influence Energy Performance'. In: (2014), p. 9 (cited on page 61).

[168] Didier Beloin-Saint-Pierre et al. 'Implementing a Dynamic Life Cycle Assessment Methodology with a Case Study on Domestic Hot Water Production: Implementing a Dynamic LCA Methodology'. In: *Journal of Industrial Ecology* 21.5 (Oct. 2017), pp. 1128–1138. DOI: 10.1111/jiec.12499. (Visited on 09/05/2022) (cited on page 62).

[169] Hyun-Jung Choi et al. 'Analysis of Long-Term Change in the Thermal Resistance of Extruded Insulation Materials through Accelerated Tests'. In: *Applied Sciences* 11.19 (Oct. 8, 2021), p. 9354. DOI: 10.3390/app11199354. (Visited on 11/14/2022) (cited on page 62).

[170] INSEE. *Depuis 11 ans, moins de tâches ménagères, plus d'Internet*. 2011. URL: https://www.insee.fr/fr/statistiques/1281050#consulter (visited on 04/17/2023) (cited on page 62).

[171] Éric Vorger. 'Étude de l'influence du comportement des habitants sur la performance énergétique du bâtiment'. PhD thesis. Ecole Nationale Supérieure des Mines de Paris, Apr. 12, 2014 (cited on page 62).

[172] Liesje Van Gelder et al. 'Comparative study of metamodelling techniques in building energy simulation: Guidelines for practitioners'. In: *Simulation Modelling Practice and Theory* 49 (Dec. 2014), pp. 245–257. DOI: 10.1016/j.simpat.2014.10.004. (Visited on 12/25/2023) (cited on page 66).

[173] Sandrine Duprez et al. 'Improving life cycle-based exploration methods by coupling sensitivity analysis and metamodels'. In: *Sustainable Cities and Society* 44 (Jan. 2019), pp. 70–84. DOI: 10.1016/j.scs.2018.09.032. (Visited on 01/27/2021) (cited on pages 69, 71, 72, 81).

[174] Shady Attia et al. 'Simulation-based decision support tool for early stages of zero-energy building design'. In: *Energy and Buildings* 49 (June 2012), pp. 2–15. DOI: 10.1016/j.enbuild.2012.01.028. (Visited on 09/05/2023) (cited on pages 70, 71).

[175] Paul Westermann and Ralph Evins. 'Surrogate modelling for sustainable building design – A review'. In: *Energy and Buildings* 198 (Sept. 2019), pp. 170–186. DOI: 10.1016/j.enbuild.2019.05.057. (Visited on 01/26/2023) (cited on pages 70, 71).

[176] Hwang Yi, Ravi S. Srinivasan, and William W. Braham. 'An integrated energy–emergy approach to building form optimization: Use of EnergyPlus, emergy analysis and Taguchi-regression method'. In: *Building and Environment* 84 (Jan. 1, 2015), pp. 89–104. DOI: 10.1016/j.buildenv.2014.10.013. (Visited on 06/19/2023) (cited on page 71).

[177] Sundaravelpandian Singaravel, Johan Suykens, and Philipp Geyer. 'Deep-learning neural-network architectures and methods: Using component-based models in building-design energy prediction'. In: *Advanced Engineering Informatics* 38 (Oct. 2018), pp. 81–90. DOI: 10.1016/j.aei.2018.06.004. (Visited on 01/31/2023) (cited on page 71).

[178] Joshua Hester, Jeremy Gregory, and Randolph Kirchain. 'Sequential early-design guidance for residential single-family buildings using a probabilistic metamodel of energy consumption'. In: *Energy and Buildings* 134 (Jan. 2017), pp. 202–211. DOI: 10.1016/j.enbuild.2016.10.047. (Visited on 10/02/2023) (cited on page 71).

[179] Lisa Rivalin et al. 'A comparison of methods for uncertainty and sensitivity analysis applied to the energy performance of new commercial buildings'. In: *Energy and Buildings* 166 (May 2018), pp. 489–504. DOI: 10.1016/j.enbuild.2018.02.021. (Visited on 10/02/2023) (cited on page 71).

[180] Louis-Gabriel Maltais and Louis Gosselin. 'Daylighting 'energy and comfort' performance in office buildings: Sensitivity analysis, metamodel and pareto front'. In: *Journal of Building Engineering* 14 (Nov. 2017), pp. 61–72. DOI: 10.1016/j.jobe.2017.09.012. (Visited on 10/02/2023) (cited on page 71).

[181] Xi Chen and Hongxing Yang. 'Integrated energy performance optimization of a passively designed high-rise residential building in different climatic zones of China'. In: *Applied Energy* 215 (Apr. 2018), pp. 145–158. DOI: 10.1016/j.apenergy.2018.01.099. (Visited on 10/02/2023) (cited on page 71).

[182] Bryan Eisenhower et al. 'A methodology for meta-model based optimization in building energy models'. In: *Energy and Buildings* 47 (Apr. 2012), pp. 292–301. DOI: 10.1016/j.enbuild.2011.12.001. (Visited on 10/02/2023) (cited on page 71).

[183] A. Prada, A. Gasparella, and P. Baggio. 'On the performance of meta-models in building design optimization'. In: *Applied Energy* 225 (Sept. 2018), pp. 814–826. DOI: 10.1016/j.apenergy.2018.04.129. (Visited on 01/26/2023) (cited on page 71).

[184] Seyed Amirhosain Sharif and Amin Hammad. 'Developing surrogate ANN for selecting near-optimal building energy renovation methods considering energy consumption, LCC and LCA'. In: *Journal of Building Engineering* 25 (Sept. 2019), p. 100790. DOI: 10.1016/j.jobe.2019.100790. (Visited on 01/31/2023) (cited on page 71).

[185] Benedek Kiss and Zsuzsa Szalay. 'Modular approach to multi-objective environmental optimization of buildings'. In: *Automation in Construction* 111 (Mar. 2020), p. 103044. DOI: 10.1016/j.autcon.2019.103044. (Visited on 05/09/2023) (cited on page 71).

[186] Torben Østergård, Rasmus Lund Jensen, and Steffen Enersen Maagaard. 'A comparison of six metamodeling techniques applied to building performance simulations'. In: *Applied Energy* 211 (Feb. 2018), pp. 89–103. DOI: 10.1016/j.apenergy.2017.10.102. (Visited on 01/31/2023) (cited on pages 71, 72).

[187] Eduardo C. Garrido-Merchán and Daniel Hernández-Lobato. 'Dealing with categorical and integer-valued variables in Bayesian Optimization with Gaussian processes'. In: *Neurocomputing* 380 (Mar. 2020), pp. 20–35. DOI: 10.1016/j.neucom.2019.11.004. (Visited on 01/26/2023) (cited on page 72).

[188] Mathilde Grandjacques, Benoît Delinchant, and Olivier Adrot. 'Pick and Freeze estimation for dynamic models with dependent inputs'. In: (Aug. 9, 2015) (cited on page 78).

[189] M Ramaswami and R Bhaskaran. 'A Study on Feature Selection Techniques in Educational Data Mining'. In: 1.1 (2009) (cited on page 79).

[190] Liang Zhang. 'Data-driven building energy modeling with feature selection and active learning for data predictive control'. In: *Energy and Buildings* 252 (Dec. 2021), p. 111436. DOI: 10.1016/j.enbuild.2021.111436. (Visited on 12/27/2023) (cited on page 79).

[191] Liang Zhang and Jin Wen. 'A systematic feature selection procedure for short-term data-driven building energy forecasting model development'. In: *Energy and Buildings* 183 (Jan. 2019), pp. 428–442. DOI: 10.1016/j.enbuild.2018.11.010. (Visited on 12/27/2023) (cited on page 79).

[192] Qingyao Qiao, Akilu Yunusa-Kaltungo, and Rodger E. Edwards. 'Feature selection strategy for machine learning methods in building energy consumption prediction'. In: *Energy Reports* 8 (Nov. 2022), pp. 13621–13654. DOI: 10.1016/j.egyr.2022.10.125. (Visited on 12/27/2023) (cited on page 79).

[193] Xue Liu et al. 'Investigating the performance of machine learning models combined with different feature selection methods to estimate the energy consumption of buildings'. In: *Energy and Buildings* 273 (Oct. 2022), p. 112408. DOI: 10.1016/j.enbuild.2022.112408. (Visited on 12/27/2023) (cited on page 79).

[194] Pablo Rodriguez-Mier, Manuel Mucientes, and Alberto Bugarín. 'Feature Selection and Evolutionary Rule Learning for Big Data in Smart Building Energy Management'. In: *Cognitive Computation* 11.3 (June 2019), pp. 418–433. DOI: 10.1007/s12559-019-09630-6. (Visited on 12/27/2023) (cited on page 79).

[195] John Neale et al. 'Accurate identification of influential building parameters through an integration of global sensitivity and feature selection techniques'. In: *Applied Energy* 315 (June 2022), p. 118956. DOI: 10.1016/j.apenergy.2022.118956. (Visited on 12/27/2023) (cited on page 79).

[196] Shu Chen et al. 'Long-Term Prediction of Weather for Analysis of Residential Building Energy Consumption in Australia'. In: *Energies* 14.16 (Aug. 6, 2021), p. 4805. DOI: 10.3390/en14164805. (Visited on 11/14/2022) (cited on page 81).

[197] Delphine Ramon et al. 'Dynamic modelling of operational energy use in a building LCA: a case study of a Belgian office building'. In: *Energy and Buildings* (Nov. 2022), p. 112634. DOI: 10.1016/j.enbuild.2022.112634. (Visited on 11/09/2022) (cited on page 81).

[198] Lucas Rosse Caldas et al. 'Bamboo bio-concrete as an alternative for buildings' climate change mitigation and adaptation'. In: *Construction and Building Materials* 263 (Dec. 2020), p. 120652. DOI: 10.1016/j.conbuildmat.2020.120652. (Visited on 02/01/2023) (cited on page 81).

[199] David A. Waddicor et al. 'Climate change and building ageing impact on building energy performance and mitigation measures application: A case study in Turin, northern Italy'. In: *Building and Environment* 102 (June 2016), pp. 13–25. DOI: 10.1016/j.buildenv.2016.03.003. (Visited on 09/15/2022) (cited on page 81).

[200] Tatiana de Meester et al. 'Impacts of occupant behaviours on residential heating consumption for detached houses in a temperate climate in the northern part of Europe'. In: *Energy and Buildings* 57 (Feb. 2013), pp. 313–323. DOI: 10.1016/j.enbuild.2012.11.005. (Visited on 10/11/2022) (cited on page 81).

[201] Linus Walker, Illias Hischier, and Arno Schlueter. 'The impact of modeling assumptions on retrofit decision-making for low-carbon buildings'. In: *Building and Environment* 226 (Dec. 2022), p. 109683. DOI: 10.1016/j.buildenv.2022.109683. (Visited on 09/20/2023) (cited on pages 81, 100).

[202] Andrea Saltelli et al. 'Variance based sensitivity analysis of model output. Design and estimator for the total sensitivity index'. In: *Computer Physics Communications* 181.2 (Feb. 2010), pp. 259–270. DOI: 10.1016/j.cpc.2009.09.018. (Visited on 11/14/2022) (cited on page 82).

[203] Marie-Lise Pannier, Patrick Schalbart, and Bruno Peuportier. 'Comprehensive assessment of sensitivity analysis methods for the identification of influential factors in building life cycle assessment'. In: *Journal of Cleaner Production* 199 (Oct. 2018), pp. 466–480. DOI: 10.1016/j.jclepro.2018.07.070. (Visited on 11/16/2022) (cited on page 82).

[204] Linus Walker. 'Scenario-based Robustness Assessment for low-emission Building Retrofit'. Artwork Size: 179 p. Medium: application/pdf Pages: 179 p. PhD thesis. ETH Zurich, 2022. DOI: 10.3929/ETHZ-B-000584675. (Visited on 09/20/2023) (cited on pages 83, 92).

[205] R. Sacchi et al. 'PRospective EnvironMental Impact asSEment (premise): A streamlined approach to producing databases for prospective life cycle assessment using integrated assessment models'. In: *Renewable and Sustainable Energy Reviews* 160 (May 2022), p. 112311. DOI: 10.1016/j.rser.2022.112311. (Visited on 05/05/2024) (cited on page 85).

[206] Sheida Shahi et al. 'A definition framework for building adaptation projects'. In: *Sustainable Cities and Society* 63 (Dec. 2020), p. 102345. DOI: 10.1016/j.scs.2020.102345. (Visited on 10/03/2023) (cited on page 90).

[207] European Comitee for Standardization. *EN 15804:2012+A2:2019 Contribution des ouvrages de construction au développement durable - Déclarations environnementales sur les produits - Règles régissant les catégories de produits de construction*. 2014 (cited on page 91).

[208] Linus Walker et al. 'Comparing Metrics for Scenario-based Robustness Assessment of Building Performance'. In: *Journal of Physics: Conference Series* 2042.1 (Nov. 1, 2021), p. 012150. DOI: 10.1088/1742-6596/2042/1/012150. (Visited on 09/20/2023) (cited on page 93).

[209] Thomas Lützkendorf and Rolf Frischknecht. '(Net-) zero-emission buildings: a typology of terms and definitions'. In: *Buildings and Cities* 1.1 (Sept. 25, 2020), pp. 662–675. DOI: 10.5334/bc.66. (Visited on 01/05/2024) (cited on page 100).

[210] P Saves et al. 'A new mixed-categorical correlation kernel for Gaussian process'. In: 2023 (2023) (cited on page 103).

[211] Abdelaziz Maalej, Nancy Rodriguez, and Olivier Strauss. 'Survey of multidimensional visualization techniques'. In: () (cited on page 105).

[212] Julian Heinrich and Daniel Weiskopf. 'State of the Art of Parallel Coordinates'. In: *Eurographics 2013 - State of the Art Reports*. Artwork Size: 22 pages ISSN: 1017-4656. The Eurographics Association, 2012, 22 pages. DOI: 10.2312/CONF/EG2013/STARS/095-116. (Visited on 11/17/2023) (cited on page 105).

[213] J.J. McArthur. 'A Building Information Management (BIM) Framework and Supporting Case Study for Existing Building Operations, Maintenance and Sustainability'. In: *Procedia Engineering* 118 (2015), pp. 1104–1111. DOI: 10.1016/j.proeng.2015.08.450. (Visited on 02/24/2023) (cited on page 129).

[214] Zoran Pučko et al. 'Application of 6D Building Information Model (6D BIM) for Business-storage Building in Slovenia'. In: *IOP Conference Series: Materials Science and Engineering* 245 (Oct. 2017), p. 062028. DOI: 10.1088/1757-899X/245/6/062028. (Visited on 02/24/2023) (cited on page 129).

[215] Christiana Panteli, Angeliki Kylili, and Paris A. Fokaides. 'Building information modelling applications in smart buildings: From design to commissioning and beyond A critical review'. In: *Journal of Cleaner Production* 265 (Aug. 2020), p. 121766. DOI: 10.1016/j.jclepro.2020.121766. (Visited on 03/25/2021) (cited on page 129).

[216] Lavinia Chiara Tagliabue et al. 'Leveraging Digital Twin for Sustainability Assessment of an Educational Building'. In: *Sustainability* 13.2 (Jan. 6, 2021), p. 480. DOI: 10.3390/su13020480. (Visited on 02/10/2024) (cited on page 129).

[217] Chen Chen et al. 'A Conceptual Framework for Estimating Building Embodied Carbon Based on Digital Twin Technology and Life Cycle Assessment'. In: *Sustainability* 13.24 (Dec. 15, 2021), p. 13875. DOI: 10.3390/su132413875. (Visited on 02/10/2024) (cited on page 129).

Appendix

A

Case-Study Model

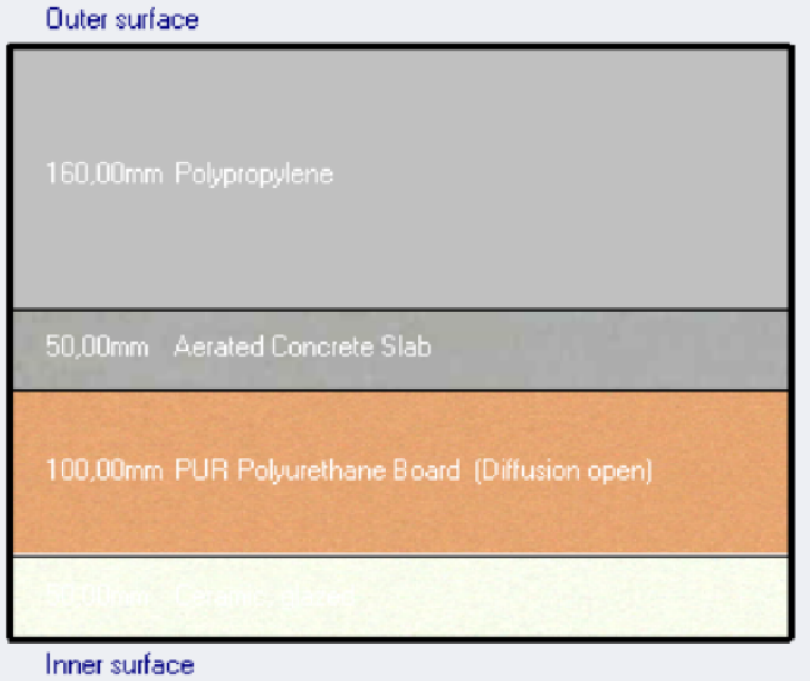

Figure A.1: Floor composition of the case-study. U-value: 0.19 W/m²·K.

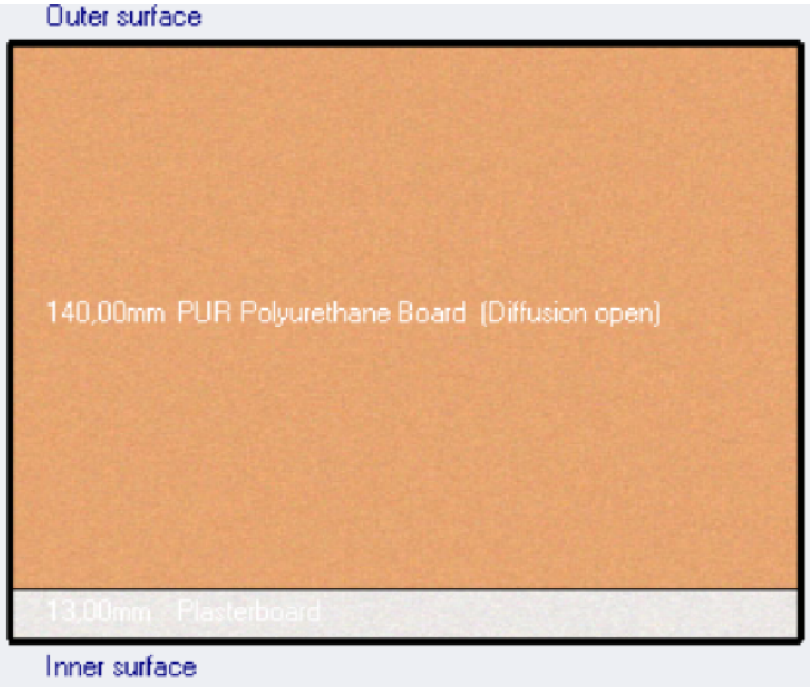

Figure A.2: Roof composition of the case-study. U-value: 0.17 W/m²·K.

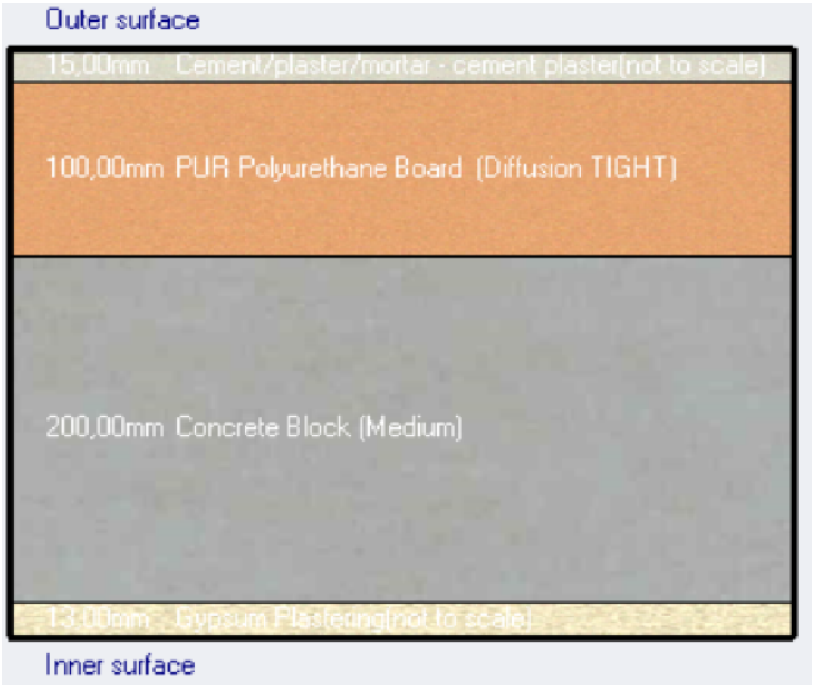

Figure A.3: Wall composition of the case-study. U-value: 0.23 W/m²·K.

Scenarios (Occupancy hours per day)	0	1	2	3	4	5	6	7	8	9	10	11	12	13	14	15	16	17	18	19	20	21	22	23
0	0	0	0	0	0	0	0	0	0	0	0	0	0	0	0	0	0	0	0	0	0	0	0	0
1	1	0	0	0	0	0	0	0	0	0	0	0	0	0	0	0	0	0	0	0	0	0	0	0
2	1	1	0	0	0	0	0	0	0	0	0	0	0	0	0	0	0	0	0	0	0	0	0	0
3	1	1	1	0	0	0	0	0	0	0	0	0	0	0	0	0	0	0	0	0	0	0	0	0
4	1	1	1	1	0	0	0	0	0	0	0	0	0	0	0	0	0	0	0	0	0	0	0	0
5	1	1	1	1	1	0	0	0	0	0	0	0	0	0	0	0	0	0	0	0	0	0	0	0
6	1	1	1	1	1	1	0	0	0	0	0	0	0	0	0	0	0	0	0	0	0	0	0	0
7	1	1	1	1	1	1	0	0	0	0	0	0	0	0	0	0	0	0	0	0	0	0	0	1
8	1	1	1	1	1	1	0	0	0	0	0	0	0	0	0	0	0	0	0	0	0	0	1	1
9	1	1	1	1	1	1	0	0	0	0	0	0	0	0	0	0	0	0	0	0	0	1	1	1
10	1	1	1	1	1	1	0	0	0	0	0	0	0	0	0	0	0	0	0	0	1	1	1	1
11	1	1	1	1	1	1	0	0	0	0	0	0	0	0	0	0	0	0	0	1	1	1	1	1
12	1	1	1	1	1	1	0	0	0	0	0	0	0	1	0	0	0	0	0	1	1	1	1	1
13	1	1	1	1	1	1	1	0	0	0	0	0	0	1	0	0	0	0	0	1	1	1	1	1
14	1	1	1	1	1	1	1	0	0	0	0	0	0	1	0	0	0	0	1	1	1	1	1	1
15	1	1	1	1	1	1	1	0	0	0	0	0	0	1	1	0	0	0	1	1	1	1	1	1
16	1	1	1	1	1	1	1	1	0	0	0	0	0	1	1	0	0	0	1	1	1	1	1	1
17	1	1	1	1	1	1	1	1	1	0	0	0	0	1	1	0	0	0	1	1	1	1	1	1
18	1	1	1	1	1	1	1	1	1	1	0	0	0	1	1	0	0	0	1	1	1	1	1	1
19	1	1	1	1	1	1	1	1	1	1	0	0	0	1	1	0	0	1	1	1	1	1	1	1
20	1	1	1	1	1	1	1	1	1	1	1	0	0	1	1	0	0	1	1	1	1	1	1	1
21	1	1	1	1	1	1	1	1	1	1	1	0	0	1	1	0	1	1	1	1	1	1	1	1
22	1	1	1	1	1	1	1	1	1	1	1	1	0	1	1	0	1	1	1	1	1	1	1	1
23	1	1	1	1	1	1	1	1	1	1	1	1	1	1	1	0	1	1	1	1	1	1	1	1
24	1	1	1	1	1	1	1	1	1	1	1	1	1	1	1	1	1	1	1	1	1	1	1	1

Figure A.4: In the the columns are the hours of the day and in the rows are how many hours, on average, the occupants is present in the building. The cells in green represent the hours of the day someone is present. For instance, if a building is occupied 22 hours in a day, the only hours it is unoccupied are 13:00 and 16:00 This variable is therefore, defined categorically.

B

Case-Study Inventory

This appendix intends to give the information on the case-study used in this thesis. Indeed, in Table B.1 the reader will find all the information used on the components and their respective EPDs as taken from the French INIES database [143]. As consequence, the component names in this table are in French.

Table B.1: Table containing the PV and thermostat EPDs used in the DM process.

ID	Component	DVR	Quantity	Unit	A1-3	A3-5	B1-3	C1-4	D
26899	Dalles de voirie et revêtements extérieurs en béton préfabriqué [ép. = 5 cm] - DONNEE ENVIRONNEMENTALE PAR DEFAUT	50	50	m²	14.46	8.69	0	1.68	0
31707	Réseaux d'adduction d'eau en PVC [Diam entre 110 et 200 mm] - DONNEE ENVIRONNEMENTALE PAR DEFAUT (v.1.2)	50	40	Unit(s)	35.1	2.54	0	0	0
31707	Réseau d'adduction d'eau en cuivre [Diam. 18 mm] - DONNEE ENVIRONNEMENTALE PAR DEFAUT	50	40	Unit(s)	1.08	0.28	0	0.13	0
30551	Béton pour fondations en milieu agressif	100	25	m²	178.73	14.58	-0.72	4.4814	-3.84
26899	Entrevous LEADER EMS EcoVS sans Isorupteur	100	61	m²	8.50	0.43	0	0.31	0
26899	Chapes / chapes flottantes en béton et mortier à base de ciment [ép.5cm] - DONNEE ENVIRONNEMENTALE PAR DEFAUT	50	61	m²	32.64	1.99	0	1.03	0
26899	Chapes / chapes flottantes en béton et mortier à base de ciment [ép.5cm] - DONNEE ENVIRONNEMENTALE PAR DEFAUT	50	61	m²	32.64	1.99	0	1.03	0
26899	Entrevous LEADER EMS EcoVS sans Isorupteur	100	61	m²	8.5	0.43	0	0.31	0
26899	Entrevous LEADER EMS EcoVS sans Isorupteur	100	5.79	m²	8.5	0.43	0	0.31	0
26899	Bloc de coffrage en béton - avec béton de remplissage	100	120	m²	9.48	25.2	-3.47	5.56	-0.88
26899	Bloc de coffrage en béton - avec béton de remplissage	100	120	m²	9.48	25.2	-3.47	5.56	-0.88
26899	Bloc de coffrage en béton - avec béton de remplissage	100	120	m²	9.48	25.2	-3.47	5.56	-0.88
28731	GR 32 Revêtu Kraft 60 mm	50	18	m²	1.37	0.22	0	0.03	0
28731	GR 32 Revêtu Kraft 100	50	18	m²	2.7	0.46	0	0.03	0
28256	Mur ossature bois avec montant d'une largeur de 145 mm et un entraxe de 60 cm non isolé, fabriqué en France	100	90	m²	-13.40	3.13	0	19.1	-3.58
28731	Isoconfort 32 100mm	50	90	m²	2.49	0.36	0	0.03	0
26899	Complexe de doublage SIS REVE SI® constitué d'un panneau en mousse rigide de polyuréthane de 50 mm d'épaisseur et d'une plaque de plâtre de 13 mm d'épaisseur, R= 2,35 m².K/W	50	90	m²	7.56	1.35	0	1.18	0
26899	Escalier droit en béton armé [larg. = 80 cm] - DONNEE ENVIRONNEMENTALE PAR DEFAUT	100	3.78	m²	367.69	59.45	0	13.27	0
31707	Tuile de terre cuite à emboitement	100	22	Unit(s)	12.1	1.46	0	0.23	-2.39
28256	Membrane synthétique en PVC-P pour étanchéité de toiture - DONNEE ENVIRONNEMENTALE PAR DEFAUT	20	22	m²	12.2	6.5	36.45	5.32	0
26899	Charpente en bois reconstitué [Gestion durable] - DONNEE ENVIRONNEMENTALE PAR DEFAUT	100	40	m²	-349.93	104	0	813	0
31707	Voligeage en bois massif ep 26 mm [gestion durable] - DONNEE ENVIRONNEMENTALE PAR DEFAUT	50	22	Unit(s)	-14.87	5.15	0	19.87	0
26899	Entrevous LEADER EMS EcoVS sans Isorupteur	100	61	m²	8.5	0.43	0	0.31	0
26899	Chapes / chapes flottantes anhydrite [ép. 5 cm] - DONNEE ENVIRONNEMENTALE PAR DEFAUT	50	61	m²	2.97	0.44	0	0.07	0
28256	Monospace 35 Revêtu Kraft 75 mm	50	25	m²	0.99	0.13	0	0.02	0
28256	Monospace 35 Revêtu Kraft 75 mm	50	6	m²	0.99	0.13	0	0.02	0
26899	Complexe de doublage SIS REVE SI® constitué d'un panneau en mousse rigide de polyuréthane de 50 mm d'épaisseur et d'une plaque de plâtre de 13 mm d'épaisseur, R= 2,35 m².K/W	50	6	m²	7.56	1.35	0	1.18	0
26899	Complexe de doublage SIS REVE SI® constitué d'un panneau en mousse rigide de polyuréthane de 50 mm d'épaisseur et d'une plaque de plâtre de 13 mm d'épaisseur, R= 2,35 m².K/W	50	25	m²	7.56	1.35	0	1.18	0
28256	Panneau d'isolation en mousse rigide de polyuréthane TMS® 48 mm d'épaisseur, R= 2,20 m².K/W (hors accessoires de pose)	50	61	m²	5.38	0.37	0	0.41	0
28256	Monospace 35 revetu kraft 45 mm	50	140	m²	0.78	0.10	0	0.01	0

ID	Component	DVR	Quantity	Unit	A1-3	A3-5	B1-3	C1-4	D
28256	Panneau d'isolation en mousse rigide de polyuréthane EFIMUR® 97 mm d'épaisseur, R= 4,5 m².K/W (hors accessoires de pose)	50	140	m²	9.55	0.76	0	0.70	0
28731	Isolant thermique et acoustique sous chape en laine de roche [R=2,5m².K/W] - DONNEE ENVIRONNEMENTALE PAR DEFAUT	50	220	m²	21.20	1.72	0	0.32	0
26899	Bloc porte métallique (porte de locaux techniques, de caves, de service) [ép.42mm] - DONNEE ENVIRONNEMENTALE PAR DEFAUT	25	5.22	m²	99.33	13.25	115.65	3.06	0
28256	Porte extérieure en bois massif [Gestion durable] - DONNEE ENVIRONNEMENTALE PAR DEFAUT	35	1.935	m²	29.36	8.09	40.46	51.31	0
28256	Porte extérieure en bois massif [Gestion durable] - DONNEE ENVIRONNEMENTALE PAR DEFAUT	35	1.963	m²	28.94	7.98	39.8	50.58	0
31582	Fenêtres et portes fenêtres mixtes Aluminium/PVC - DONNEE ENVIRONNEMENTALE PAR DEFAUT	30	0.57	m²	180.6	28.26	0	9.71	0
31582	Fenêtres et portes fenêtres mixtes Aluminium/PVC - DONNEE ENVIRONNEMENTALE PAR DEFAUT	30	2.1	m²	49.04	7.67	0	2.63	0
31582	Fenêtres et portes fenêtres mixtes Aluminium/PVC - DONNEE ENVIRONNEMENTALE PAR DEFAUT	30	2.58	m²	180.69	28.26	0	9.71	0
31582	Fenêtres et portes fenêtres mixtes Aluminium/PVC - DONNEE ENVIRONNEMENTALE PAR DEFAUT	30	4.73	m²	98.55	15.41	0	5.29	0
28256	Motorisation de volets roulants - DONNEE ENVIRONNEMENTALE PAR DEFAUT	15	4	m²	30.55	3.34	127.91	7.954	0
28256	Motorisation de volets roulants - DONNEE ENVIRONNEMENTALE PAR DEFAUT	15	6	m²	30.55	3.34	127.91	7.95	0
28256	Portes intérieures de communication en bois avec huisserie bois [Gestion durable] - DONNEE ENVIRONNEMENTALE PAR DEFAUT (v.1.3)	30	12	m²	26.1	17.7	12.6	22.2	-3.28
31707	Revêtement de sol dur en céramique [ép. 7mm] - DONNEE ENVIRONNEMENTALE PAR DEFAUT	50	61	Unit(s)	20.58	6.13	5.42	0.64	0
31707	Revêtement de sol dur en céramique [ép. 7mm] - DONNEE ENVIRONNEMENTALE PAR DEFAUT	50	61	Unit(s)	20.58	6.13	5.42	0.64	0
26899	Cloisonnement en plaque de plâtre [ép. entre 12.5 et 18 mm] - DONNEE ENVIRONNEMENTALE PAR DEFAUT	50	90	m²	9.96	3.16	0.60	0.81	0
26899	Cloisonnement en plaque de plâtre [ép. entre 12.5 et 18 mm] - DONNEE ENVIRONNEMENTALE PAR DEFAUT	50	18	m²	9.96	3.16	0.60	0.81	0
26899	Cloisonnement en plaque de plâtre [ép. entre 12.5 et 18 mm] - DONNEE ENVIRONNEMENTALE PAR DEFAUT	50	140	m²	9.96	3.16	0.60	0.81	0
26899	Enduit de peinture extérieure - DONNEE ENVIRONNEMENTALE PAR DEFAUT	30	145	m²	7.69	1.90	6.99	0.89	0
26899	Enduit de peinture extérieure - DONNEE ENVIRONNEMENTALE PAR DEFAUT	30	90	m²	7.69	1.90	6.99	0.89	0
26899	Enduit de peinture extérieure - DONNEE ENVIRONNEMENTALE PAR DEFAUT	30	18	m²	7.69	1.90	6.99	0.89	0
28256	Membrane synthétique en PVC-P pour étanchéité de toiture - DONNEE ENVIRONNEMENTALE PAR DEFAUT (v.1.3)	20	70	m²	12.1	6.5	0.16	5.35	0
31707	Radiateur électrique [P=1kW] - DONNEE ENVIRONNEMENTALE PAR DEFAUT	17	12	Unit(s)	25.39	0.90	0	1.46	0
31707	VMC simple flux Hygro B [Débit = 59m3/h] - DONNEE ENVIRONNEMENTALE PAR DEFAUT	17	1	Unit(s)	44.33	1.51	97.09	4.173	0
31707	Réseaux d'adduction d'eau en PVC [Diam 110mm] - DONNEE ENVIRONNEMENTALE PAR DEFAUT	50	40	Unit(s)	9.67	0.70	0	0	0
28105	Baignoire en matériau de synthèse - DONNEE ENVIRONNEMENTALE PAR DEFAUT	20	1	m²	377.40	19.15	61.61	4.08	0
26899	Colonne de douche avec robinet mitigeur - DONNEE ENVIRONNEMENTALE PAR DEFAUT	16	2	m²	17.44	0.85	298.09	0.22	0
31707	Receveur de douche en matériau de synthèse [Long. 90 cm Larg. 90 cm] - DONNEE ENVIRONNEMENTALE PAR DEFAUT	20	2	Unit(s)	163.70	17.18	296.54	16.79	0
31707	Robinetterie (non électronique) en laiton - DONNEE ENVIRONNEMENTALE PAR DEFAUT	12	4	Unit(s)	35.84	2.11	395.08	4.23	0

ID	Component	DVR	Quantity	Unit	A1-3	A3-5	B1-3	C1-4	D
26899	Evier en acier inoxydable [Long. 860 mm Larg. 500 mm Haut. 140 mm] - DONNEE ENVIRONNEMENTALE PAR DEFAUT	20	1	m²	52.72	6.07	99.17	3.83	0
28256	Lavabo en céramique (robinetterie et vidange non inclus) - DONNEE ENVIRONNEMENTALE PAR DEFAUT	20	3	m²	124	22.8	225.62	0.69	0
31707	WC en céramique - DONNEE ENVIRONNEMENTALE PAR DEFAUT	20	3	Unit(s)	173.4	13.5	500	6.1	0
31707	Réseaux d'évacuation et d'assainissement en PVC [Diamètre 315 mm] - DONNEE ENVIRONNEMENTALE PAR DEFAUT	50	30	Unit(s)	25.94	9.08	0	4.99	0
28731	Interrupteurs - DONNEE ENVIRONNEMENTALE PAR DEFAUT	10	26	m²	3.37	0.13	14.08	0.02	0
31884	Prises de courant fort - DONNEE ENVIRONNEMENTALE PAR DEFAUT	20	10	Unit(s)	1.41	0.02	2.18625	0.03	0
31707	Prises diverses (TV, HP, informatique...) - DONNEE ENVIRONNEMENTALE PAR DEFAUT	20	25	Unit(s)	3.44	0.10	5.39	0.05	0
26899	Chemin de câble dalle en PVC - DONNEE ENVIRONNEMENTALE PAR DEFAUT	20	50	m²	22.54	0.31	3.55	0.83	0
26899	Câble basse tension 0,6/1kV [Section conductrice de 5 mm² à 120 mm²] - DONNEE ENVIRONNEMENTALE PAR DEFAUT	30	100	m²	13.47	3.56	12.65	1.95	0
26899	Coupe-circuit - DONNEE ENVIRONNEMENTALE PAR DEFAUT	20	8	m²	0.39	0.14	0.88	0.05	0
31707	Relais différentiel - DONNEE ENVIRONNEMENTALE PAR DEFAUT	10	4	Unit(s)	15.74	0.08	64.55	0.31	0
26899	Encastrés intérieurs linéaires pour éclairage tertiaire [P=20W] - DONNEE ENVIRONNEMENTALE PAR DEFAUT	25	20	m²	90.56	14.64	11.20	6.81	0
26899	Cadre et portes pour coffrets encastrés - DONNEE ENVIRONNEMENTALE PAR DEFAUT	20	1	m²	11.50	1.93	20.98	0.54	0

C

Renovation and replacement components

This annex is dedicated to listing the components that are used in Annex 4 in the investigation of renovation and replacement measures. Much like in the case-study LCI, these components were found in the INIES database [143].

Table C.1: Table containing the HVAC-related EPDs used in the DM process.

ID	Component	DVR	Quantity	Unit	A1-3	A3-5	B1-3	C1-4	D
31811	Chaudière bois granulés assurant le chauffage seul [P = 17 kW]	17	unit	0.53	1520	113	0	386	0
36623	LG PAC Air-Eau 6kW	17	1.5	unit	1118.8	9.67	138.5	119	0
36698	LG PAC Air-Air 7kW	17	1.3	unit	1016.3	14.0	201.82	212E	0
33725	Chauffe-eau thermodynamique sur air extrait T.Flow®	17	1	unit	414.02	9.76	97	55.38	0
28379	Réseau d'adduction d'eau en cuivre [Diam. entre 18 et 40 mm] - DONNEE ENVIRONNEMENTALE PAR DEFAUT (v.1.2)	100	40	m	2.4	0.631	0	0.293	0
32040	Conduits rigides PVC [DN=160mm] - DONNEE ENVIRONNEMENTALE PAR DEFAUT (v.1.3)	30	30	m	4.73	1.62	0	0.931	0
32081	Diffuseur d'air circulaire sur plénum [débit = 100m3/h] - DONNEE ENVIRONNEMENTALE PAR DEFAUT (v.1.3)	17	9	unit	24.2	5.16	0	0.933	0
36713	ARTIS décor classique vertical (v.1.2)	50	9	kW	75.19	0.309	0	3.83	0

Table C.2: Table containing the glazing EPDs used in the DM process.

ID	Component	DVR	Quantity	Unit	A1-3	A3-5	B1-3	C1-4	D
31582	Fenêtres et portes fenêtres mixtes Aluminium/PVC - DONNEE ENVIRONNEMENTALE PAR DEFAUT	30	14	m^2	180.69	28.26	0	9.71	0
30583	Fenêtre et porte-fenêtre double vitrage, fabriquée en France, en Bois d'essence tempérée européen (v.1.3)	30	14	m^2	30.1	10.6	1.82	12.3	-4.33
30584	Fenêtre et porte-fenêtre triple vitrage, fabriquée en France, en Bois d'essence tempérée européen (v.1.3)	30	14	m^2	42.7	11	1.82	15.9	-5.75
28196	Fenêtre double vitrage en bois-aluminium [Uw = 1,3 W/(m^2.K)] [Gestion durable] - DONNEE ENVIRONNEMENTALE PAR DEFAUT (v.1.3)	30	14	m^2	129	17.6	19.6	30.3	-1.3
28211	Fenêtre triple vitrage en bois-aluminium [Uw = 0,8 W/(m^2.K)] [Gestion durable] - DONNEE ENVIRONNEMENTALE PAR DEFAUT (v.1.2)	30	14	m^2	313	30.8	4.77	22.9	-3.63

Table C.3: Table containing the insulation EPDs used in the DM process.

Component	DVR	Quantity	A1-3	A3-5	B1-3	C1-4	D
Panneaux Rigides Isolants en Polyuréthane Ep 100 mm KNAUF Thane Mur B2i	50	1	12.6	1.11	0	0.0114	0
Panneaux Rigides Isolants en Polyuréthane Ep 120 mm KNAUF Thane Mur B2i	50	1	15.9	1.28	0	0.0135	0
Panneaux Rigides Isolants en Polyuréthane Ep 140 mm KNAUF Thane Mur B2i	50	1	18.8	1.42	0	0.0155	0
Isolant Biofib' Trio épaisseur 60 mm (v.1.1)	50	1	-1.44	0.178	0	1.66	-0.7
Isolant Biofib' Trio épaisseur 80 mm (v.1.1)	50	1	-1.92	0.241	0	2.22	-0.93

Component	DVR	Quantity	A1-3	A3-5	B1-3	C1-4	D
Isolant Biofib' Trio épaisseur 100 mm (v.1.1)	50	1	-2.37	0.311	0	2.77	-1.16
Isolant Biofib' Trio épaisseur 160 mm (v.1.1)	50	1	-3.83	0.481	0	4.43	-1.86
KNAUF INSULATION Laine de Verre ECOSE Acoustilaine 035 140 mm	50	1	2.27	0.47	0	0.47	0
KNAUF INSULATION Laine de Verre ECOSE Acoustilaine 035 160 mm	50	1	2.67	0.536	0	0.563	0
KNAUF INSULATION Laine de Verre ECOSE Acoustilaine 035 220 mm	50	1	3.67	0.784	0	0.766	0
KNAUF INSULATION Laine de Verre ECOSE Acoustilaine 035 280 mm	50	1	4.52	0.955	0	0.919	0
FLEX 40 40 mm	50	1	-0.504	0.212	0	0.777	-0.614
FLEX 40 80 mm	50	1	-1.187	0.3725	0	1.5935	-1.2615
FLEX 55 100 mm	50	1	-1.87	0.533	0	2.41	-1.909
FLEX 55 200 mm	50	1	-4.5	1.05	0	4.88	-3.875
FBT PR (v.1.4) 100mm	50	1	-2.6	0.508	0	3.92	-1.61
FBT PR (v.1.4) 200mm	50	1	-5.2	1.016	0	7.84	-3.22
FBT PR (v.1.4) 300mm	50	1	-7.8	1.524	0	11.76	-4.83
FBT PR (v.1.4) 400mm	50	1	-10.4	2.032	0	15.68	-6.44

Table C.4: Table containing the PV and thermostat EPDs used in the DM process.

ID	Component	DVR	Quantity	Unit	A1-3	A3-5	B1-3	C1-4	D
25861	VOLTEC SOLAR TARKA 120	30	1	m^2	135.895	0.0247	1.37	0.128	0
31866	Inters horaires - DONNEE ENVIRONNEMENTALE PAR DEFAUT (v.1.2)	10	1	unit	134	0.108	0	0.145	0

D

Complementary Results

In Chapter 4, the results of the DM methodology were presented only for the upper-edge scenario. In this Annex D, the optimization and statistical simulation results will be shown under the lower-edge and the RE2020 scenarios.

D.0.1 Lower-Edge Scenario

Having presented all results for DM support under the "Upper-Edge" scenario, this section of the thesis will now be dedicated to the "Lower-Edge" case, as defined in Table 4.2. As a reminder, in this scenario, the building is expected to have the lowest GWP results due to the DP assumptions.

D.0.1.1 Optimization Results

The Pareto solution of under this scenario then, is presented in Figure D.1. The first takeaway is the overall position of the solutions in relation to the thresholds. Most importantly, the BAU case, with a green contour is within both the operational budget and the future 2025 embodied budget, indicating that no measures are required for threshold compliance. This recommendation is true even though the case-study building relies on electrical radiators for heating, since in this scenario, the average CI of electricity goes down to 17 gCO_2/kWh.

Another detail worth highlighting from the Pareto plot is that the minimal overall emissions solution (represented by the red +) has distanced itself from the minimal OE solution. Indeed, by looking at the solutions' details in Table D.1, the addition of PV is not worth the EE investments and the best overall solution has no renewable energy generation at all. The same solution in the preceding scenario recommended 29 m² of panels to be installed, positioning it much closer to minimal OE solution.

This phenomenon, again, is explained by the low-carbon electricity, making CMMs that reduce consumption of energy from the grid, either from energy efficiency improvements or renewable energy production, less interesting.

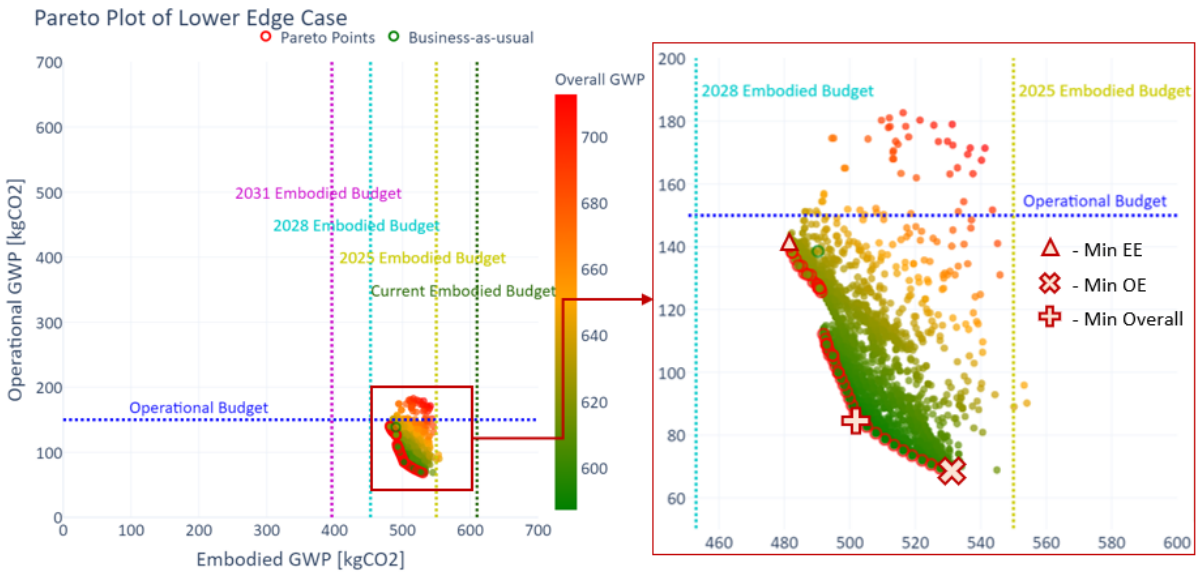

Figure D.1: Pareto solutions of the optimization solution found in the Lower-Edge case-study.

In fact, this trend can also be seen in glazing, where all solutions chosen are double glazed, again supporting the idea that improving energy performance is not as much a priority under this scenario than it was with the Upper-Edge case.

At the same time however, some CMM remained invariably the same when compared to the other scenario, namely the ventilation system replacement and the insulation renovation: Double-flow ventilation was never judged necessary and wood straw is always recommended. This can be observed in the solution frequency plot in Figure D.2.

The fact that these solutions appear in the Pareto front under the Upper and Lower-Edge scenarios, lead to the conclusion that these are pretty robust decisions that will perform well independently of the external factors represented by the DPs.

D.0.1.2 Quasi-Random Evaluation

An optimization does not tell the whole story, however. In this Saltelli sampling then, the Sobol indices and the measures' frequencies that appear in threshold compliant solutions will be made. The PCP is shown in Figure D.3.

The Sobol results in this Lower-Edge scenario is displayed in Figure D.4 and it differs a lot from the one presented in Figure 4.5. Clearly, heating system choice is much much more influential here, which is justified by the fast and drastic decarbonization process of electricity, which, of course, does not affect the wood-pellet heating system's CI. This means the variance caused by the change from an electrified to a biomass system is accentuated

Table D.1: This table includes 3 sets of solutions found in the Pareto front and identifies all CMMs to achieve the resulting GWP displayed.

CMM	Best Overall Solution	Minimal OE Solution	Minimal EE Solution	BAU
	1	2	3	
Heat recovery CMV	Simple flow Ventilation	Simple flow Ventilation	Simple flow Ventilation	Simple flow Ventilation
CMV replacement year	17	17	17	17
Glazing type	Double Glaz PVC	Double Glaz PVC	Double Glaz PVC	Double Glaz PVC
Glazing replacement year	30	30	30	30
Insulation material	Wood Straw	Wood Straw	Wood Straw	EPS
Insulation thickness	Thickest	Thickest	Thickest	Thinnest
Insulation addition year	5	5	5	5
Heating system	Air-water HP	Air-water HP	Electric rad	Electric rad
Heating replacement year	5	5	17	17
PV surface [m^2]	0	32.0	0.0	0.0
PV addition year	-	5	5	5
Thermostat	Thermostat	Thermostat	No Thermostat	No Thermostat
Operational GWP	84.89	68.30	140.04	138.54
Embodied GWP	502.39	530.40	481.52	490.27
Overall GWP	587.28	598.70	621.57	628.81

under this scenario. All other indices are in a similar order as in the Upper-Edge scenario.

Another interesting plot that should aggregate information here is the solution frequency analysis for threshold compliant CMMs. However, as observed in the Pareto plot, even the BAU solution already follows the current embodied carbon budgets[1]. Thus, such an analysis should yield a somewhat uniform frequency for most measures. In order to validate this, the analysis was done for this threshold and it has been included in Figure D.5.

More interesting though, should be to analyse the solution frequency in the solutions that follow operational and 2025 embodied budgets instead and that is what Figure D.6 shows. Here, although subtle, some tendencies are observable, namely in heating system replacement and scheduling, where electric radiators are clearly unpreferred, with wood pellet appearing the most likely to satisfy the future embodied budget. This can be explained by the higher EEs of the heat pump alternatives, despite being more interesting in terms of OE. The tendency of realizing earlier heating system

1: Of the 13312 samples evaluated, 8161 were found to follow current embodied and operational budgets, simultaneously. For the 2025 embodied budget, that number is not very heavily affected, jumping down to 8124.

Figure D.2: Solution Frequency of Pareto front under Lower-Edge scenario.

replacement is also notable.

In terms of PV installation, 15% of threshold-compliant solutions recommend no PV installation, however, when it is recommended, it clearly should be done as early as possible.

The two spikes at year 5 in "Insulation Addition Year" and in "PV Addition Year" merit some more explaining as well. In fact, when no insulation or PV is added, the renovation year for these CMMs have no meaning, since no renovation is recommended. Therefore, in the DLCA workflow, when BAU is selected for either of these measures, insulation and PV addition years are automatically set to 5. Of course this number doesn't represent anything, since no intervention will be realized at year 5, but this justifies the

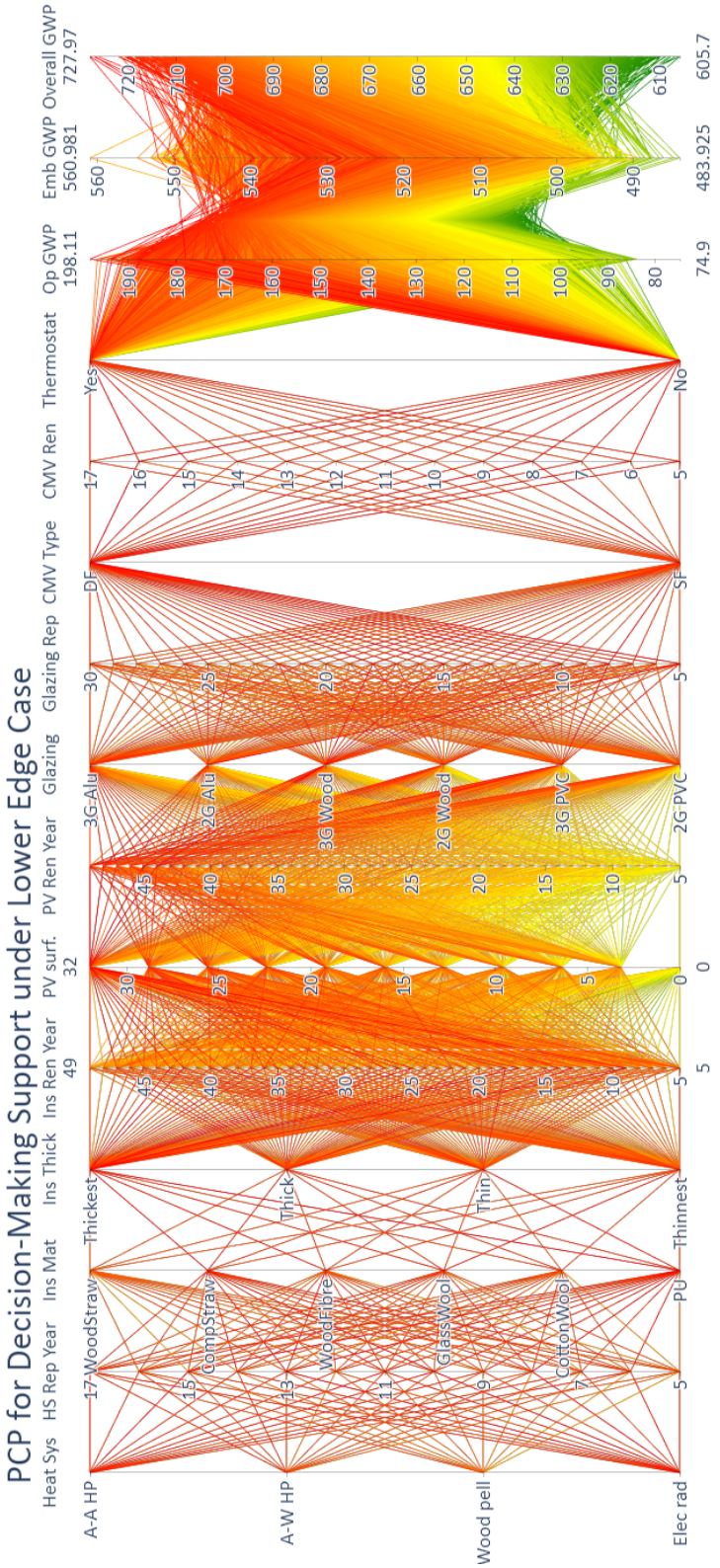

Figure D.3: Pareto solutions of the optimization solution found in the Lower-Edge case-study.

aforementioned peaks in the frequency.

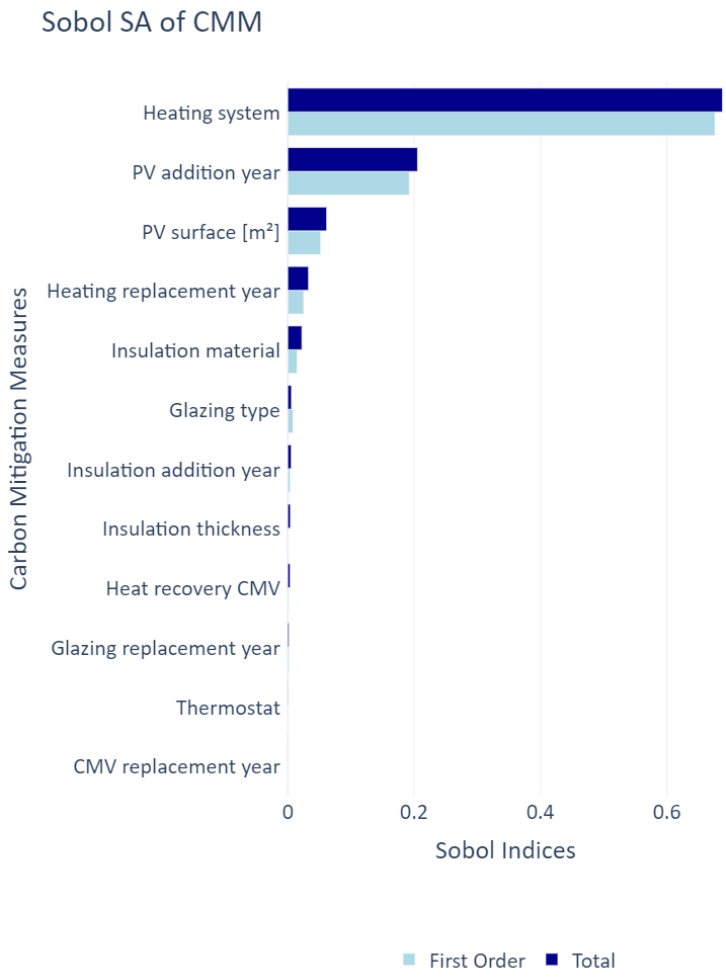

Figure D.4: Sobol indices of CMMs under lower-edge case.

D.0.2 RE2020's Dynamic LCA

Finally, with the results of the upper and lower-edge scenarios visualized, we can now explore the solutions given by the RE2020 DLCA methodology.

D.0.2.1 Optimization Results

In this short subsection then, the optimization results with the RE2020's weighting factor will be presented, starting with the Pareto in Figure D.7.

The immediate observable conclusion is the fact that much fewer solutions follow the current embodied and operational budgets under this new scenario than in the Lower-Edge case, with the Pareto front being close to where the Upper-Edge case used to be.

Indeed, Figure 4.6 and Figure D.7 are very similar, however, a key distinction from the preceding optimization results is the

Figure D.5: Pareto solutions of the optimization solution found in the Lower-Edge case-study.

fact that the minimal OE solution (represented by the "x") also is the minimal overall GWP solution. This indicates that, under the RE2020 scenario, the EE investments in the form of CMMs, are more often compensated by the subsequent OE savings.

The solution frequency plot of the Pareto solutions, displayed in Figure D.8, was found to also resemble the Upper-Edge scenario's, with exception to the wood pellet boiler appearing in close to 20% of solutions here. This increased in interest in the bio-mass fuel is due to the fact that the weighting factor[2] affect all emission values, while in the preceding scenarios, the DPs only accounted for the improvement of the electricity grid's mix, thus not affecting the CI of burning wood pellets.

2: As a reminder, the weighting factor is defined by the RE2020 and is a multiplier for all GWP values as a function of the year, affecting both OE and EE.

Figure D.6: Pareto solutions of the optimization solution found in the Lower-Edge case-study.

D.0.2.2 Quasi-Random Evaluation

After the Saltelli sample was evaluated, the Sobol indices were calculated leading to the results in Figure D.9. But much like the optimization results, no substantial difference was identified neither here, in the Sobol results nor in any other result of the quasi-random evaluation.

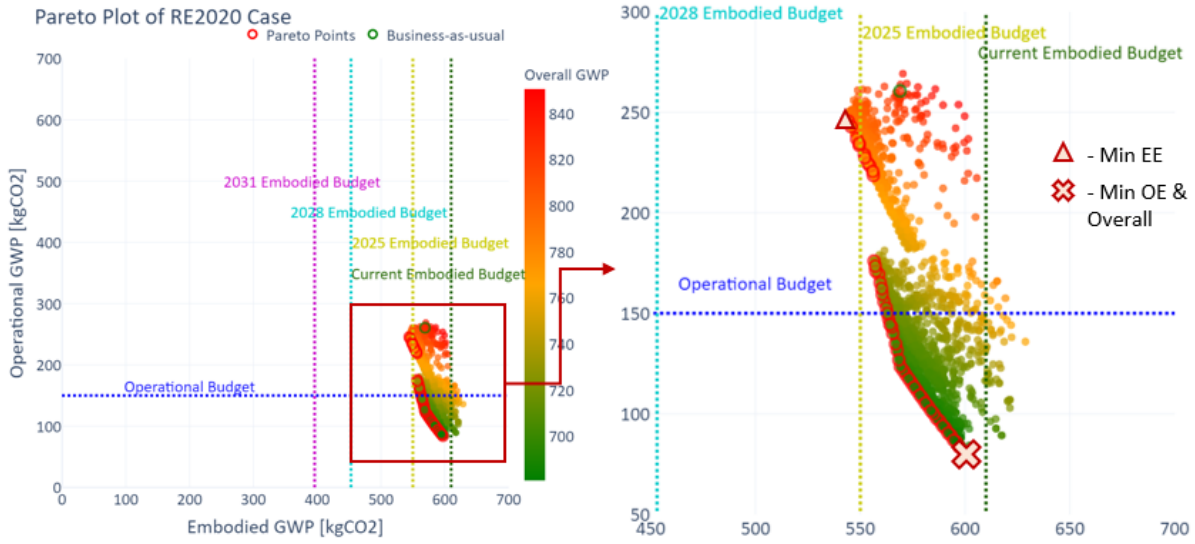

Figure D.7: Pareto solutions of the optimization solution found in the Lower-Edge case-study.

D.0.3 Static Scenario

D.0.3.1 Optimization Results

The last scenario to be investigated is the static LCA, where the building's environment and its conditions do not evolve with time and thus, the first year of operation are subject to the same assumptions of the last. The same DM workflow was applied to this scenario and so we will start again with the optimization results.

In the Pareto plot found in Figure D.10, the most notable difference is that now, all solutions are much farther than before from the carbon thresholds, most notably the embodied budget. Indeed, no combination of CMMs is capable of amending the deviation in EE. This highlights how pessimistic a static LCA approach is. Indeed, despite having modelled DPs that assume deterioration of the building's performance, in Annex 3 we found that these parameters have little to no impact in overall GWP when compared to the decarbonization processes of the building-adjacent sectors.

This result also highlights the importance of getting the EEs of a building right from design and conception stage, since there is very little "room for corrections" once the building is constructed. Another significant chunk is emitted at the building's EOL, which also is largely determined by the material and components chosen during design-stage.

Another interesting point from Figure D.10 is the fact that OEs does not seem to have been as heavily impacted as EE from not taking any dynamic factors into account. In fact, some Pareto front solutions still allow compliance with the operational budget. This

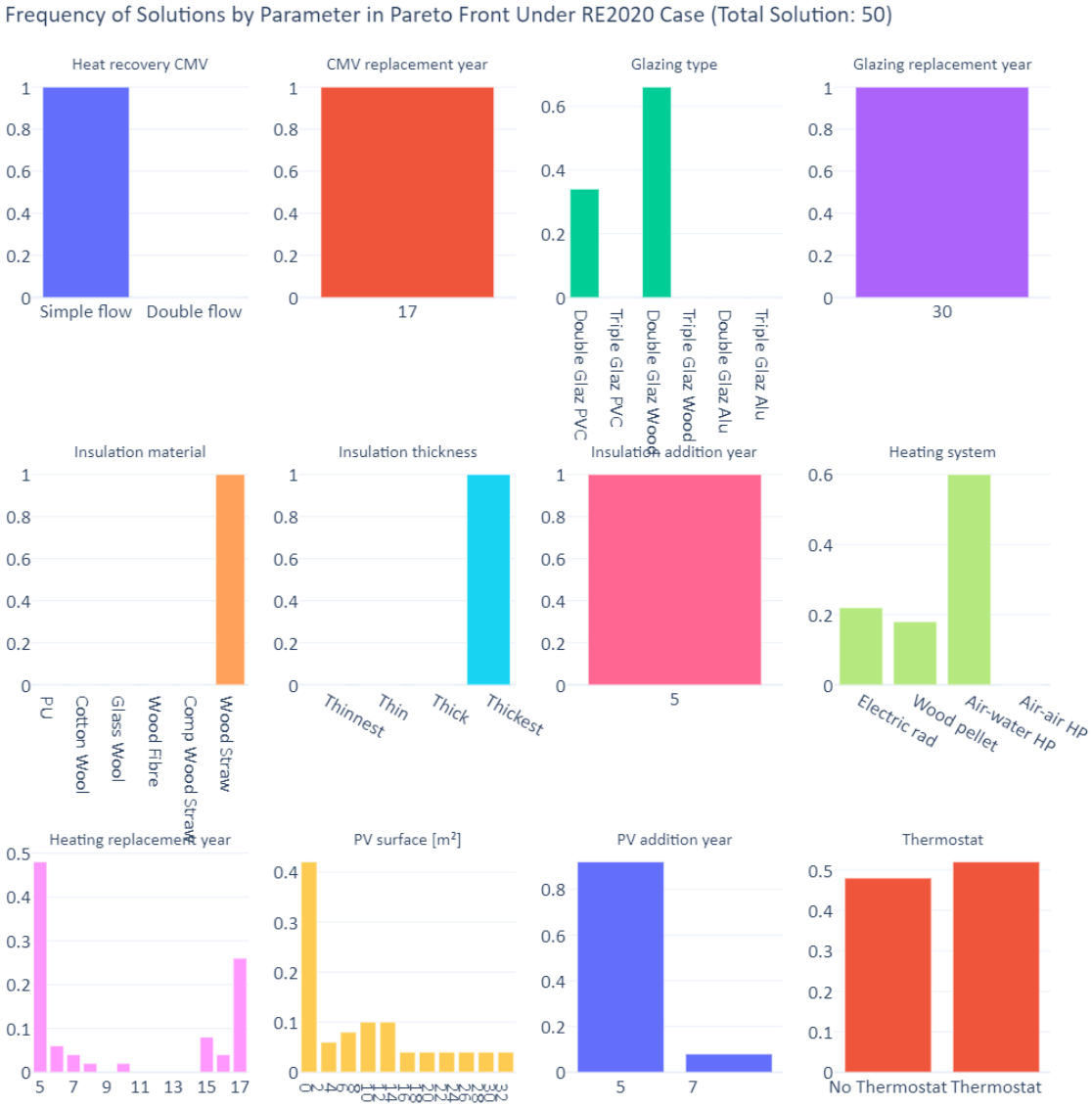

Figure D.8: Solution frequency of Pareto solutions under RE2020 case.

is also linked to the aforementioned peak in emission at year 50, when DPs have the most impact in the resulting GWP. Meanwhile, OEs are more evenly spread throughout the building's life cycle, meaning its impact by the various DPs are attenuated.

To study more closely the results, the three solutions identified in Figure D.10 have been detailed in Table D.2. However, despite the grossly different results in terms of raw GWP values from dynamic to static LCA, the solutions are identical to the RE2020 approach. This is explained by the fact that the weighting factor multiplies OE and EE the same value indiscriminately, unlike in the Upper and Lower-Edge scenarios.

The solution frequency of the Pareto solutions shown in Figure D.11

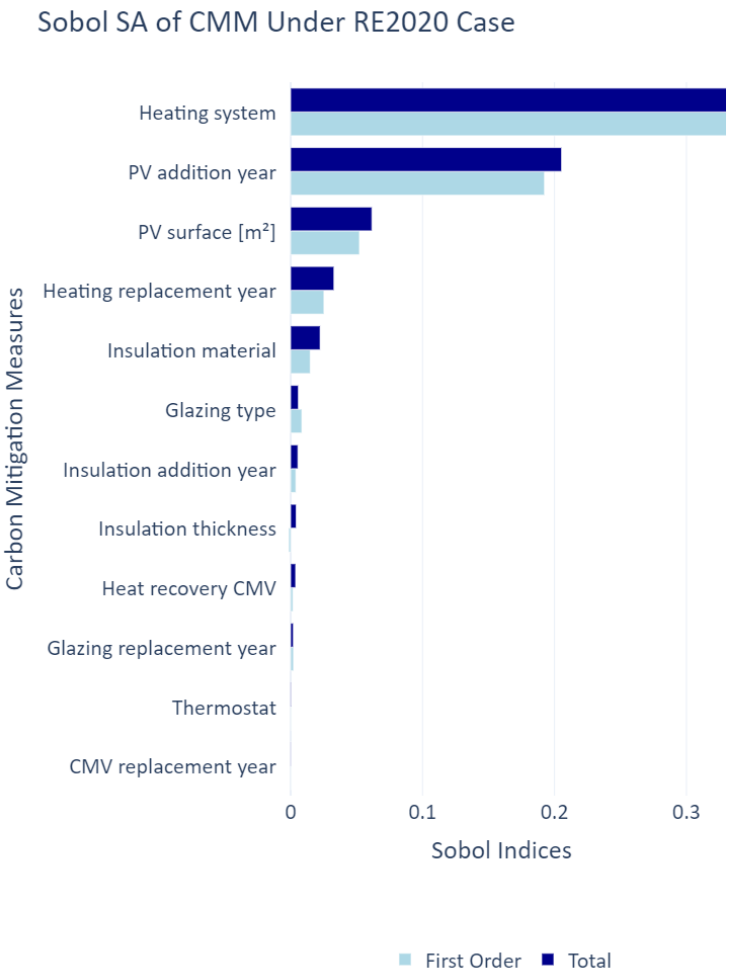

Figure D.9: Sobol indices of CMM under RE2020 scenario.

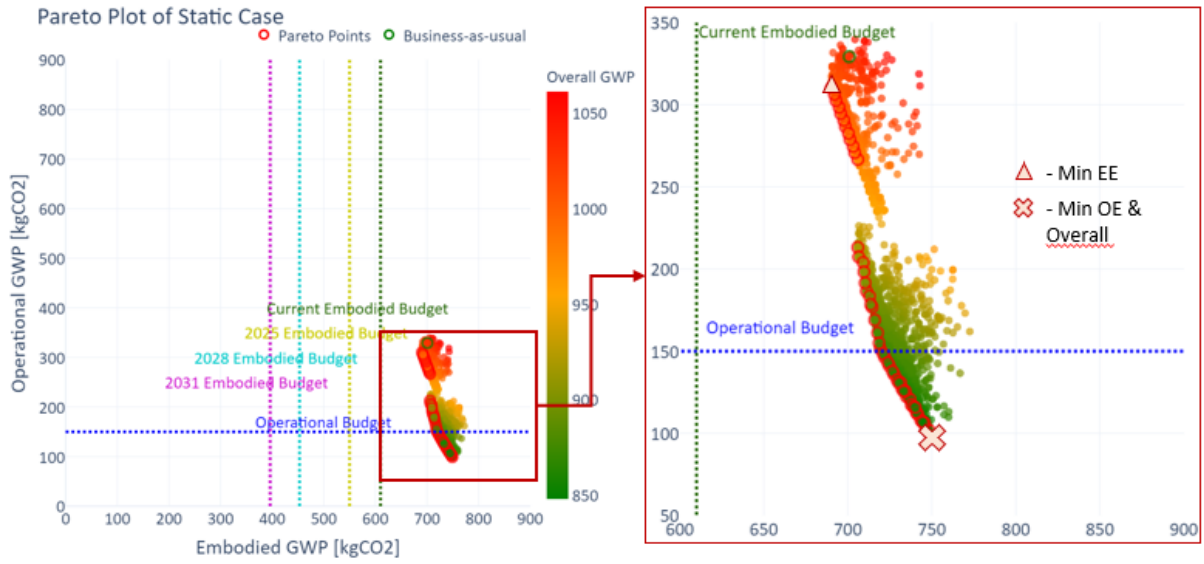

Figure D.10: Pareto plot under static scenario.

also are very similar to the RE2020's, the only notable difference being the glazing replacement year not unanimously being recom-

Table D.2: This table includes 3 sets of solutions found in the Pareto front and identifies all CMMs to achieve the resulting GWP displayed.

CMM	Minimal OE & Overall Solution	Minimal EE Solution	BAU
	1	2	
Heat recovery CMV	Simple flow Ventilation	Simple flow Ventilation	Simple flow Ventilation
CMV replacement year	17	17	17
Glazing type	Double Glaz PVC	Double Glaz Wood	Double Glaz PVC
Glazing replacement year	25	30	30
Insulation material	Wood Straw	Wood Straw	PU
Insulation thickness	Thickest	Thickest	Thinnest
Insulation addition year	5	5	5
Heating system	Air-water HP	Electric rad	Electric rad
Heating replacement year	5	17	17
PV surface [m²]	32.0	0.0	0.0
PV addition year	5	5	5
Thermostat	Thermostat	No Thermostat	No Thermostat
Operational GWP	98.92	310.35	329.31
Embodied GWP	749.11	690.24	700.82
Overall GWP	848.04	1000.59	1030.13

mended to be done at year 30, going back to year 24. This is because the weighting factor used to incentivizes delaying replacements, as emissions have reduced impact with time. However, in this static approach, the only thing the optimizer will avoid is increasing the number replacements further down the line. Otherwise, the earlier an energy efficiency improvement is implemented, the greater to OE savings.

D.0.3.2 Quasi-Random Evaluation

To continue this investigation of the static solutions, the PCP has been plotted in Figure D.12, where it is clear, by the range available under the EE axis, that no solution comes close to the embodied budget of 610 $kgCO_2/m^2$. The OE can still be corrected though and so the operational budget has been brushed under the resulting operational axis.

A much more limited array of solutions is available here, despite there being only one filter. In fact this PCP informs that, no electrical

Figure D.11: Solution frequency of Pareto front under static scenario.

radiator solution is threshold-compliant and at least 10 m² of PV surface will be necessary.

A Sobol analysis was also deemed interesting application in this scenario, and so the results are displayed in Figure D.13. Here, the largest gap can be observed between the PV addtion year and the heating system replacement choice. This confirms the superfluity of including the renovation and replacement years as CMMs in a static approach. Indeed, since the EE investments and OE have constant values, there's no real need to calculate year-by-year emissions. Thus, a simple "payback" time analysis would be as useful for a less intensive computational cost.

With all the results under the four established scenarios presented,

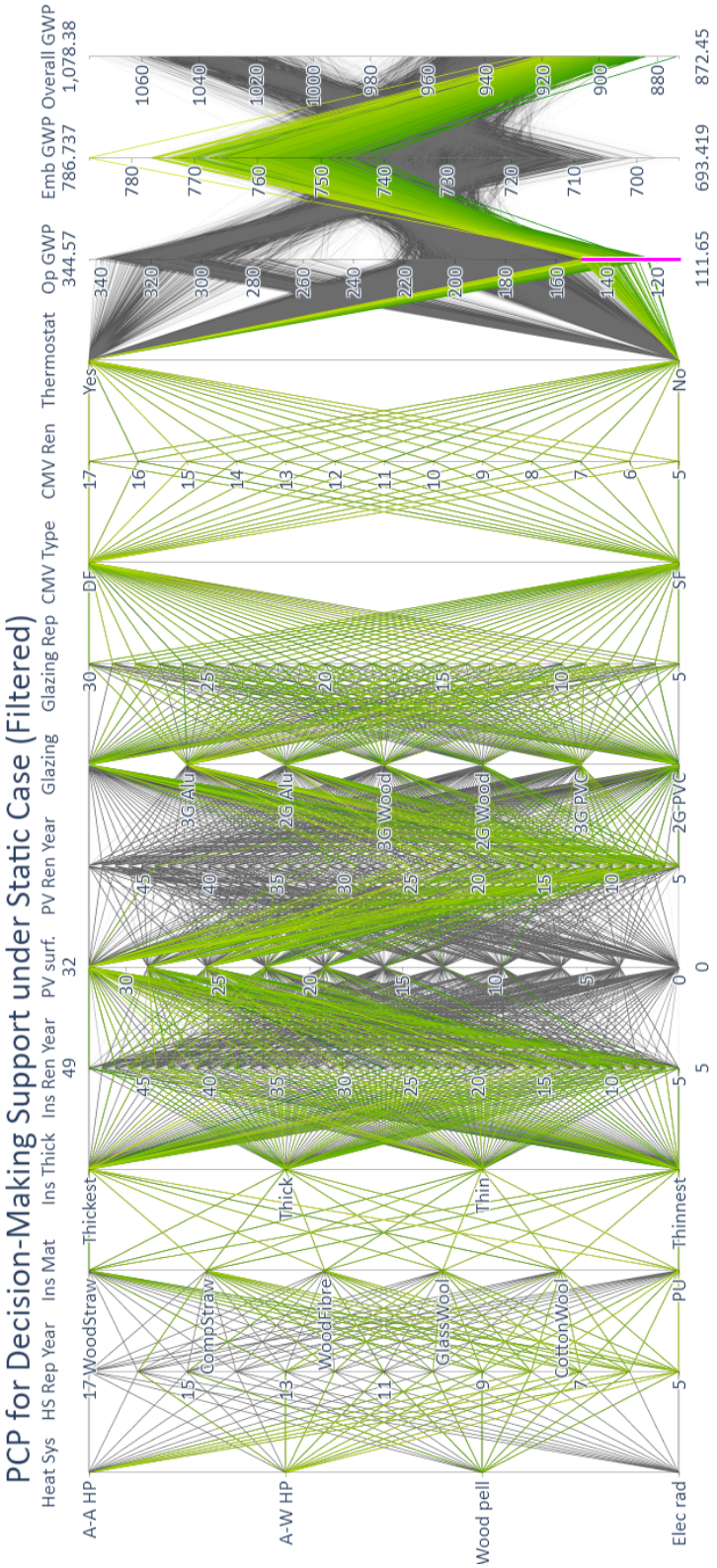

Figure D.12: Pareto solutions of the optimization solution found in the Lower-Edge case-study.

we will now move on to the comparison and discussion section of this fourth chapter.

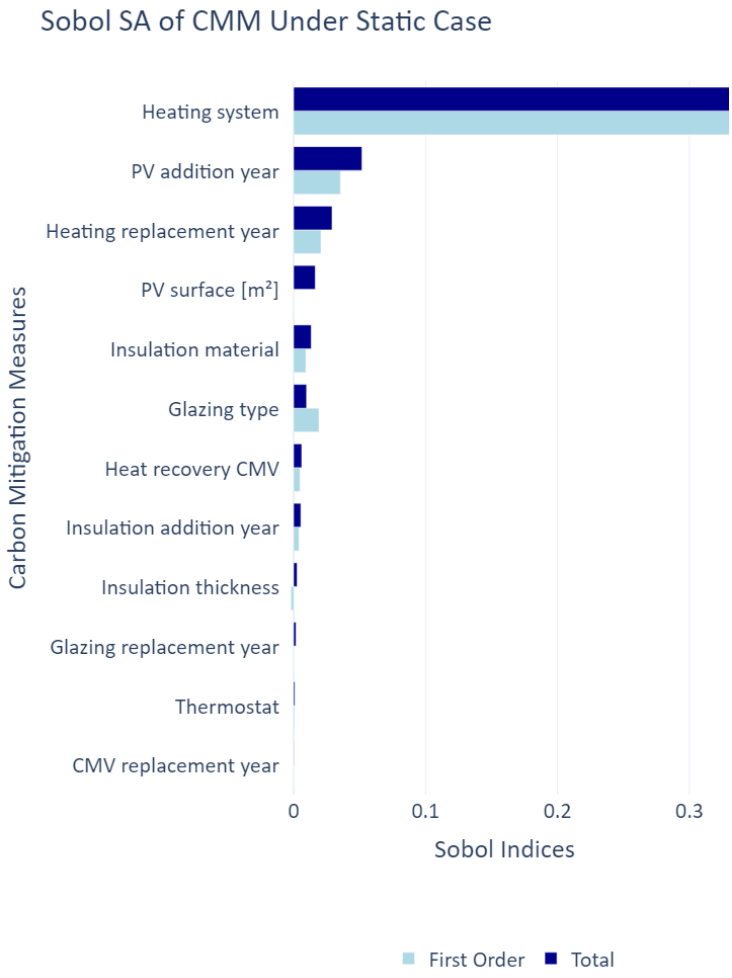

Figure D.13: Pareto solutions of the optimization solution found in the Lower-Edge case-study.